The involvement of phytohormones, tissue and age in the response to photoperiod stress in *Arabidopsis thaliana*

Dissertation

zur Erlangung des akademischen Grades

des Doktors der Naturwissenschaften (Dr. rer. nat.)

eingereicht im Fachbereich Biologie, Chemie, Pharmazie

der Freien Universität Berlin

vorgelegt von

Manuel Frank

aus Duisburg

2019

Diese Arbeit wurde von September 2015 bis September 2019 unter der Leitung von Prof. Dr. Thomas Schmülling am Institut für Biologie/Angewandte Genetik der Freien Universität Berlin angefertigt.

1. Gutachter: Prof. Dr. Thomas Schmülling

2. Gutachter: Prof. Dr. Wolfgang Schuster

Disputation am_____05.11.2019_____

Table of contents

List of Figures ..... **V**
List of tables ..... **VII**
List of abbreviations ..... **VIII**
1 Introduction **1**
1.1 The photoperiod stress syndrome 1
1.2 Cytokinin 2
1.2.1 Cytokinin biosynthesis and metabolism 2
1.2.2 Cytokinin transport 4
1.2.3 Cytokinin signaling 5
1.3 Auxin 6
1.3.1 Auxin biosynthesis and metabolism 7
1.3.2 Auxin signaling 8
1.4 Ethylene 9
1.4.1 Ethylene biosynthesis 10
1.4.2 Ethylene signaling 11
1.5 Gibberellic acid (GA) 12
1.5.1 GA biosynthesis and metabolism 12
1.5.2 GA signaling 14
1.6 Phases of plant and leaf development 15
1.6.1 Juvenile-to-adult transition 15
1.6.2 Leaf aging 16
1.7 Research aims 18
2 Materials and Methods **20**
2.1 Databases and software 20
2.2 Kits 20
2.3 Enzymes 21
2.4 Generation of *SUCROSE-PROTON SYMPORTER2* (*SUC2)::CKX1-Myc* plants 21
2.4.1 Microorganisms and growth conditions 21
2.4.2 Transformation of microorganisms 23
2.4.3 Vectors used and plasmids generated 23
2.4.4 Amplification of *SUC2* promoter 23
2.4.5 Cloning of *SUC2* constructs 24
2.4.6 Colony PCR 25
2.4.7 Purification of PCR products 26
2.4.8 Transformation of *Arabidopsis thaliana* plants 26
2.4.9 Selection and segregation analysis of *SUC2::CKX1-4xMyc* transformants 26

2.5 *Arabidopsis thaliana* plants ... 27
2.6 Growth conditions for *Arabidopsis thaliana* plants ... 28
2.7 Genetic crosses ... 29
2.8 Nucleic acid methods ... 29
2.8.1 Quantification of transcript abundance via quantitative RT-PCR ... 29
2.8.2 Genotyping of Arabidopsis plants ... 33
2.9 Determination of cytokinin, auxin and GA levels ... 36
2.10 Photoperiod stress treatment and evaluation of physiological and molecular parameters ... 36
2.10.1 Quantification of lesions ... 36
2.10.2 Chlorophyll Fluorometry (Fv/Fm ratio) ... 37
2.10.3 Determination of hydrogen peroxide (H_2O_2) content ... 37
2.10.4 Sampling for expression analysis of stress marker genes ... 38
2.10.5 RNA sequencing (RNAseq) analysis ... 38
2.11 Statistical analysis ... 38
3 Results ... 39
3.1 *t*Z-type cytokinins are essential to cope with photoperiod stress and require AHPs and ARRs to transduce their signal ... 39
3.1.1 Photoperiod stress increases the cytokinin content in wild-type plants ... 39
3.1.2 Transcript levels of genes involved in cytokinin metabolism, transport and signaling change upon photoperiod stress ... 41
3.1.3 Root-derived *t*Z-type cytokinins protect plants from photoperiod stress ... 44
3.1.4 Watering of *cypDM* plants with either *t*Z or *t*ZR reduces the sensitivity to photoperiod stress ... 46
3.1.5 Impairment in synthesis of bioactive cytokinins does not increase photoperiod stress sensitivity ... 48
3.1.6 AHP2, AHP3 and AHP5 act redundantly in photoperiod stress signaling ... 48
3.1.7 Loss of ARR10 and ARR12 rescues photoperiod stress sensitivity of *arr2* mutants ... 50
3.2 The sensitivity to photoperiod stress is tissue- and age-specific ... 52
3.2.1 Leaves of the same plant differ in their photoperiod stress responsiveness ... 52
3.2.2 The leaf identity does not influence the response to photoperiod stress ... 53
3.2.3 The sensitivity to photoperiod stress is age-dependent ... 55
3.2.4 Establishment of tissue-specific cytokinin decreases influences the sensitivity to photoperiod stress ... 58
3.2.5 The responsiveness to photoperiod stress varies in different tissues ... 59
3.3 Formation of photoperiod stress requires the perception of auxin and ethylene ... 61
3.3.1 Photoperiod stress treatment increases content of free IAA in wild-type plants ... 61
3.3.2 *GH3* transcripts are more abundant in response to photoperiod stress ... 62
3.3.3 Plants with an impaired auxin perception are less sensitive to photoperiod stress ... 64

3.3.4 Impairment in auxin perception reduces photoperiod stress sensitivity of cytokinin signaling mutants ... 66
3.3.5 The abundance of genes involved in ethylene synthesis is increased in plants in the night after exposure to a prolonged light period ... 67
3.3.6 A constitutively active ethylene pathway protects plants from photoperiod stress ... 69
3.3.7 The GA content does not change in wild-type plants in response to a prolonged light period ... 72
3.3.8 Expression of genes encoding GA receptors is altered in response to photoperiod stress ... 74
3.3.9 Plants with an impaired GA synthesis are less sensitive to photoperiod stress ... 76

4 Discussion ... 78

4.1 *tZ*-type cytokinins protect plants against photoperiod stress ... 78

4.1.1 The cytokinin concentration is increased in response to photoperiod stress ... 78
4.1.2 *tZ*-type cytokinins act as protectants against photoperiod stress ... 79
4.1.3 *logS* plants are insensitive to photoperiod stress ... 80
4.1.4 ARR2, ARR10 and ARR12 regulate the response to photoperiod stress in a complex manner ... 81

4.2 The response to photoperiod stress is age- and tissue-specific ... 82

4.2.1 The age of plants and specific leaves influences the photoperiod stress sensitivity ... 82
4.2.2 The responsiveness to photoperiod stress differs between leaves and roots ... 83

4.3 The sensitivity to photoperiod stress is influenced by the auxin and ethylene status ... 84

4.3.1 The regulation of auxin homeostasis is crucial to cope with photoperiod stress ... 84
4.3.2 An interaction of cytokinin and auxin during the regulation of photoperiod stress ... 86
4.3.3 Loss of type-II ethylene receptors causes a reduced photoperiod stress sensitivity ... 87
4.3.4 Potential interactions of ethylene with cytokinin in the context of photoperiod stress ... 89
4.3.5 Potential interactions of ethylene with auxin in the context of photoperiod stress ... 90
4.3.6 The GA status has a minor influence on the sensitivity to photoperiod stress ... 91

4.4 Differences between RNAseq and qRT data ... 92
4.5 Future perspectives ... 93

4.5.1 Role of cytokinin synthesis, metabolism and signaling in photoperiod stress ... 93
4.5.2 The importance of leaf/plant age and different tissues in photoperiod stress and a potential influence of cytokinin ... 94
4.5.3 Deciphering the crosstalk between cytokinin, auxin and ethylene in photoperiod stress ... 95
4.5.4 Photoperiod stress as a system to study the ability of plants to adapt to seasonal changes in daylength ... 97

5 Summary **98**
6 Zusammenfassung **99**
7 References **101**
Supplementary Information **124**
Acknowledgements **130**

List of Figures

		Page
Figure 1	Schematic overview of the photoperiod stress regime and physiological and molecular markers measured in this thesis.	1
Figure 2	Simplified scheme of cytokinin biosynthesis and metabolism.	3
Figure 3	Simplified scheme of cytokinin signaling in Arabidopsis.	6
Figure 4	Simplified scheme of auxin biosynthesis and metabolism.	7
Figure 5	Simplified scheme of auxin signaling.	9
Figure 6	Simplified scheme of ethylene biosynthesis.	10
Figure 7	Simplified Scheme of ethylene signaling.	11
Figure 8	Simplified scheme of GA biosynthesis and metabolism.	13
Figure 9	Simplified scheme of GA signaling in Arabidopsis.	14
Figure 10	Regulation of the juvenile-to-adult transition through miRNA156 and miRNA172.	16
Figure 11	Model of the regulation of leaf senescence by integration of environmental signals and age-related changes (ARCs).	17
Figure 12	Photoperiod stress causes an increased cytokinin content in wild-type plants.	40
Figure 13	Expression of cytokinin synthesis and metabolism genes during photoperiod stress in wild type and *ahk2ahk3.*	42
Figure 14	Expression of cytokinin transporter genes during photoperiod stress in wild type and *ahk2ahk3.*	43
Figure 15	Expression of cytokinin signaling genes during photoperiod stress in wild type and *ahk2ahk3.*	44
Figure 16	Plants deficient in *tZ-type* cytokinins are strongly affected by photoperiod stress.	45
Figure 17	Pretreatment of cytokinin-deficient plants with *tZ-type* cytokinins for five weeks reduces the damage caused by photoperiod stress.	47
Figure 18	Plants deficient in bioactive cytokinins are less affected by photoperiod stress.	48
Figure 19	AHP2, AHP3 and AHP5 act redundantly during photoperiod stress.	49
Figure 20	Loss of ARR10 or ARR12 rescues the *arr2* photoperiod stress phenotype.	51
Figure 21	Distinct leaves of an Arabidopsis rosette differ in their photoperiod stress sensitivity.	53
Figure 22	The responsiveness to photoperiod stress does not depend on the leaf identity.	54
Figure 23	The responsiveness to photoperiod stress depends on the plant age.	56
Figure 24	The responsiveness to photoperiod stress depends on the leaf age.	57
Figure 25	A tissue specific *CKX1* overexpression results in an increased photoperiod stress sensitivity.	58
Figure 26	Leaves and roots respond differently to photoperiod stress.	60

Figure 27	Photoperiod stress causes an increased content of IAA and IAA-Asp in wild-type plants.	62
Figure 28	Expression of auxin biosynthesis and metabolism genes during photoperiod stress in wild type and *ahk2ahk3.*	63
Figure 29	Expression of auxin signaling genes during photoperiod stress in wild type and *ahk2ahk3.*	64
Figure 30	Plants impaired in auxin perception are less sensitive to photoperiod stress.	65
Figure 31	Plants with an increased auxin status are more sensitive to photoperiod stress.	66
Figure 32	An impairment of auxin perception in *ahk2ahk3* decreases the sensitivity to photoperiod stress.	67
Figure 33	Expression of ethylene biosynthesis and metabolism genes during photoperiod stress in wild type and *ahk2ahk3.*	68
Figure 34	Expression of ethylene signaling genes during photoperiod stress in wild type and *ahk2ahk3.*	69
Figure 35	Plants with an impaired ethylene signaling are more sensitive to photoperiod stress.	70
Figure 36	Loss of CTR1 causes a reduced sensitivity to photoperiod stress.	71
Figure 37	Loss of type-II ethylene receptors causes a reduced sensitivity to photoperiod stress.	72
Figure 38	Photoperiod stress does not change levels of bioactive GAs in wild-type plants.	73
Figure 39	Expression of GA biosynthesis and metabolism genes during photoperiod stress in wild type and *ahk2ahk3.*	75
Figure 40	Expression of GA signaling genes during photoperiod stress in wild type and *ahk2ahk3.*	76
Figure 41	*ga20ox* mutants are less sensitive to photoperiod stress.	77
Supplemental Figure 1	Maps of vectors used and cloned in this study.	124
Supplemental Figure 2	Expression of CKX1 in *SUC2::CKX1-4xMyc* lines and shoot phenotypes.	125
Supplemental Figure 3	Confirmation of RNAseq results via qRT-PCR.	126
Supplemental Figure 4	Photoperiod stress does not change levels of GA-precursors in wild-type plants.	127
Supplemental Figure 5	Photoperiod stress does not change levels of deactivated GAs in wild-type plants.	128

List of tables

		Page
Table 1	Databases and software programs used in this thesis.	20
Table 2	Kits used in this thesis.	20
Table 3	Enzymes used in this thesis.	21
Table 4	Microorganisms used in this thesis.	21
Table 5	Composition of lysogeny broth (LB) medium (Bertani, 1951).	22
Table 6	Composition of super optimal broth with catabolite repression (SOC) medium (Hanahan, 1983).	22
Table 7	Composition of yeast extract broth (YEB) medium (Vervliet et al., 1975).	22
Table 8	Vectors and plasmids used and generated in this thesis.	23
Table 9	Reaction mixture for amplification of the *SUC2* promoter.	24
Table 10	BP reaction mixture used in this thesis for generation of *pDONRTMP4P1R-SUC2.*	24
Table 11	LR reaction mixture use for generation of *pB7m34GW-SUC2::CKX1-4xMyc.*	25
Table 12	Primer sequences for construction of plasmids, colony PCR and sequencing.	25
Table 13	PCR reaction mixture used for colony PCR.	26
Table 14	Composition of plant culture medium.	27
Table 15	Mutant and transgenic Arabidopsis plants.	27
Table 16	Reaction mixtures for cDNA synthesis from total RNA.	30
Table 17	Reaction mixtures for cDNA synthesis from miRNAs.	30
Table 18	Primer used for cDNA synthesis from miRNAs.	31
Table 19	Primer sequences for qRT-PCR.	31
Table 20	Reaction mix for qRT-PCR.	32
Table 21	Insertion-specific primers used for genotyping.	33
Table 22	Gene-specific primers used for genotyping.	34
Table 23	Genotyping of tir1 with CAPS markers.	35
Table 24	PCR reaction mixture used for genotyping of Arabidopsis plants.	35
Table 25	iP-type cytokinin content in control and PL plants at the time points depicted in Figure 12A.	41
Table 26	*tZ-type* cytokinin content in control and PL plants at the time points depicted in Figure 12A.	41
Supplemental Table 1	DHZ-type cytokinin content in control and PL plants at the time points depicted in Figure 12A.	129
Supplemental Table 2	*cZ-type* cytokinin content in control and PL plants at the time points depicted in Figure 12A.	129

List of abbreviations

4-Cl-IAA	4-chloroindole-3-acetic acid
A	Adenine
A. tumefaciens	*Agrobacterium tumefaciens*
ABC	ATP-BINDING CASSETTE
ACC	1-aminocyclopropane-1-carboxylic acid
ACD1	ACC DEAMINASE1
ACS	ACC-SYNTHASE
ACO	ACC-OXIDASE
ADP	Adenosine diphosphate
AFB	AUXIN SIGNALING F-BOX
AHK	ARABIDOPSIS HISTIDINE KINASE
AHP	ARABIDOPSIS HISTIDINE PHOSPHOTRANSFER PROTEIN
αKB	α-ketobutyrate
AMP	Adenosine monophosphate
AN3	ANGUSTIFOLIA3
ANT	AINTEGUMENTA
AP2	APETALA2
APX	ASCORBATE PEROXIDASE
ARC	Age-related change
ARF	AUXIN RESPONSE FACTOR
ARGOS	AUXIN-REGULATED GENE INVOLVED IN ORGAN SIZE
ARR	ARABIDOPSIS RESPONSE REGULATOR
ATML	ARABIDOPSIS THALIANA MERISTEM LAYER
ATP	Adenosine triphosphate
att	Attachment site
BAP1	BON ASSOCIATION PROTEIN1
bp	Base pairs
C	Cytosine
°C	Degree Celsius
CAB2	CHLOROPHYLL A/B BINDING PROTEIN2
CCA1	CIRCADIAN CLOCK ASSOCIATED1
CI	Chloroform isoamyl alcohol
CK	cytokinin
CKX	CYTOKININ OXIDASE
Cm	Chloramphenicol
CLV1	CLAVATA1
Col-0	Ecotype/accession Columbia-0
CPS	*ent*-COPALYL DIPHOSPHATE SYNTHASE
CRF6	CYTOKININ RESPONSE FACTOR6

CTR1	CONSTITUTIVE TRIPLE RESPONSE1
CUC	CUP-SHAPED COTYLEDON
CYP735A	CYTOCHROME P450 MONOOXYGENASE 735A
cypDM	*cyp735a1cyp735a2* double mutant
*c*Z	*cis*-zeatin
*c*ZPR	*c*Z riboside
*c*ZRDP	*c*ZR diphosphate
*c*ZRMP	*c*ZR monophosphate
*c*ZRTP	*c*ZR triphosphate
DAO	DIOXYGENASE FOR AUXIN OXIDATION
D-CDES	D-CYSTEINE DESULFHYDRASE
DHZ	Dihydrozeatin
DMAPP	Dimethylallyl diphosphate
DMSO	Dimethyl sulfoxide
DNA	Deoxyribonucleic acid
DVL	DEVIL
E. coli	*Escherichia coli*
EBF	EIN3-BINDING F-BOX PROTEIN
EIN	ETHYLENE INSENSITIVE
EIL	EIN3-LIKE
ENT	EQUILIBRATIVE NUCLEOSIDE TRANSPORTER
ent-C	*ent*-copalyl diphosphate
ent-K	*ent*-kaurene
ent-KA	*ent*-kaurenoic acid
ER	Endoplasmic reticulum
eto	*ethylene-overproducer*
ERS	ETHYLENE RESPONSE SENSOR
ETP	EIN2 TARGETING PROTEIN
ETR	ETHYLENE RESPONSE
FW	Fresh weight
G	Guanine
GA	Gibberellic acid
GA2OX	GIBBERELLIN 2-OXIDASE
GA3OX	GIBBERELLIN 3-OXIDASE
GA13OX	GIBBERELLIN 13-OXIDASE
GA20OX	GIBBERELLIN 20-OXIDASE
GAI	GIBBERELLIC ACID INSENSITIVE
G-ACC	γ-glutamyl-ACC
GGDP	Geranylgeranyl diphosphate
GGT	γ-GLUTAMYL-TRANSPEPTIDASE
GH3	GRETCHEN HAGEN3

GID1	GIBBERELLIN INSENSITIVE DWARF1
GIF1	GRF-INTERACTING FACTOR1
GR	GLUTATHIONE REDUCTASE
GRF	GROWTH REGULATING FACTOR
h	Hours
IAA	Indole-3-acetic acid
IAA-Asp	IAA aspartic acid
IAA-Glu	IAA glutamic acid
IAR3	IAA-ALANINE RESISTANT3
ILL	IAA-LEUCINE RESISTANT-LIKE
ILR1	IAA-LEUCINE RESISTANT1
iP	N^6-isopentenyladenine
IPA	Indole-3-pyruvic acid
iPR	iP riboside
iPRDP	iPR diphosphate
iPRMP	iPR monophosphate
iPRTP	iPR triphosphate
IPT	ISOPENTENYLTRANSFERASE
JA	Jasmonic acid
Kan	Kanamycin
KAO	*ent*-KAURENOIC ACID OXIDASE
kb	Kilo base pairs
KO	*ent*-KAURENE OXIDASE
KS	*ent*-KAURENE SYNTHASE
LB	Lysogeny broth
LHY	LATE ELONGATED HYPOCOTYL
LOG	LONELY GUY
logS	*log* septuple mutant
MEP	Methylerythritol phosphate
Met	Methionine
MIM	miRNA mimicry
min	Minutes
miRNA	microRNA
MVA	Mevalonate
NAC	NO APICAL MERISTEM (NAM)/ATAF/CUP-SHAPED COTYLEDON
NAM	NO APICAL MERISTEM
oxIAA	2-oxoindole-3-acetic acid
PAM	Pulse-amplitude-modulated
PCD	Programmed cell death
PCI	Phenol chloroform isoamyl alcohol

PCR	Polymerase chain reaction
PIF	PHYTOCHROME-INTERACTING FACTOR
PL	Prolonged light period treated (stressed)
PLP	Prolonged light period
PP2AA2	PROTEIN PHOSPHATASE2A SUBUNIT A2
ppt	Phosphinothricin
PRR1	PSEUDO RESPONSE REGULATOR1
PUP	PURINE PERMEASE
qRT	Quantitative real time
REV	REVOLUTA
RGA	REPRESSOR-OF-GA1-3
RGL	RGA-LIKE
RHL41/ZAT12	RESPONSIVE TO HIGH LIGHT 41
RNA	Ribonucleic acid
RNAseq	RNA sequencing
ROS	Reactive oxygen species
ROT4	ROTUNDOFOLIA4
RTFL	ROTUNDOFOLIA4-LIKE
S-AM	S-adenosyl-L-methionine
SAG	SENESCENCE-ASSOCIATED GENE
SAM	SAM-SYNTHETASE
SCF	Skp1-Cullin-F-box
SD	Short-day/ standard deviation
SDG	SENESCENCE-DOWN-REGULATED GENE
sec	Seconds
sis1	*sugar-insensitive1*
SLY1	SLEEPY1
SNE	SNEEZY
SnRK2	SUCROSE NON-FERMENTING1-RELATED PROTEIN KINASE2
SOC	Super optimal broth with catabolite repression
SOD	SUPEROXIDE DISMUTASE
Spec	Spectinomycin
SPL	SQUAMOSA PROMOTER BINDING PROTEIN-LIKE
SPT	SPATULA
SUC2	SUCROSE-PROTON SYMPORTER2
SWP	STRUWWELPETER
T	Thymine
TAA1	TRYPTOPHAN AMIDOTRANSFERASE OF ARABIDOPSIS1
Taq	*Thermus aquaticus*
TAR	TRYPTOPHAN AMINOTRANSFERASE RELATED

TE	Tris-EDTA
TIR1	TRANSPORT INHIBITOR RESISTANT1
TOC1	TIMING OF CAB EXPRESSION1
tRNA	Transfer ribonucleic acid
*t*Z	*trans*-zeatin
*t*ZPR	*t*Z riboside
*t*ZRDP	*t*ZR diphosphate
*t*ZRMP	*t*ZR monophosphate
*t*ZRTP	*t*ZR triphosphate
UBC10	UBIQUITIN-CONJUGATING ENZYME10
UGT76C	URIDINE DIPHOSPHATE GLYCOSYLTRANSFERASE76C
UGT85A	URIDINE DIPHOSPHATE GLYCOSYLTRANSFERASE85A
V	Volt
WUS	WUSCHEL
YEB	Yeast extract broth
YUC	YUCCA

1 Introduction

1.1 The photoperiod stress syndrome

Plants are exposed to several environmental stimuli that can act as potential stressors. One of these stimuli is the alteration of the light-dark cycle. As shown recently, a novel type of abiotic stress caused by an exposure to a prolonged light period (PLP) - coined photoperiod stress - has been described in *Arabidopsis* (Nitschke *et al*., 2016, 2017). The standard photoperiod stress regime consists of a five-week-long short-day (SD) entrainment that is interrupted once by a 32 h-lasting PLP (Figure 1).

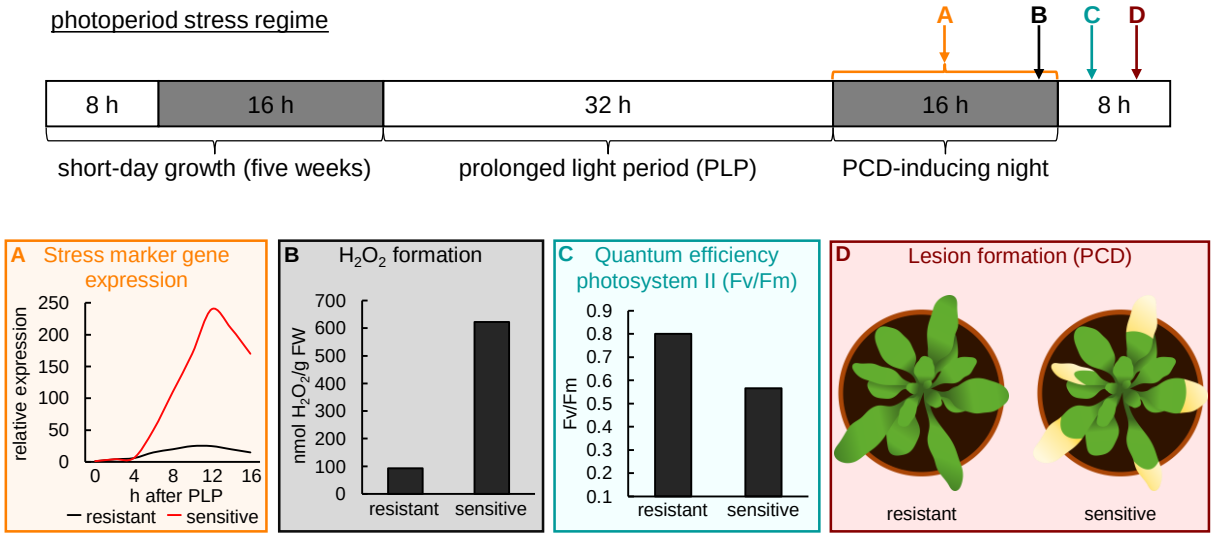

Figure 1: Schematic overview of the photoperiod stress regime and physiological and molecular markers measured in this thesis.
After five weeks of short-day entrainment, a prolonged light period (PLP) of 32 h is given. (A) During the night following the PLP, photoperiod sensitive plants show an altered expression of stress marker genes compared to resistant plants (Induction of marker genes in A serves as one example but a downregulation is also possible). (B) 15 h after the PLP-treatment, sensitive plants accumulate more H_2O_2 compared to resistant plants. The next day, a reduction in photosystem II maximum quantum efficiency (Fv/Fm) is noted in leaves of sensitive plants (C), and the formation of lesions becomes visible which ultimately results in programmed cell death (PCD, D). Adapted from Nitschke et al*., 2017.*

Characteristic for the response to photoperiod stress is, amongst others, an altered expression of stress and cell death marker genes - for example *BON ASSOCIATION PROTEIN1* (*BAP1*), *RESPONSIVE TO HIGH LIGHT41* (*RHL41*/*ZAT12*) and *CHLOROPHYLL A/B BINDING PROTEIN2* (*CAB2*) - in sensitive plants compared to resistant plants during the night following the PLP (Figure 1A). In addition to the differential expression of marker genes, an accumulation of reactive oxygen species (ROS) in form of H_2O_2 is detected during and especially at the end of the night after the PLP in sensitive plants (Figure 1B). The next day, sensitive plants display a reduced photosynthetic efficiency compared to resistant plants (Figure 1C). Lastly, an increased number of leaves that are lesioned is visible in sensitive plants compared to resistant ones resulting eventually in programmed cell death (PCD; Figure 1D). Notably, while a PLP of 32 h was applied in the first description of the stress syndrome (Nitschke *et al*., 2016, 2017), an extension of the light period by four hours is sufficient to trigger a photoperiod stress response in terms of lesion formation (Nitschke, 2014), while a prolongation by two hours is sufficient to cause

photoperiod stress at the molecular level (Abdelsloud *et al*., unpublished). Furthermore, only mature, fully expanded leaves are fully sensitive and especially young leaves that are still growing are not or less responsive to photoperiod stress (Nitschke, 2014).
So far, two pathways have been described to be crucial for the sensitivity to photoperiod stress (Nitschke *et al*., 2016, 2017). The first one is the circadian clock. An impairment of the circadian oscillations by the loss of the circadian oscillators CIRCADIAN CLOCK ASSOCIATED1 (CCA1) and LATE ELONGATED HYPOCOTYL (LHY) as well as an overexpression of *PSEUDO RESPONSE REGULATOR1* (*PRR1*)/*TIMING OF CAB EXPRESSION1* (*TOC1*) led to an increased sensitivity to photoperiod stress (Nitschke *et al*., 2016). Moreover, the synthesis, metabolism and signaling of the phytohormone cytokinin has been found to be of major importance for the photoperiod stress sensitivity (Nitschke *et al*., 2016). Central components in this context are ISOPENTENYLTRANSFERASE3 (IPT3), IPT5, IPT7, CYTOKININ OXIDASEs (CKXs), ARABIDOPSIS HISTIDINE KINASE3, ARABIDOPSIS RESPONSE REGULATOR2 (ARR2), ARR10 and ARR12 (Nitschke *et al*., 2016). In plants with either an impaired circadian clock or a decreased cytokinin status, expression of jasmonic acid (JA) synthesis and signaling genes were misregulated upon photoperiod stress (Nitschke *et al*., 2016). Furthermore, cytokinin receptor and metabolism mutants accumulated several JA derivatives including bioactive JA-isoleucine. The loss of JA-isoleucine synthesis in the cytokinin mutant background rescued the photoperiod stress phenotype of these plants (Nitschke *et al*., 2016). As the expression of circadian clock genes was also misregulated in plants with a decreased cytokinin status compared to wild type after exposure to photoperiod stress, a model has been proposed that puts the circadian clock in the center of photoperiod stress regulation and places cytokinin as one factor influencing the circadian clock by regulating the transcription of its components (Nitschke *et al*., 2016, 2017).

1.2 Cytokinin

Cytokinins are one major group of phytohormones and have been named originally after their ability to regulate cell division. In the 1950s, Miller and colleagues isolated the first cytokinin derivative by autoclaving DNA and demonstrated its cell division-inducing properties in tissue cultures (Miller *et al*., 1955, 1956). Since then, experimental evidence suggests that cytokinins are involved in nearly all aspects of plant growth and development like e.g. shoot initiation, shoot and root growth in general, embryonic development, nutrient acquisition, flowering, leaf senescence and in the resistance against biotic and abiotic stresses (Werner and Schmülling, 2009; Kieber and Schaller, 2014; Cortleven *et al*., 2019b). Furthermore, its biosynthesis and metabolism, transport and signaling pathway has been studied extensively in the last decades.

1.2.1 Cytokinin biosynthesis and metabolism

Structurally, natural cytokinins are adenine derivatives that are either isoprenylated or carry an aromatic side chain at the N^6-residue (Sakakibara, 2006). The four biologically most important types - N^6-isopentenyladenine (iP), *cis*-zeatin (*c*Z), *trans*-zeatin (*t*Z) and dihydrozeatin (DHZ) - belong to the isoprenoid class. All can exist either as *O*- and *N*-glucosides, ribotides, ribosides or as a bioactive free

base (Sakakibara, 2006). In *Arabidopsis*, iP and *t*Z are the biologically most relevant cytokinins. iP is predominantly important for root development and *t*Z is crucial for most developmental processes in shoot tissue (Miyawaki *et al*., 2006; Kiba *et al*., 2013). They are initially synthesized by the addition of dimethylallyl diphosphate (DMAPP), which mainly derives from the methylerythritol phosphate (MEP) pathway, to adenosine mono-/di-/triphosphate (AMP/ADP/ATP) (Sakakibara, 2006; Figure 2).

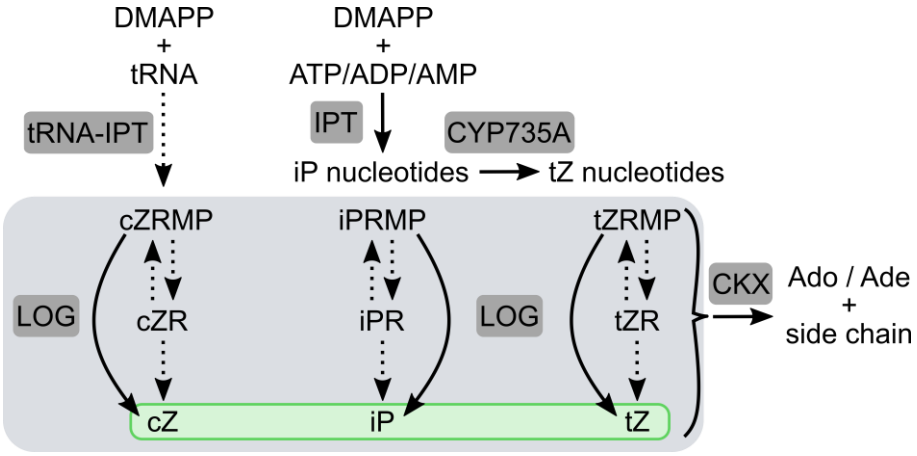

Figure 2: Simplified scheme of cytokinin biosynthesis and metabolism.
As a first step of synthesis, isopentenyl adenine (iP) nucleotides are formed by ISOPENTENYLTRANSFERASE (IPT) enzymes. Conversion to the respective trans*-zeatin (*t*Z)-nucleotides is catalyzed by CYTOCHROME P450 MONOOXYGENASEs (CYP735As). In addition,* cis*-zeatin (*c*Z)-type CKs are formed by tRNA-IPT enzymes. iP riboside monophosphate (iPRMP),* t*Z riboside monophosphate (*tZRMP*) and* c*Z riboside monophosphate (*cZRMP*) can be directly converted to biologically active free bases (green box) by LONELY GUY (LOG) enzymes. Inactivation of all metabolites is catalyzed by CYTOKININ OXIDASES/DEHYDROGENASE (CKX) enzymes. Modified after Cortleven* et al*., 2019.*

This reaction is catalyzed by ISOPENTENYLTRANSFERASEs (IPTs) that constitute a nine-member family in *Arabidopsis* (Takei *et al*., 2001; Kakimoto, 2001). Seven of these nine members are involved in iP nucleotide (iP riboside (iPR) mono-/di-/triphosphate (iPRMP/iPRDP/iPRTP)) formation. Cytokinin measurements as well as phenotypic analyses of *ipt* single and higher order mutants indicates that iP-type cytokinins are mainly formed by IPT3 and that IPT3, IPT5 and IPT7 are the most relevant enzymes (Miyawaki *et al*., 2006). They are expressed in the phloem (*IPT3*), lateral root primordia (*IPT5*) as well as root tips and the endodermis (*IPT7*) (Miyawaki *et al*., 2004). It is assumed that cytokinin is mainly synthesized in plastids as studies revealed that IPT1, IPT3, IPT5 and IPT8 are localized in plastids, while IPT4 is localized in the cytosol and IPT7 in mitochondria (Kasahara *et al*., 2004). Formed iP nucleotides are converted further to *t*Z nucleotides by two cytochrome P450 monooxygenases - CYP735A1 and CYP735A2 (Takei *et al*., 2004). *CYP735A1* is predominantly expressed in flowers and roots and *CYP735A2* predominantly expressed in roots but also in the hypocotyl close to the shoot apical meristem (Takei *et al*., 2004; Kiba *et al*., 2013). Characterization of *t*Z-deficient *cyp735a* mutants indicated that both isoforms act redundantly (Kiba *et al*., 2013). In *cypDM* double mutants, *t*Z-type cytokinin content is strongly reduced but total cytokinin levels are unchanged as the reduction is compensated by an increased content of iP-type cytokinins (Kiba *et al*., 2013).

*c*Z-type cytokinins are formed via a different pathway that involves transfer ribonucleic acid (tRNA)-IPTs IPT2 and IPT9. These enzymes catalyze the reaction of DMAPP, which mainly derives from the mevalonate (MVA) pathway, with tRNAs which results in the formation of *c*Z ribotides (Takei *et al*., 2001;

Miyawaki *et al*., 2006). On the one hand, studies suggest that *c*Z-type cytokinins are formed in the cytosol as IPT2 is localized there (Kasahara *et al*., 2004). On the other hand, *ipt2ipt9* mutant analysis indicates that *c*Z-type cytokinins are involved in primary root growth and protoxylem formation (Köllmer *et al*., 2014).

All isoprenoid class cytokinins are converted to their bioactive form by cytokinin nucleoside 5'-monophosphate phosphoribohydrolase enzymes named LONELY GUY (LOGs) through dephosphorylation of respective riboside monophosphate precursors (Kurakawa *et al*., 2007). In *Arabidopsis*, seven out of nine *LOG* genes are functional, each one being expressed in different tissues and mutant analysis indicates that they act redundantly in various processes (Kuroha *et al*., 2009; Tokunaga *et al*., 2012). In *log* septuple mutant (*logS*), levels of bioactive cytokinins are reduced by more than 50 %, while levels of cytokinin ribosides and nucleotides are strongly increased (Tokunaga *et al*., 2012).

Bioactive cytokinins are degraded irreversibly by either N-glucosylation or by side chain cleavage. Further, zeatin-type cytokinins can be inactivated temporarily by O-glucosylation and it is believed that they are reactivated by hydrolases. From the five genes encoding glucosyl transferases in *Arabidopsis*, N-glucosylation is catalyzed by two enzymes - URIDINE DIPHOSPHATE GLYCOSYLTRANS-FERASE76C1 (UGT76C1) and UGT76C2 (Hou *et al*., 2004; Wang *et al*., 2011, 2013). CYTOKININ OXIDASEs (CKXs) cleave bioactive cytokinins irreversibly. Seven *CKX* genes are present in *Arabidopsis* and they are localized mainly in the ER and vacuoles and have distinct expression patterns (Werner *et al*., 2003). Further, constitutive overexpression of *CKX* genes as well as *ckx* mutant analysis showed the importance for plant development (Werner *et al*., 2001, 2003; Bartrina *et al*., 2011; Werner *et al*., 2010; Köllmer *et al*., 2014). O-glucosylation is catalyzed by the other three enzymes of the glucosyl transferase family (Hou *et al*., 2004; Jin *et al*., 2013). Studies indicate that UGT85A1 is the enzyme with the biggest impact on O-glucosylation by regulating *t*Z homeostasis (Jin *et al*., 2013).

1.2.2 Cytokinin transport

After their synthesis, cytokinins either signal directly at or are transported to the site of action (Kang *et al*., 2017). iP-type and *t*Z-type cytokinins are carried over long distances via the vasculature. The direction of their transport reflects the side of their biological function. iP-type cytokinins move basipetally in the phloem (Matsumoto-Kitano *et al*., 2008; Bishopp *et al*., 2011), while *t*Z-type cytokinins move acropetally in the xylem mainly as ribosides but also as free bases (Kiba *et al*., 2013; Osugi *et al*., 2017). Crucial for the long-distance translocation of *t*Z-type cytokinins is ABCG14, a member of the 28-member containing subfamily G of ATP-BINDING CASSETTE (ABC) proteins. It is mainly expressed in the root and as a consequence, *abcg14* mutants accumulate *t*Z-type cytokinins in root tissue (Ko *et al*., 2014; Zhang *et al*., 2014).

Apart from ABCGs, members of two other transporter families are also involved in cytokinin translocation and either transport inactive cytokinin ribosides or bioactive cytokinins. EQUILIBRATIVE NUCLEOSIDE TRANSPORTER (ENT) proteins translocate cytokinin ribosides (Hirose *et al*., 2005; Sun *et al*., 2005). In *Arabidopsis*, ENTs constitute an eight-member family and so far, cytokinin riboside transport through ENT3, ENT6 ENT7 and ENT8 has been experimentally proven (Hirose *et al*., 2005, 2008). From these, all *ENTs* are expressed to different extends in leaves and while *ENT6* is expressed vasculature specific

throughout the plant, *ENT8* is expressed strongly in hypocotyls and petioles (Li *et al*., 2003; Sun *et al*., 2005; Hirose *et al*., 2008).

Plasma membrane-localized PURINE PERMEASE (PUP) symporters are involved in H^+-dependent transport of cytokinin free bases and are encoded by 21 genes in *Arabidopsis* (Durán-Medina *et al*., 2017). PUP1 and PUP2 were the first family members identified (Gillissen *et al*., 2000; Bürkle *et al*., 2003) and while *PUP1* is predominantly expressed in hydathodes but also in stigma tissue, *PUP2* is expressed specifically in the vasculature (Bürkle *et al*., 2003; Cedzich *et al*., 2008). Recently, PUP14 has been identified to be crucial for seedling development as amiRNA lines were strongly impaired (Zürcher *et al*., 2016). Interestingly, *PUP14* expression was inversely correlated to cytokinin signaling output and as PUP14 is also localized at the plasma membrane, a discussion started whether cytokinin perception is taking place at the plasma membrane or the endoplasmic reticulum (ER) (Zürcher *et al*., 2016; Kang *et al*., 2017; Romanov *et al*., 2018).

1.2.3 Cytokinin signaling

After cytokinins are synthesized and transported, bioactive cytokinins activate the cytokinin signaling pathway, which is a histidine/aspartate phosphorylation cascade (reviewed in e.g. Werner and Schmülling, 2009; Kieber and Schaller, 2014). In *Arabidopsis*, cytokinins are bound by a three-member family of ARABIDOPSIS HISTIDINE KINASE (AHK) receptors (Inoue *et al*., 2001; Suzuki *et al*., 2001a; Ueguchi *et al*., 2001; Yamada *et al*., 2001) (Figure 3). Activated receptors phosphorylate the histidine residue of ARABIDOPSIS HISTIDINE PHOSPHOTRANSFER PROTEINS (AHPs) (Hutchison *et al*., 2006). Five redundant genes encode AHPs with histidine residues in *Arabidopsis* (Hutchison *et al*., 2006). AHP6 does not contain the histidine residue and acts as a negative regulator of cytokinin signaling (Mähönen *et al*., 2006). The phosphorylation signal of AHP1 to AHP5 is transferred to and thus activates type-B ARABIDOPSIS RESPONSE REGULATOR (type-B ARR) transcription factors, which ultimately regulate cytokinin- dependent gene expression (Imamura *et al*., 1999). Type-B ARRs contain a phosphorylation domain as well as a DNA-binding domain (Sakai *et al*., 1998a). Thus, they act as positive regulators of cytokinin signaling in most cases. However, some studies suggest that gene regulation by type-B ARRs is more complex (Mason *et al*., 2005; Ramireddy *et al*., 2013).

Part of cytokinin regulated genes encode for type-A ARRs that act as negative regulators, thereby establishing a feedback mechanism (Brandstatter and Kieber, 1998; Sakai *et al*., 1998a). As known from bacterial RRs (Mack *et al*., 2009), some ARRs like ARR18 can homo- and heterodimerize in a phosphorylation-dependent manner (Veerabagu *et al*., 2012). Further, they can interact with transcription factors of other hormone signaling pathways like ETHYLENE INSENSITIVE3 (EIN3) or PHYTOCHROME-INTERACTING FACTORs (PIFs) (Marín-de la Rosa *et al*., 2015; Yan *et al*., 2017).

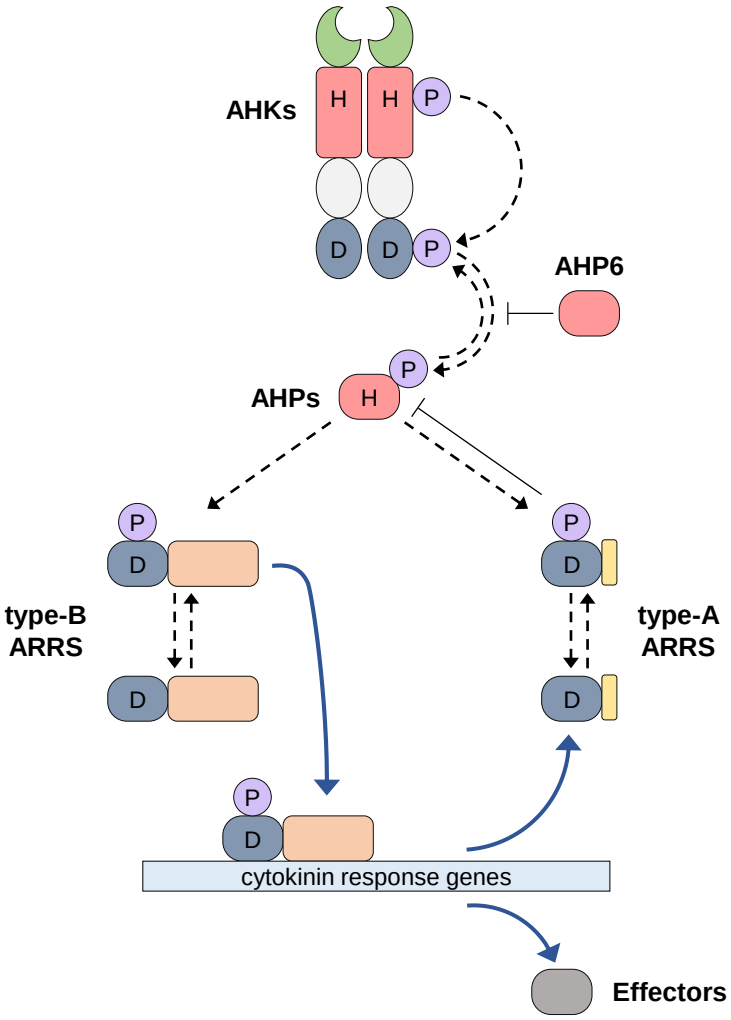

***Figure 3: Simplified scheme of cytokinin signaling in* Arabidopsis.**
Bioactive cytokinins bind to the CHASE-domain (green) of ARABIDOPSIS HISTIDINE KINASE (AHK) receptors thereby initiating a histidine (H)/aspartate (D) phosphorylation (P; purple) cascade. The phosphorylation signal is transduced by ARABIDOPSIS HISTIDINE PHOSPHOTRANSFER PROTEINs (AHPs) that contain H residues and ultimately given to type-B ARABIDOPSIS RESPONSE REGULATORs (ARRs). Upon phosphorylation, they activate cytokinin response genes by binding to DNA via their DNA-binding domain (orange). Among cytokinin response genes are type-A ARRs. These act as negative feedback regulators as they compete with type-B ARRs for phosphorylation but are unable to bind DNA. Modified after Werner and Schmülling (2009).

1.3 Auxin

Auxins are another group of molecules that belong to the 'classical' phytohormones and are named after their ability to regulate plant growth. Already in the 19th century, Charles Darwin and his son Francis studied the bending of coleoptiles towards light, which is an auxin-regulated process (Darwin and Darwin, 1880). Since then, it was discovered that auxins are mobile molecules (Went, 1926) and that they not only regulate coleoptile bending but are also crucial for developmental processes of e.g. embryos, primary and lateral roots and the vascular tissue (Teale *et al*., 2006). During many of these processes, auxin and cytokinin interact with each other by regulating the others metabolism, signaling and transport (Coenen and Lomax, 1997; El-Showk *et al*., 2013).

1.3.1 Auxin biosynthesis and metabolism

So far, three naturally occurring active auxins - indole-3-acetic acid (IAA), 4-chloroindole-3-acetic acid (4-Cl-IAA), and phenylacetic acid (PAA) - have been identified (reviewed in Korasick *et al*., 2013). From these, only IAA has been found in *Arabidopsis* and originates from indole. It can be formed tryptophan-independently or tryptophan-dependently (reviewed in Woodward and Bartel, 2005). One of the three proposed tryptophan-dependent branches - the indole-3-pyruvic acid (IPA) pathway – appears to be the main contributor of IAA formation in *Arabidopsis* and it is the only one where all genes have been described (reviewed in Zhao, 2012; Korasick *et al*., 2013).

As the initial step of the IPA pathway, TRYPTOPHAN AMIDOTRANSFERASE OF ARABIDOPSIS1 (TAA1) and TRYPTOPHAN AMINOTRANSFERASE RELATED (TAR) proteins convert tryptophan to IPA (Stepanova *et al*., 2008) (Figure 4).

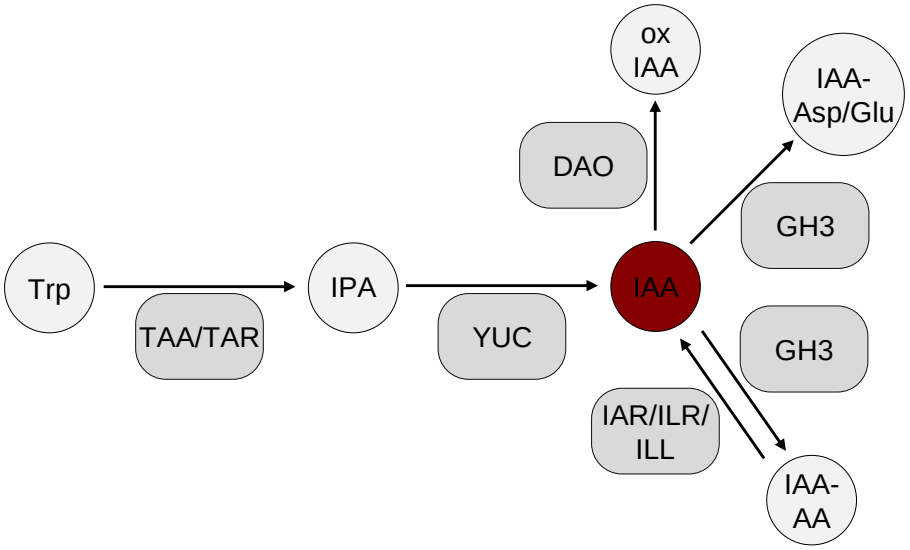

Figure 4: Simplified scheme of auxin biosynthesis and metabolism.
First, TRYPTOPHAN AMIDOTRANSFERASE OF ARABIDOPSIS (TAA1) and TRYPTOPHAN AMINOTRANS-FERASE RELATED (TAR) proteins convert tryptophan (Trp) to indole-3-pyruvic acid (IPA), which is converted to bioactive free IAA by YUCCA (YUC) proteins. IAA can be inactivated irreversibly to 2-oxoindole-3-acetic acid (oxIAA) by DIOXYGENASE FOR AUXIN OXIDATION (DAO) proteins or to either IAA aspartic acid (IAA-Asp) and IAA glutamic acid (IAA-Glu) by GRETCHEN HAGEN3 (GH3) proteins. GH3s catalyze also the reversible inactivation to other IAA-amino acid conjugates. Reversion of the reaction is catalyzed by IAA-ALANINE RESISTANT3 (IAR3), IAA-LEUCINE RESISTANT1 (ILR1) and IAA-LEUCINE RESISTANT-LIKE (ILL) proteins.

taa1 mutants were initially found in screens for weak ethylene insensitivity and loss of shade avoidance in seedlings (Stepanova *et al*., 2008). Further, only *taa1* single mutant and respective higher order *taa1tar* mutants showed auxin-related phenotypes such as reduced vascular patterning or a reduced gravitropic response and in most cases, *taa1tar1tar2* triple mutants were seedling lethal (Stepanova *et al*., 2008). After its formation, IPA is converted further to bioactive free IAA by YUCCA (YUC) proteins. *Arabidopsis* harbors eleven *YUC* genes that are expressed in various tissues at different developmental stages (Cheng *et al*., 2006; Müller-Moulé *et al*., 2016). A gain-of-function *YUC1* mutant - named *yuc1D* hereafter – had severe developmental alterations due to an increased content of free IAA (Zhao *et al*., 2001) as had other *35S::YUC* lines (Cheng *et al*., 2006). *yuc* loss-of-function mutants on the other hand

had increased levels of IPA and showed phenotypes related to a lowered auxin status (Cheng *et al*., 2006; Mashiguchi *et al*., 2011; Müller-Moulé *et al*., 2016).

IAA is modified/inactivated in many ways like oxidation or amino acid and carbohydrate conjugation. The most important irreversible inactive forms in *Arabidopsis* are 2-oxoindole-3-acetic acid (oxIAA), IAA aspartic acid (IAA-Asp) and IAA glutamic acid (IAA-Glu). Oxidation of IAA to oxIAA is catalyzed by two DIOXYGENASE FOR AUXIN OXIDATION (DAO) homologs (Porco *et al*., 2016; Zhang *et al*., 2016a). Amino acid conjugation of IAA is catalyzed by subfamily II of GRETCHEN HAGEN3 (GH3) proteins (Staswick *et al*., 2002, 2005). Both inactivation branches act redundantly, as IAA levels in *dao1* mutants were not altered compared to wild type due to increased IAA-Asp and IAA-Glu levels that compensated the impaired oxIAA formation (Porco *et al*., 2016). Further, a *gh3.1-6* sextuple mutant had increased IAA and IAA-Glu levels while IAA-Asp formation was abolished (Porco *et al*., 2016). Apart from conjugating Asp and Glu to IAA, GH3s also catalyze the reversible inactivation to other IAA-amino acid conjugates like IAA-Leu and IAA-Ala. Hydrolysis of these IAA conjugates is catalyzed by IAA-ALANINE RESISTANT3 (IAR3), IAA-LEUCINE RESISTANT1 (ILR1) and IAA-LEUCINE RESISTANT-LIKE (ILL) proteins (Davies *et al*., 1999; LeClere *et al*., 2002). From seven genes in *Arabidopsis*, IAR3, ILR1, ILL1 and ILL2 are able to release free IAA from amino acid conjugates and ILL5 has been suggested to be a pseudogene (LeClere *et al*., 2002). Genetic analysis further indicated that the release of IAA is of importance for hypocotyl growth and root development (LeClere *et al*., 2002; Rampey, 2004).

1.3.2 Auxin signaling

Formed IAA can activate signaling pathways whose receptors are in either the apoplast or in the inside of cells. While extracellular AUXIN-BINDING-PROTEINs (ABP1)-dependent IAA perception is only of minor importance in *Arabidopsis* (Gao *et al*., 2015), intracellular perception of IAA is accomplished by TRANSPORT INHIBITOR RESISTANT1 (TIR1)/AUXIN SIGNALING F-BOX (AFB) receptors and thus represents the major auxin perception pathway (Dharmasiri *et al*., 2005a, 2005b; Parry *et al*., 2009). *TIR1*/*AFBs* are expressed ubiquitously and genetic analysis demonstrated their functional redundancy in leaf development as well as in root development (Dharmasiri *et al*., 2005b; Parry *et al*., 2009). In absence of IAA, TIR/AFBs are inactive (Figure 5).

As a result, AUX/IAA proteins - *Arabidopsis* harbors 29 *Aux*/*IAA* genes - are present and inhibit the function of AUXIN RESPONSE FACTOR (ARF) transcription factors by interacting directly through domain III and IV (Ulmasov *et al*., 1997b, 1999b). There are 23 *ARF* genes in *Arabidopsis* of which one is a pseudogene (*ARF23*). Structurally, ARFs can be divided in class A ARFs, whose members share a Q-rich middle region and act mostly as transcriptional activators, and class B and class C ARFs that act as repressors of auxin signaling (Ulmasov *et al*., 1999a; Tiwari *et al*., 2003; Guilfoyle and Hagen, 2007).

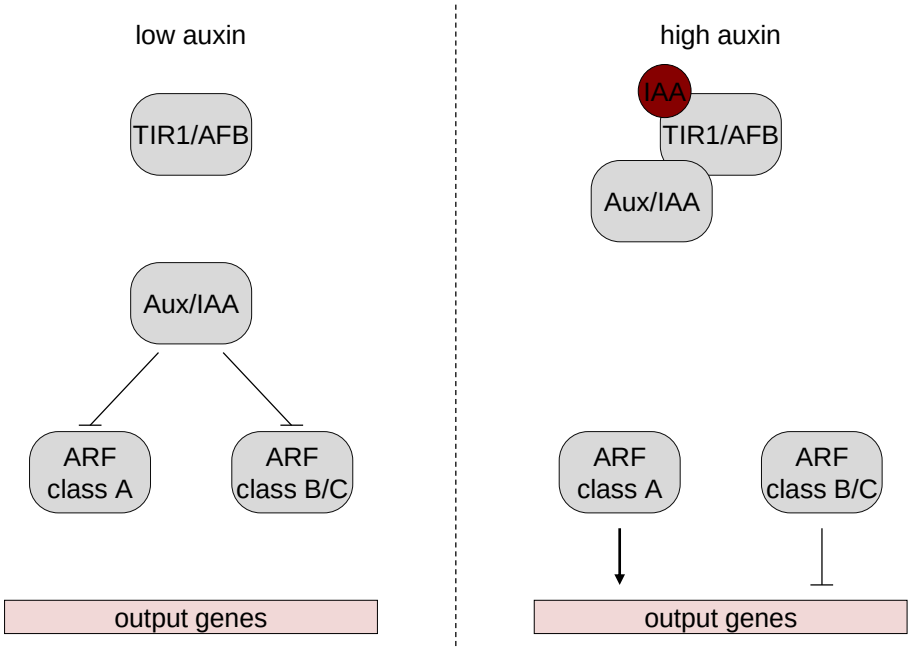

Figure 5: Simplified scheme of auxin signaling.
In absence of auxin (IAA), TRANSPORT INHIBITOR RESISTANT1 (TIR1)/AUXIN SIGNALING F-BOX (AFB) receptors are inactive. Consequently, Aux/IAA proteins inhibit the function of class A, B and C AUXIN RESPONSE FACTOR (ARF) transcription factors. With perception of IAA by TIR1/AFB receptors, the latter interact with and thus inhibit Aux/IAAs by mediating their ubiquitin-dependent degradation. In consequence, class A ARFs act as transcriptional activators while class B and C ARFs mostly act as transcriptional repressors.

With perception of IAA by TIR1/AFB receptors, a Skp1-Cullin-F-box (SCF)-TIR1/AFB complex is formed that inhibits Aux/IAA function by mediating their ubiquitination and consequently, their proteasome-dependent degradation. Domain II of Aux/IAA is crucial for this process (Worley *et al*., 2000; Ramos *et al*., 2001). Characterization of *aux*/*iaa* single and higher order mutants did not show any differences from wild type but gain-of-function mutations as in *IAA17* led to strong changes in auxin sensitivity (Overvoorde *et al*., 2005). As a consequence of Aux/IAA degradation, ARFs get active, can form dimers and positively or negatively regulate the transcription of output genes via binding to auxin response elements (Ulmasov *et al*., 1997a, 1999a, 1999b). Genetic studies indicate that *arf* single mutants do not exhibit strong phenotypes, but higher order mutants like *arf7arf19* and *arf6arf8* show severe root and/or shoot phenotypes (Okushima *et al*., 2005).

1.4 Ethylene

Belonging to the ‘classical’ phytohormones, ethylene is a gaseous hormone that is involved in regulating numerous developmental processes like seedling growth, fruit ripening, leaf and root development, the juvenile-to-adult transition or senescence (Abeles *et al*., 1992; Bleecker and Kende, 2000; Schaller and Kieber, 2002; Schaller, 2012). Further, ethylene is crucial for the tolerance to a variety of biotic and abiotic stresses (Wang *et al*., 2002; Kazan, 2015). Structurally, ethylene displays the simplest unsaturated hydrocarbon (C_2H_4) and had already been discovered at the end of the 19th century (Neljubow, 1901; Abeles *et al*., 1992). First mutants have been identified by screening for the ethylene-triggered ‘triple response’, characterized by the formation of an exaggerated apical hook, hypocotyl

shortening and thickening and the inhibition of root elongation of dark-grown *Arabidopsis* seedlings (Guzman and Ecker, 1990). Mutant screens in the early 1980s and 1990s further led to the identification of pathways involved in ethylene biosynthesis, metabolism and signaling.

1.4.1 Ethylene biosynthesis

The metabolism of ethylene has been summarized elsewhere (Wang *et al*., 2002) and thus will be covered briefly in this section. As the first step of ethylene synthesis, SAM-SYNTHETASE (SAM) proteins convert methionine (Met) and ATP to S-adenosyl-L-methionine (S-AM) (Figure 6).

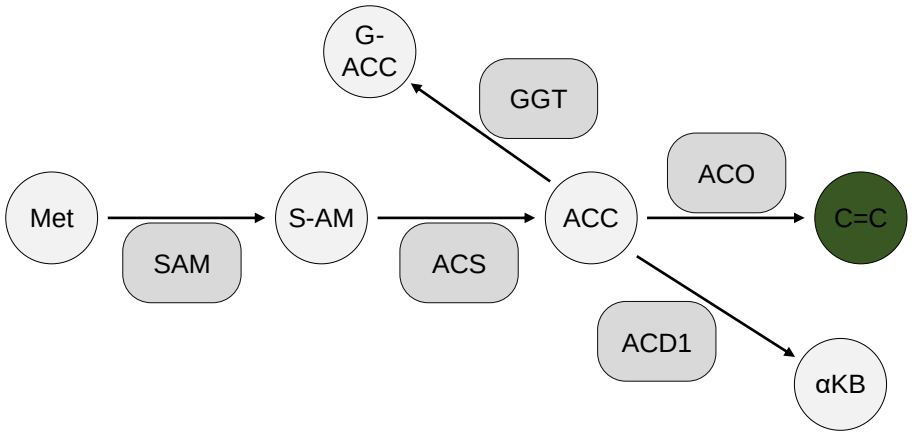

Figure 6: Simplified scheme of ethylene biosynthesis.
Schematic presentation of ethylene metabolism. First, SAM-SYNTHETASE (SAM) proteins convert methionine (Met) to S-adenosyl-L-methionine (S-AM), which is converted to 1-aminocyclopropane-1-carboxylic acid (ACC) by ACC-SYNTHASE (ACS) enzymes. ACC can be converted to either α-ketobutyrate (αKB) by ACC DEAMINASE1 (ACD1) or γ-glutamyl-ACC (G-ACC) by γ-GLUTAMYL-TRANSPEPTIDASE (GGT) proteins. Ethylene itself (C=C) is synthesized from ACC by ACC-OXIDASE (ACO) enzymes. Please note that other ACC conjugates exist that are not depicted in this figure.

S-AM is not only a precursor during ethylene production, but is also a methyl-group donor during DNA and protein methylation (Yang and Hoffman, 1984; Wang *et al*., 2002; Shyh-Chang *et al*., 2013). Consequently, changes in S-AM levels in *sam1sam2* plants and *SAM* overexpression lines mimic ethylene related phenotypes (Mao *et al*., 2015). The next step of ethylene synthesis is the conversion of S-AM to 1-aminocyclopropane-1-carboxylic acid (ACC) by ACC-SYNTHASE (ACS) enzymes. The *Arabidopsis* genome harbors 12 *ACS* genes from which eight catalyze the reaction as *ACS3* is a pseudogene, *ACS1* is not functional and *ACS10* and *ACS12* encode for aminotransferases (Liang *et al*., 1995; Yamagami *et al*., 2003). In *ethylene-overproducer* (*eto*) mutants *eto1*, *eto2* and *eto3*, ACS5 and ACS9 protein levels are increased due to impairment of their degradation (Vogel *et al*., 1998; Woeste *et al*., 1999b). Characterization of *acs* single and higher order mutants on the other hand indicates a crucial role in general shoot development, flowering time, seed and silique development and ethylene production (Tsuchisaka *et al*., 2009).
ACC can be conjugated or irreversibly degraded. The conjugation to γ-glutamyl-ACC (G-ACC) catalyzed by γ-GLUTAMYL-TRANSPEPTIDASE (GGT) proteins. Four genes encode GGTs in *Arabidopsis* and while phenotypic analysis of *ggt* mutants indicates a role for GGT1 and GGT3, determination of catalytic activity indicates that GGT1 and GGT2 are active (Martin *et al*., 2007). ACC is irreversibly degraded to

α-ketobutyrate (αKB) by ACC DEAMINASEs (ACDs). ACDs can be found in many bacteria and fungi and recently, one gene encoding ACD1 (also D-CYSTEINE DESULFHYDRASE, D-CDES) has been identified and characterized in *Arabidopsis* (McDonnell *et al*., 2009). If not conjugated or degraded, ACC is oxidized by ACC-OXIDASE (ACO) enzymes, leading to ethylene formation. So far, only few *aco* mutants have been characterized. For example, ACO2 functionality is crucial to counteract ABA-mediated inhibition of seed germination through ACC (Linkies *et al*., 2009).

1.4.2 Ethylene signaling

At the end of its synthesis, ethylene can activate a signaling cascade that has certain similarities to the cytokinin signaling pathway and bacterial two component systems. In its resting state without ethylene, ETHYLENE RESPONSE (ETR)/ETHYLENE RESPONSE SENSOR (ERS)/ETHYLENE INSENSITIVE4 (EIN4) receptors act as negative regulators of ethylene signaling (Figure 7) (Ecker, 1995; Hua *et al*., 1995; Sakai *et al*., 1998b).

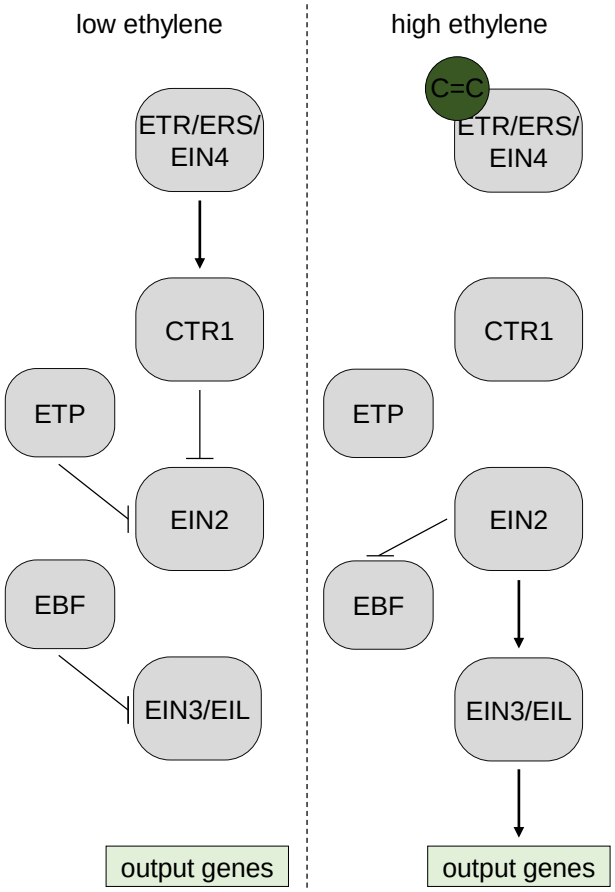

Figure 7: Simplified Scheme of ethylene signaling.
In absence of ethylene (C=C), ETHYLENE RESPONSE (ETR)/ETHYLENE RESPONSE SENSOR (ERS)/ETHYLENE INSENSITIVE4 (EIN4) receptors act as negative regulators of ethylene signaling by interacting with CONSTITUTIVE TRIPLE RESPONSE1 (CTR1), which inactivates EIN2. In addition, EIN2 can be degraded 26S proteasome-dependently, which is mediated by F-box proteins EIN2 TARGETING PROTEIN (ETP) F-box proteins. Because of EIN2 inactivation and degradation, EIN3/EIN3-LIKE1 (EIL1)/EIL2 transcription factors get degraded mediated by EIN3-BINDING F-BOX PROTEINs (EBFs). Upon ethylene perception, ETR/ERS/EIN4 receptors get inactive and consequently CTR1. This leads to an activation of EIN2, which stabilizes EIN3/EIL proteins and mediates EBF degradation, leading to the activation of ethylene-regulated genes.

In *Arabidopsis*, five genes encode ETR/ERS/EIN4 proteins and based on the N-terminal structure, they are divided in type I receptors (ETR1 and ERS1) that have three transmembrane domains and type II receptors (ETR2, ERS2 and EIN4) that have four transmembrane domains (Hua *et al*., 1998). ETR/ERS/EIN4 interact with and thus activate CONSTITUTIVE TRIPLE RESPONSE1 (CTR1) - a Ser/Thr kinase (Kieber *et al*., 1993). CTR1 phosphorylates EIN2 at its C-terminus, causing its inactivation (Ju *et al*., 2012). In addition, EIN2 can be degraded 26S proteasome-dependently, which needs the function of F-box proteins EIN2 TARGETING PROTEIN1 (ETP1) and ETP2 (Qiao *et al*., 2009). In consequence of EIN2 inactivation and degradation, EIN3/EIN3-LIKE1 (EIL1)/EIL2 transcription factors become degraded with help of two other F-box proteins - EIN3-BINDING F-BOX PROTEIN1 (EBF1) and EBF2 (Guo and Ecker, 2003; Potuschak *et al*., 2003; An *et al*., 2010). The lack in EIN3/EIL1/EIL2 ultimately causes an absence of ethylene-response genes transcription.
Upon ethylene perception, ETR/ERS/EIN4 receptors get inactive, causing CTR1 inactivation. Simultaneously, EIN2 interacts with ETR/ERS/EIN4 in a phosphorylation dependent manner which protects EIN2 from degradation (Bisson and Groth, 2010). Further, inactivation of CTR1 enables the cleavage of the EIN2 C-terminus, which migrates into the nucleus and stabilizes EIN3/EIL proteins directly but also indirectly by mediating EBF degradation (Wen *et al*., 2012; An *et al*., 2010). In addition, ethylene perception leads to a downregulation of *EBF1* and *EBF2* (An *et al*., 2010). EIN3/EIL1/EIL2 accumulation finally leads to the transcriptional regulation of ethylene-response genes (Chao *et al*., 1997; Guo and Ecker, 2003; Potuschak *et al*., 2003).

1.5 Gibberellic acid (GA)

Like all formerly introduced phytohormones, GAs belong to the ‘classical’ phytohormones and the research can be followed back to the end of the 19th century. Back then, it was found that fungal pathogens were able to cause uncontrolled seedling elongation and infertility (Hori, 1898). Later, the growth promoting substance was isolated from the fungus *Gibberella fujikuroi* and was named accordingly (Yabuta and Sumiki, 1938). Since then, GA function has been studied extensively. It has been assumed that GAs regulate various developmental processes like seed germination and development, leaf expansion, flowering or regulation of the juvenile-to-adult transition and the underlying metabolism and signaling has been deciphered (Hedden and Phillips, 2000; Yamaguchi, 2008; Sun, 2008; Davière and Achard, 2013; Hedden and Sponsel, 2015).

1.5.1 GA biosynthesis and metabolism

Since its discovery, over 130 GAs have been found but only a small number has been suggested to be bioactive (Yamaguchi, 2008). In *Arabidopsis*, the main GA-precursor GA_{12} is formed through multiple consecutive reactions from geranylgeranyl diphosphate (GGDP; Figure 8).

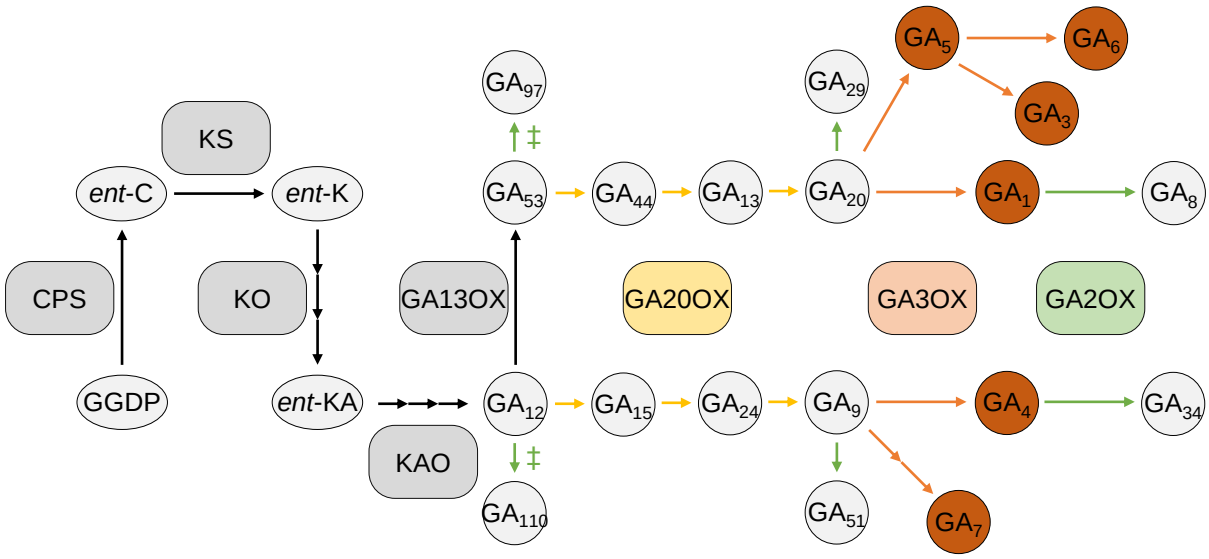

Figure 8: Simplified scheme of GA biosynthesis and metabolism.
Starting from geranylgeranyl diphosphate (GGDP), the main GA-precursor GA_{12} is formed through multiple consecutive reactions involving ent-COPALYL DIPHOSPHATE SYNTHASE (CPS) that forms ent-copalyl diphosphate (ent-C), ent-KAURENE SYNTHASE (KS) that forms ent-kaurene (ent-K), ent-KAURENE OXIDASE (KO) that forms ent-kaurenoic acid (ent-KA) and ultimately ent-KAURENOIC ACID OXIDASE (KAO) enzymes. GA_{12} can be converted to either GA_{53} via GIBBERELLIN 13-OXIDASE (GA13OX) enzymes (genes have not been identified yet) or to GA_9 via GIBBERELLIN 20-OXIDASE (GA20OX) enzymes (yellow arrows). The latter also catalyze the conversion of GA_{53} to GA_{20}. GIBBERELLIN 3-OXIDASE (GA3OX) enzymes convert GA_9 to bioactive GA_4 and GA_7 (dark orange) and GA_{20} to bioactive GA_1, GA_3, GA_5 and GA_6. Inactivation of GA_1 and GA_4 is facilitated by GIBBERELLIN 2-OXIDASE (GA2OX) enzymes, which also convert GA_9 and GA_{20} precursors to inactive forms. GA2OX7 and GA2OX8 inactivate GA_{12} and GA_{53} precursors (indicated by ‡). Double arrows indicate multiple reaction steps catalyzed by the same enzyme.

First, *ent*-COPALYL DIPHOSPHATE SYNTHASE (CPS) forms *ent*-copalyl diphosphate (*ent*-C) from GGDP (Sun and Kamiya, 1994). Formed *ent*-C is converted to *ent*-kaurene (*ent*-K) by *ent*-KAURENE SYNTHASE (KS) (Yamaguchi *et al*., 1998). *ent*-K is used as a substrate by *ent*-KAURENE OXIDASE (KO) to form *ent*-kaurenoic acid (*ent*-KA) (Helliwell *et al*., 1998). Ultimately, *ent*-KAURENOIC ACID OXIDASE (KAO) enzymes use *ent*-KA as a substrate to form GA_{12} (Helliwell *et al*., 2001). *Arabidopsis* harbors two *KAO* genes that have overlapping expression patterns as in the root meristem and in flowers but are also expressed distinctly as in the vasculature (*KAO2*). Further, mutant analysis indicates that they act redundantly (Regnault *et al*., 2014).

After its formation, GA_{12} itself is transported over long distances through the vasculature (Regnault *et al*., 2015) and is converted afterwards to either GA_{53} by GIBBERELLIN 13-OXIDASEs (GA13OXs) of which the coding genes have not been identified yet or to GA_9 by GIBBERELLIN 20-OXIDASEs (GA20OXs). The latter also catalyze the conversion of GA_{53} to GA_{20} (Phillips *et al*., 1995). Mutant analysis indicates that from the five isoforms in *Arabidopsis*, GA20OX1 GA20OX2 have the major role while GA20OX4 and GA20OX5 are of minor importance (Plackett *et al*., 2012). The reactions leading to the formation of bioactive GAs are catalyzed by GA3OX enzymes. On the one hand, GIBBERELLIN 3-OXIDASEs (GA3OXs) convert GA_9 to bioactive GA_4 and GA_7. On the other hand, they convert GA_{20} to bioactive GA_1, GA_3, GA_5 and GA_6. Four genes encode GA3OX proteins in *Arabidopsis* and from these, *GA3OX1* and *GA3OX2* are expressed throughout the plant (Mitchum *et al*., 2006; Sun, 2008). Characterization of *ga3ox* single and higher order mutants further indicates that GA3OX1 and GA3OX2

are the most important isoforms for general shoot development while GA3OX1 and GA3OX3 are of major importance for GA production in the flower (Hu *et al*., 2008).
Following their formation and potential action, bioactive GAs are inactivated by different mechanisms. The best studied pathway involves GIBBERELLIN 2-OXIDASEs (GA2OXs) that inactivate GA_1 and GA_4 but also the direct precursors GA_9 and GA_{20} (Thomas *et al*., 1999). Recently, two GA2OX7 and GA2OX8 have been found to deactivate bioactive GAs but GA_{20} and GA_{53} precursors (Schomburg *et al*., 2003). Conclusively, *ga2ox* mutants have increased levels of bioactive GAs and resemble phenotypes indicative for an increased GA status (Schomburg *et al*., 2003; Wang *et al*., 2004).

1.5.2 GA signaling

Synthesized bioactive GAs can activate a nucleus-localized signaling pathway that involves GIBBERELLIN INSENSITIVE DWARF1 (GID1) receptors, DELLA proteins GIBBERELLIC ACID INSENSITIVE (GAI)/ REPRESSOR-OF-GA1-3 (RGA)/RGA-LIKE (RGL), F-box proteins SLEEPY1 (SLY1) and SNEEZY (SNE) and transcription factors like e.g. PHYTOCHROME-INTERACTING FACTORs (PIFs) (Sun, 2008; Schwechheimer, 2012; Davière and Achard, 2013). In the absence of bioactive GA, GID1 receptors are inactive (Figure 9).

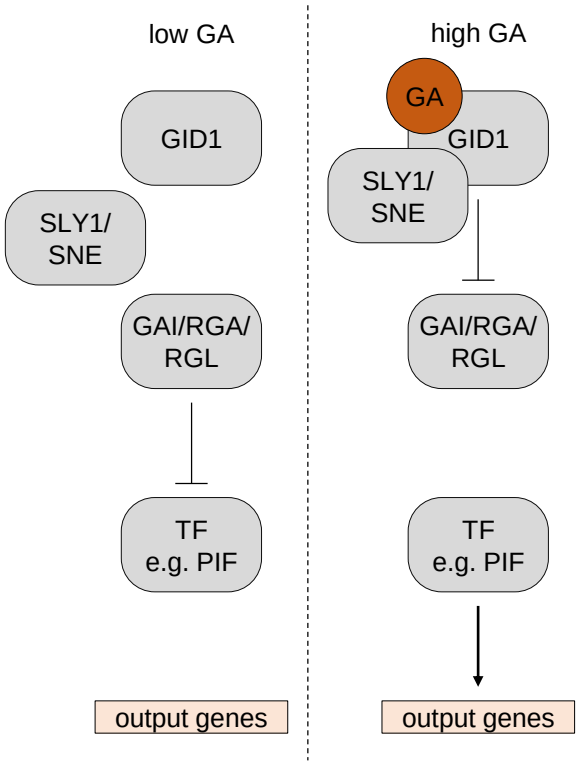

***Figure 9: Simplified scheme of GA signaling in* Arabidopsis.**
In the absence of GA (dark orange), GIBBERELLIN INSENSITIVE DWARF1 (GID1) receptors are inactive. Consequently, DELLA proteins GIBBERELLIC ACID INSENSITIVE (GAI)/ REPRESSOR OF GA1-3 (RGA)/RGA-LIKE (RGL) inhibit the function of transcription factors (TF) like e.g. PHYTOCHROME-INTERACTING FACTOR (PIF) proteins. With perception of GA by GID1 receptors, the latter associate with F-box proteins SLEEPY1 (SLY1) or SNEEZY (SNE) and inhibit DELLA function by mediating their degradation. In consequence, TFs are active and mediate the transcription of output genes.

GID1 was originally found in rice in which it is encoded by only one gene (Ueguchi-Tanaka *et al*., 2005). In comparison, three genes encode for GID1 receptors in *Arabidopsis* and characterization of *gid1* mutants indicates that GID1A and GID1C are the major GA receptors (Griffiths *et al*., 2006). Because of GID1 inactivity, DELLA proteins GAI/RGA/RGL inhibit the GA signaling pathway (Peng and Harberd, 1993; Silverstone *et al*., 1998; Lee *et al*., 2002; Cheng, 2004). Mechanistically, GAI/RGA/RGL repress the function of transcription factors like PIFs by e.g. binding to their DNA-recognition domain (De Lucas *et al*., 2008; Feng *et al*., 2008).
With perception of GA by GID1 receptors, the latter become active and inhibit DELLA function together with F-box proteins SLY and SNE by causing their ubiquitination and subsequent 26S proteasome-dependent degradation (McGinnis *et al*., 2003; Dill *et al*., 2004; Ariizumi *et al*., 2011). Consequently, formerly repressed transcription factors get active and mediate the transcription of output genes.

1.6 Phases of plant and leaf development

During its lifetime, a plant itself but also each of its leaves individually undergo various developmental programs characteristic for certain developmental stages. Previous work has shown that young leaves of a plant are less responsive to photoperiod stress compared to mature ones (Nitschke, 2014; Nitschke *et al*., 2016). However, which age-related developmental processes are involved could not be solved. In order to deepen the understanding of this process, two distinct developmental programs that are influenced by cytokinin - the so-called juvenile-to-adult transition and leaf aging itself - were investigated and therefore will be introduced in this section.

1.6.1 Juvenile-to-adult transition

As plants develop, they undergo distinct phases that follow one another and that normally cannot be skipped (Poethig, 2003; Huijser and Schmid, 2011). The length of the phases is influenced by environmental stimuli like the light-dark rhythm (Martínez-Zapater *et al*., 1995; Chien and Sussex, 1996). Generally, plants grow vegetatively after germination. During this period, plants increase their biomass and form leaves. Further, vegetative growth starts with a juvenile phase that progresses to an adult phase. Plants then enter a phase of reproductive growth in which they flower and produce seeds. Ultimately, plants end their life cycle by entering the phase of senescence. All phases possess distinct morphological and genetic traits. In the following, the focus will lie on the vegetative growth phase.
Morphologically, leaves formed during juvenile vegetative growth have long petioles, roundly shaped blades with smooth margins and lack abaxial trichomes while on the other hand, adult leaves have shorter petioles, elongated blades with serrations and abaxial trichomes (Martínez-Zapater *et al*., 1995; Chien and Sussex, 1996; Telfer *et al*., 1997). The presence of both juvenile and adult traits on one plant has been termed heteroblasty. Molecularly, vegetative growth and the so-called juvenile-to-adult transition is regulated by two microRNAs - miRNA156 and miRNA172 (Figure 10). Expression of *MIRNA156* is high in young plants while expression of *MIRNA172* is low (Axtell and Bartel, 2005), which leads to the formation of juvenile leaves. Plants constitutively overexpressing either *MIRNA156* (*35S::MIRNA156*) or miRNA172 mimicry targets (*35S::MIM172*) form many juvenile leaves and have a

delayed flowering as they leave vegetative growth later (Schwab *et al*., 2005; Wu and Poethig, 2006; Todesco *et al*., 2010). With age, miRNA156 levels decrease while miRNA172 accumulates until a certain threshold is reached and the juvenile-to-adult transition has progressed to a point where newly formed leaves possess adult traits. Supportively, *35S::MIRNA172a* and *35S::MIM156* plants form only few adult leaves until flowering (Franco-Zorrilla *et al*., 2007; Todesco *et al*., 2010).

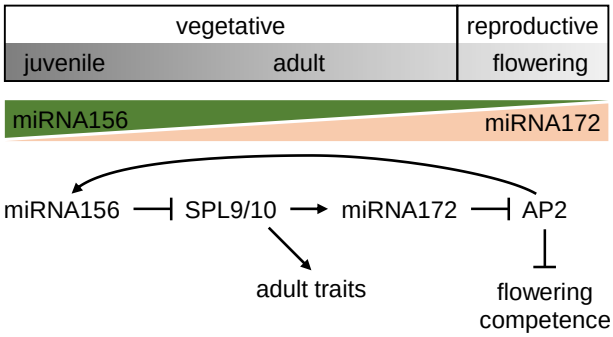

Figure 10: Regulation of the juvenile-to-adult transition through miRNA156 and miRNA172.
Abundance of miR156 is high in early stages of plant development and thus positively regulates the juvenile vegetative growth phase within these phases. As the plant matures, the abundance of miRNA156 decreases, which results in the accumulation of SQUAMOSA PROMOTER BINDING PROTEIN-LIKE9 (SPL9) and SPL10 proteins that promote adult leaf traits. Simultaneously, SPL9 and SPL10 induce the expression of MIR172 *genes. An accumulation of miRNA172 results in a negative regulation of AP2-like transcription factors, which repress flowering. A loss of this repression enables the development of flowering competence. Moreover, some AP2-like transcription factors positively regulate miRNA156. Altered after Huijser and Schmid, 2011.*

Both miRNAs are connected via miRNA156 downstream targets SQUAMOSA PROMOTER BINDING PROTEIN-LIKEs (SPLs) (Wu and Poethig, 2006; Franco-Zorrilla *et al*., 2007). With age, SPLs accumulate and induce the transition to the adult growth phase and loss-of-function mutants possess more juvenile leaves (Cardon *et al*., 1999; Wu and Poethig, 2006; Wu *et al*., 2009). Further, SPL9 and SPL10 regulate *MIRNA172* transcription (Wu *et al*., 2009). Subsequently, miRNA172 represses APETALA2 (AP2)-type transcription factors that act downstream not only during vegetative growth but also during flowering induction (Aukerman and Sakai, 2003; Chen, 2004; Mathieu *et al*., 2009). Apart from miRNAs, the length of juvenile and adult vegetative growth is regulated by different phytohormones. For example, GA acts as a positive regulator of the juvenile growth phase by regulating *SPL* transcript levels through the chromatin remodeling enzyme PICKLE (Telfer *et al*., 1997; Park *et al*., 2017). Further, it has been reported that *t*Z-type cytokinins are regulators of the juvenile-to-adult transition (Kiba *et al*., 2013) as well as ethylene (Lumba *et al*., 2012).

1.6.2 Leaf aging

With age, individual leaves undergo several developmental phases that go hand in hand with morphological and molecular alterations. After their initiation, leaves undergo phases of growth, maturation and senescence until eventually they die off (Gonzalez *et al*., 2012; Tsukaya, 2013; Woo *et al*., 2013; Schippers, 2015; Nelissen *et al*., 2016). During growth, young leaves sequester nutrients and carbohydrates to grow and build up the photosynthetic apparatus. Further, they are not responsive to

external stimuli that induce senescence (Figure 11) (Jing *et al*., 2005; Jibran *et al*., 2013; Kanojia and Dijkwel, 2018).

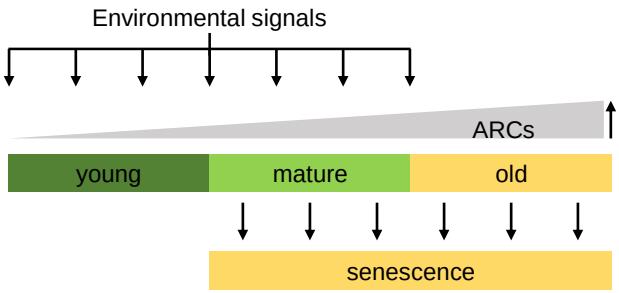

Figure 11: Model of the regulation of leaf senescence by integration of environmental signals and age-related changes (ARCs).
Over time, ARCs accumulate during plant development (right-angled triangle). They are integrated together with environmental signals and, depending on the occurrence of certain ARCs, senescence is induced. Environmental signals alone cannot induce senescence in young leaves as these lack ARCs. With leaf maturation through ARCs, they become responsive to external senescence-inducing signals. In old leaves, a critical number of ARCs has occurred that triggers senescence regardless of environmental signals. Altered after Jibran et al*., 2013.*

The major drivers of leaf growth - cell division and cell expansion - change with progression. In its early development, leaf tissue grows due to cell proliferation, which displays a combination of cell division and cell expansion (Donnelly *et al*., 1999; Granier *et al*., 2002). Eventually, a so-called cell-cycle arrest front is formed at which an area of cell expansion at the tip and the proliferating tissues of the basal leaf meet (Donnelly *et al*., 1999; Kazama *et al*., 2010; Andriankaja *et al*., 2012). Starting from the leaf tip, the cell-cycle arrest front migrates to the base but then stays at a certain position. Afterwards, it disappears abruptly and cell expansion becomes the major form of leaf growth (Kazama *et al*., 2010; Andriankaja *et al*., 2012). At the molecular level, cell proliferation is positively regulated by many factors like AINTEGUMENTA (ANT) (Mizukami and Fischer, 2000), GROWTH REGULATING FACTORs (GRFs) (Kim and Kende, 2004; Horiguchi *et al*., 2005), ANGUSTIFOLIA3 (AN3)/GRF-INTERACTING FACTOR1 (GIF1) (Kim and Kende, 2004; Lee *et al*., 2009), AUXIN-REGULATED GENE INVOLVED IN ORGAN SIZE (ARGOS) (Hu *et al*., 2003) or STRUWWELPETER (SWP) (Autran *et al*., 2002). Respective loss-of-function mutants possess smaller leaves than wild type. Analysis of *spatula* (*spt*) plants (Ichihashi *et al*., 2010) and *ROTUNDOFOLIA4* (*ROT4*)*-LIKE* (*RTFL*)/*DEVIL* (*DVL*) overexpressors indicates that these factors are negative regulators (Narita *et al*., 2004; Wen *et al*., 2004).

With the end of growth and differentiation, leaves enter the maturation phase (Gonzalez *et al*., 2012; Bar and Ori, 2014). Here, they are photosynthetically active and thus crucial for the plant's energy supply in form of carbohydrates. Over time, leaves undergo more and more age-related changes (ARCs) that are irreversible and make them responsive to stress-triggered senescence (Figure 11) (Jibran *et al*., 2013; Kanojia and Dijkwel, 2018). Examples of ARCs are an increased sensitivity and production of ROS, a gradual decline in the antioxidant system (by e.g. a decrease in ascorbic acid content), an increased sensitivity to ethylene, an altered transcriptional responsiveness, a reduced repairment of damaged DNA or a decrease in cytokinin content (Dertinger *et al*., 2003; Jing *et al*., 2005; Kotchoni *et al*., 2009; Breeze *et al*., 2011; Jibran *et al*., 2013; Kanojia and Dijkwel, 2018; Skalák *et al*., 2019). The

entrance into stress-independent senescence displays the final phase in the life cycle of a leaf (Woo *et al*., 2013; Schippers, 2015; Kim *et al*., 2018b) Physiologically, senescent leaves gradually lose their chlorophyll/photosynthetic activity and degrade proteins and nucleic acids (Dertinger *et al*., 2003). Furthermore, nutrients are relocated to non-senescing tissues (Hensel *et al*., 1993; Breeze *et al*., 2011). The molecular mechanisms behind the onset of senescence have been studied thoroughly. Many transcription factors regulating senescence belong to two families - *NACs* (standing for *NO APICAL MERISTEM* (*NAM*)/*ATAF*/*CUP-SHAPED COTYLEDON* (*CUC*)) and *WRKYs*. In *Arabidopsis*, over 100 genes encode *NACs* and many of them have been genetically characterized (Ooka *et al*., 2003; Kim *et al*., 2016). Recently, three of them - *ANAC017*, *ANAC082*, and *ANAC090* - have been identified as negative regulators of senescence and to be crucial already in a pre-senescent state (Kim *et al*., 2018a). WRKYs comprise 74 members in *Arabidopsis* and characterization of *wrky53* (positive regulator), *wrky54* and *wrky70* mutants (negative regulators) demonstrated their important regulatory function (Miao *et al*., 2004; Besseau *et al*., 2012). Further, REVOLUTA (REV) transcription factors induce *WRKY53* expression in an H_2O_2-dependent manner (Xie *et al*., 2014). Apart from transcription factors, other genes upregulated (*SENESCENCE-ASSOCIATED GENES*, *SAGs*) or downregulated (*SENESCENCE-DOWN-REGULATED GENES*, *SDGs*) during senescence have been described (Hensel *et al*., 1993; Lohman *et al*., 1994; Li *et al*., 2012).

Numerous phytohormones have been found to regulate leaf development and senescence. Among them, cytokinin acts positively on cell proliferation (Miller *et al*., 1955; Werner and Schmülling, 2009; Kieber and Schaller, 2014) and - by signaling through AHK3, ARR2 and CYTOKININ RESPONSE FACTOR6 (CRF6) - negatively regulates senescence (Kim *et al*., 2006; Zwack *et al*., 2013; Bartrina *et al*., 2017). In agreement with this, cytokinin levels in young tobacco and poplar leaves are high and decrease with age (Hewett and Wareing, 1973; Singh *et al*., 1992a, 1992b) and *t*Z levels are higher in young, proliferating *Arabidopsis* leaves (Skalák *et al*., 2019). Furthermore, senescence can be delayed by *IPT* expression under control of the senescence-induced *SAG12* promoter (Gan and Amasino, 1995).

1.7 Research aims

Based on previous findings in the context of photoperiod stress (Nitschke, 2014; Nitschke *et al*., 2016), my work aimed to deepen the understanding of photoperiod stress in three directions.

The first research question aimed to further specify which type of cytokinin is protective and which signaling components act during photoperiod stress. Therefore, mutants lacking certain cytokinin biosynthesis enzymes, cytokinin transporters or cytokinin signaling components were exposed to photoperiod stress and characterized at the phenotypic and molecular level. To provide further experimental evidence, watering of plants with cytokinin was performed to protect photoperiod stress sensitive cytokinin-deficient mutants. Cytokinin levels were monitored throughout photoperiod stress treatment and development of stress symptoms in wild-type plants to get insight into the direct temporal regulation.

The second part dealt with the question of what causes the differences in photoperiod stress competence of young and mature leaves and which tissues contribute to the photoperiod stress

response. Therefore, the focus of my experiments was on two different developmental programs of leaves and plants. On the one hand, the involvement of plant and leaf age was investigated by testing the photoperiod stress sensitivity of wild-type and *ahk2ahk3* plants and specific leaves of different age. On the other hand, it was evaluated which leaves of a single rosette are photoperiod stress responsive and if correlation between leaves and their age could be made. Further, the involvement of the leaf identity (juvenile vs. adult leaves) was investigated by characterizing mutants with either a prolonged or shortened juvenile vegetative growth phase for their response to photoperiod stress. Apart from the importance of leaf tissue in responding to photoperiod stress, the molecular response to alterations of the light-dark-cycle was investigated in wild-type and *ahk2ahk3* roots and compared to that of leaves.
The third question aimed to elaborate if other phytohormones apart from cytokinin and jasmonic acid are involved in the response to photoperiod stress. Here, the focus was on the phytohormones auxin, ethylene and GA. As a first step, auxin and GA levels were determined in the same setup as for cytokinin. To get insights into the regulation of these hormones in photoperiod stress resistant and sensitive plants, transcript levels of genes involved in hormone synthesis, metabolism and signaling were analyzed via RNA sequencing (RNAseq) and quantitative real time (qRT)-polymerase chain reaction (PCR) in wild type and *ahk2ahk3*. Mutants with a higher or lower hormone status were exposed to photoperiod stress and analyzed for their phenotypic and molecular response to decipher the importance of hormone homeostasis for photoperiod stress sensitivity. As the experiments pointed to a contribution of ethylene and auxin, first experiments studying the genetic interaction of auxin and cytokinin signaling have been conducted.

2 Materials and Methods

2.1 Databases and software

The databases and software programs used in this thesis are displayed in Table 1.

Table 1: Databases and software programs used in this thesis.

Name	Company, reference or internet link	Purpose of use
NCBI	The National Center for Biotechnology Information (http://www.ncbi.nlm.nih.gov/)	Literature (PubMed), BLAST and others
Excel	Microsoft Office	Calculations, statistical analysis and graph design
PowerPoint	Microsoft Office	Figure design
ImageJ	Abramoff *et al*., 2004	Image analysis
NEBcutter	New England BioLabs Inc. (http://tools.neb.com/NEBcutter2/)	Search for restriction sites
Bio-Rad CFX Manager	Bio-Rad®	Quantitative real time-PCR (qRT- PCR), primer quality assessment
NASC	The European Arabidopsis Stock Centre (http://arabidopsis.info/)	Ordering *Arabidopsis* seeds
ThaleMine (Araport)	Krishnakumar *et al*., 2017 (https://apps.araport.org/thalemine/begin.do)	*Arabidopsis* gene information search
SIGnAL T-DNA Express	Salk Institute Genomic Analysis Laboratory (http://signal.salk.edu/cgi-bin/tdnaexpress), Alonso *et al*., 2003	Search for *Arabidopsis* T-DNA insertion mutants
SIGnAL T-DNA Primer Design	Salk Institute Genomic Analysis Laboratory (http://signal.salk.edu/tdnaprimers.2.html)	Primer design for T-DNA insertion mutants
QuantPrime	Max-Planck Institute of Molecular Plant Physiology (http://quantprime.mpimp-golm.mpg.de/), Arvidsson *et al*., 2008	Primer design for qRT-PCR
Gen5™ Reader Control and Data Analysis Software	Biotek®, Winooski, Vermont, U.S.A.	controlling of Synergy™ 2 Multi-Detection Microplate Reader for ROS measurements
GenoCapture	Synoptics Ltd., Cambridge, UK	Agarose gel documentation

2.2 Kits

Kits used in this thesis are displayed in Table 2.

Table 2: Kits used in this thesis.

Name	Manufacturer and Cat. No.	Purpose of use
NucleoSpin® Gel and PCR Clean-up	Macherey-Nagel, Cat. No. 740609.250	DNA gel extraction/ PCR purification
NucleoSpin® RNA Plant	Macherey-Nagel, Cat. No. 740949.250	RNA purification for RNAseq
NucleoSpin® Plasmid EasyPure	Macherey-Nagel, Cat. No. 740727.250	Plasmid purification
Pierce™ Quantitative Peroxide Assay Kit	Thermo Scientific, Cat. No. 23280	Quantification of the H_2O_2 content in *Arabidopsis* leaves

2.3 Enzymes

Enzymes used in this thesis are displayed in Table 3.

Table 3: Enzymes used in this thesis.

Name	Manufacturer and Cat. No.	Purpose of use
Taq DNA Polymerase	AG Schuster Institute of Biology/Applied Genetics, FU Berlin	PCR analysis for genotyping
Phusion High-Fidelity DNA Polymerase	Fermentas/Thermo Scientific, Cat. No. F530S	Cloning-PCRs
RNAseOUT™ Recombinant Ribonuclease Inhibitor	Invitrogen/Life Technologies, Cat. No. 10777019	RNase-inhibitor during stem-loop-cDNA-synthesis
Gateway® BP Clonase® Enzyme Mix	Invitrogen/Life Technologies, Cat. No. 11789013	Cloning
Gateway® BP Clonase® II Enzyme Mix	Invitrogen/Life Technologies, Cat. No. 11789020	Cloning
Gateway® LR Clonase® Enzyme Mix Gateway®	Invitrogen/Life Technologies, Cat. No. 11791019	Cloning
Gateway® LR Clonase® II Enzyme Mix	Invitrogen/Life Technologies, Cat. No. 11791020	Cloning
SuperScript III Reverse Transcriptase	Invitrogen/Thermo Scientific, Cat. No. 18080-044	cDNA synthesis
DNaseI	Thermo Scientific, EN0521	DNase digestion during RNA purification
Immolase DNA Polymerase	Bioline, Cat. No. BIO-21047	qRT-PCR
Restriction enzymes	Fermentas/Thermo Scientific	Restriction digestion for genotyping (CAPS marker)

2.4 Generation of *SUCROSE-PROTON SYMPORTER2* (*SUC2)::CKX1-Myc* plants

2.4.1 Microorganisms and growth conditions

Escherichia coli and *Agrobacterium tumefaciens* stems used in this study are listed in Table 4. *E. coli* stem DH5α was used for plasmid/vector replication with exception for replication of Gateway® empty vectors that were replicated in DB3.1.

Table 4: Microorganisms used in this thesis.

Species	Stem	Genotype	Reference
E. coli	DH5α	F^- Φ80dlacZΔM15 Δ(lacZYA-argF)-U169 endA1 recA1 glnV44 thi-1 relA1 gyrA96 deoR nupG hsdR17 (r_K^- m_K^+) λ^-	Grant *et al*., 1990
	DB3.1	F^- gyrA462 endA1 glnV44 Δ(sr1-recA) mcrB mrr hsdS20(r_B^-, m_B^-) ara14 galK2 lacY1 proA2 rpsL20(Sm^r) xyl5 Δleu mtl1	Hanahan, 1983; Bernard and Couturier, 1992
A. tumefaciens	GV3101:pMP90	pMP90 (pTiC58ΔT-DNA); Rif^R, $Gent^R$	Koncz and Schell, 1986

Usually, *E. coli* were cultivated at 37 °C in either LB solid or liquid medium. After transformation of *E. coli* (section 2.4.2), SOC medium was used to let bacteria recover. For transformation of *A. thaliana* plants (section 2.4.8), *A. tumefaciens* stem GV3101::pMP90 was used. Generally, *A. tumefaciens* were cultivated at 28 °C on either LB solid medium or YEB liquid medium. Media used are listed in Table 5, Table 6 and Table 7.

Table 5: Composition of lysogeny broth (LB) medium (Bertani, 1951).

Components	Concentration
tryptone	1.0 % (w/v)
yeast extract	0.5 % (w/v)
NaCl	10 % (w/v)
agar (for solid medium)	1.5 % (w/v)
pH 7.0 adjusted with NaOH	
Kanamycin[1)] or Spectinomycin[1)]	50 µg/mL

1) Added after autoclaving at a temperature of ca. 60 °C

Table 6: Composition of super optimal broth with catabolite repression (SOC) medium (Hanahan, 1983).

Components	Concentration
tryptone	2.0 % (w/v)
yeast extract	0.5 % (w/v)
NaCl	10 mM
KCl	2.5 mM
pH 7.4 adjusted with NaOH	
$MgCl_2$ (after autoclaving)	10 mM
$MgSO_4$ (after autoclaving)	10 mM
glucose (after autoclaving)	20 mM

Table 7: Composition of yeast extract broth (YEB) medium (Vervliet* et al*., 1975).

Components	Concentration
meat extract	0.5 % (w/v)
yeast extract	0.1% (w/v)
peptone	0.5 % (w/v)
sucrose	0.5 % (w/v)
$MgSO_4$	2 mM
pH 7.2 adjusted with NaOH	

2.4.2 Transformation of microorganisms

In this study, chemo-competent *E.coli* cells were used for transformation. Aliquots were thawed for 20 minutes on ice. Thereafter, plasmid DNA was added to aliquots and mixed carefully. After a 20 minute incubation on ice, a heat shock of 45 sec at 42 °C was given by placing the aliquots in a water bath. 800 µL SOC medium (Table 6) was given to the cells directly after the heat shock, reaction tubes were carefully mixed and incubated for 60 minutes at 37 °C and 180 rpm for regeneration of cells and formation of resistance to antibiotics. Afterwards, cells were distributed on LB plates that contained plasmid-specific antibiotics (Table 5) and were incubated overnight at 37 °C.
For transformation of *A. tumefaciens*, an aliquot of electro-competent cells (kindly provided by Dr. Sören Werner) per transformation was thawed for 20 minutes on ice. Thereafter, plasmid DNA was added, carefully mixed and put into a cooled electroporation cuvette. After another 20 minutes on ice, cuvettes were dried from the outside and cells were electroporated with a MicroPulser™ (Bio-Rad, Munich, Germany) with 2,4 kV for 5 ms. 1 mL YEB-Medium (Table 7) was added directly, briefly mixed and put into a fresh 1.5 mL Eppendorf tube. Cells were incubated for 1 h at 28 °C and 180 rpm and placed on LB plates for selective growth for two days at 28 °C.

2.4.3 Vectors used and plasmids generated

Vectors used and plasmids generated in this work are listed with their respective resistances in Table 8.

Table 8: Vectors and plasmids used and generated in this thesis.

Name	Resistance in bacteria	Resistance in plants	Reference
pDONR™P4P1R	Kan[R1]	---	Invitrogen/Life Technologies (Carlsbad, CA)
pB7m34GW	Spec[R3], Cm[R2]	Basta[R]/PPT[R4]	Karimi *et al*., (2005)
pDONR™P2RP3-4xMyc	Kan[R1]	---	Dr. Sören Werner FU Berlin
pDONR™221-CKX1(w/o stopp)	Kan[R1]	---	Dr. Sören Werner FU Berlin
pDONR™P4P1R-pSUC2	Kan[R1]	---	This study
pB7m34GW-SUC2::CKX1-4xMyc	Spec[R3]	Basta[R]/PPT[R4]	This study

1) Kanamycin resistance
2) Chloramphenicol resistance
3) Spectinomycin resistance
4) Phosphinothricin resistance

2.4.4 Amplification of SUC2 promoter

For the amplification of the *SUC2* promoter (An *et al*., 2004; Endo *et al*., 2014) with Gateway attachment sites attB4 and attBR1, PCR reactions were conducted with Phusion High-Fidelity DNA Polymerase (Thermo Scientific). The reaction mixture used is depicted in Table 9.

Table 9: Reaction mixture for amplification of the* SUC2 *promoter.

Components	Volume [µL].	Final concentration
5 x *Phusion* buffer	4	1 x
5 mM dNTPs	0.8	200 µM
50 µM forward primer	0.25	625 nM
50 µM reverse primer	0.25	625 nM
Phusion High-Fidelity DNA Polymerase	0.5	---
water	ad 19	---
Template (undiluted DNA extract)	1	---

Primer pairs used can be found in sections 2.4.3. The respective product of ca. 3500 bp was amplified as follows: Initial denaturation step (95 °C, 5 min), 40 PCR cycles comprised of denaturation (95 °C, 15 sec), annealing (55 °C, 30 sec), and elongation (72 °C, 210 sec). The final elongation step (at 72 °C) was five minutes long.

2.4.5 Cloning of SUC2 *constructs*

After promoter amplification, the fragment was cloned into *pDONR^{TM}P4P1R* by BP reaction at 25 °C for 3 h (Table 10).

Table 10: BP reaction mixture used in this thesis for generation of pDONR^{TM}P4P1R-SUC2.

Component	Volume [µL].
5 x BP buffer	2
pDONR^{TM}P4P1R	1
attB4-pSUC2-attBR1	5
BP Clonase	2

Afterwards, the final *pB7m34GW-SUC2::CKX1-4xMyc* construct was created by Gateway LR reaction at 25 °C over night (Table 11). Calculation of amounts of vectors needed for the reaction was done as follows:

$$ng = fmol_{vector}\ x\ bp_{vector}\ x\ \left(\frac{660\ fg}{fmol}\right) x\ \left(\frac{1\ ng}{10^6 fg}\right)$$

Table 11: LR reaction mixture use for generation of pB7m34GW-SUC2::CKX1-4xMyc.

Component	Volume [µL].
pDONR^{TM}P2RP3-4xMyc	0.25
pDONR^{TM}221-CKX1(w/o Stopp)	0.75
pDONR^{TM}P4P1R-pSUC2	0.32
pB7m34GW	2.38
Clonase	2
1 x TE	ad 10

The final construct was used for transformation of *Arabidopsis* plants, respectively (section 2.4.8). Respective primer sequences for fragment amplification (section 2.4.4), colony PCR (section 2.4.6) and sequencing can be found in Table 12. Sequencing of constructs was performed by GATC Biotech (Konstanz, Germany).

Table 12: Primer sequences for construction of plasmids, colony PCR and sequencing.
Underlined sequences represent the attB-sequences, respectively.

Name	Primer sequences wild-type allele (5' → 3')	Annealing temperature used [°C]	Purpose
pSUC2-Fwd	GGGGACAACTTTGTATAGAAAAGTTGTC TTTGTCATACATTTATTTGCCACAAG	55	amplification of SUC2 promoter
pSUC2-Rev	GGGGACTGCTTTTTTGTACAAACTTGC ATTTGACAAACCAAGAAAGTAAGAAAAAA		
M13 fwd	CTGGCCGTCGTTTTAC	55	colony PCR and sequencing of pDONR^{TM}P4P1R-pSUC2
M13 rev	CAGGAAACAGCTATGAC		
CKX1-intern2rev	CCAGCATTAGATAGTGTACC	55	colony PCR pB7m34GW-SUC2::CKX1-4xMyc
pSUC2-Fwd2	GCAAAACACATGTTGCCGAGTC	---	sequencing of pDONR^{TM}P4P1R-pSUC2
pSUC2-Fwd3	CTAATTGGTTGTTCGTAAATGGTGC	---	
pSUC2-Fwd4	GCCTGAGGATACTATTATTCTCTGTC	55	colony PCR with CKX1-intern2rev, sequencing of pDONR^{TM}P4P1R-pSUC2

2.4.6 Colony PCR

Colony PCR was performed to test if *E. coli* and *A. tumefaciens* colonies carry the correct plasmids. Here, thermostable DNA polymerase from *Thermus aquaticus* (*Taq*, see Table 3) was used to amplify DNA. The 10x Taq PCR buffer consisted of 500 mM KCl, 100 mM Tris/HCl pH 9, and 1 % Triton X-100. A typical colony PCR reaction mixture is displayed in Table 13.

Table 13: PCR reaction mixture used for colony PCR.

Components	Volume [µL].	Final concentration
10 x *Taq* buffer incl. $MgCl_2$	2	1 x
5 mM dNTPs	0.8	200 µM
50 µM forward primer	0.25	625 nM
50 µM reverse primer	0.25	625 nM
Taq DNA Polymerase	0.5	---
water	ad 20	---
Template (undiluted colony)	toothpick tip	---

Primer pairs used can be found in section 2.4.5. The elongation time was changed to the product sizes, respectively. PCR setup was as follows: Initial denaturation step (95 °C, 5 min), 35 PCR cycles comprising denaturation (95 °C, 15 sec), annealing (55 °C, 40 sec), and elongation (72 °C, 1 kb/min). A final elongation step (at 72 °C) of five minutes.

2.4.7 Purification of PCR products

PCR products were either purified by direct PCR cleanup or by gel extraction using the NucleoSpin® Gel and PCR Clean-up kit by Macherey-Nagel (see Table 2) and plasmid DNA was purified with the NucleoSpin® Plasmid EasyPure kit following the manufacturer's protocols. DNA concentration determination was facilitated by photometrical measurement using the NanoDrop ND-1000 spectrophotometer with the 'DNA-50' program.

2.4.8 Transformation of **Arabidopsis thaliana** *plants*

Stable transformation of *Arabidopsis* plants was performed as described previously (Clough and Bent, 1998; Davis *et al*., 2009). Flowers of four- to five-week-old plants, cultivated under long-day conditions in the greenhouse, were dipped twice for ten seconds in a 500 mL YEB over-night liquid culture containing *Agrobacteria* that were successfully transformed with the binary *pB7m34GW-SUC2::CKX1-4xMyc* plasmid and 200 µl Silwet L-77 that was added immediately before the floral dip (Lehle Seeds, Round Rock, Texas, USA). Afterwards, dipped plants were stored humidly in the dark over night at room temperature and placed back in the greenhouse for seed production.

2.4.9 Selection and segregation analysis of **SUC2::CKX1-4xMyc** *transformants*

After transformation, primary selection of T_0 transformants was performed by spraying soil-grown plants, cultivated in the greenhouse under long day (LD) conditions (see also section 2.6), one and two weeks after germination with Basta® (Bayer, Leverkusen, Germany). T_1 and T_2 segregation analysis of ppt-resistant *SUC2::CKX1-4xMyc* lines was conducted on sterile ½ Murashige and Skoog (MS)-medium containing Petri dishes. Composition of respective MS-medium is displayed in Table 14.

Table 14: Composition of plant culture medium.

Components	Concentration
MS basal salt mixture, Duchefa	2.15 g/L
MES	0.5 g/L
Emprove® Essential, BP Agar extra pure, Merck	10 g/L
pH 5.7 adjusted with 1 N KOH	
ppt[1)]	10 µg/mL

1) Added after autoclaving at a temperature of ca. 60 °C

Sterilization of seeds was achieved under a sterile hood by soaking and shaking for one minute in absolute ethanol. After this, seeds were rinsed twice with 70 % ethanol. After being washed once with water, seeds were homogenously distributed in 0.1 % agarose solution. The seeds were then transferred onto the medium using sterile pipette tips. After the seeds were sown on the medium, the Petri dishes were sealed with Leukopor tape. Petri plates were grown in a culture room at 22 °C under long day conditions.

2.5 *Arabidopsis thaliana* plants

For experiments of this study, Columbia-0 (Col-0) was used as wild type. Table 15 lists all mutant and transgenic *Arabidopsis* plants that were used.

Table 15: Mutant and transgenic* Arabidopsis *plants.

Name[1)]	References	Source[2)]
Cytokinin-related		
abcg14-2 (SK15918, *abcg14*)	Ko *et al*., 2014; Zhang *et al*., 2014	PhD Youngsook Lee, Pohang University of Science and Technology (Pohang, Korea)
ahk2-5 (*ahk2*) *ahk3-7* (*ahk3*)	Riefler *et al*., 2006	Dr. Anne Cortleven, FU Berlin
ahp2-1 (*ahp2*) *ahp3* *ahp2 ahp5-2* (*ahp5*) *ahp3 ahp5* *ahp2 ahp3 ahp5*	Hutchison *et al*., 2006	N860151 Daniela Pezzetta, FU Berlin N860155 Daniela Pezzetta, FU Berlin
arr2-1 (*arr2*), GK269G01	Nitschke, 2014	Dr. Sören Werner, FU Berlin
arr10-5 (*arr10*) *arr12-1* (*arr12*) *arr10 arr12*	Mason *et al*., 2005; Ishida *et al*., 2008	Dr. Sören Werner, FU Berlin
arr2 arr10 *arr2 arr12* *arr2 arr10 arr12*	---	Dr. Sören Werner, FU Berlin
cyp735a1-2 (*cyp735a1*) *cyp735a2-2* (*cyp735a2*) (*cypDM*)	Kiba *et al*., 2013	Dr. Sören Werner, FU Berlin
log1-2 (*log1*) *log2-1* (*log2*) *log3-1* (*log3*) *log4-3* (*log4*) *log5-1* (*log5*) *log7-1* (*log7*) *log8-1* (*log8*) (*logS*)	Kuroha *et al*., 2009; Tokunaga *et al*., 2012	Prof. Hitoshi Sakakibara, RIKEN Center for Sustainable Resource Science (Yokohama, Japan)
35S::CKX1	Werner *et al*., 2003	Daniela Pezzetta, FU Berlin
ATML::CKX1-4xMyc	Werner, 2016	Dr. Sören Werner, FU Berlin

CLV1::CKX1	Otto, 2013	Daniela Pezzetta, FU Berlin
SUC2::CKX1-4xMyc[3)]	This study	---
WUS::CKX1	Otto, 2013	Daniela Pezzetta, FU Berlin
Auxin-related		
tir1-1 (*tir1*) *afb2-3* (*afb2*) *afb3-4* (*afb3*) *tir1 afb2* *tir1 afb2 afb3*	Dharmasiri *et al*., 2005a Parry *et al*., 2009	N3798 N69651 N69652 N69691 N69653
yuc1D	Zhao *et al*., 2001 Cheng *et al*., 2006	Prof. Christine Beveridge, The University of Queensland (St. Lucia, Australia)
ahk2 ahk3 tir1 afb2[3)]	This study	---
Ethylene-related		
ctr1-1 (*ctr1*)	Kieber *et al*., 1993	N8057; Dr. Anne Cortleven, FU Berlin
ctr/sis1-1	Gibson *et al*., 2001	N3874; Dr. Anne Cortleven, FU Berlin
etr1-1	Guzman and Ecker, 1990	N237, Dr. Silvia Nitschke (formerly FU Berlin)
etr1-6 (*etr1*) *etr2-3* (*etr2*) *ein4-4* (*ein4*) *etr2 ers2-3* (*ers2*) *ein4*	Hua and Meyerowitz, 1998	Prof. Eric Schaller, Dartmouth College (Hanover, USA)
ein2-1 (*ein2*)	Guzman and Ecker, 1990	N3071, Tanja Rublack (formerly FU Berlin)
ein3-1 (*ein3*)	Rothenberg and Ecker, 1993	N8052, Tanja Rublack (formerly FU Berlin)
GA-related		
gid1a-1 (*gid1a*) *gid1b-1* (*gid1b*) *gid1a gid1c-1* (*gid1c*) *gid1b gid1c*	Griffiths *et al*., 2006	Dr. Stephen Thomas, Rothamsted Research (Harpenden, United Kingdom)
ga20ox1 ga20ox2 *ga20ox1 ga20ox3* *ga20ox2 ga20ox3*	Plackett *et al*., 2012	Dr. Stephen Thomas, Rothamsted Research (Harpenden, United Kingdom)
gai	Matschi *et al*., 2015	Daniela Pezzetta, FU Berlin
rga28 (*rga1*)	Park *et al*., 2013	Daniela Pezzetta, FU Berlin
miRNA-related		
35S::MIR156B	---	Dr. Sören Werner, FU Berlin
35S::MIM172	Werner, 2016	Dr. Sören Werner, FU Berlin

1) Written in parentheses are the names used throughout this study
2) NASC ID if ordered from stock centre or seeds kindly provided by the indicated researcher
3) Generated in this study

2.6 Growth conditions for *Arabidopsis thaliana* plants

For photoperiod stress experiments *Arabidopsis* plants were grown under short day (SD) conditions (light/dark: 8 h/16 h) in a phytochamber at 22 °C and light intensities of 100-150 µmol $m^{-2}s^{-1}$. For these experiments seeds were sown on ‘sowing soil’ (2:2:1, Soil Type P:Soil Type T:Sand). In experiments that aimed to harvest root material, ‘sowing soil’ and sand were mixed in a ratio of 1:3. Seeds were stratified at 4 °C for two days before they were transferred to the phytochamber. For the first few days, seedlings were cultivated under a plastic hood to ensure sufficient humidity. After two weeks of growth, plants were separated and further cultivated on “sowing soil”.

For genotyping, propagation, crossing and segregation analyses, plants were cultivated under long day (LD) conditions (light/dark: 16 h/8 h) in the greenhouse. Plants in the greenhouse were cultivated under temperature cycles (light/dark: 22/18 °C) and were sown on “sowing soil” and cultivated under a plastic hood. After separation, seedlings were transferred to soil containing Perligran G instead of sand.

2.7 Genetic crosses

Genetic crosses were performed on two consecutive days. On the first day, female organs of two or three flower buds that were still closed were prepared. After removing all other siliques, leaves, younger flower buds and open flowers near the chosen flower buds using precision tweezers, gynoecia were prepared by removing sepals, petals, and all six stamens on the selected flower buds, respectively. Afterwards, it was checked that gynoecia were intact. Inspected plants were grown in the green house for one more day. Thereafter, development of ‘stigma hairs’ was checked as an indicator that gynoecia were not pollinated before and pollination was conducted by removing a complete open flower of the male parent and brushing its anthers over the stigma of the gynoecium. Pollination was visually inspected under the binocular microscope. Elongation of siliques was observed after two to three days if plants were successfully crossed. Seeds of respective siliques were collected in paper bags and sown out for propagation after ripening. Segregation analyses and genotyping were conducted in the F2 and F3 generation, respectively.

2.8 Nucleic acid methods

2.8.1 Quantification of transcript abundance via quantitative RT-PCR

2.8.1.1 Isolation and purification of total RNA

For RNA isolation, frozen samples (100 mg fresh weight) were ground using a Retsch mill in pre-cooled adapters. Afterwards, samples were dissolved in 750 µL extraction buffer (0.6 M NaCl, 10 mM EDTA, 4 % (w/v) SDS, 100 mM Tris/HCl pH 8) and 750 µL phenol chloroform isoamyl alcohol (PCI; 25:24:1) solution was added. Samples were vortexed, shaken for 20 minutes at room temperature and centrifuged at 19.000 x *g* for five minutes at 4 °C. The supernatants were transferred into fresh 1.5 mL Eppendorf tubes and chloroform isoamyl alcohol (CI, 24:1) solution was added in a 1:1 ratio. Samples were vortexed briefly and centrifuged at 19.000 x *g* for five minutes at 4 °C. Supernatants were transferred into fresh tubes and RNA was precipitated for 2 h on ice by adding 0.75 volumes of 8 M LiCl. After centrifugation at 19.000 *g* for 15 minutes at 4 °C, supernatants were removed and resolved in 300 µL RNase-free water. RNA was precipitated again by the addition of 30 µL 3 M sodium acetate and 750 µL absolute ethanol and incubation at -70 °C for 30 minutes. Samples were centrifuged at 19.000 *g* for ten minutes at 4 °C and the supernatant was discarded. Pellets were washed either with 200 µL 70 % ethanol (v/v) or - to avoid loss of miRNAs - with 80 % ethanol (v/v) and after centrifugation, pellets were dried at room temperature and resolved in 40 µL RNase-free water.

2.8.1.2 cDNA synthesis from total RNA

Following isolation, 16 µL of RNA were firstly incubated with DNaseI (Thermo Scientific) for 30 minutes at 37 °C and inactivated in the presence of 2.5 mM EDTA for ten minutes at 65 °C. After total RNA measurement at the Nanodrop®, 150 - 500 ng of total RNA (same amount in each distinct experiment, respectively) were used per sample, put into a new test tube and filled to a volume of 10 µL with RNase-free water. Thereafter, two reaction mixtures were prepared that are displayed in Table 16.

Table 16: Reaction mixtures for cDNA synthesis from total RNA.

Mix 1		**Mix 2**	
Components (stock conc.)	**Volume [µL]**	**Components (stock conc.)**	**Volume [µL]**
Oligo-dT-Primer T_{25} (50 µM)	1	First Strand Buffer (5x)	4
Random-Primer N_9 (50 µM)	1.8	DTT (100 mM)	1
5 mM dNTPs	2	SuperScript® III Reverse Transcriptase (200 U/µL)	0.5

For cDNA synthesis, 4,8 µL of Mix 1 were added and incubated for five minutes at 65 °C. After cooling down on ice, 5,5 µL of the Mix 2 were added and cDNA was ultimately synthesized by incubation for five minutes at 25 °C, following 60 minutes at 50 °C and 15 minutes at 70 °C. After its synthesis, cDNA was diluted to a concentration of 50 ng/µL using 1 x TE buffer and stored in either the fridge or freezer until usage.

2.8.1.3 cDNA synthesis from miRNAs

For cDNA synthesis of miRNAs (Chen *et al*., 2005; Pant *et al*., 2008), 500 ng of DNaseI-digested total RNA was used for Mix 1 Table 17.

Table 17: Reaction mixtures for cDNA synthesis from miRNAs.

Mix 1		**Mix 2**	
Components (stock conc.)	**Volume [µL]**	**Components (stock conc.)**	**Volume [µL]**
total RNA	x (500 ng)	First Strand Buffer (5x)	2.5
miRNA-specific StLp-Primer (50 µM)	0.125	DTT (100 mM)	0.5
TAFII15-qRT_rev (50 µM)	0.125	SuperScript® III Reverse Transcriptase (200 U/µL)	0.5
5 mM dNTPs	1	RNaseOUT (40 U/µl)	0.3
dd H_2O (RNase-free)	ad 8.7		

Mix 1 was incubated for five minutes at 65 °C and put on ice afterwards. Following the addition of 3.8 µL Mix 2 to Mix 1, samples were incubated for 30 minutes at 16 °C, 30 minutes at 50 °C and for 15 minutes at 70 °C. cDNA synthesized was stored in either fridge or freezer until usage (undiluted). Primer for synthesis of cDNA from miRNAs and their sequences are displayed in Table 18.

Table 18: Primer used for cDNA synthesis from miRNAs.

Primer	Sequence	Source
miR156-StLp	GTCGTATCCAGTGCAGGGTCCGAGGTATTCGCACTGGATACGACGTGCT[1)]	Werner, 2016
miR172abe-StLp	GTCGTATCCAGTGCAGGGTCCGAGGTATTCGCACTGGATACGACATGCA[1)]	Werner, 2016
TAFII15-qRT_rev	ACTCTTAGCCAAGTAGTGCTCC	Werner, 2016

1) underlined sequences are miRNA-specific

2.8.1.4 Primer design for qRT-PCR analysis and primer sequences

Apart from already established primer pairs, all new primer pairs were designed using the QuantPrime software (see Table 1) under the following conditions:
Design mode: Primer pair (SYBR Green or EtBr detection); Limit 3' G/C content within the 5 last bases of each primer, allow max 3 G/C bases; Specificity prefiltering BLAST E-value: 1; Specificity prefiltering splice variant options: Primer pairs perfectly matching splice variants will neither be filtered out nor required; Prefer 3' tail of transcript for amplicons (recommended when using oligo-dT for cDNA synthesis), Use the last 1000 bp of transcript 3' tail as preferred range; Hybridization probe options: Don't allow a G at the 5' end, use the strand with most C's. Force strand for hybridization probe: No Taqman; Primer3 parameters: PRIMER_MAX_POLY_X = 3, PRIMER_GC_CLAMP = 1, PRIMER_TM_SANTALUCIA = 1, PRIMER_SALT_CORRECTIONS = 1, PRIMER_DNTP_CONC = 0.4, PRIMER_DIVALENT_CONC = 1.5, PRIMER_DNA_CONC = 50.0, PRIMER_SALT_CONC = 50.0, PRIMER_MIN_SIZE = 20, PRIMER_OPT_SIZE = 22, PRIMER_MAX_SIZE = 24, PRIMER_PRODUCT_SIZE_RANGE = 150-250 250-350, PRIMER_PRODUCT_MIN_TM = 75.0, #PRIMER_PRODUCT_OPT_TM = 80.0, PRIMER_PRODUCT_MAX_TM = 95.0, PRIMER_MIN_GC = 45.0, PRIMER_OPT_GC_PERCENT = 50.0, PRIMER_MAX_GC = 55.0, PRIMER_MIN_TM = 59.0, PRIMER_OPT_TM = 60.0, PRIMER_MAX_TM = 61.0, PRIMER_MAX_DIFF_TM = 2.0; Specificity test parameter set: BLAST expectation: 200, require a possible amplicon, up to a maximum size of 1500 bp. Suitable primer pairs were ordered from ThermoFisher Scientific. In Table 19 all qRT-PCR primers (for genes of interest (GOI) and reference genes) used in this work are listed.

Table 19: Primer sequences for qRT-PCR.

Gene	AGI number	Forward Primer	Reverse Primer	Source
Genes of Interest (GOI)				
ABCG14	AT1G31770	TTCTGGAGGAAGAACAGTCGTC	CTGAGTATCAGGTGGGATTCCG	---
ARR5	AT3G48100	CTACTCGCAGCTAAAACGC	GCCGAAAGAATCAGGACA	Louisa Brock
ARR6	AT5G62920	GAGCTCTCCGATGCAAAT	GAAAAAGGCCATAGGGGT	Louisa Brock
BAP1	AT3G61190	CCAGAGATTACGGCGCGTGTT	TACAGACCCCAAACCGGAACTCC	Nitschke, 2014
CAB2	AT1G29920	AGAGGCCGAGGACTTGCTTTAC	GCCAATCTTCCGTTCTTGAGC	Nitschke, 2014
CTR1	AT5G03730	CGTTTCTTTCCTCGAAGTCAGC	AACCGCAGCTACAACCTGAG	---

CYP735A1	AT5G38450	CAACGGTGTTAGTGGAAGATCG	CATATGCCTTGCGTATCCCTTG	---
CYP735A2	AT1G67110	GTCTCTTGGTCCAAACAATATGGG	AGAAGCCCACGCCCTATAAAC	---
ETR1	AT1G66340	CCGATCAATTCTTCCCAAGTGTG	GCACCAAACTGAACAAGTACCC	---
GAI	AT1G14920	GATCGGTTTACTGAGTCGTTGC	AACGTTTCATGACGCTCAACTC	---
GID1A	AT3G05120	AGCAGAACAGTGGTTCCTCTC	CCTGCGATCAATCAAGACATCG	---
LOG8	AT5G11950	GAACTCGGCAATGAACTCGTG	TCATGCATGTCTGCAACAACTC	---
MIRNA156	---	CAGTGCAGGGTCCGAGGT[1)]	CCGTGGTGACAGAAGAGAGTGA[2)]	Werner, 2016
MIRNA172	---	CAGTGCAGGGTCCGAGGT[1)]	GTCCGTGGAGAATCTTGATGATG[2)]	Werner, 2016
TAA1	AT1G70560	TGTCTAAGGAGTCACAGGTTCG	CAAACGCAGGGTAAGATTCGAG	---
TIR1	AT3G62980	ACTTGCAGGAATCTGAAAGAGC	GAGATTGGGACACCTAGTCACC	---
ZAT12	AT5G59820	CGCTTTGTCGTCTGGATTG	AGCAGCCCCACTCTCGTT	Nitschke, 2014
Reference genes				
MCP2D	AT1G79340	AACCCGCTATGCAGACACACG	CAGTTGGTTTCCCCGCTGGA	Nitschke, 2014
PP2AA2	AT3G25800	CCATTAGATCTTGTCTCTCTGCT	GACAAAACCCGTACCGAG	Nitschke, 2014
TAFII15	AT4G31720	GAATCACGGCCAACAATC	ACTCTTAGCCAAGTAGTGCTCC	Werner, 2016
UBC10	AT5G53300	CCATGGGCTAAATGGAAA	TTCATTTGGTCCTGTCTTCAG	Nitschke, 2014

1) StLp-qRT_for: stem loop specific
2) underlined sequences represent binding sequences to respective miRNA

2.8.1.5 Quantitative reverse transcription PCR (qRT-PCR)

qRT-PCR was performed with the CFX96™ Real-Time Touch System (Bio-Rad®) using SYBR Green I as DNA-binding dye. The reaction mix is listed in Table 20.

Table 20: Reaction mix for qRT-PCR.

Components	Volume [µL].	Final concentration
10 x Immolase buffer	2	1 x
50 µM $MgCl_2$	0.8	2 mM
5 mM dNTPs	0.4	100 µM
10 x SYBR Green I	0.2	0.1 x
50 µM forward primer	0.12	300 nM
50 µM reverse primer	0.12	300 nM
Immolase (5 U/µL)	0.04	0.01 U/µL
water	ad 18 µL	---
Template (50 ng/µL)	2	5 ng/µL

All components except for the template DNA were mixed together and 18 µL of that master-mix were added to each well of a 96-well-plate. Afterwards, template DNA or water was added.

The following PCR setup was used: heat activation of the Immolase for 15 minutes at 95 °C, 40 cycles of five seconds at 95 °C (denaturation), 15 seconds at 55 °C (annealing), and ten seconds at 72 °C (elongation). After PCR, the Bio-Rad CFX Manager generated a dissociation curve which was checked to ensure specificity of the amplification.

Primer efficiencies for newly designed primers were tested by mixing all cDNAs (50 ng/µL) from one experimental setup and making a 1:10 dilution series consisting of five dilutions. After respective PCR, efficiencies (E in %) were calculated by Bio-Rad CFX Manager. Only primers with an efficiency between 90 % and 110 % were used for further studies. Expression of GOI was normalized against reference genes according to Vandesompele *et al*., 2002 using Microsoft Excel by calculation of a normalization factor (NF) for each sample. It represented the geometric mean of the $2^{-\Delta Ct}$ values of all reference genes tested. The relative expression of the GOI tested was finally determined as $2^{-\Delta Ct}$ (GOI)/NF. In general, these relative expression values were normalized to wild-type control which was set to 1. Data in which the relative expression was normalized to other controls/samples are described in the figure description, respectively.

2.8.2 Genotyping of Arabidopsis *plants*

2.8.2.1 Genotyping strategies

Plants were genotyped after ordering seeds from NASC or in all generations following genetic crosses (also parental plants). Mutants with clear phenotypical characteristics in the homozygous state were selected by phenotype, respectively. Such mutants were *ctr1* and *ctr/sis1-1* (dwarfed shoot, dark green leaves, late flowering), *etr1etr2ein4* and *etr2ers2ein4* (different degree of dwarfed shoot and dark green leaves), *ga20ox1ga20ox2*, *ga20ox1ga20ox3* and *ga20ox2ga20ox3* (reduced germination rates that can be rescued by addition of active GAs, different degrees of reduced shoot size with different degrees of small, dark green roundish leaves) and *yuc1D* (long petioles, reduced plastochron, curled down leaves). T-DNA insertions mutants were genotyped via PCR using two primer pairs, one flanking the insertion to amplify the wild-type allele if no insertion was existent and another pair with a gene-specific and an insertion (T-DNA)- specific primer to amplify the mutant allele. In Table 21 all insertion-specific primers that were used are listed and Table 22 contains all gene-specific primer pairs with further information about primer combinations that detect the mutant alleles, respectively.

Table 21: Insertion-specific primers used for genotyping.

Name	Primer	Purpose of use
SAIL-IT1_F (SAIL)	GCCTTTTCAGAAATGGATAAATAGCCTTGCTTCC	Genotyping of SAIL lines
GABI-Kat (GABI)	CCCATTTGGACGTGTAGACAC	Genotyping of GABI-Kat lines
LBaI (SALK1)	TGGTTCACGTAGTGGGCCATCG	Genotyping of SALK lines
LBbI (SALK2)	GCGTGGACCGCTTGCTGCAACT	Genotyping of SALK lines
SLAT-3’	CTTATTTCAGTAAGAGTGTGGGGTTTTGG	*gid1b-1* genotyping
JMLB1	GGCAATCAGCTGTTGCCCGTCTCACTGGTG	*ahp* mutant genotyping
pSKTAIL-L1 (TAIL)	TTCTCATCTAAGCCCCCATTTGG	*abcg14-2* genotyping

Table 22: Gene-specific primers used for genotyping.

Mutant	Primer sequences[1)] wild-type allele (5' → 3')	Product size [bp]	Primer combination mutant allele	Annealing temperature used [°C]
abcg14	F-ATGCCTCAGAACTGCATAGC R-TTACCGCAACTTCACCCGAT	2100	F + TAIL (~650 bp)	60
afb2	F-TCAACGGTCAAGATCCATCTC R-CTGCAATTAGCGGCAATAGAG	1100	R + SALK1 (~900 bp)	59
afb3	F-TCATGTTGCTTACAAATTGCG R-TCTGCAAACAGATGACAAACG	1100	R + SALK1 (~800 bp)	59
ahk2	F-GCAAGAGGCTTTAGCTCCAA R-TTGCCCGTAAGATGTTTTCA	672	F + SAIL (650 bp)	59
ahk3	F-CCTTGTTGCCTCTCGAACTC R-CGCAAGCTATGGAGAAGAGG	558	R + GABI (450 bp)	59
ahp2	F-TCATGAGGTCAAGTTGATGAGAG TATATG R-TTTGTATTTGACAGTGAGACTG CGTTGAC	1308	F + JMLB1 (~850 bp)	57
ahp3	F-TCATGAGGTCAAGTTGATGAGAG TATATG R-TTTGTATTTGACAGTGAGACTGC GTTGAC	2320	F + JMLB1 (~1100 bp)	57
ahp5	F-ATTTTTCCTGTTTTGTAACTGTGG ACGAT R-TCCTTTCTCAATCTATTGTCACA ATCATG	2156	R + JMLB1 (~750 bp)	57
cyp735a1	F-CTTGCGGTTACGTCGGCTC R-ATCCTCATGAAACCAATGGCTTC	1357	R + SALK2 (~500 bp)	55
cyp735a2	F-CCAAGATGGTGTCCCTTCCG R-CTTGGTAAAAGTGTGGCAGGAG	1518	R + SALK2 (~700 bp)	55
gid1a	F-GAATTATCGGCGTGCACCA R-TGATTGTTATTAGGCAAGAGGTAAA ACC	552	R + SALK1 (684 bp)	55
gid1b	F-TCTCCTGTCCACCAAACATTG R-CTGGGTTTTGGAGACTATGGC	897	R + SLAT3' (354 bp)	55
gid1c	F-ATGGCTGGAAGTGAAGAAGTTAA TCT R-CAGGGCGACGCAGGAG	570	R + SALK1 (559 bp)	55
log1	F-ATGGAGATAGAATCAAAGTTCAAGA R-CCAATGCTCCCTCCACCATAGACAA	1173	F + SALK1 (~1500 bp)	55
log2	F-GTGGCATGGGTTGAAGTCTATATTC R-TGGAAGTCTCAATGCTTGGAAAATG	935	F + SALK1 (~800 bp)	55
log3	F-CATTCCCAAGACCCTCATGCCTAGA R-CTAATTTTAAGTGCCAGATGTTGAT	1037	F + SALK1 (~700 bp)	55
log4	F-GGTTTGCTTTGTAATGATTTCTGGG R-TCAGTCTTCAGAAGAGTAGTCAATC	923	R + SALK1 (~700 bp)	55
log5	F-ATGGAAATAGTGAAGTCGAGGTTCA R-CTAAAGGGCAATCTCAGTCTGCATG	1367	F + GABI (~1000 bp)	55
log7	F-GTCATTACATGGGCTCAACTCGGTA R-TCACAATCAGGGGTTATGTAGTCGT	449	R + SALK1 (~800 bp)	55
log8	F-CACTTTACTTTGTTTGCCCCCCTTT R-AGAAACAATCCCAAACTAATCAAC	1346	F + SALK1 (~900 bp)	55
tir1	F-GACGGATGGGGAGGTTACGTG R-CTGCAGTGTACCCACCAGTGC	~1200 bp	*Bsa*I digest: wild type 1000 + 200 bp, mutant resistant → 1200 bp	55

1) F: forward primer; R: reverse primer

The *tir1* mutants carries a point mutation (derived from EMS mutagenesis) and was genotyped using cleaved amplified polymorphic sequences (CAPS) markers. The point mutation resulted in a loss of a *Bsa*I in the fragment amplified via PCR. Table 23 displays the primers used as well as further information about the *tir1* mutation, respectively.

Table 23: Genotyping of* tir1 *with CAPS markers.

Mutant	Primer sequences[1)] wild-type allele (5' → 3')	Annealing temperature used [°C]	Restriction enzyme	Wild-type allele/ mutant allele [bp]	Mutation
tir1	F-GACGGATGGGGAGGTTACGTG R-CTGCAGTGTACCCACCAGTGC	55	*Bsa*I	1000 + 200/ 1200	Gly147Asp (GGT→GAT)

2.8.2.2 Extraction of genomic DNA from *Arabidopsis*

For isolation of genomic DNA, a small piece of leaf tissue was placed in a tube of an 8x stripe filled with 400 µL extraction buffer and ground for two minutes from each side using a Retsch mill. Afterwards, samples were centrifuged at maximum speed for 15 minutes. 300 µL of each supernatant were transferred into fresh 8x stripes filled with 300 µL 2-propanol per tube. After inverting tubes briefly, samples were centrifuged at maximum speed for 1 hour at 4 °C. Supernatants were discarded and pellets were washed with 300 µL 70 % ethanol. After centrifugation at maximum speed for 15 minutes at 4 °C, pellets were dried at 60 °C and resolved in 100 µL Tris-EDTA (TE) buffer.

2.8.2.3 PCR analysis

PCR analysis was performed in order to genotype *Arabidopsis* plants using genomic DNA extracts (see section 2.8.2.2). For that purpose, *Taq* Polymerase (see 2.4.6) was used to amplify DNA. A typical PCR reaction mixture (20 µL) for *Arabidopsis* genotyping is depicted in Table 24.

Table 24: PCR reaction mixture used for genotyping of* Arabidopsis *plants.

Components	Volume [µL].	Final concentration
10 x *Taq* buffer incl. $MgCl_2$	2	1 x
5 mM dNTPs	0.8	200 µM
50 µM forward primer	0.25	625 nM
50 µM reverse primer	0.25	625 nM
Taq DNA Polymerase	0.5	---
water	ad 19 µL	---
Template (undiluted DNA extract)	1	---

Primer pairs used can be found in sections 2.8.2.1. The respective product size changed between different approaches (Tables 11 and 12, section 2.8.2.1). After the initial denaturation step (95 °C, 5 min) between 30 and 35 PCR cycles followed consisting of denaturation (95 °C, 15 sec), annealing (55-65 °C, 30 sec), and elongation (72 °C, 1 kb/min). The final elongation step (at 72 °C) was five minutes long.

2.8.2.4 Restriction digestion

Restriction enzymes for genotyping using CAPS markers (section 2.8.2.1) and cloning of *SUC2* constructs (section 2.4.5) were purchased from Fermentas/Thermo Scientific or New England BioLabs. For CAPS marker analysis, restriction enzymes were directly added to PCR reaction mixture after PCR. For cloning of *SUC2* constructs, supplied reaction buffers were used. A typical reaction mixture consisted of ca. 1 µg DNA, 5-10 U of the restriction enzyme, 1x of the recommended reaction buffer and water to a final volume of 40 µL or for CAPS genotyping, 5-10 U of the restriction enzyme was added directly to each PCR reaction mixture after PCR (section 2.8.2.3). The reaction mixtures were incubated at 37 °C in either a PCR machine or an incubator for at least one hour. For enzyme inactivation, samples were heated (> 70 °C) for five minutes.

2.8.2.5 Agarose gel electrophoresis

Following PCR or restriction digestion, DNA fragments were separated by size via agarose gel electrophoresis. Samples were prepared for electrophoresis by addition of 6x loading dye (30 % glycerol, 0.25 % bromophenol blue, 0.25 % xylene cyanol FF) so that the final loading dye concentration was 1x. In most experiments, gels consisted of 1 to 1.5 % (w/v) agarose and ethidium bromide (0.75 µL/mL gel) solved in 1x TAE (40 mM Tris, 20 mM acetic acid and1 mM EDTA, pH 8). To determine DNA size, the 100 bp DNA ladder Hyperladder I (Thermo Scientific) was used in most experiments. DNA was stained with ethidium bromide and visualized with an ultraviolet (UV) transilluminator (Genoplex, VWR International GmbH, Darmstadt, Germany) using the GenoCapture sofware.

2.9 Determination of cytokinin, auxin and GA levels

For hormone measurements, 100 mg fresh weight of leaf tissue per sample and hormone was collected and shock-frozen in liquid nitrogen under white light (time points during light exposure) or green safety light (time points during night). Samples were sent to Prof. Ondrej Novak (Palacký University & Institute of Experimental Botany AS CR, Olomouc, Czech Republic). Analysis of hormones was carried out using ultra-performance liquid chromatography-electrospray tandem mass spectrometry as described (Novák *et al*., 2008; Pěnčík *et al*., 2009; Urbanová *et al*., 2013) with 15 mg/techn. or biol. replicate/hormone. All samples were measured in quintuplicate for each genotype and each timepoint.

2.10 Photoperiod stress treatment and evaluation of physiological and molecular parameters

2.10.1 Quantification of lesions

Lesions were quantified three to four hours after the night following PLP treatment. First, the total number of fully expanded leaves (except for leaf 1 and 2 as well as cotyledons) of a plant was counted.

Afterwards, the total number of lesioned leaves was determined (0 = not lesioned, 0.5 = less than 50 % lesioned, 1 = more than 50 % lesioned) and the percentage was calculated by dividing the number of lesioned leaves by the total number of fully expanded leaves (for each plant, respectively).

2.10.2 Chlorophyll Fluorometry (Fv/Fm ratio)

As a measure of stress and progress of cell death, the photosystem II maximum quantum efficiency (F_v/F_m ratio, Baker, 2008) was determined six to seven hours after the night following the prolonged light period. First, healthy and lesioned leaves of several plants (3 leaves per plant) were detached in a ratio reflecting the determined lesion percentage of the respective genotype in the same experiment. Detached leaves were placed in Petri dishes filled with water with the abaxial part of the leaf directly facing the water.

After 20 minutes of incubation in darkness, pulse-amplitude-modulated (PAM) measurements were performed with the chlorophyll fluorometer FluorCam (Photon Systems Instruments). First, the minimum fluorescence emission signal F_0 was recorded. Afterwards, the maximum fluorescence yield F_m (induced by a saturating light pulse of 1500 µmol m^{-2} s^{-1}) was recorded. The variable fluorescence F_v is defined as the difference F_m - F_0. As a result, the full equation is defined as $F_v/F_m = (F_m - F_0)/F_m$.

2.10.3 Determination of hydrogen peroxide (H_2O_2) content

For H_2O_2 measurements, ca. 100 mg of leaf material was harvested per sample, put into a 2 mL Eppendorf tube and shock-frozen in liquid nitrogen under green safety light. After samples were ground in pre-cooled adapters in a Retsch mill, 700 µL of 0.1 % (v/v) trichloroacetic acid (TCA) were added, samples were vortexed and put on ice. Samples were consecutively vortexed every five minutes for 15 minutes and centrifuged at 16000 g at 4 °C for 15 minutes. 300 µL per supernatant were transferred to a fresh 1.5 mL Eppendorf tube. 20 µL of each supernatant were used and mixed with 200 µL of a freshly prepared working solution in a well of a 96 well plate (ratio 1:100, colorless solution one: yellow solution two; Pierce™ Quantitative Peroxide Assay Kit). For H_2O_2 quantification, a 1000 µM H_2O_2 stock solution was prepared and a dilution series was made (100 µM, 80 µM, 60 µM, 40 µM, 20 µM and 0 µM H_2O_2, respectively). 20 µL of each dilution were used in the same manner as for the other samples. In addition, 20 µL of 0.1 % (v/v) TCA were used as a blank. After ten minutes of incubation, absorption was measured with a Synergy™ 2 Multi-Detection Microplate Reader (Biotek®, Winooski, Vermont, USA) at a wavelength of 595 nm using the Gen5™ Reader Control and Data Analysis Software. As a plate control, absorption of a second plate was measured with the same wells filled with samples/controls/blank but with 200 µL of water instead of working solution. H_2O_2 quantities were determined by subtracting either the TCA blank or the lowest value measured from all other values and calculating the linear function y = mx + b (m = slope, b = 0) of the dilution series first. Afterwards, the final quantity was calculated using the equation: $H_2O_2\ content_{nm/g\ FW} = absorption_{595nm}$ * mL TCA solution added / weight [g] * m.

2.10.4 Sampling for expression analysis of stress marker genes

For expression analysis, ca. 100 mg of leaf material were harvested into 2 mL Eppendorf tubes and shock-frosted in liquid nitrogen under white light (0 h time points) or green safety light (7.5, 15 h time points). Root samples were harvested by washing out soil and sand with water under the same light conditions as described before. Roots were then dried briefly using paper towels, weighed (50 to 100 mg) and shock-frozen in liquid nitrogen. Methods for determination of marker gene expression are described in section 2.8.1.

2.10.5 RNA sequencing (RNAseq) analysis

For RNAseq analysis, ca. 100 mg of leaf material was harvested into 2 mL Eppendorf tubes and shock-frozen in liquid nitrogen under white light (0 h time points) or green safety light (4 h, 6 h, 8 h and 12 h time points). After RNA isolation (NucleoSpin® RNA Plant Kit, section 2.2), samples were sent to the Beijing Genomics Institute (BGI) Co., Ltd. (Hongkong, China) for quality and integrity control, library construction and sequencing. Concentration and integrity of RNA and the extent of rRNA contamination were determined by the Nanodrop NA-1000 and the Bioanalyzer Agilent 2100 (Agilent Technologies, Santa Clara, CA, USA). RNA was treated with DNaseI and an enrichment and fragmentation of mRNA was achieved by using oligo-dT magnetic beads. Hereafter, random hexamer primers were used for first-strand cDNA synthesis and after that, second strand synthesis was performed. Following purification, end repair, and 3' end single-nucleotide A addition, sequence adaptors were ligated. Prior to the sequencing of the library products with the BGISEQ-500 platform (Zhu *et al*., 2018), quality control was conducted with the Agilent 2100 Bioanalyzer and PCR amplification was performed using the ABI StepOnePlus Real-Time PCR System (Thermo Fischer Scientific, Waltham, MA, USA). Bioinformatics analysis of RNAseq data including mapping against the *Arabidopsis* genome (TAIR10) and statistical analysis with DESeq2 (pairwise comparisons: Bonferroni correction) was performed by Dr. Anne Cortleven using R®.

2.11 Statistical analysis

For statistical analysis of most data, SAS®Studio (https://odamid.oda.sas.com/SASStudio) was used. One- and two-way ANOVA were performed after testing the homogeny (Shapiro-Wilk test; $p \geq 0.95$) of samples. In sets with an equal variance (Levenes test; $p \geq 0.01$) Tukey post-hoc-test was performed. If assumptions were not applicable, transformations were performed. A Wilcoxon test was performed in the case that assumptions were still not met after transformation.
For cytokinin auxin and GA measurements, the significance of differences between control and PLP-treated samples was calculated with a paired Student’s t-test in Microsoft Excel®.

3 Results

3.1 *t*Z-type cytokinins are essential to cope with photoperiod stress and require AHPs and ARRs to transduce their signal

3.1.1 Photoperiod stress increases the cytokinin content in wild-type plants

Plants impaired in cytokinin biosynthesis and signaling are sensitive to alterations of the light-dark cycle (Nitschke *et al*., 2016). To investigate whether photoperiod stress directly influences the hormone level, cytokinin concentrations were measured in leaves of short-day grown wild-type plants exposed to a 32 h light period, which is the standard stress treatment (in cooperation with Assoc. Prof. Ondrej Novak, Palacký University, Olomouc) (Figure 12A).

Plants experiencing photoperiod stress had an elevated total cytokinin content at the end of the PLP treatment and in the middle of the following night (Figure 12B; time points 2 and 3). Furthermore, content of CK free bases was elevated up to three-fold in PL plants compared to control plants at the end of PLP and in the middle and at the end of the following night (Figure 12C; time points 2, 3 and 4). A similar pattern could be observed for the content of CK ribosides. Here, an increase in PL plants compared to control plants was measured already during PLP and at the end of the night following PLP treatment, 0.25 pmol CK ribosides/g FW were measured in PL plants, which reflected a three-fold increase compared to control plants (Figure 12D, time points 1 and 4). Moreover, cytokinin nucleotides were increased two-fold in PL plants compared to control after 16 h of additional light (Figure 12E; time point 1). Nucleotide content stayed elevated in PL plants in comparison to control plants until the end of the night following PLP (time points 2 and 3). While concentrations of total cytokinin *N*-glucosides did not differ between control and PL, O-glucoside content was elevated 20 - 30 % in PL samples compared to control in the middle and the end of the night following PLP (Figure 12F, G).

The increase in free bases, nucleosides, nucleotides and O-glucosides was reflected by the concentrations of iP- and *t*Z-type cytokinin metabolites respectively. With 0.234 pmol/g FW, iP content was elevated the most (three-fold) in PL compared to control at the end of the night following treatment (Table 25; time point 4). In response to exposure to PLP, iPR content was increased directly after treatment and further increased until the end of the following night (Table 25; time points 2 to 4). The biggest difference in cytokinin content between stressed and control plants was detected for iPRMP, as its content was elevated more than four-fold already during PLP-treatment (Table 25; time point 1). Similar to the regulation of iP-type cytokinin content, an increased *t*Z, *t*ZR and *t*ZRMP content could be detected at several time points throughout photoperiod stress treatment (Table 26). Strikingly, *t*ZRMP content was decreased by 25 % in PL plants compared to control plants the day after experiencing photoperiod stress (Table 26; time point 5). During the night after the PLP, the content of *t*Z-type O-glucosides was elevated as much as 40 % in PL plants (Table 26; time points 3 and 4).

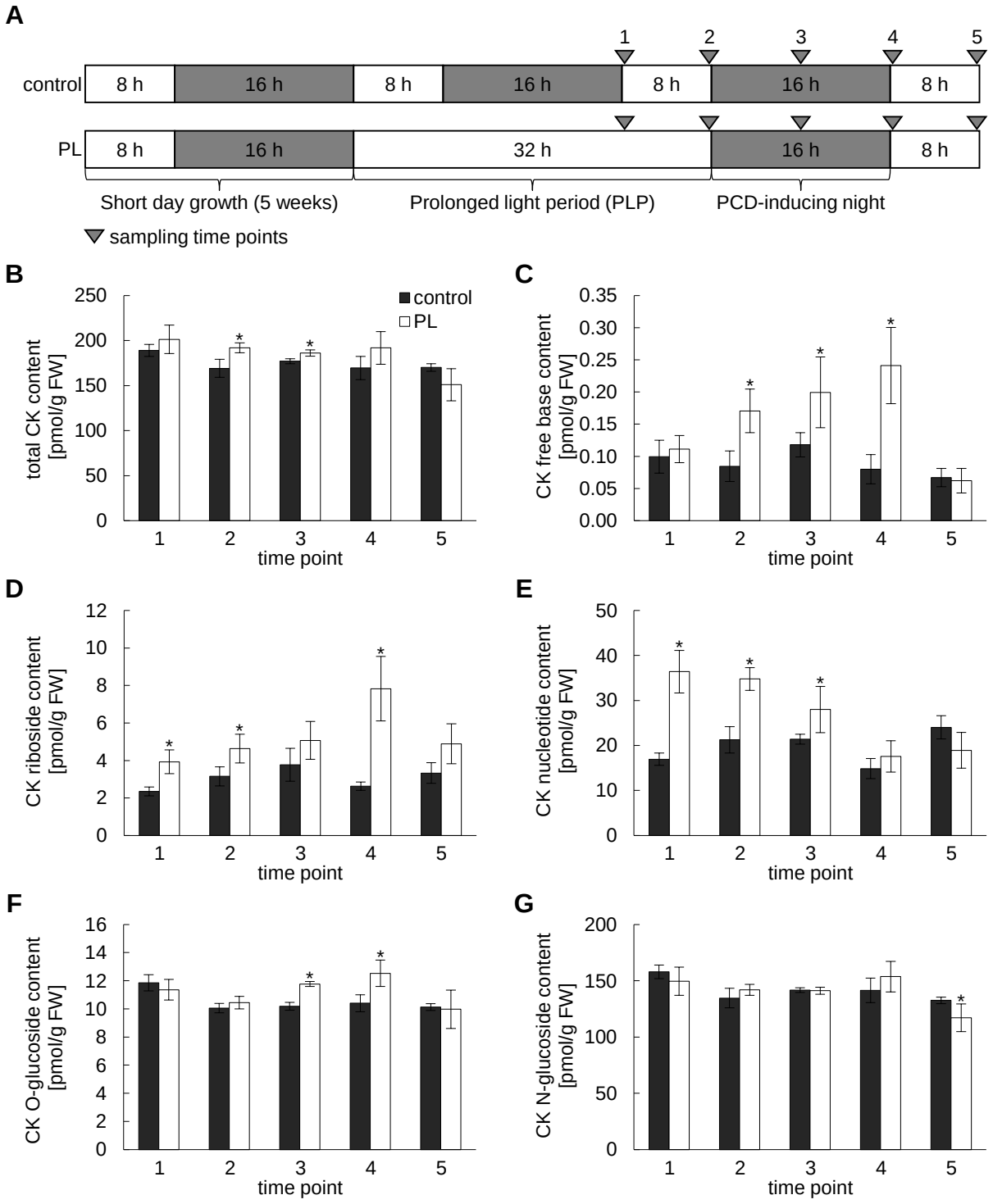

Figure 12: Photoperiod stress causes an increased cytokinin content in wild-type plants.
(A) Schematic overview of sampling time points (grey arrows) for CK measurements. Five-week-old wild-type plants were either cultivated under SD conditions (control) or were treated with a prolonged light period (PLP) of 32 h (PL). (B - G) Content of total CK (B), CK free bases (C), CK ribosides (D) CK nucleotides (E), CK O-glucosides (F) and CK N-glucosides (G) in control (black bars) and PL samples (white bars) at the time points depicted in A. Stars indicate a statistically a significant difference between PL and respective control samples at the given time point (1 - 5) in a paired Student's t-test ($p \leq 0.05$). Error bars indicate SD (n = 5).

Similar tendencies were also detected for DHZ-type cytokinins (Supplemental Table 1). In contrast, the concentrations of *c*ZR and *c*ZRMP were decreased in PL plants during PLP-treatment but were elevated

up to eightfold at the end of the following night and nearly tenfold 16 hours later (Supplemental Table 2; time points 1, 4 and 5).

Table 25: iP-type cytokinin content in control and PL plants at the time points depicted in Figure 12A.
Bold numbers indicate a statistically significant difference in PL samples versus the controls under each sampling time point (1 - 5) in a paired Student's t-test. Values indicate pmol/g FW ± SD.

Condition	Total iP-types	iP	iPR	iPRMP	iP7G	iP9G
control 1	29.4 ± 1.3	0.090±0.027	0.24 ± 0.06	5.13 ± 0.74	22.04± 1.25	1.90 ± 0.11
PL 1	**48.1 ± 4.1**	0.103±0.021	**0.75 ± 0.11**	**21.61± 1.81**	23.56± 2.89	2.10 ± 0.25
control 2	33.1 ± 2.0	0.078±0.024	0.40 ± 0.10	10.86± 1.77	20.03± 0.74	1.70 ± 0.04
PL 2	**44.7 ± 2.6**	**0.161±0.034**	**0.87 ± 0.10**	**20.66± 1.46**	21.10± 1.31	1.91 ± 0.19
control 3	36.8 ± 2.9	0.115±0.018	0.51 ± 0.05	10.98± 1.02	23.19± 1.66	2.01 ± 0.22
PL 3	41.4 ± 3.1	**0.193±0.056**	0.61 ± 0.13	14.69± 3.15	23.91± 0.85	2.04 ± 0.07
control 4	28.0 ± 1.8	0.074±0.022	0.27 ± 0.05	5.27 ± 1.22	20.64± 0.58	1.78 ± 0.11
PL 4	**34.5 ± 3.6**	**0.234±0.059**	**1.11 ± 0.25**	6.56 ± 1.97	**24.65± 1.92**	1.96 ± 0.18
control 5	38.0 ± 0.6	0.063±0.014	0.56 ± 0.16	14.44± 1.19	21.19± 0.98	1.76 ± 0.10
PL 5	33.1 ± 5.9	0.059±0.019	0.54 ± 0.17	**10.32± 2.84**	20.59± 2.74	1.58 ± 0.23

To sum up, the content of all types of cytokinin changed upon photoperiod stress treatment and more importantly led to an increase of the bioactive cytokinins iP and *t*Z as well as their transport forms and precursors.

Table 26: tZ-type cytokinin content in control and PL plants at the time points depicted in Figure 12A.
Bold numbers indicate a statistically significant difference in PL samples versus the controls under each sampling time point (1 - 5) in a paired Student's t-test. Values indicate pmol/g FW ± SD.

Condition	Total *t*Z-types	*t*Z	*t*ZR	*t*ZRMP	*t*ZOG	*t*ZROG	*t*Z7G	*t*Z9G
control 1	132.1 ± 4.9	0.009 ± 0.003	1.67 ± 0.19	8.11 ± 1.20	6.77 ± 0.43	1.10 ± 0.05	87.53 ± 3.94	26.97 ± 0.60
PL 1	129.3 ± 11.5	0.009 ± 0.002	**3.03 ± 0.53**	**13.25 ± 3.13**	6.47 ± 0.49	1.08 ± 0.11	81.79 ± 6.96	**23.71 ± 2.26**
control 2	113.6 ± 8.9	0.007 ± 0.001	2.43 ± 0.43	7.56 ± 1.65	5.64 ± 0.31	0.98 ± 0.08	74.79 ± 5.97	22.16 ± 1.99
PL 2	124.7 ± 3.7	**0.010 ± 0.002**	**3.51 ± 0.77**	**11.89 ± 2.17**	6.02 ± 0.24	1.06 ± 0.05	79.45 ± 2.35	22.78 ± 0.76
control 3	113.4 ± 3.2	0.003 ± 0.001	2.90 ± 0.90	6.01 ± 0.31	5.37 ± 0.17	0.90 ± 0.04	77.34 ± 2.45	20.82 ± 1.05
PL 3	116.3 ± 1.5	**0.006 ± 0.001**	4.04 ± 0.89	**8.88 ± 1.75**	5.88 ± 0.26	**1.24 ± 0.09**	76.07 ± 2.10	20.23 ± 0.73
control 4	116.5 ± 10.5	0.006 ± 0.001	1.90 ± 0.24	6.04 ± 1.13	5.52 ± 0.46	1.05 ± 0.08	79.79 ± 6.84	22.18 ± 2.32
PL 4	126.1 ± 12.3	0.007 ± 0.001	**3.36 ± 0.78**	4.83 ± 1.25	**6.42 ± 0.61**	**1.46 ± 0.17**	85.25 ± 8.16	24.80 ± 2.21
control 5	110.3 ± 4.4	0.004 ± 0.001	2.59 ± 0.47	7.85 ± 1.61	5.52 ± 0.16	0.93 ± 0.04	73.74 ± 1.31	19.62 ± 1.60
PL 5	**92.7 ± 10.6**	0.003 ± 0.001	2.73 ± 0.46	**3.98 ± 0.91**	**4.67 ± 0.57**	0.90 ± 0.15	**63.65 ± 6.76**	16.82 ± 2.49

3.1.2 Transcript levels of genes involved in cytokinin metabolism, transport and signaling change upon photoperiod stress

To elucidate which genes might be involved in coping with photoperiod stress, Dr. Anne Cortleven and I collected wild-type and *ahk2ahk3* leaf samples of control and stressed (PL) plants during the night following PLP (0 h, 4 h, 6 h, 12 h). These samples were sent in for RNAseq analysis to get an overview over the whole transcriptional response in both genotypes. Analysis of RNAseq raw data and statistical analysis was performed by Dr. Anne Cortleven and for this thesis, I filtered results specifically for certain gene families, specifically.

In the night following the prolonged light period of 32 h, several *ARRs* were differentially regulated in wild type but even more pronounced in photoperiod stress sensitive plants (Nitschke, 2014; Nitschke *et al*., 2016). To get further insights into the cytokinin-related transcriptome, transcript abundances of

cytokinin metabolism, transport and signaling genes were extracted from RNAseq data. In comparison to wild type control, the transcript abundance of *LOG7* was increased at all investigated time points in *ahk2ahk3* control (Figure 13B).

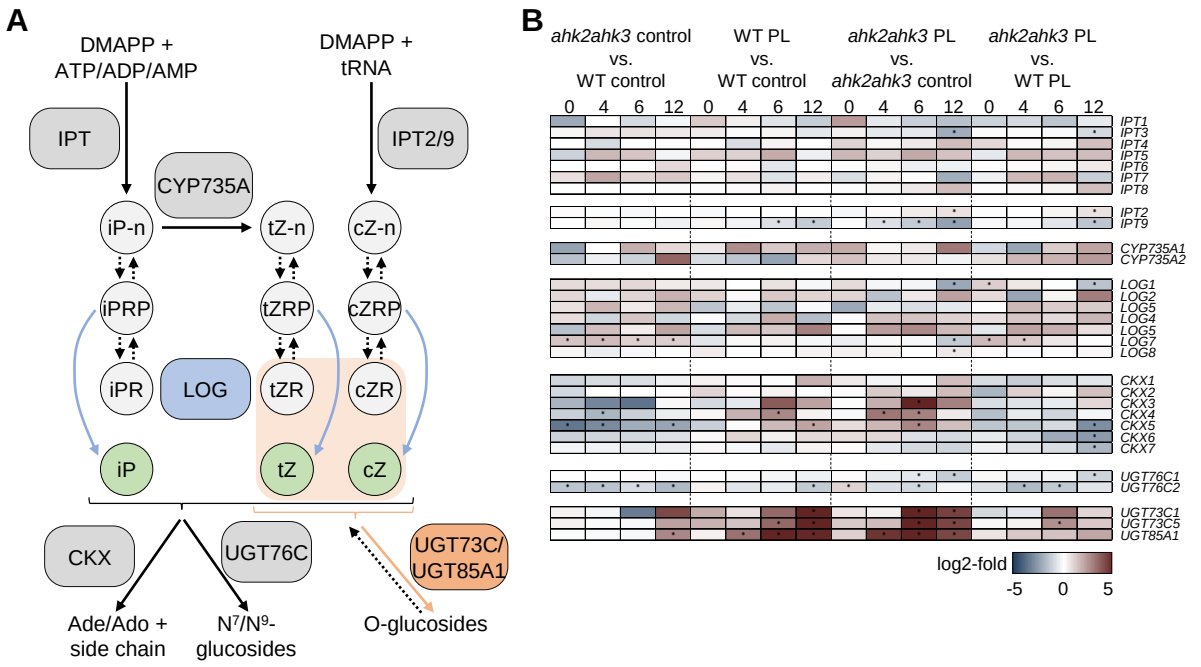

***Figure 13: Expression of cytokinin synthesis and metabolism genes during photoperiod stress in wild type and* ahk2ahk3.**
(A) Simplified scheme of cytokinin metabolism in Arabidopsis*. As a first step of synthesis, isopentenyl adenine (iP) nucleotides are formed by ISOPENTENYLTRANSFERASE (IPT) enzymes. Conversion to the respective* trans*-zeatin (*tZ*)-nucleotides (*tZ*-n) is catalyzed by CYTOCHROME P450 MONOOXYGENASEs (CYP735As). In addition,* cis*-zeatin (*cZ*)-type CKs are formed by the tRNA-IPTs IPT2 and IPT9. iP riboside monophosphate (iPRP),* tZ *riboside monophosphate (*tZRP*) and* cZ *riboside monophosphate (*cZRP*) can be directly converted to biologically active free bases (green) by LONELY GUY (LOG) enzymes (blue arrows). Irreversible inactivation of all metabolites is catalyzed by CYTOKININ OXIDASES/DEHYDROGENASE (CKX) and URIDINE DIPHOSPHATE GLYCOSYLTRANSFERASE76C (UGT76C) enzymes. Furthermore, O-glucosylation of zeatin-type free bases and ribosides is catalyzed by UGT73Cs and UGT85A1 and displays a reversible inactivation step (orange items). (B) Transcript levels 0, 4, 6 and 12 hours after the PLP in either PL plants or control plants of wild type and ahk2ahk3. Stars indicate a significant difference between groups at the given time point after Bonferroni correction ($p \leq 0.05$; $n = 3$).*

Furthermore, *CKX4* and *CKX5* abundances were decreased 4 h after nightfall. *UGT76C2* abundance was reduced at all time points investigated, while the abundance of *UGT85A1* was increased sixfold 12 h after nightfall. Upon photoperiod stress treatment, transcriptional changes were similarly induced in both genotypes. Most strikingly, the abundance of genes involved in O-glucosylation of zeatin-type cytokinins was strongly enhanced (up to 1000-fold) compared to their respective controls 6 and 12 h after the PLP. Direct comparison between *ahk2ahk3* and wild type PL revealed that 12 h after the PLP, the abundance of *IPT3*, *IPT9*, *LOG1*, *CKX5-7* and *UGT76C1* was reduced in *ahk2ahk3*.

Next, abundances of genes known to be involved in cytokinin transport in the leaf were analyzed. Except for the reduced abundance of *PUP1* in *ahk2ahk3* 12 h after nightfall, no alterations were found between controls of *ahk2ahk3* and wild type (Figure 14B)

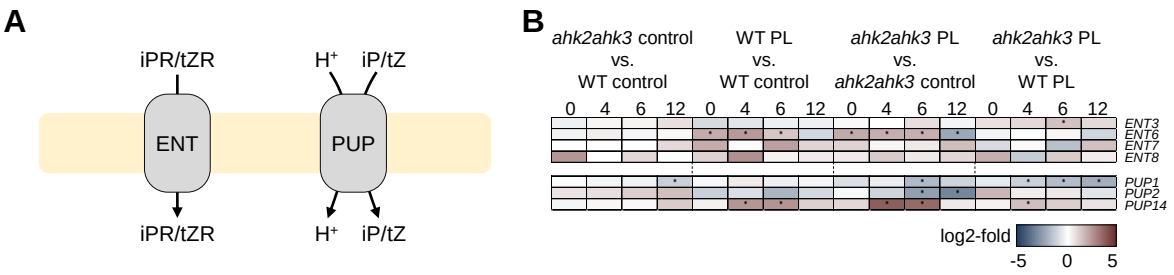

***Figure 14: Expression of cytokinin transporter genes during photoperiod stress in wild type and* ahk2ahk3.** *(A) Schematic view over cytokinin transport. EQUILIBRATIVE NUCLEOSIDE TRANSPORTER (ENT) proteins translocate cytokinin ribosides. Plasma membrane-localized PURINE PERMEASE (PUP) symporters are involved in H^+-dependent transport of cytokinin free bases like iP or tZ. Modified after Kudo* et al*. (2010). (B) Transcript levels 0, 4, 6 and 12 hours after the PLP in either PL plants or control plants of wild type and ahk2ahk3. Stars indicate a significant difference between groups at the given time point after Bonferroni correction ($p \leq 0.05$; $n = 3$).*

Photoperiod stress treatment led to several changes in transcript abundance in both genotypes. First, both genotypes responded to the applied PLP with an increased abundance of *ENT6* and *PUP14* compared to respective controls, which was most pronounced 4 and 6 h after the PLP. Moreover, *PUP1* and *PUP2* transcript abundance was reduced more than threefold in *ahk2ahk3* PL compared to its control 6 h after the PLP. Lastly, *PUP1* abundance was reduced in *ahk2ahk3* PL plants compared to wild-type PL plants as early as 4 h after the PLP-treatment, while that of *PUP14* was increased 2.8-fold. Expression analysis of genes involved in cytokinin signaling proved that the sent in samples belonged to the respective genotypes as *AHK2* and *AHK3* expression was strongly reduced in *ahk2ahk3* control plants compared to wild type (Figure 15B). In addition, the transcript abundance of *AHK4* as well as of several type-A *ARRs* (*ARR4*-7, *ARR15* and *ARR16*) was reduced in *ahk2ahk3*, mostly 4, 6 and 12 h after nightfall but the abundance of *AHPs* and type-B *ARRs* was not altered. Further changes in transcript abundance were induced with application of photoperiod stress in both genotypes. In comparison to their respective controls, *AHP1* and *AHP5* were more abundant in PL samples 6 h after treatment. Moreover, the abundance of type-A *ARR6* to *ARR9* and *ARR16* was reduced as much as nine-fold in *ahk2ahk3* PL and wild type PL 12 h after the exposure to a PLP. Differences in the abundance of type-B *ARRs* were only detected in *ahk2ahk3* PL compared to its respective controls. Here, *ARR1*, *ARR11* and *ARR14* were less abundant as early as 4 h after the PLP-treatment, while *ARR18* was over eleven-fold more abundant in 12 h after the PLP-treatment. In *ahk2ahk3* PL plants compared to wild-type PL plants, all *AHK* and most type-A *ARR* transcripts were less abundant at nearly all time points investigated. The biggest difference was detected for *ARR15*, which was over 80 times less abundant in *ahk2ahk3* PL plants.

Summing up, both wild type and *ahk2ahk3* modulated the transcript abundance of genes involved in cytokinin synthesis, metabolism, transport and signaling in response to the exposure to photoperiod stress with *ahk2ahk3* being similarly more responsive.

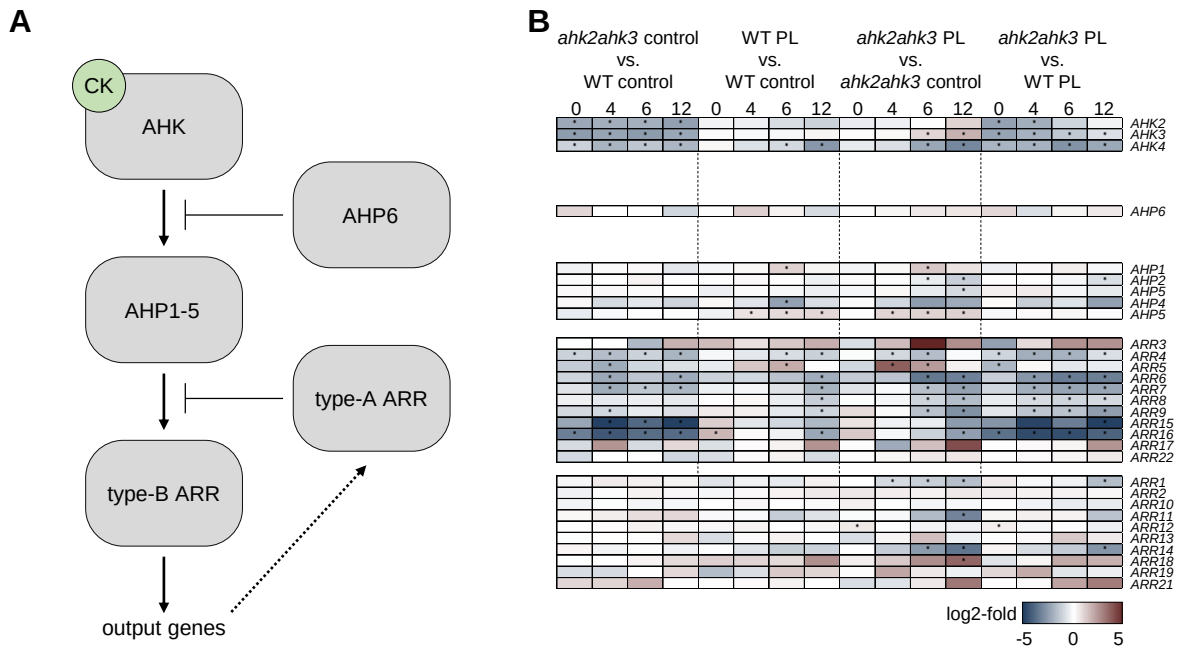

***Figure 15: Expression of cytokinin signaling genes during photoperiod stress in wild type and* ahk2ahk3.**
(A) Simplified scheme of cytokinin signaling in Arabidopsis*. Bioactive cytokinins (CK, green) bind to ARABIDOPSIS HISTIDINE KINASE (AHK) receptors thereby initiating phosphorylation cascade. The phosphorylation signal is transduced by ARABIDOPSIS HISTIDINE PHOSPHOTRANSFER PROTEINs (AHPs) and is ultimately given to type-B ARABIDOPSIS RESPONSE REGULATORs (ARRs). AHP6 competes with other AHPs for phosphorylation but does not phosphorylate type-B ARRs. Activated type-B ARRs transcriptionally regulate output genes. Among them are type-A ARRs, which act as negative feedback regulators as they compete with type-B ARRs for phosphorylation but are unable to bind DNA. (B) Transcript levels 0, 4, 6 and 12 hours after the PLP in either PL plants or control plants of wild type and ahk2ahk3. Stars indicate a significant difference between groups at the given time point after Bonferroni correction ($p \leq 0.05$; $n = 3$).*

3.1.3 Root-derived tZ-type cytokinins protect plants from photoperiod stress

Stressed wild-type plants regulated the concentrations of both functionally relevant cytokinins - iP and *t*Z. To decipher which of these two forms might be protective against photoperiod stress, the involvement of *t*Z-type cytokinins was investigated by exposing mutants that are impaired in either the biosynthesis of *t*Z-type cytokinins (*cypDM*; Kiba *et al*., 2013) or their transport from the root to the shoot (*abcg14-2*; Ko *et al*., 2014) to photoperiod stress.

Over 80 % of *cypDM* and *abcg14* leaves were lesioned after photoperiod stress treatment, which reflected a four-fold increase compared to wild-type plants (Figure 16B). Furthermore, photoperiod stress caused a drop in Fv/Fm of over 50 percent in these mutants compared to wild type (Figure 16C). At the molecular level, *cypDM* leaves accumulated six times more H_2O_2 than wild type (Figure 16D) and 7.5 and 15 hours after the PLP-treatment, abundances of stress marker genes *BAP1* and *ZAT12* were increased two- to threefold in *cypDM* and *abcg14* (Figure 16E, F). The abundance of *CAB2* on the other hand was markedly decreased in both mutants compared to wild type (Figure 16G). Summing up, these results support a protective function of root-derived *t*Z-type cytokinins against photoperiod stress.

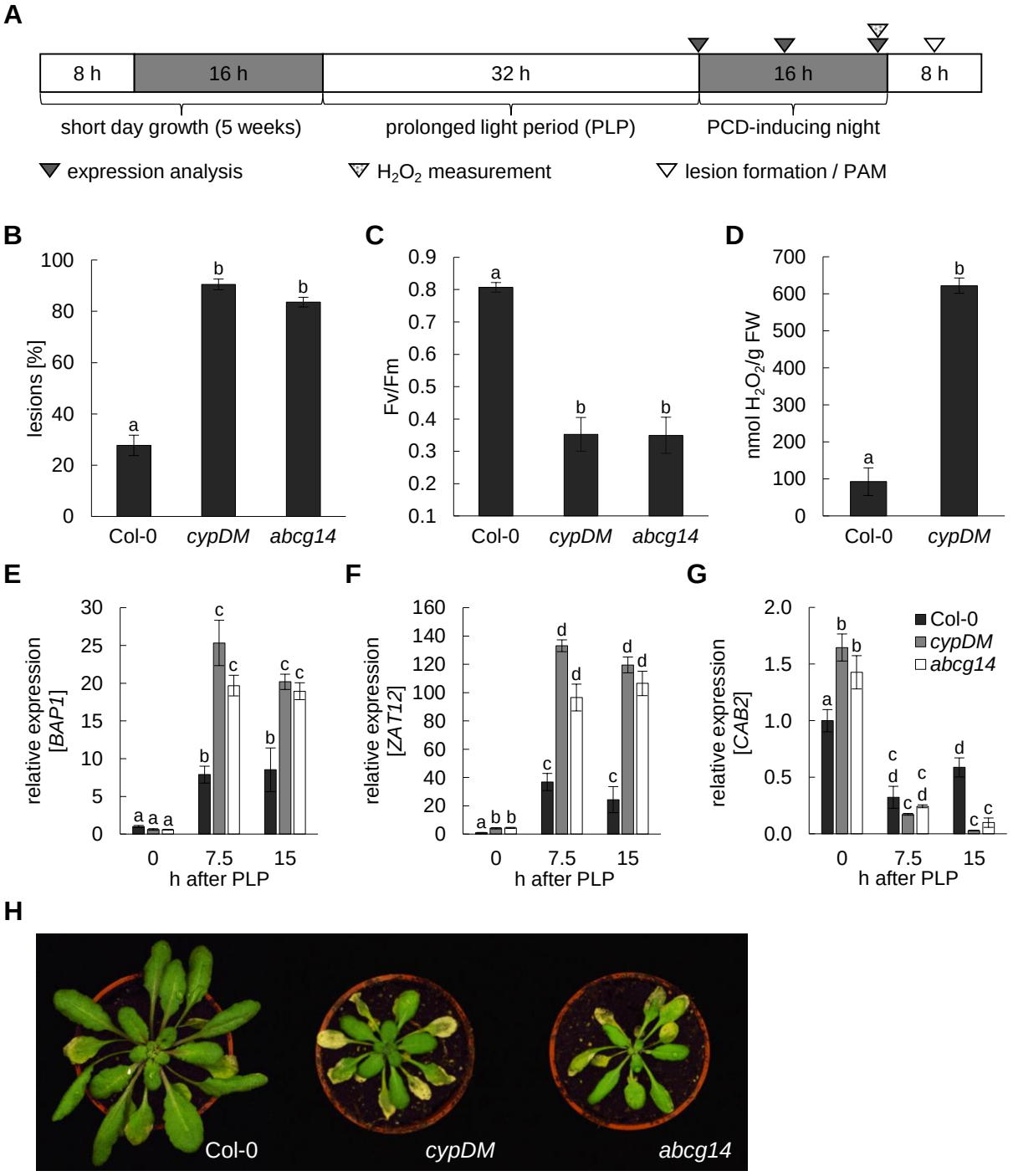

Figure 16: Plants deficient in tZ-type cytokinins are strongly affected by photoperiod stress.
(A) Schematic overview of photoperiod stress treatment. Time points for quantification of lesion formation, PAM measurements as well as sample taking for gene expression analysis and H_2O_2 measurements are depicted. (B) Lesion formation of leaves at five-week-old Col-0, cypDM *and* abcg14 *plants the day after the PCD-inducing night (n = 15). (C) PAM measurements of leaves the day after PCD-inducing night (n = 15). (D) H_2O_2 measurements of Col-0 and* cypDM *15 h after the PLP treatment (n = 4). (E - G) Expression of marker genes (*BAP1, ZAT12, CAB2*) 0 h, 7.5 h and 15 h after the PLP (n ≥ 3). (H) Pictures of representative plants that experienced a PLP. Letters indicate significant differences between groups (p ≤ 0.05). Error bars indicate SE.*

3.1.4 Watering of cypDM plants with either t*Z or* t*ZR reduces the sensitivity to photoperiod stress*

Recent studies by Osugi *et al*., 2017 demonstrated that under long-day conditions, root-derived *t*Z has distinct functions in the shoot (e.g. in regulating the size of leaves or the SAM) compared to root-derived *t*ZR that is converted to *t*Z later. In order to dissect the role of root-derived *t*Z and *t*ZR in photoperiod stress, we watered *cypDM* plants with either 10 µM *t*Z or 10 µM *t*ZR daily during the whole cultivation period and exposed them to photoperiod stress.

*t*ZR application reduced lesion formation about 10 % compared to untreated *cypDM* plants (Figure 17A). In addition, the decrease in photosynthetic capacity of *t*ZR-treated plants was lower compared to untreated *cypDM* controls. These results indicate that *t*ZR might render plants less sensitive to photoperiod stress. Watering plants with *t*Z suppressed the photoperiod stress syndrome almost completely showing that the transport of *t*Z from the root to the shoot protects plants during photoperiod stress (Figure 17B). At the molecular level, treatment with either *t*ZR or *t*Z reduced the photoperiod stress-induced misregulation of stress marker genes 15 h after the PLP (Figure 17C-E). Furthermore, the twofold decrease in the abundance of cytokinin response genes *ARR5 and ARR6* in control *cypDM* plants compared to wild type was abolished by application of *t*ZR and *t*Z (Figure 17F-G).

In summary, watering experiments indicated that lesion formation, the decrease in photosynthetic capacity and the transcriptional response can be rescued nearly completely by *t*Z while *t*ZR was able to fully rescue the stress response at the transcriptional level as well as the deregulation of cytokinin response genes. However, the phenotypic changes upon photoperiod stress treatment were not fully rescued by *t*ZR.

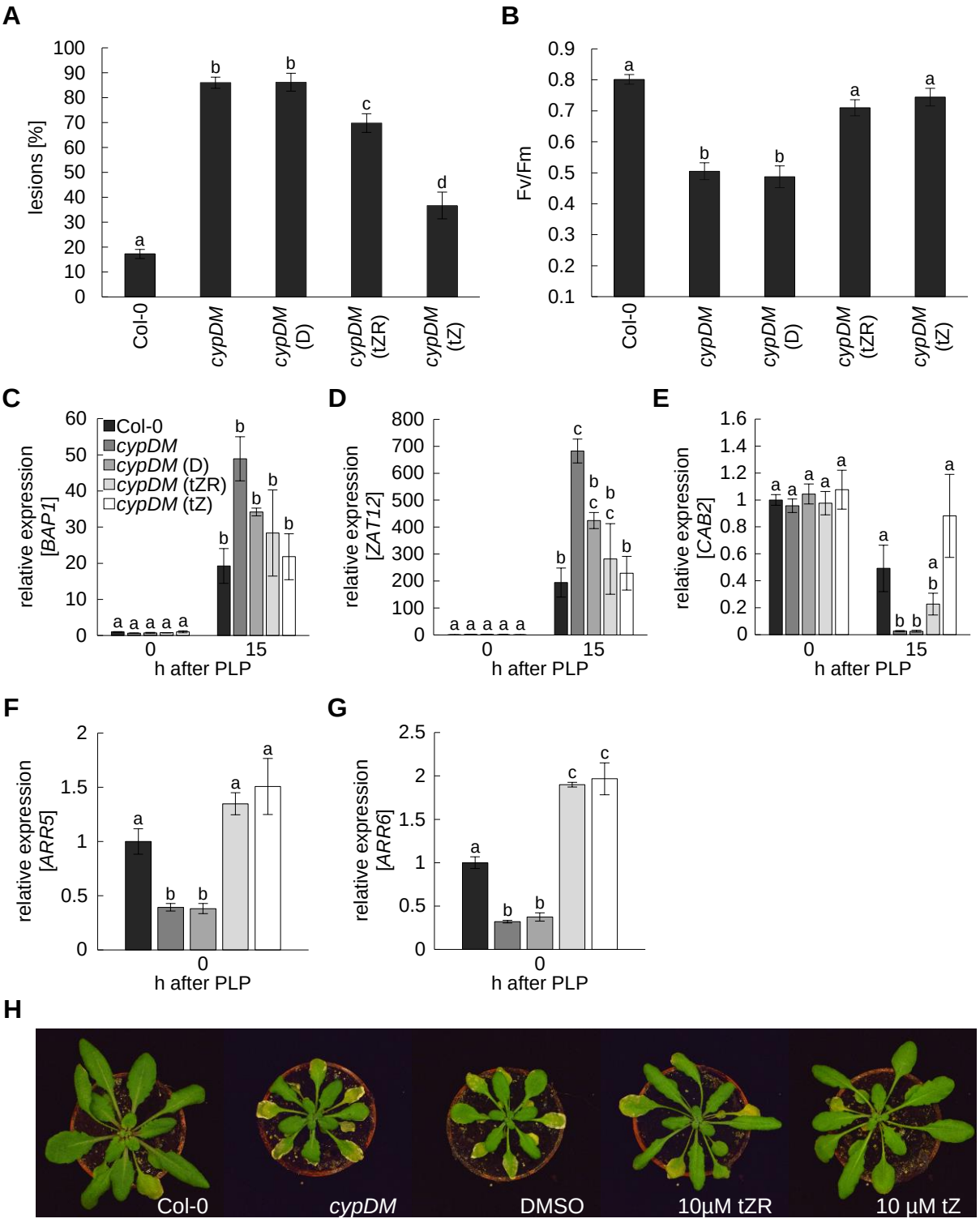

Figure 17: Pretreatment of cytokinin-deficient plants with tZ-type cytokinins for five weeks reduces the damage caused by photoperiod stress.
*(A) Percentage of lesion formation in five-week-old short day-grown plants the day after the PCD-inducing night (n = 12). (B) Photosystem II maximum quantum efficiency (Fv/Fm) of leaves evaluated in A (n = 15). (C - E) Expression of marker genes (*BAP1, ZAT12, CAB2*) 0 h and 15 h after the PLP treatment (n ≥ 3). (F, G) Expression of cytokinin output genes (*ARR5, ARR6*) 0 h after the PLP treatment (n ≥ 3). (H) Pictures of representative plants tested after the PLP-treatment. Abbreviations: D, DMSO;* tZ, trans*-zeatin (10 µM);* tZR, trans*-zeatin-riboside (10 µM). Letters indicate significant differences between groups (p ≤ 0.05). Error bars indicate SE.*

3.1.5 Impairment in synthesis of bioactive cytokinins does not increase photoperiod stress sensitivity

In *Arabidopsis*, the conversion of inactive iP- and *t*Z-type cytokinins to their active forms is catalyzed via a nine-member family of LOG enzymes of which seven are functionally relevant (Kuroha *et al*., 2009). To demonstrate the necessity for plants to form bioactive *t*Z as a protectant against photoperiod stress, the *log septuple* (*logS*) mutant (Tokunaga *et al*., 2012) was tested. 20 % of leaves were lesioned in *logS* as well as wild-type plants after photoperiod stress (Figure 18A).

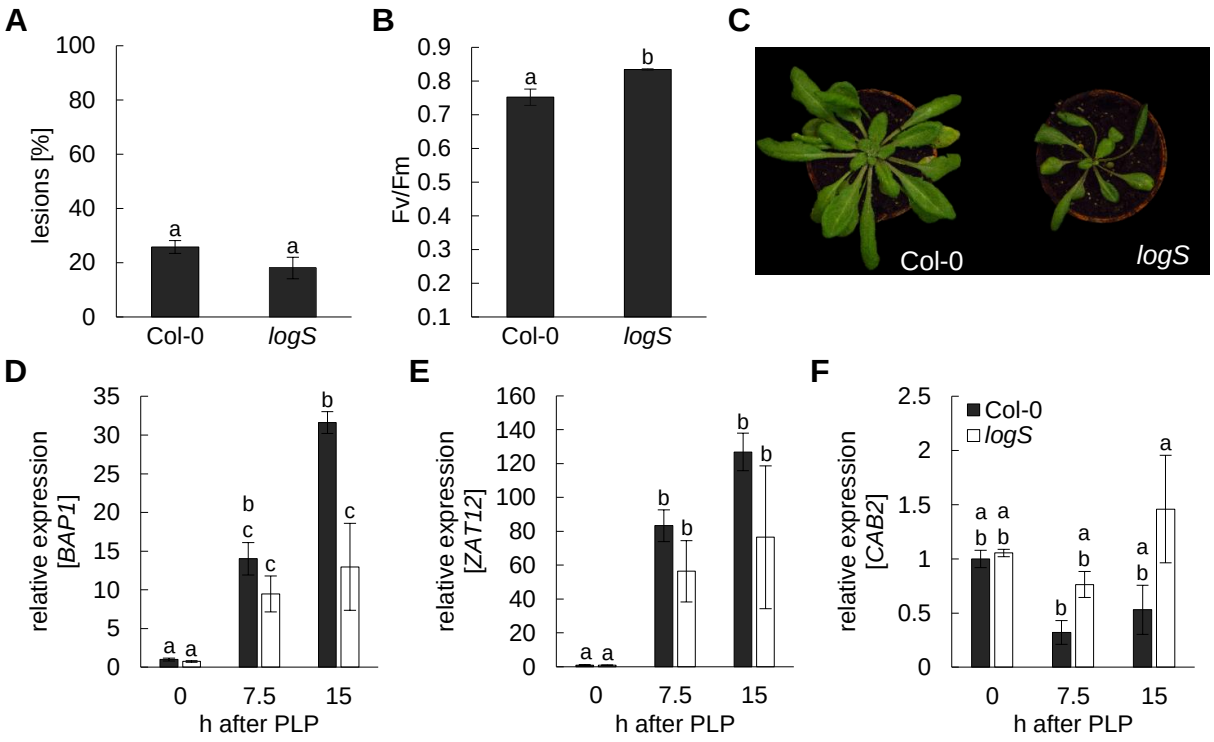

Figure 18: Plants deficient in bioactive cytokinins are less affected by photoperiod stress.
(A) Quantification of lesioned leaves at five-week-old Col-0 and log septuple mutant (logS) *plants the day after PCD-inducing night (n = 15). (B) Fv/Fm measurements of leaves the day after PCD-inducing night (n = 15). (C) Pictures of representative plants that experienced a PLP. (D - F) Expression of marker genes (*BAP1, ZAT12, CAB2*) 0 h, 7.5 h and 15 h after the PLP-treatment (n ≥ 3). Letters indicate significant differences between groups (p ≤ 0.05). Error bars indicate SE.*

Consistently, no decrease in photosynthetic capacity was observed in *logS* (Figure 18B). At the transcriptional level, *logS* plants showed no differences to wild type plants or performed even better (Figure 18B-E). All in all, a lack of free base cytokinins in *logS* plants had no effect on the sensitivity to photoperiod stress.

3.1.6 AHP2, AHP3 and AHP5 act redundantly in photoperiod stress signaling

In *Arabidopsis*, AHK receptors transduce the cytokinin signal to AHPs via phosphorylation and phosphorylated AHPs activate type-B ARRs. Although AHPs are involved in several developmental processes and responses to stress (Hutchison *et al*., 2006), their role during photoperiod stress has not been investigated so far. Thus *ahp2ahp3ahp5* triple mutants as well as the corresponding double

mutants (Hutchison *et al*., 2006) were exposed to photoperiod stress. 25 % of leaves were lesioned in wild-type plants, while 50 % were lesioned in *ahp2ahp3* and *ahp2ahp3ahp5* (Figure 19A).

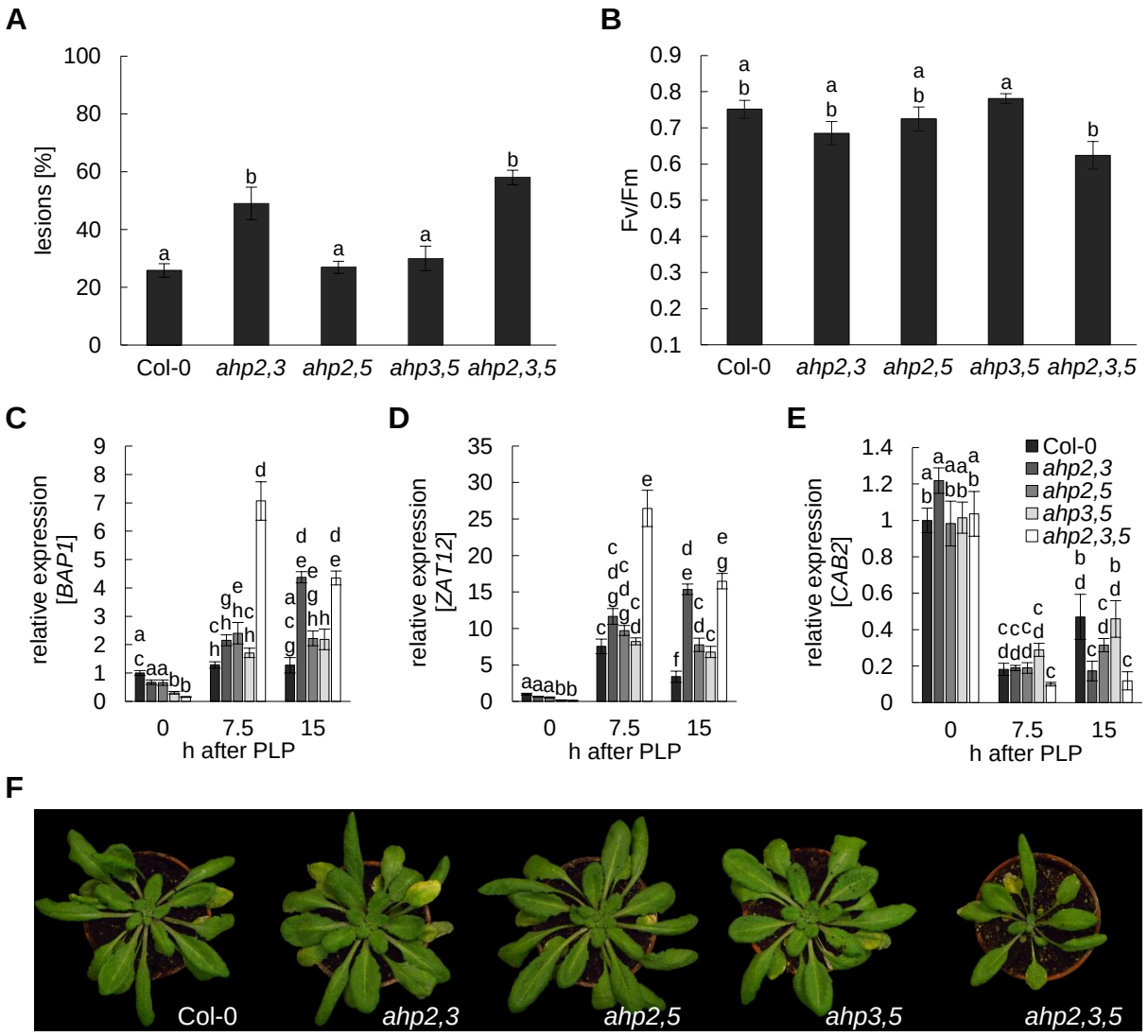

Figure 19: AHP2, AHP3 and AHP5 act redundantly during photoperiod stress.
(A) Lesion formation in five-week-old Col-0, ahp2ahp3 *(*ahp2,3*),* ahp2ahp5 *(*ahp2,5*),* ahp3ahp5 *(*ahp3,5*) and* ahp2ahp3ahp5 *(*ahp2,3,5*) plants the day after PCD-inducing night (n = 15). (B) Fv/Fm measurements of leaves the day after PCD-inducing night (n = 15). (C - E) Expression of marker genes (*BAP1, ZAT12, CAB2*) 0 h, 7.5 h and 15 h after the PLP-treatment. (F) Pictures of representative plants that experienced a PLP. Letters indicate significant differences between groups (p ≤ 0.05; n ≥ 3). Error bars indicate SE.*

Correspondingly, the photosynthetic capacity of *ahp2ahp3ahp5* plants was decreased compared to all other genotypes (Figure 19B). A functional redundancy of AHPs was also reflected at the molecular level (Figure 19C-E). While the increase in *BAP1* and *ZAT12* abundance was apparent in all *ahp* double and triple mutants compared to wild type 15 hours after the PLP-treatment, the amplitude was highest in *ahp2ahp3* and *ahp2ahp3ahp5* (Figure 19C, D). Similar to the differential impact on *BAP1* and *ZAT12* expression, a decrease of *CAB2* transcript levels was more apparent in *ahp2ahp3* and *ahp2ahp3ahp5* plants 15 hours after exposure to a PLP (Figure 19E). To sum up, AHPs act redundantly in photoperiod stress signaling with AHP2 and AHP3 having a more prominent role in comparison to AHP5.

3.1.7 Loss of ARR10 and ARR12 rescues photoperiod stress sensitivity of arr2 *mutants*

After phosphorylation by AHPs, type-B ARRs regulate the cytokinin signaling output. As demonstrated by Nitschke *et al*. (2016), three members of the type-B ARR family - namely ARR2, ARR10 and ARR12 - act in photoperiod stress signaling. Their functional redundancy in this signaling pathway has, however, not been demonstrated. Characterization of the function of type-B ARRs hint at a complex genetic interaction in other developmental processes (Mason *et al*., 2005). Hence, *arr2arr10arr12* triple mutants and corresponding double and single mutants (created by Dr. Sören Werner) were exposed to a prolonged light period.

Consistent with the findings of Nitschke *et al*., (2016), 2.5-fold more leaves were lesioned in *arr2* plants compared to wild-type plants after photoperiod stress treatment and *arr10* and *arr12* plants did not differ from wild type with respect to lesion formation (Figure 20A). Surprisingly, *arr2,10* and *arr2arr12* plants were also indistinguishable from wild type and lesion formation in *arr2arr10arr12* plants was increased four-fold compared to respective double mutants and wild-type plants. This indicated that ARR2, ARR10 and ARR12 may interact in regulating the response to photoperiod stress. Measurement of the photosynthetic capacity confirmed that *arr2* leaves were more affected by the given prolonged light period compared to all other genotypes except for *arr2arr10arr12*, which were similarly affected (Figure 20B). At the molecular level, the response of the different *arr* mutants varied (Figure 20C-E). While the abundances of *BAP1* and *ZAT12* did not give clear indications whether tested mutants differed in their photoperiod stress response (Figure 20C, D), *CAB2* abundance in *arr2* and *arr2arr10arr12* decreased considerably compared to all other genotypes 15 hours after the PLP (Figure 20E). Confirmative to the observed phenotypical differences, *CAB2* abundance in *arr2arr10* and *arr2arr12* was similarly regulated as in wild type at all time points and its abundance was increased compared to wild type in *arr10,12* 7.5 and 15 hours after the PLP.

Summing up, the results confirm the previously described positive regulatory function of ARR2 in photoperiod stress and additionally demonstrate that ARR10 and ARR12 act in a more complex manner than previously described.

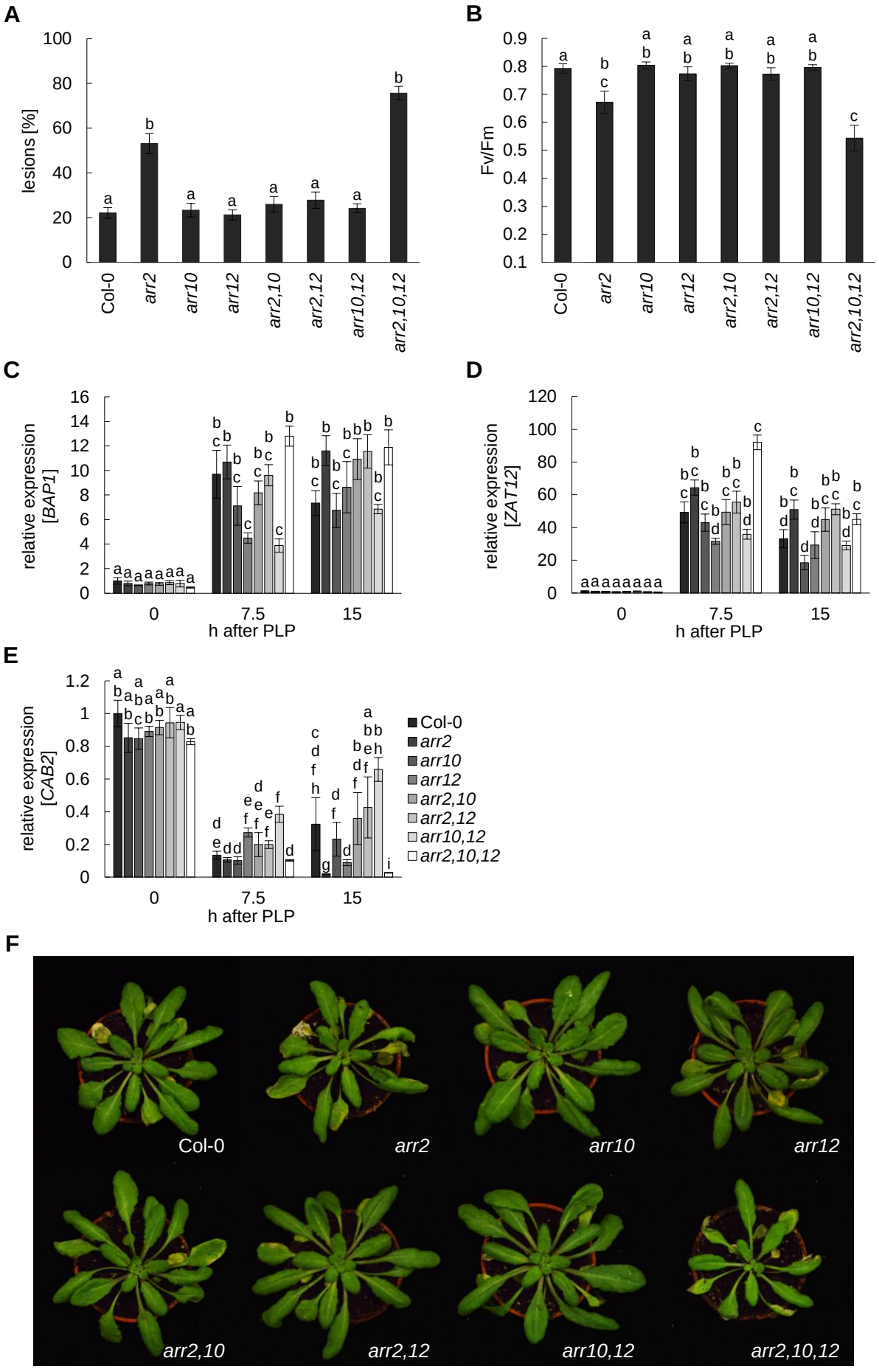

Figure 20: Loss of ARR10 or ARR12 rescues the* arr2 *photoperiod stress phenotype.

Lesion formation in five-week-old Col-0, arr2*,* arr10*,* arr12*,* arr2arr10 *(*arr2,10*),* arr2arr12 *(*arr2,12*),* arr10arr12 *(*arr10,12*) and* arr2arr10arr12 *(*arr2,10,12*) plants the day after the PCD-inducing night (n = 15). (B) Fv/Fm measurements of leaves the day after PCD-inducing night (n = 15). (C - E) Expression of marker genes (*BAP1*,* ZAT12*,* CAB2*) 0 h, 7.5 h and 15 h after the PLP-treatment. (F) Pictures of representative plants that experienced a PLP. Letters indicate significant differences between groups (p ≤ 0.05; n ≥ 3). Error bars indicate SE.*

3.2 The sensitivity to photoperiod stress is tissue- and age-specific

3.2.1 Leaves of the same plant differ in their photoperiod stress responsiveness

As described in Nitschke (2014), not all leaves were equally sensitive to photoperiod stress. Mature, fully expanded leaves were highly responsive to photoperiod stress while young, still growing leaves did respond much less, both in wild type and *ahk2ahk3*. As a first approach to understanding the mechanism behind this observation further, the photoperiod stress sensitivity of distinct leaves was evaluated in the same genotypes as mentioned previously. Leaf one to leaf four were already senescent or dead in most plants before the actual treatment and therefore excluded from analysis. 40 % of all wild-type and *ahk2ahk3* plants had a fifth leaf that was lesioned after experiencing photoperiod stress (Figure 21B).
From leaf five to leaf eight, wild type and *ahk2ahk3* did not differ in lesion formation. Starting from leaf 9, differences were observed as 20 % of wild-type leaves nine to twelve were lesioned and 90 % of *ahk2ahk3*. No lesions were formed by leaves 13 and 14 of wild-type plants. The photosynthetic capacity of the tested leaves was more affected in *ahk2ahk3*, especially between leaves seven and 13 (Figure 21C).
Representative of these observations on the phenotypical level, leaves six, eight, ten and twelve were chosen for the expression analysis of marker genes. 18 hours after the PLP-treatment, *BAP1* expression was increased in all *ahk2ahk3* leaves compared to wild type except for leaf eight (Figure 21D). In comparison to that, the abundance of *ZAT12* was not altered in leaves six to ten, but was increased 20-fold in leaf twelve of *ahk2ahk3* compared to that of wild type (Figure 21E). In support of the observed reduction of the photosynthetic capacity in *ahk2ahk3* compared to wild type, the abundance of *CAB2* was reduced more than 80-fold in *ahk2ahk3* leaves compared to the respective wild-type leaves (Figure 21E).
Summing up, sensitivity to photoperiod stress was highest in *ahk2ahk3* leaves nine to twelve. The same leaves of wild-type plants were the ones in which the sensitivity slowly decreased until in leaf 13 and 14, lesion formation and a reduction of the photosynthetic capacity were absent.

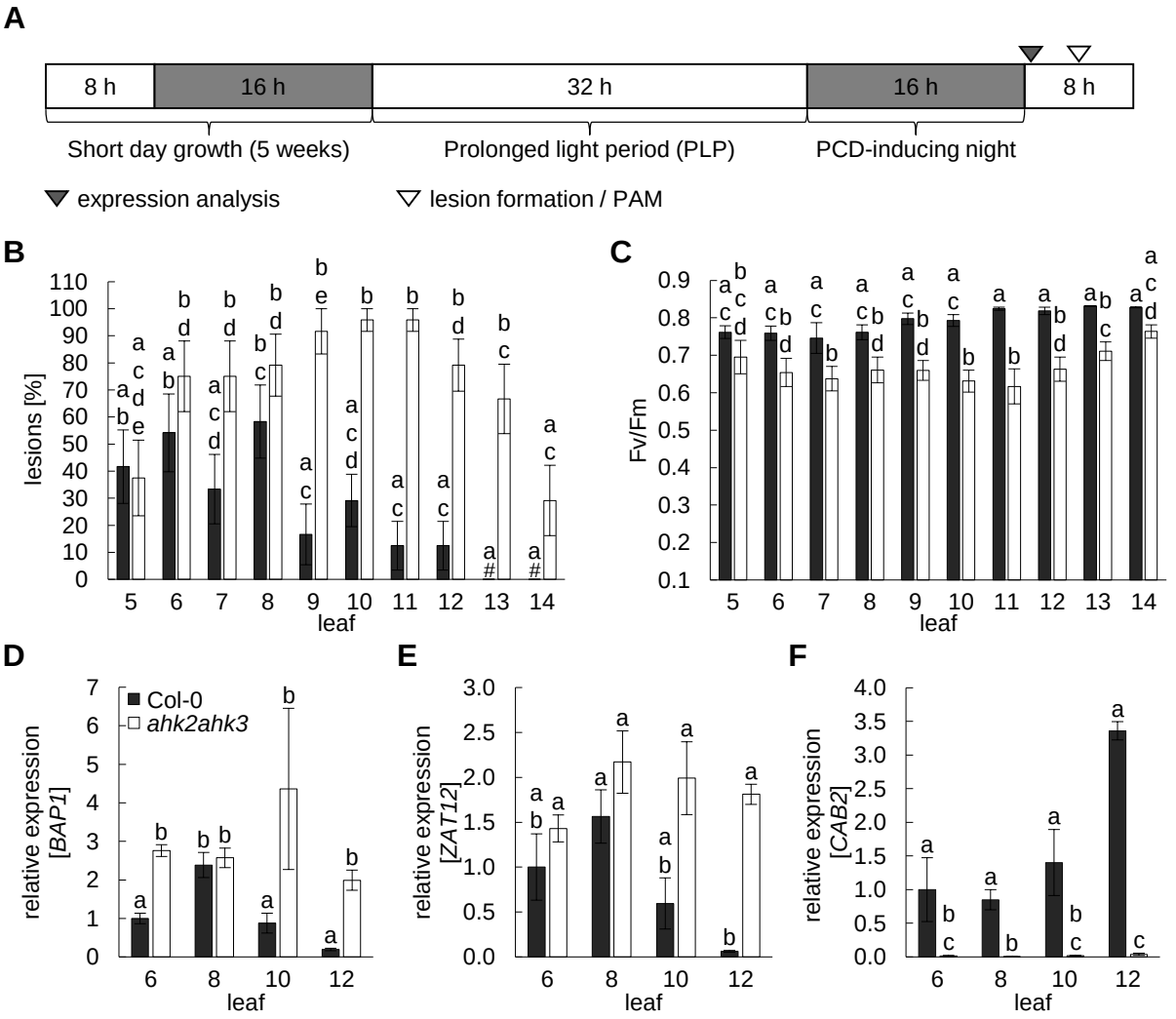

Figure 21: Distinct leaves of an* Arabidopsis *rosette differ in their photoperiod stress sensitivity.
(A) Schematic overview of photoperiod stress treatment. Time points for quantification of lesion formation, PAM measurements (both white arrows) as well as sampling for gene expression analysis (grey arrows) are depicted. (B) Lesion formation of leaves six to 14 in five-week-old Col-0 (black bars) and ahk2ahk3 *plants (white bars) the day after PCD-inducing night (n = 12). # indicates that no leaves were lesioned (C) PAM measurements of leaves six to 14 the day after PCD-inducing night (n = 12). (D - F) Expression of marker genes (*BAP1*,* ZAT12*,* CAB2*) 0 h and 18 h after the PLP-treatment (n ≥ 3) relative to leaf six of Col-0 at 0 h. Letters indicate significant differences between groups (p ≤ 0.05). Error bars indicate SE.*

3.2.2 The leaf identity does not influence the response to photoperiod stress

Because mature leaves were more sensitive to photoperiod stress, further experiments were conducted to clarify which developmental program might be involved in modulating the sensitivity to photoperiod stress. Two cytokinin-dependent developmental programs were considered. Firstly, the juvenile-to-adult transition and secondly, leaf and plant aging itself.

Previously, it was reported that *tZ*-type cytokinins negatively regulate the formation of juvenile leaves by regulating the miRNA172 abundance (Kiba *et al.*, 2013; Werner, 2016). In agreement with these reports, formation of juvenile leaves was increased in *ahk2ahk3*. The receptor double mutant formed eleven juvenile leaves on average while wild type formed seven (Figure 22A). Moreover, *MIRNA172* were less abundant in *ahk2ahk3* compared to wild type, while the abundance of *MIRNA156* did not differ (Figure 22B - D). The influence of the leaf identity was further analyzed by using plants that form more juvenile

leaves as they have altered miRNA156 and miRNA172 levels. While lesion formation was not altered in *35S::MIRNA156B*, 1.75-fold more leaves of 35S::*MIM172* were lesioned compared to wild type in response to photoperiod stress (Figure 22E). However, Fv/Fm values did not differ between the genotypes (Figure 22F).

All in all, results indicate that the increased formation of juvenile leaves in *ahk2ahk3* is not causative for its increased sensitivity to photoperiod stress as *35S::MIRNA156B* and *35S::MIM172* only showed minor phenotypic alterations upon exposure to photoperiod stress.

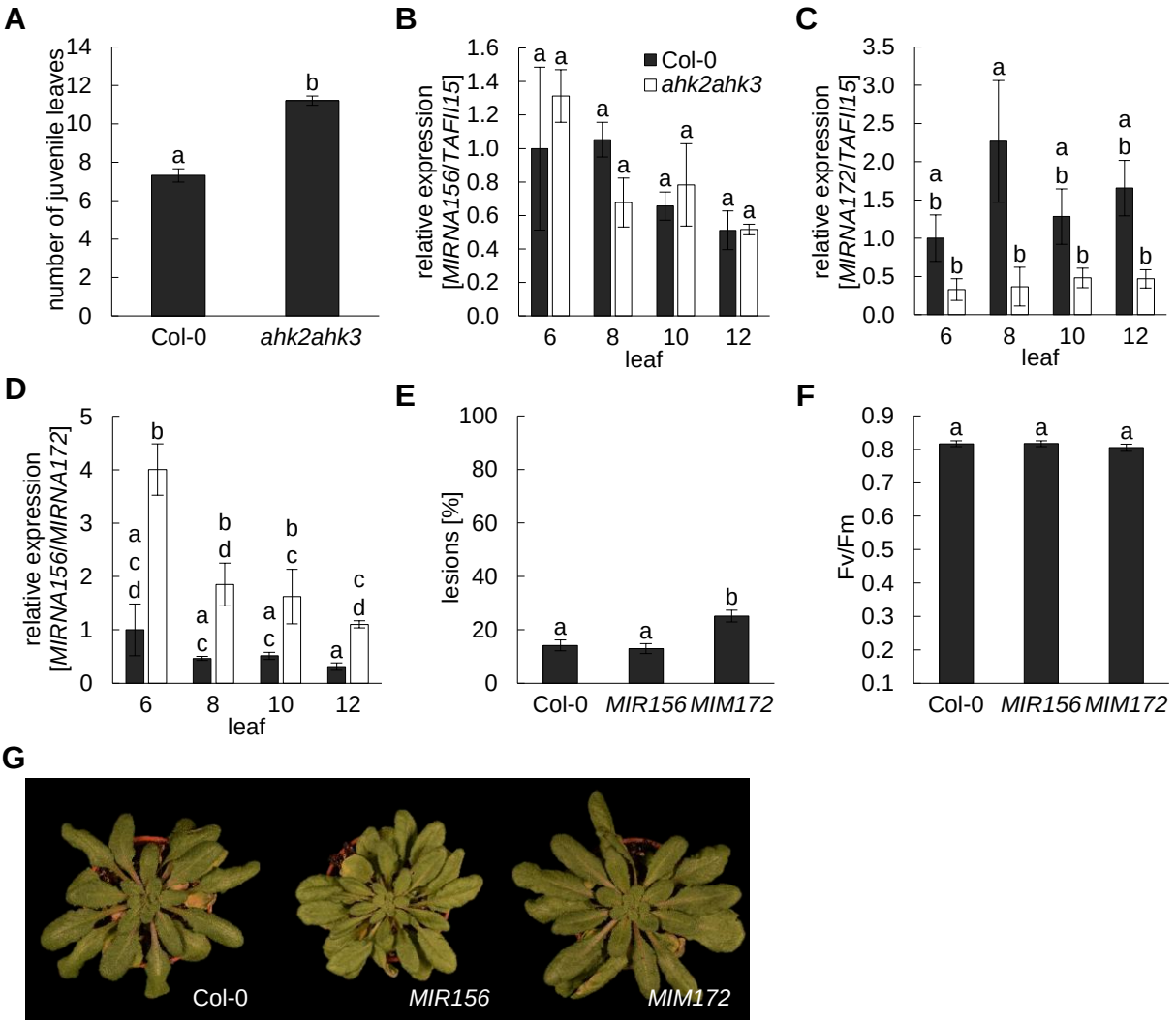

Figure 22: The responsiveness to photoperiod stress does not depend on the leaf identity.
(A) Number of juvenile leaves in five-week-old short day-grown Col-0 and ahk2ahk3 plants (n = 12). (B, C) Transcript abundance of MIRNA156 *(B) and* MIRNA172 *(C) in Col-0 (black bars) and* ahk2ahk3 *(white bars) (n ≥ 3). (D) Ratio between* MIRNA156 *and* MIRNA172 *based on the results in B and C. (E) Lesion formation of five-week-old Col-0,* 35S::MIRNA156B *(*MIR156*) and* 35S::MIM172 *(*MIM172*) the day after the PCD-inducing night (n ≥ 15). (F) PAM measurements of leaves the day after PCD-inducing night (n = 15). (G) Pictures of representative plants from experiments depicted in E and F. Letters indicate significant differences between groups (p ≤ 0.05). Error bars indicate SE.*

3.2.3 The sensitivity to photoperiod stress is age-dependent

Since the identity of leaves was of minor importance for the sensitivity to photoperiod stress, it was evaluated whether and how the age of the whole plant and of specific leaves correlated with the photoperiod stress responsiveness. Three-, four- and five-week-old wild-type and *ahk2ahk3* plants were exposed to a PLP. Whereas the plant age did not affect lesion formation of wild type, 20 % of leaves were lesioned in three-week-old *ahk2ahk3* plants and 50 % in four- and five-week-old plants (Figure 23A). However, Fv/Fm ratios did not differ between leaves of both genotypes independent of plant age (Figure 23B).

At the molecular level, *BAP1*, *ZAT12* and *CAB2* transcript abundance indicated that plants of all ages were photoperiod stress responsive (Figure 23E - G). 15 hours after the PLP, *BAP1* abundance was increased by 50 % in three-week-old *ahk2ahk3* compared to wild-type plants of the same age (Figure 15E). A similar expression pattern was observed for five-week-old plants of both genotypes. The highest abundance of *BAP1* was detected in five-week-old *ahk2ahk3* plants, which was 50 % higher than in wild-type plants of the same age. Simultaneously, this abundance displayed also a 50 % increase compared to three- and four-week-old *ahk2ahk3*. *ZAT12* expression was similarly induced by photoperiod stress. Here, the transcript abundance was twofold higher in four- and five-week-old *ahk2ahk3* compared to respective wild-type plants 15 hours after nightfall (Figure 23F). Furthermore, photoperiod stress led to a decrease in *CAB2* abundance in both genotypes independent of age (Figure 23G). However, 15 hours after experiencing a PLP, the abundance was decreased more than 20-fold in five-week-old *ahk2ahk3* plants compared to all other groups tested.

As the results indicated that the responsiveness to photoperiod stress was at least partially plant age-dependent, further experiments evaluated whether the age of specific leaves was also important. Here, leaf eight was chosen as it was one of the leaves that were very responsive to photoperiod stress in five-week-old wild type and *ahk2ahk3*. Leaf eight was formed shortly before plants were three weeks old and thus, leaf areas were determined as a measure of leaf maturity in three-, four- and five-week-old plants. Within the fourth week of growth, area of leaf eight in wild type plants increased tenfold (Figure 24A)

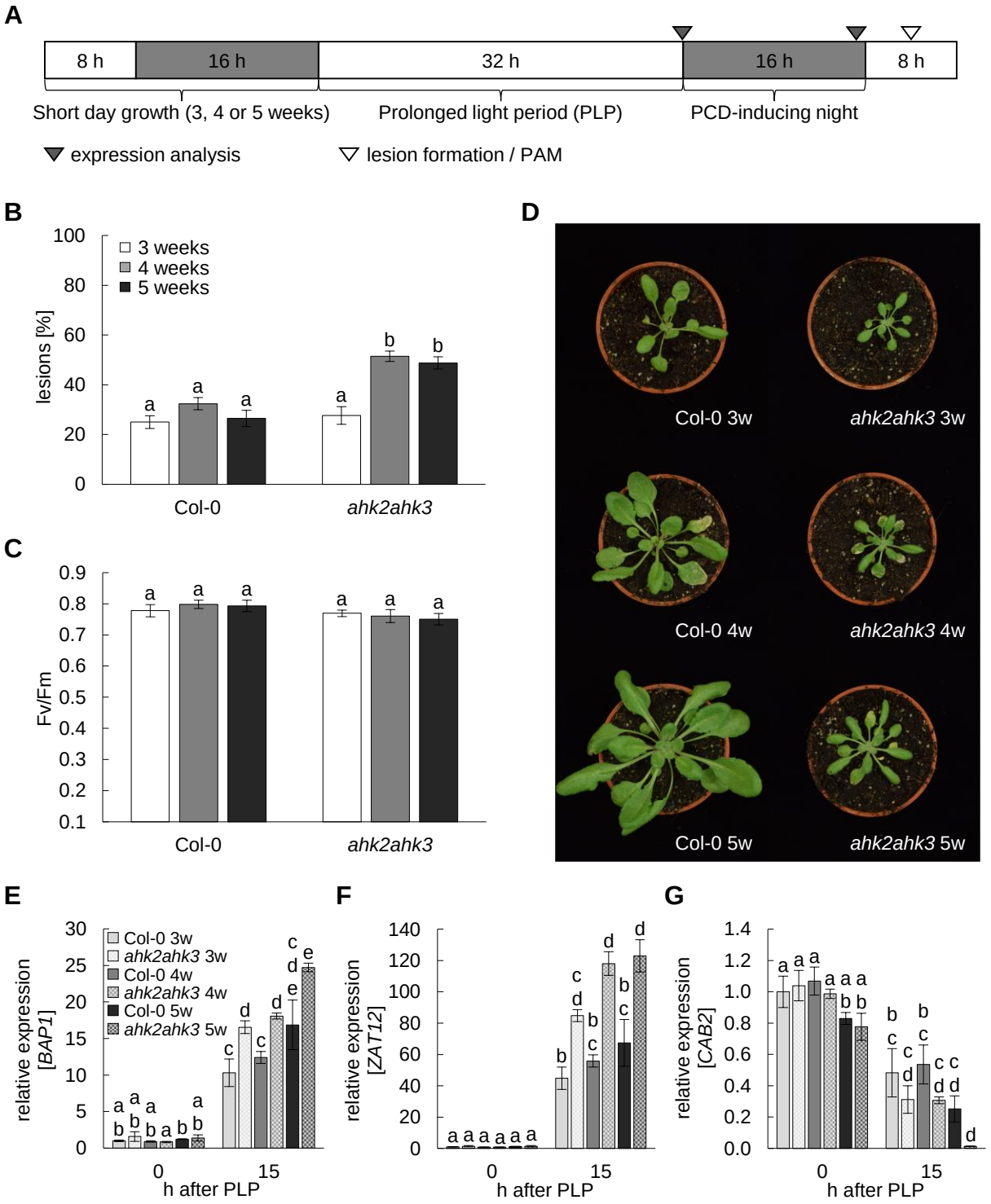

Figure 23:The responsiveness to photoperiod stress depends on the plant age.
(A) Schematic overview of photoperiod stress treatment. Time points for quantification of lesion formation, PAM measurements as well as sample taking for gene expression analysis are depicted. (B) Lesion formation in leaves of three-, four- and five-week-old Col-0 and ahk2ahk3 *plants the day after PCD-inducing night (n = 15). (C) PAM measurements of leaves the day after PCD-inducing night (n = 15). (D) Pictures of representative plants tested. (E - G) Expression of marker genes (*BAP1, ZAT12, CAB2*) 0 h and 15 h after the PLP-treatment. Letters indicate significant differences between groups (p ≤ 0.05; n ≥ 3). Error bars indicate SE.*

Compared to that, growth of leaf eight was reduced in *ahk2ahk3* as the increase in leaf area between week three and four was only six-fold. After week four, leaf eight did not grow significantly further in both genotypes. However, leaf eight was about five times bigger in wild type compared to *ahk2ahk3*.

After exposure to photoperiod stress, lesion formation was absent in leaf eight of three-week-old wild-type and *ahk2ahk3* plants (Figure 24B). With age, the percentage of leaf eight lesion formation increased in both genotypes, but it increased earlier in *ahk2ahk3*. 20 % of four-week-old wild-type plants had an eighth leaf that was lesioned, whereas, in comparison, lesion formation was increased four-fold in *ahk2ahk3*. Moreover, the photosynthetic capacity was reduced significantly in leaf eight of four-week-old *ahk2ahk3* plants compared to wild type (Figure 24C). At the molecular level, H_2O_2 accumulated to a greater extend in leaf eight of five-week-old plants (Figure 24D). In agreement with lesion formation, about 35 times more H_2O_2 accumulated in leaf eight of four-week-old *ahk2ahk3* plants compared to wild-type of the same age.

To sum up, the sensitivity of plants as well as of distinct leaves to photoperiod stress increased with age in both wild type and *ahk2ahk3* and after four weeks of growth, *ahk2ahk3* was already as sensitive to photoperiod stress as after five weeks.

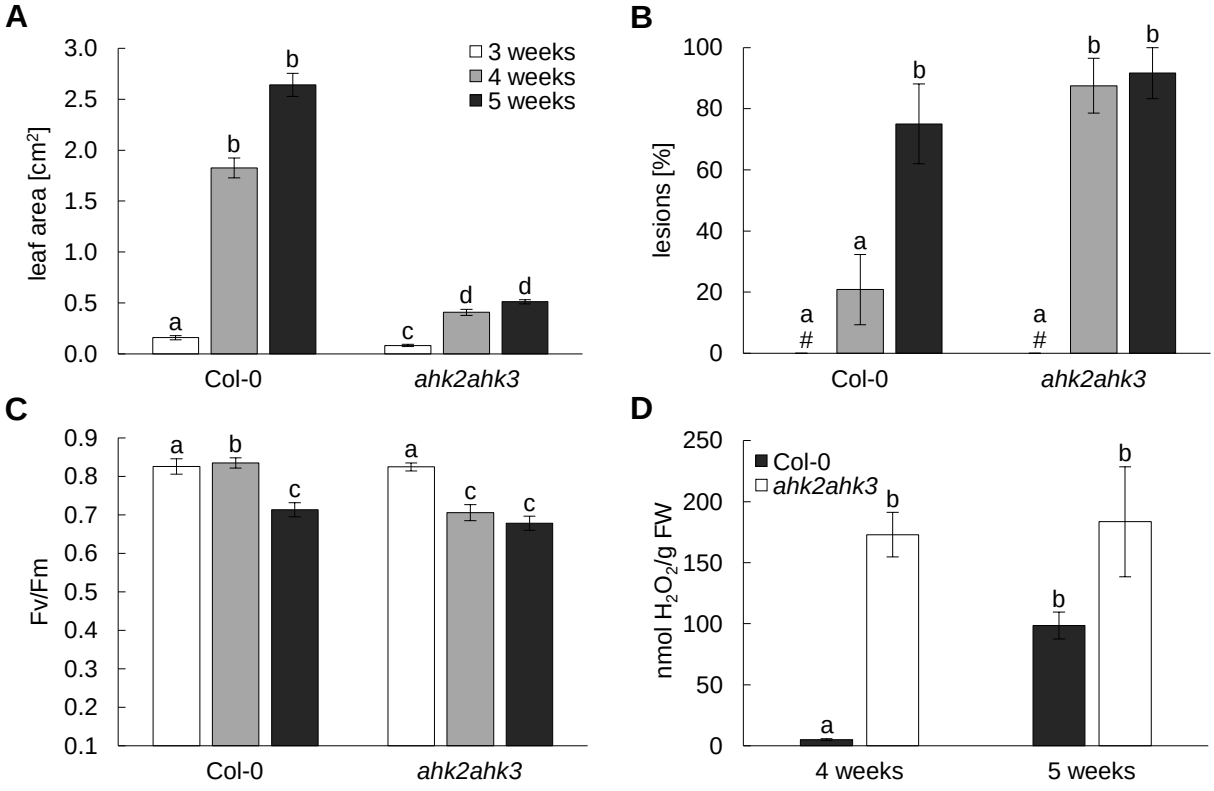

Figure 24: The responsiveness to photoperiod stress depends on the leaf age.
(A) Areas of leaf eight of three-, four- and five-week-old SD-grown wild-type and ahk2ahk3 *control plants (n = 10). (B) Percentage of leaf eight lesion formation in three-, four- and five-week-old plants the day after PCD-inducing night (n = 12). # indicates that no lesions were visible. (C) Photosystem II maximum quantum efficiency (Fv/Fm) of leaves evaluated in B (n = 12). (D) H_2O_2 levels in leaf eight of four- and five-week-old plants 15 h after the PLP-treatment (n = 4). Letters indicate significant differences between groups (p ≤ 0.05). Error bars indicate SE.*

3.2.4 Establishment of tissue-specific cytokinin decreases influences the sensitivity to photoperiod stress

As shown in 3.1.3, root-derived *t*Z-type cytokinins are important to protect plants from photoperiod stress. To further elaborate which tissues are involved in determining the cytokinin-dependent sensitivity to photoperiod stress, plants were exposed to a PLP that have a reduced cytokinin content by overexpressing *CKX1* under the constitutively active *35S* promoter (Werner *et al*., 2003), the meristem-specific *WUSCHEL* (*WUS*) promoter and the vasculature- and meristem-specific *CLAVATA1* (*CLV1*) promoter (Otto, 2013). Moreover, lines overexpressing *CKX1-4xMyc* under the leaf epidermis-specific *ARABIDOPSIS THALIANA MERISTEM LAYER* (*ATML)* promoter (Werner, 2016) as well as under the vasculature(phloem)-specific *SUCROSE-PROTON SYMPORTER2* (*SUC2*) promoter (created in this thesis, further information can be taken from Supplemental Figure 2) were exposed to photoperiod stress.

Except for *WUS::CKX1* #14, lesion formation was increased in all lines compared to wild type (Figure 25A). 90 % of *SUC2::CKX1-4xMyc* #23 leaves were lesioned, which was four times more than in wild type and the highest lesion formation percentage of all lines tested. Similarly, all lines tested had a reduced Fv/Fm except for *WUS::CKX1* #14 (Figure 25B). In agreement with the formation of lesions, the lowest Fv/Fm was detected in *SUC2::CKX1-4xMyc* #23.

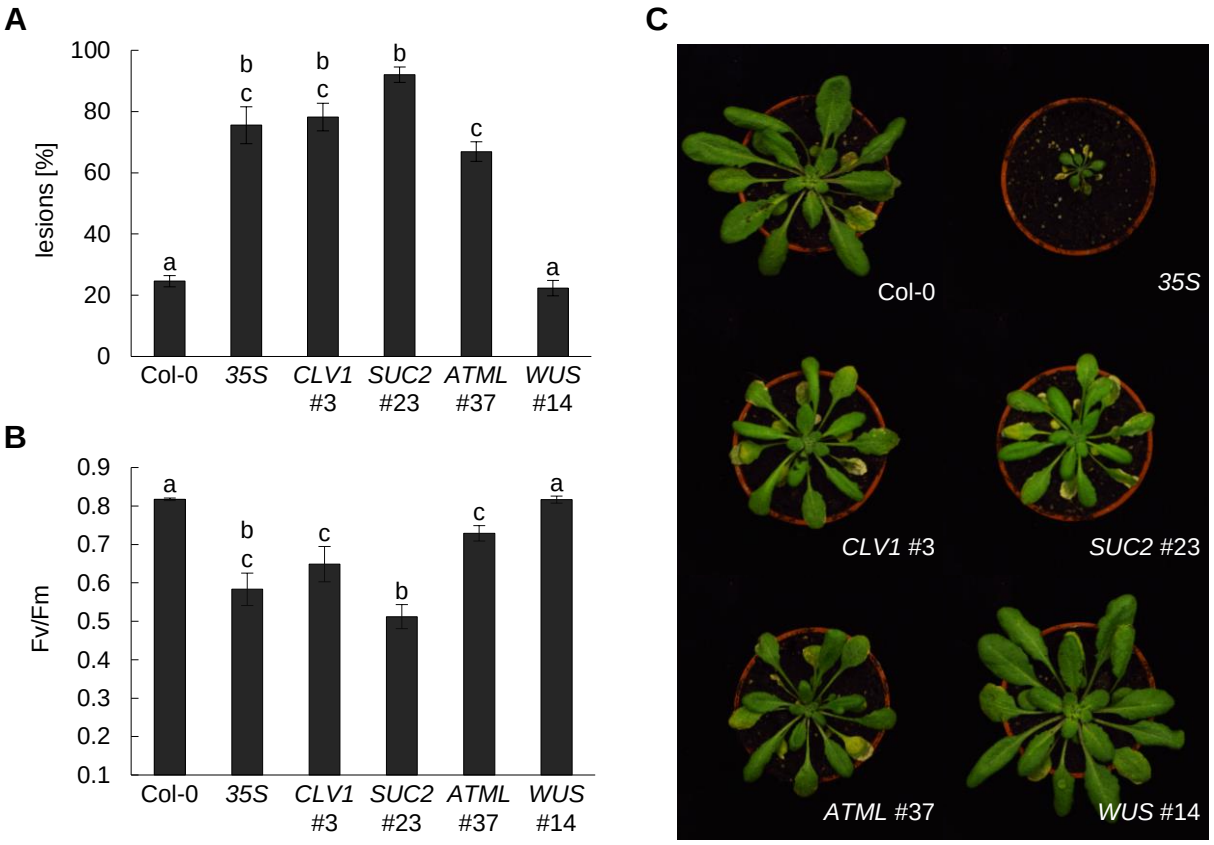

Figure 25: A tissue specific* CKX1 *overexpression results in an increased photoperiod stress sensitivity. *(A) Lesion formation of five-week-old Col-0,* 35S::CKX1 *(*35S*),* CLV1::CKX1-4xMyc *(*CLV1*),* SUC2::CKX1-4xMyc *(*SUC2*),* ATML::CKX1::4xMyc *(*ATML*) and* WUS::CKX1 *(*WUS*) plants the day after the PLP (n ≥ 12). (B) PAM measurements of leaves the day after PCD-inducing night (n = 15). (C) Pictures of representative plants after photoperiod stress treatment. Letters indicate significant differences between groups (p ≤ 0.05). Error bars indicate SE.*

All in all, overexpression of *CKX1* in both the vasculature (*SUC2* and *CLV1* lines) and leaf epidermis (*ATML* lines) caused an increase in photoperiod stress sensitivity displayed by an increased lesion formation and reduced photosynthetic capacity.

3.2.5 The responsiveness to photoperiod stress varies in different tissues

As *t*Z-type cytokinins are mainly formed in root tissue, expression of photoperiod stress marker genes and of genes involved in cytokinin synthesis and metabolism was analyzed in wild type and *ahk2ahk3*. At the end of the PLP treatment, no differences in *BAP1* and *ZAT12* transcript abundance was detected between leaf and root tissue (Figure 26A, B). 15 hours after experiencing the prolonged light period, transcript levels of *BAP1* and *ZAT12* did not differ between both genotypes in roots whereas *BAP1* (and in tendency *ZAT12*) abundance was increased threefold in *ahk2ahk3* leaves compared to wild type. As a control of tissue purity, abundance of *CAB2* was determined. While *CAB2* expression was detected in leaf samples of both genotypes, *CAB2* abundance was very low in root samples (Figure 26C).
Moreover, the abundance of *BAP1* and *ZAT12* was not affected by photoperiod stress in roots of both genotypes compared to their respective control samples (Figure 26D, E). Similarly, the abundance of *IPT3*, *CYP735A1*, *CYP735A2*, *ABCG14* and *LOG8* was unaffected by photoperiod stress (Figure 26F – J). Summing up, the transcriptional response of wild type and *ahk2ahk3* to photoperiod stress was different in roots and leaves.

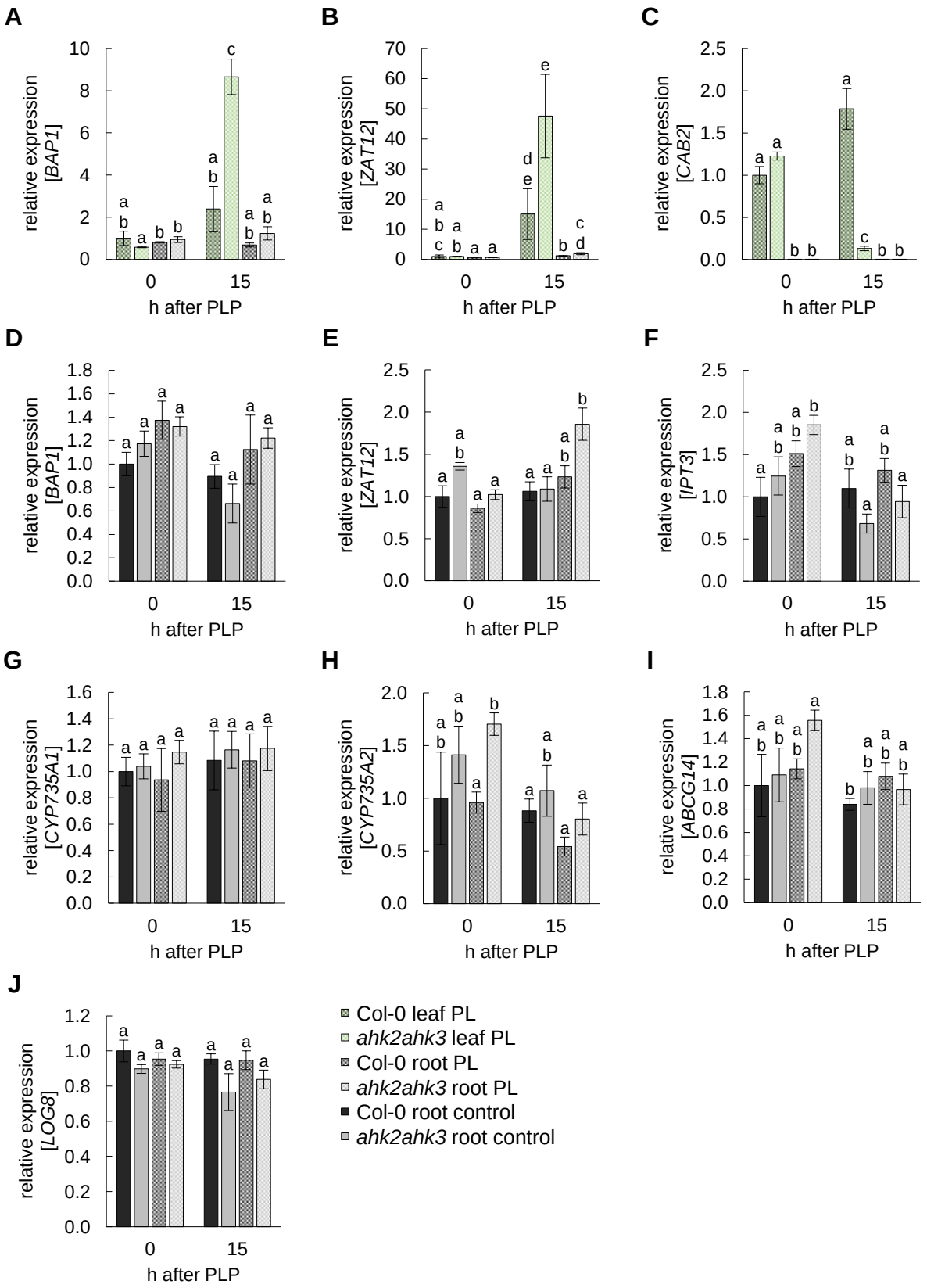

Figure 26: Leaves and roots respond differently to photoperiod stress.
*(A - C) Expression of marker genes (*BAP1, ZAT12, CAB2*) 0 h and 15 h after the PLP-treatment in PL shoots and roots of ahk2ahk3 and wild type (Col-0). Expression of* BAP1 *(D),* ZAT12 *(E),* IPT3 *(F),* CYP735A1 *(G),* CYP735A2 *(H),* ABCG14 *(I) and* LOG8 *(J) 0 h and 15 h after the PLP-treatment in control and PL roots of* ahk2ahk3 *and wild type. Letters indicate significant differences between groups (p ≤ 0.05; n ≥ 3). Error bars indicate SE.*

3.3 Formation of photoperiod stress requires the perception of auxin and ethylene

3.3.1 Photoperiod stress treatment increases content of free IAA in wild-type plants

The contents of bioactive free IAA and its irreversibly inactivated derivatives oxIAA, IAA-Asp and IAA-Glu were measured in the same leaf samples used for cytokinin measurements in section 3.1.1. During PLP-treatment (time points 1 and 2), PL plants and respective control plants did not differ in their IAA content (Figure 27B).

As the night after the PLP-treatment progressed (time points 3 and 4), endogenous IAA content increased in PL plants compared to the respective controls. At the end of the night (time point 4), IAA content was increased two-fold. In comparison, oxIAA levels were unchanged at all time points (Figure 27C)Figure 27. The most pronounced differences were detected for the content of IAA-Asp (Figure 27D). While it was decreased at the end of PLP-treatment (time point 2), it was increased 4.5-fold and 3.5-fold at the end of the night after the PLP-treatment and at the end of the following day, respectively. IAA-Glu levels were reduced directly after the PLP-treatment, in the middle of the night following the PLP and at the end of the following day (Figure 27E; time points 2, 3 and 5). All in all, contents of both bioactive IAA as well as its irreversibly inactivated derivative IAA-Asp increased due to exposure to a PLP followed by darkness.

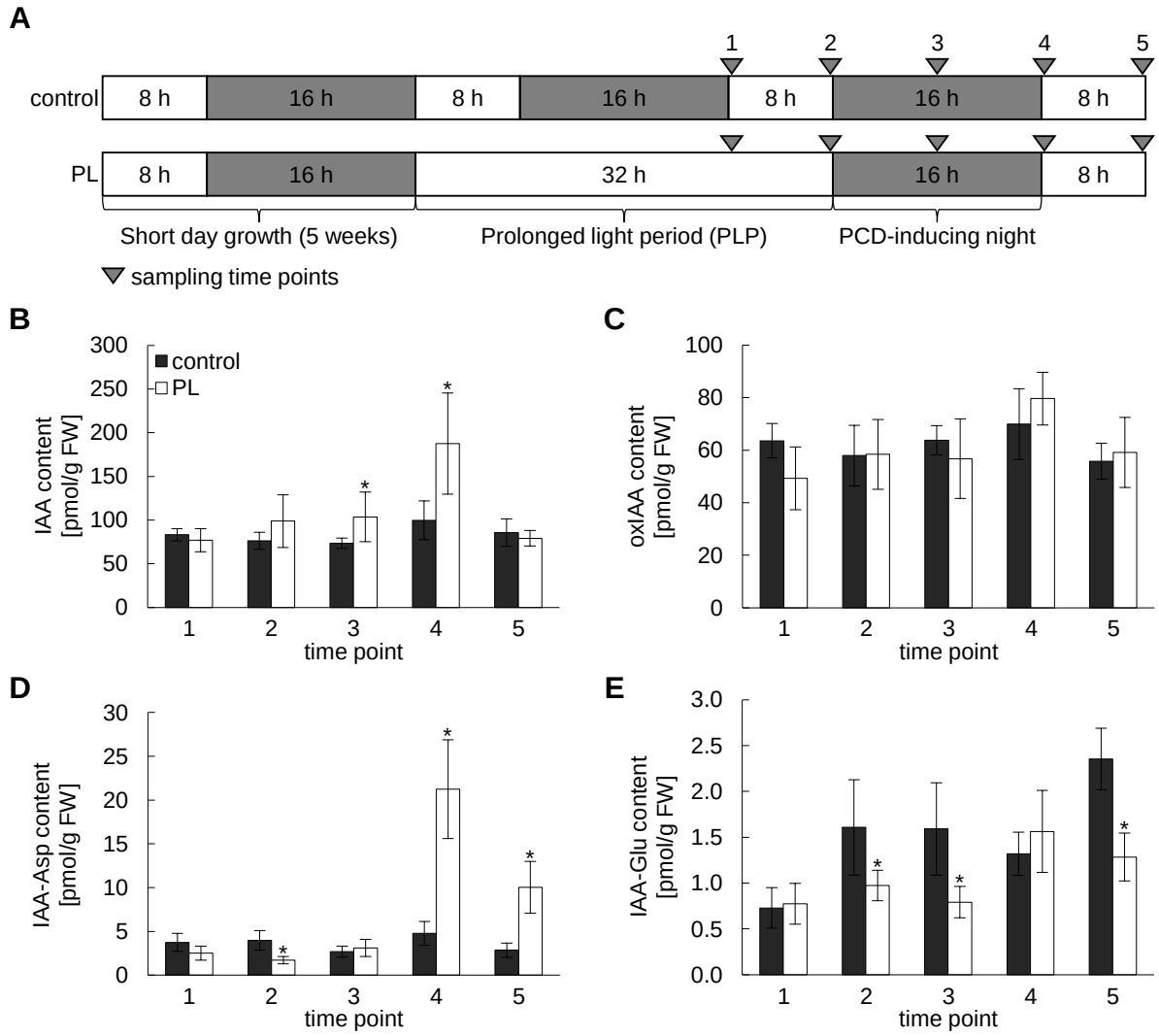

Figure 27: Photoperiod stress causes an increased content of IAA and IAA-Asp in wild-type plants.
(A) Schematic overview of sampling time points for IAA measurements. five-week-old wild type plants were either cultivated under SD conditions (control) or were treated with a prolonged light period (PLP) of 32 h (PL). (B - E) Content of free IAA (B), oxIAA (C), IAA-Asp (D) and IAA-Glu (E) in control samples and PL samples at the time points depicted in A. Stars indicate statistically a significant difference between PL and respective control samples at the given time point (1 - 5) in a paired Student's t-test ($p \leq 0.05$). Error bars indicate SD ($n \geq 3$).

3.3.2 GH3 *transcripts are more abundant in response to photoperiod stress*

To investigate whether changes in IAA and IAA-Asp content of wild-type plants are also reflected at the transcriptional level and whether photoperiod stress sensitive *ahk2ahk3* plants respond differently, genes involved in auxin metabolism were analyzed via RNAseq and qRT-PCR during the night after the PLP-treatment (Figure 28). Except for *TAA1*, the abundance of all other genes was not significantly altered in *ahk2ahk3* compared to wild type under control conditions (Figure 28B , see also Supplemental Figure 3A for the confirmation via qRT PCR).

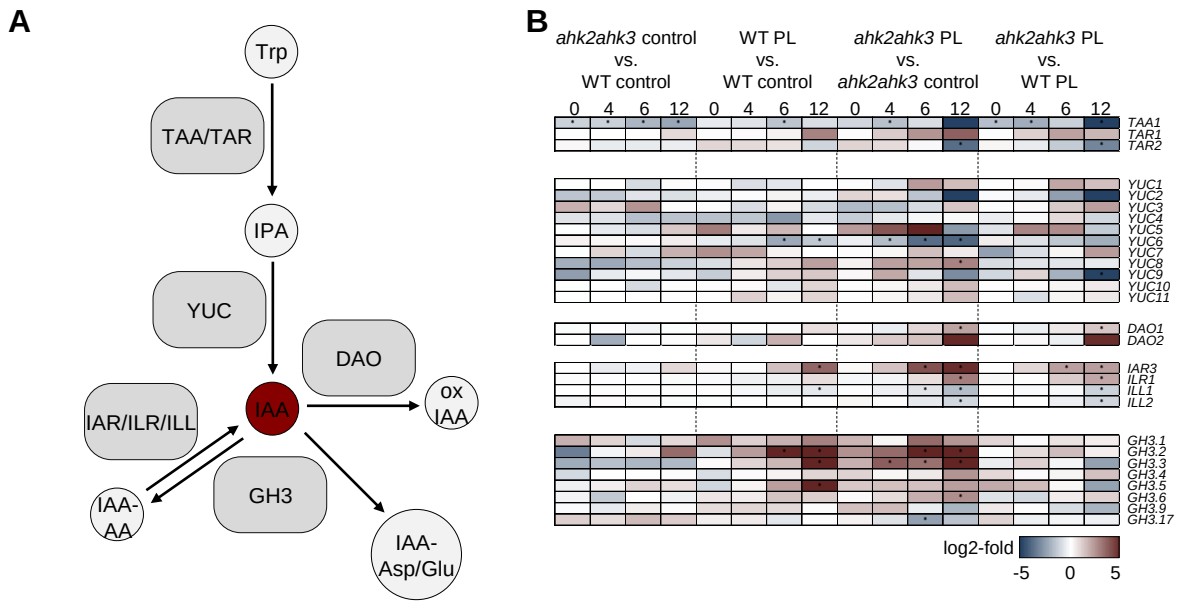

Figure 28: Expression of auxin biosynthesis and metabolism genes during photoperiod stress in wild type and* ahk2ahk3*.
(A) Schematic presentation of auxin biosynthesis and metabolism. First, TRYPTOPHAN AMIDOTRANSFERASE OF ARABIDOPSIS (TAA1) and TAA-RELATED (TAR) proteins convert tryptophan (Trp) to indole-3-pyruvic acid (IPA), which is converted to bioactive free IAA by YUCCA (YUC) proteins. IAA can be inactivated irreversibly to 2-oxoindole-3-acetic acid (oxIAA) by DIOXYGENASE FOR AUXIN OXI-DATION (DAO) proteins or to either indole-3-acetic acid aspartic acid (IAA-Asp) and indole-3-acetic acid glutamic acid (IAA-Glu) by GRETCHEN HAGEN3 (GH3) proteins. GH3s also catalyze the reversible inactivation to other IAA-amino acid conjugates. Reversion of the reaction is catalyzed by IAA-ALANINE RESISTANT3 (IAR3), IAA-LEUCINE RESISTANT1 (ILR1) and IAA-LEUCINE RESISTANT-LIKE (ILL) proteins. (B) Transcriptional regulation 0, 4, 6 and 12 hours after the PLP (PL plants) compared to respective control plants. Stars indicate a significant difference between groups ($p \leq 0.05$; $n = 3$).

Most changes in transcript abundance were detected 6 and 12 hours after the PLP-treatment in both wild type and *ahk2ahk3*. The abundance of *IAR3*, *GH3.2*, *GH3.3* and *GH3.5* was increased 12 hours after the PLP-treatment in wild-type PL plants compared to control plants while the *YUC6* and *ILL1* abundance was decreased 2.7-fold and 1.5-fold, respectively. A similar regulation could be observed in *ahk2ahk3* PL plants compared to control plants. Most genes differently expressed in wild type were also differently expressed in *ahk2ahk3* but already 4 and 6 hours after the PLP. Additionally, the abundance of *YUC8*, *DAO1* and *ILR1* was increased while the abundance of *TAR2* and *ILL2* was decreased 14-fold and two-fold in *ahk2ahk3* PL plants 12 hours after the PLP-treatment. Supportive for a stronger response of *ahk2ahk3* to photoperiod stress were differences in the transcript abundance of most previously mentioned genes in *ahk2ahk3* PL plants when compared to wild-type PL plants.

Like the differential expression of auxin metabolism genes, the abundance of auxin signaling genes did not differ in control plants of wild type and *ahk2ahk3* (Figure 29B). In wild type PL, the abundance of *TIR1* and *AFB5* was decreased twofold and 2.2-fold compared to control plants 12 hours after the PLP as well as the abundance of *IAA8* and *IAA12* and several *ARF* transcripts (confirmation of changes in *TIR1* abundance can be found in Supplemental Figure 3B). In addition, *IAA2*, *IAA10* and *IAA19* were more abundant as well as *ARF7*. In comparison to *ahk2ahk3* control, the abundance of the previously mentioned genes was also changed in *ahk2ahk3* PL 12 hours after the PLP-treatment but more strongly (e.g. *AFB5*; WT PL vs control: twofold decreased, *ahk2ahk3* PL vs control: ~eight-fold decreased). As seen for the expression of auxin metabolism genes, The abundance of these genes was different

between *ahk2ahk3* PL and *ahk2ahk3* control already 4 and 6 hours after the PLP and the difference was stronger 12 hours after the PLP. In addition, a changed abundance of several more *AFB*, *IAA* and *ARF* transcripts was detected.

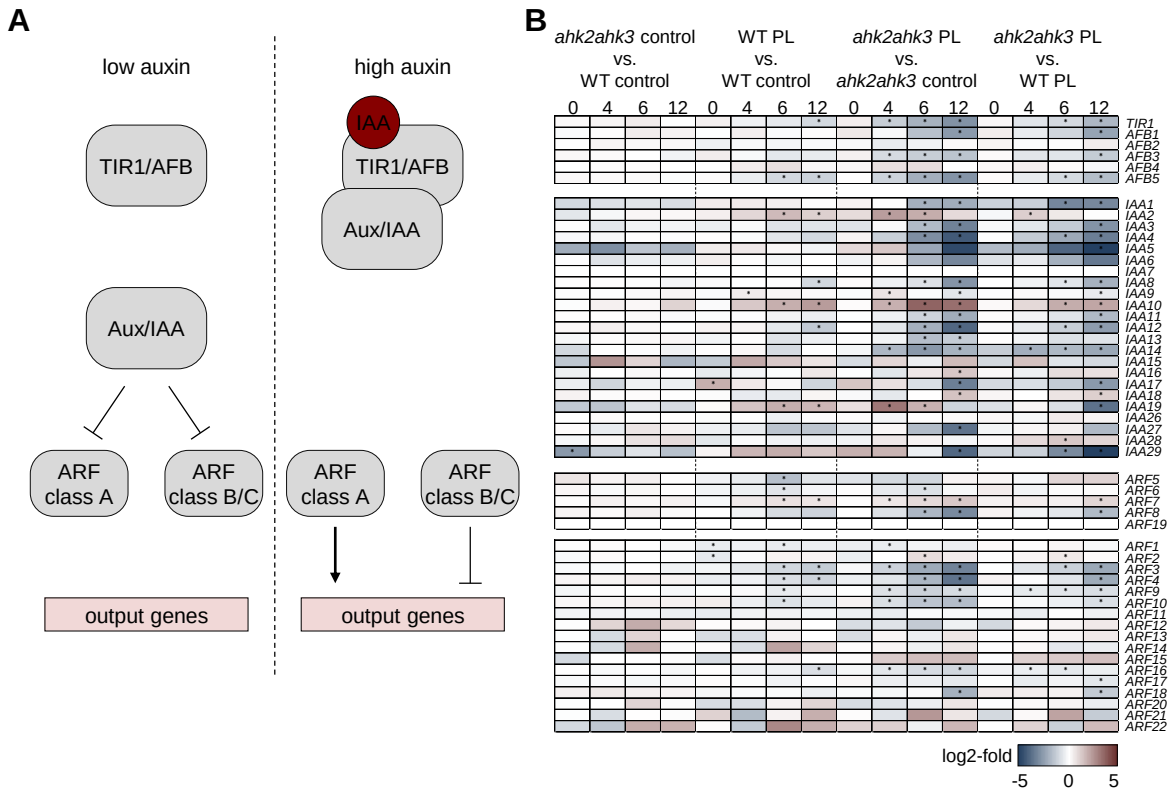

***Figure 29: Expression of auxin signaling genes during photoperiod stress in wild type and* ahk2ahk3.**
(A) Schematic presentation of auxin signaling. In absence of auxin (IAA), TRANSPORT INHIBITOR RESISTANT1 (TIR1)/AUXIN SIGNALING F-BOX (AFB) receptors are inactive. Consequently, Aux/IAA proteins inhibit the function of class A, B and C AUXIN RESPONSE FACTOR (ARF) transcription factors. With perception of IAA by TIR1/AFB receptors, the latter inhibit Aux/IAA function by mediating their ubiquitin-dependent degradation. In consequence, class A ARFs act as transcriptional activators whereas class B and C ARFs mostly act as transcriptional repressors. (B) Transcriptional regulation 0, 4, 6 and 12 hours after the PLP (PL plants) compared to respective control plants. Stars indicate a significant difference between groups ($p \leq 0.05$; $n = 3$).

In comparison with wild-type PL plants, the transcript abundance of the previously mentioned genes was also changed in the same direction as in *ahk2ahk3* PL plants, even though the differences were less pronounced. Summing up, the alterations in the abundance of auxin metabolism and signaling genes in response to photoperiod stress were more pronounced in *ahk2ahk3* plants compared to wild type.

3.3.3 Plants with an impaired auxin perception are less sensitive to photoperiod stress

As many auxin metabolism and signaling genes were differently regulated, plants with an altered auxin status were exposed to photoperiod stress. With an increasing impairment in auxin perception, plants became less photoperiod stress sensitive (Figure 30). While ca. 25 % of wild-type leaves formed lesions, less than 10 % of *tir1afb2afb3* leaves did (Figure 30A). Furthermore, all respective single mutants as well as *tir1afb2* did not differ from wild type in their photoperiod stress sensitivity. Except for *ahk2ahk3*, no receptor mutant differed in its Fv/Fm from wild type (Figure 30B).

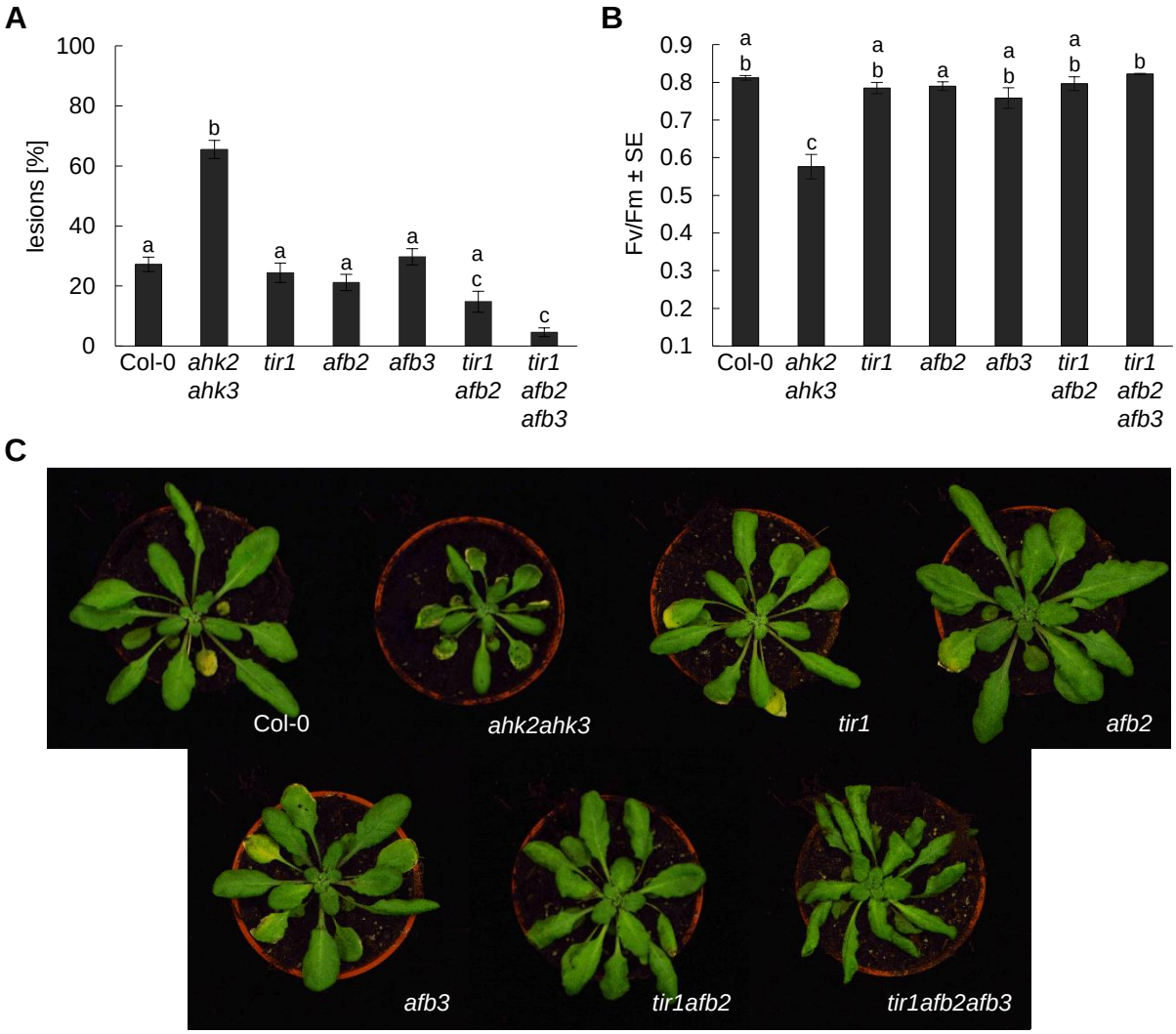

Figure 30: Plants impaired in auxin perception are less sensitive to photoperiod stress.
(A) Lesion formation of leaves at five-week-old Col-0*,* ahk2ahk3*,* tir1*,* afb2*,* afb3*,* tir1afb2 *and* tir1afb2afb3 *plants the day after the PCD-inducing night (n ≥ 12). (B) PAM measurements of leaves the day after PCD-inducing night (n = 15). (C) Pictures of representative plants that experienced a PLP. Letters indicate significant differences between groups (p ≤ 0.05). Error bars indicate SE.*

To further investigate an involvement of auxin in photoperiod stress, *tir1afb2afb3* plants as well as plants with an increased auxin status were tested not only phenotypically but also at the molecular level. While *tir1afb2afb3* plants were less sensitive to photoperiod stress, *yuc1D* plants, which have an increased auxin content, were more sensitive (Figure 31). In comparison to photoperiod sensitive *ahk2ahk3* plants, formation of lesions was less pronounced in *yuc1D* but Fv/Fm was similarly affected (Figure 31A, B). Moreover, *yuc1D* plants formed more H_2O_2 in comparison to wild type but less than *ahk2ahk3* (Figure 31C). At the transcriptional level, the abundance of *BAP1* and *ZAT12* did not differ between stressed wild-type plants and *tir1afb2afb3* 0 and 15 hours after the PLP (Figure 31D, E). 15 hours after the PLP, both genes were more abundant in *yuc1D* but still less than in *ahk2ahk3*. *CAB2* abundance decreased in wild type and *yuc1D* to a similar level 15 hours after the PLP (Figure 31F). In *ahk2ahk3*, its abundance was even further decreased to approximately a quarter of wild type level. Strikingly, no difference in abundance of *CAB2* was detected in *tir1afb2afb3* 15 h after the PLP treatment compared to 0 h.

To sum up, plants with an elevated auxin status were more sensitive to photoperiod stress while plants with a reduced auxin status were less sensitive.

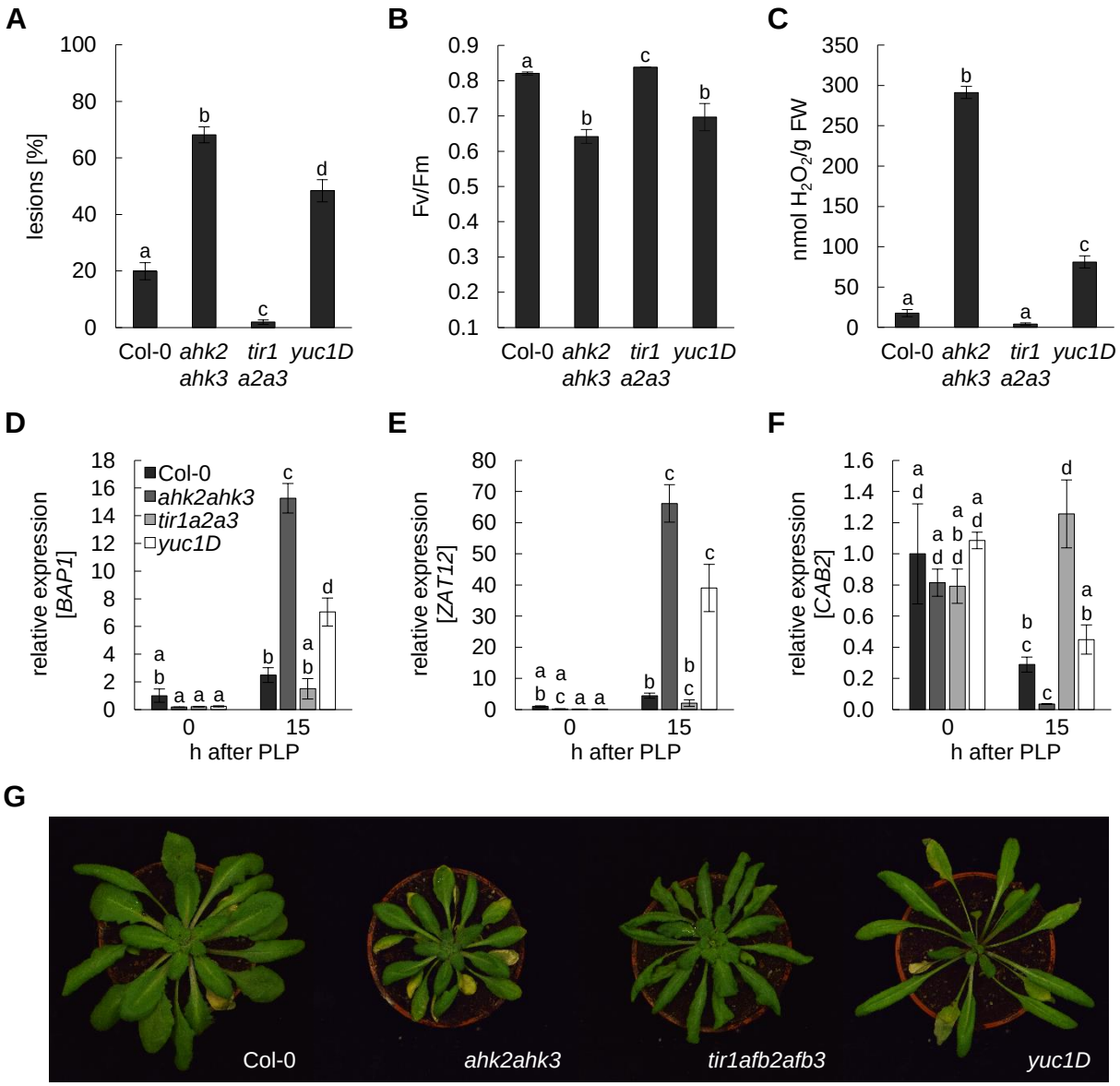

Figure 31: Plants with an increased auxin status are more sensitive to photoperiod stress.
(A) Lesion formation of leaves at five-week-old Col-0, ahk2ahk3, tir1afb2afb3 *(*tir1a2a3*) and* yuc1D *plants the day after the PCD-inducing night (n = 15). (B) PAM measurements of leaves the day after PCD-inducing night (n = 15). (C)* H_2O_2 *measurements 15 h after the PLP-treatment (n = 4). (D - F) Expression of marker genes (*BAP1, ZAT12, CAB2*) 0 h and 15 h after the PLP-treatment (n ≥ 3). (G) Pictures of representative plants that experienced a PLP. Letters indicate significant differences between groups (p ≤ 0.05). Error bars indicate SE.*

3.3.4 Impairment in auxin perception reduces photoperiod stress sensitivity of cytokinin signaling mutants

As impairment in auxin perception caused a reduction in photoperiod stress sensitivity and plants with an impaired cytokinin perception were more sensitive to photoperiod stress, a genetic interaction of both hormones was tested by generating crosses between *ahk2ahk3* and *tir1afb2afb3* and by exposing the

generated crosses to photoperiod stress. Compared to *ahk2ahk3*, lesion formation was ~ 50 % reduced in *ahk2ahk3tir1afb2* plants but it was still six times higher than in *tir1afb2afb3* (Figure 32A).

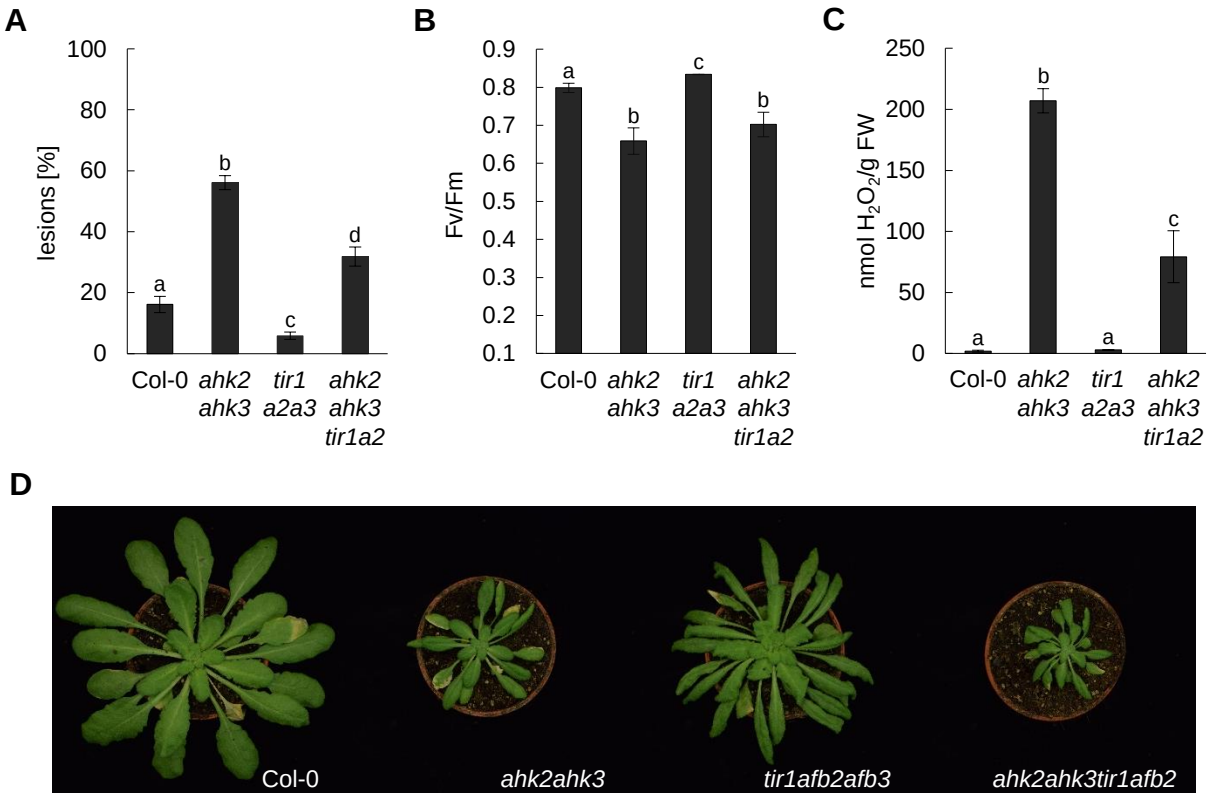

Figure 32: An impairment of auxin perception in* ahk2ahk3 *decreases the sensitivity to photoperiod stress. *(A) Lesion formation of leaves at five-week-old* Col-0*,* ahk2ahk3*,* tir1afb2afb3*(*tir1a2a3*) and* ahk2ahk3tir1afb2 *(*ahk2ahk3tir1a2*) plants the day after the PCD-inducing night (n ≥ 10). (B) PAM measurements of leaves the day after PCD-inducing night (n = 15). (C) H_2O_2 measurements 15 h after the PLP-treatment (n = 4). (D) Pictures of representative plants that experienced a PLP. Letters indicate significant differences between groups (p ≤ 0.05). Error bars indicate SE.*

Moreover, *ahk2ahk3* and *ahk2ahk3tir1afb2* showed a similar drop in Fv/Fm after exposure to photoperiod stress (Figure 32B). The molecular response, reflected by the content of H_2O_2, was similar to the percentage of lesion formation, as in *ahk2ahk3tir1afb2* less H_2O_2 was detected than in *ahk2ahk3* (Figure 32C). All in all, an impairment of auxin perception in *ahk2ahk3* partially reduced the photoperiod stress responsiveness.

3.3.5 The abundance of genes involved in ethylene synthesis is increased in plants in the night after exposure to a prolonged light period

To examine whether and how ethylene is involved in the formation of photoperiod stress, transcriptional regulation of genes involved in ethylene metabolism was investigated in wild-type and *ahk2ahk3* plants. Except for *ACS6*, which was 3.5-fold more abundant 12 hours after exposure to a PLP, no other transcripts differed in their abundance in *ahk2ahk3* control plants compared to wild type at any time point (Figure 33B).

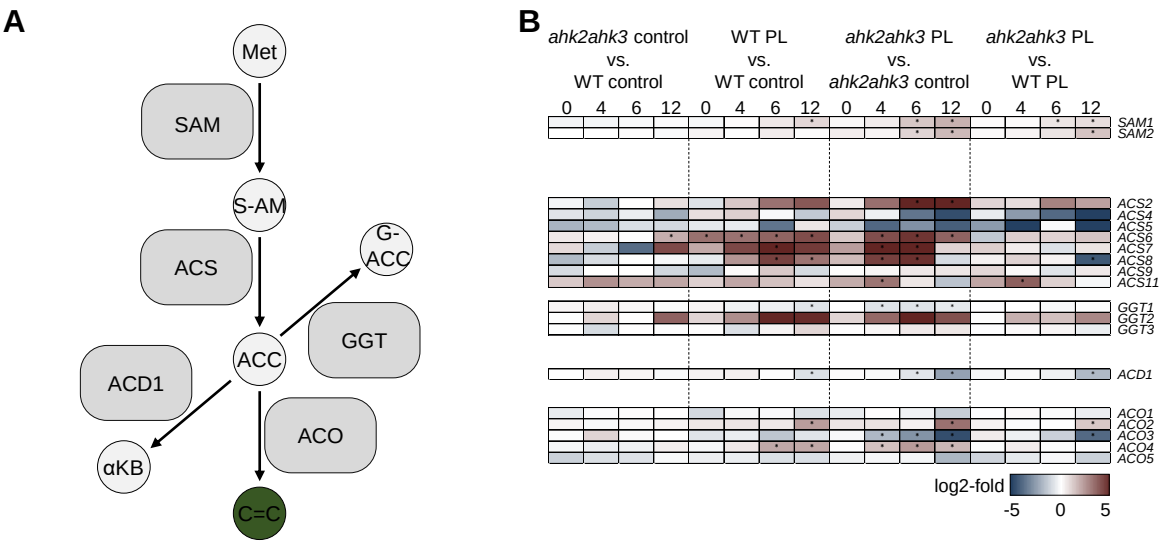

***Figure 33: Expression of ethylene biosynthesis and metabolism genes during photoperiod stress in wild type and* ahk2ahk3.**
(A) Schematic presentation of ethylene metabolism. First, SAM-SYNTHETASE (SAM) proteins convert methionine (Met) to S-adenosyl-L-methionine (S-AM), which is converted to 1-aminocyclopropane-1-carboxylic acid (ACC) by ACC-SYNTHASE (ACS) enzymes. ACC can be formed to either α-ketobutyrate (αKB) by ACC DEAMINASE1 (ACD1) or γ-glutamyl-ACC (G-ACC) by γ-GLUTAMYL-TRANSPEPTIDASE (GGT) proteins. Ethylene itself (C=C) is synthesized from ACC by ACC-OXIDASE (ACO) enzymes. Please note that other ACC conjugates exist that are not depicted in this figure. (B) Transcript levels 0, 4, 6 and 12 hours after the PLP-treatment in either PL plants or control plants of wild type and ahk2ahk3. Stars indicate a significant difference between groups at the given time point after Bonferroni correction (p ≤ 0.05; n = 3).

In wild-type PL plants, *SAM1*, *ACS6*, *ACS7* and *ACS8*, *ACO2* and *ACO4* were more abundant compared to respective control plants mostly 12 hours after the PLP-treatment. The transcript abundance of *ACS6* was increased at all time points. In addition, *GGT1* (12 hours after the PLP) and *ACD1* (12 hours after the PLP-treatment) were less abundant. A similar - but mostly stronger - change in gene expression than in wild type was observed by comparing *ahk2ahk3* PL plants with respective control plants. Furthermore, *ACS6* and *ACS7* were more abundant already 4 hours after the PLP-treatment *GGT1* was less abundant. In case of *ACD1*, a 1.5-fold decreased abundance was observed 6 hours after the PLP. The abundance of *SAM2* (6 and 12 hours after the PLP) and *ACO3* (4, 6, and 12 hours after the PLP) was increased and decreased in addition to the formerly mentioned genes in *ahk2ahk3*. The expression pattern of *SAM2* and *ACO3* similar in *ahk2ahk3* PL plants compared to wild-type PL plants 12 hours after exposure to the PLP. In addition, the abundance of *SAM1* and *ACO2* was increased 1.7-fold and 2.4-fold and abundance of *ACS8* was decreased 20-fold 12 hours after the PLP-treatment.

Apart from transcriptional regulation of genes involved in ethylene metabolism, the transcript abundance of genes involved in ethylene signaling was analyzed via RNAseq. Wild type control and *ahk2ahk3* control did not differ in expression of these genes (Figure 34B). 6 hours after the PLP-treatment, the abundance of *ETR1*, *ERS1*, *ERS2*, *EIN4*, *CTR1* and *EIN3* was increased in wild-type PL plants compared to its respective control plants (qRT experiment to confirm changes in *ETR1* and *CTR1* can be found in Supplemental Figure 3C and D). A similar regulation was observed 12 hours after the PLP-treatment with the exception that *ETR1* was not regulated but *ETR2*. The expression of the previously mentioned genes in *ahk2ahk3* plants was like that in wild type. *ERS1* and *ERS2* were 2.2-fold and 1.5-fold more abundant already 4 hours after exposure to a PLP in PL plants, while the abundance of *EIN2*

was decreased onefold and 1.6-fold 4 and 6 hours after the PLP-treatment. Additionally, *EIL1* was less abundant 6 and 12 hours after the PLP. In comparison to wild-type PL plants, the abundance of *ETR1* and *CTR1* was increased 6 and 12 hours after the PLP-treatment in *ahk2ahk3* PL plants while the abundance of *EIL1* was decreased at those time points. Furthermore, the abundance of *ERS1* was increased 1.85-fold 4 hours after exposure to the PLP.

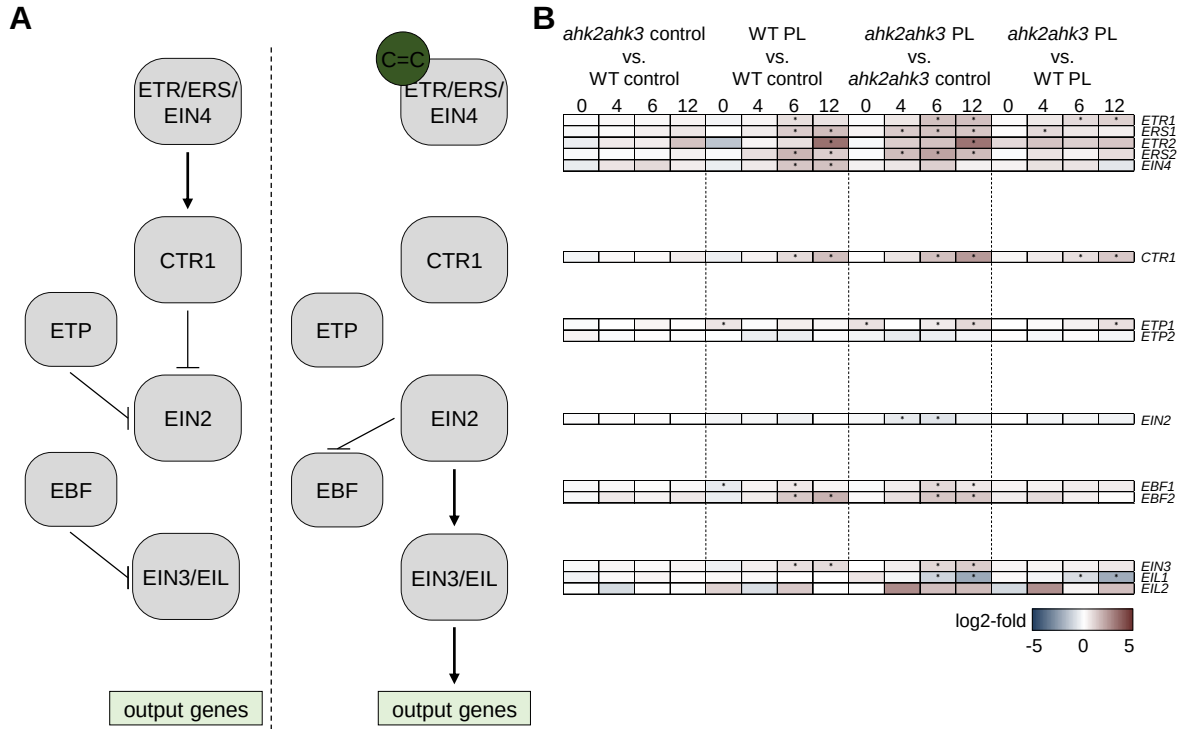

***Figure 34: Expression of ethylene signaling genes during photoperiod stress in wild type and* ahk2ahk3.**
(A) Schematic presentation of ethylene signaling. In absence of ethylene (C=C), ETHYLENE RESPONSE (ETR)/ETHYLENE RESPONSE SENSOR (ERS)/ETHYLENE INSENSITIVE4 (EIN4) receptors act as negative regulators of ethylene signaling by interacting with CONSTITUTIVE TRIPLE RESPONSE1 (CTR1), which inactivates EIN2. In addition, EIN2 can be degraded 26S proteasome-dependently, which is mediated by F-box proteins EIN2 TARGETING PROTEIN (ETP) F-box proteins. Because of EIN2 inactivation and degradation, EIN3/EIN3-LIKE1 (EIL1)/EIL2 transcription factors become degraded mediated by EIN3-BINDING F-BOX PROTEINs (EBFs). Upon ethylene perception, ETR/ERS/EIN4 receptors get inactive and consequently CTR1. This leads to an activation of EIN2, which stabilizes EIN3/EIL proteins and mediates EBF degradation, leading to the activation of ethylene-regulated genes. (B) Transcript levels 0, 4, 6 and 12 hours after the PLP in either PL plants or control plants of wild type and ahk2ahk3. Stars indicate a significant difference between groups at the given time point after Bonferroni correction ($p \leq 0.05$; $n = 3$).

Summing up, PLP-induced changes in transcript abundance were detected via RNAseq mostly for genes encoding ethylene receptors in both wild type and *ahk2ahk3*. Responses to photoperiod stress in *ahk2ahk3* were either stronger (e.g. *ETR1* transcription) or faster (*ERS1* transcription).

3.3.6 A constitutively active ethylene pathway protects plants from photoperiod stress

As transcriptional analysis of wild type and *ahk2ahk3* indicated an influence of photoperiod stress on the transcription of genes involved in ethylene metabolism and signaling, it was investigated whether a difference in ethylene status has an influence on the photoperiod stress sensitivity of plants. To do so, mutants impaired either in ethylene perception or signaling were exposed to PLP. Compared to wild

type, lesion formation was doubled in *etr1-1* and *ein2* but less in comparison with *ahk2ahk3* (Figure 35A).

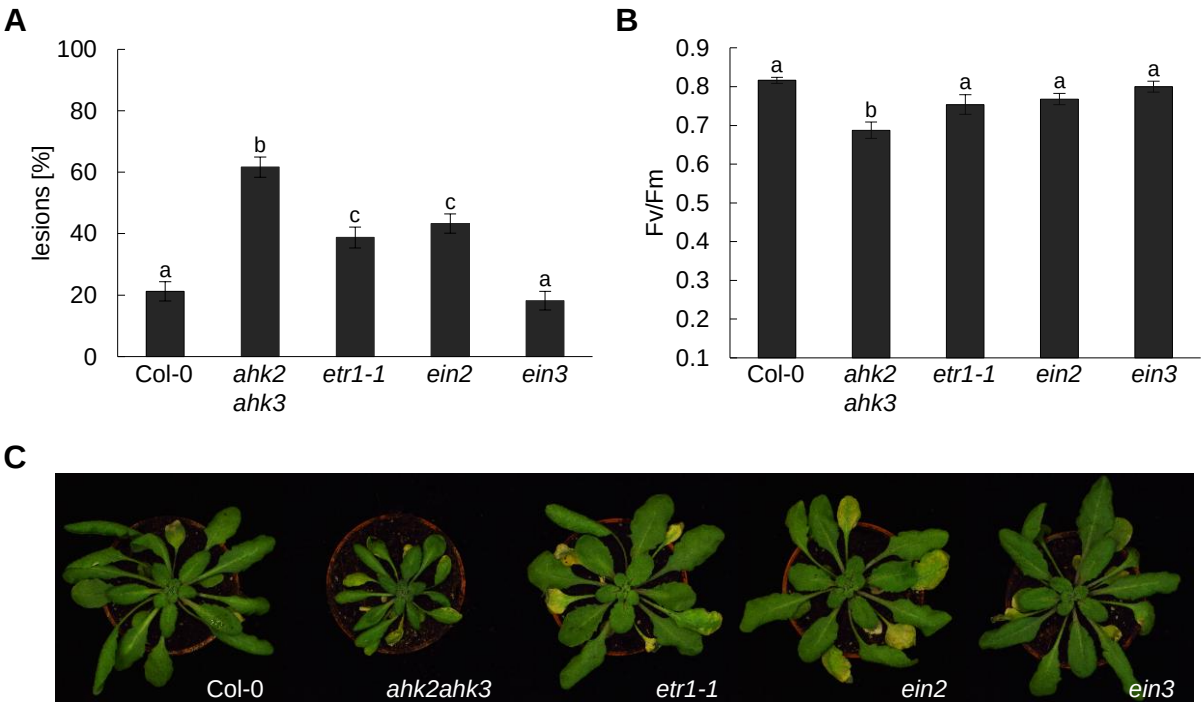

Figure 35: Plants with an impaired ethylene signaling are more sensitive to photoperiod stress.
(A) Lesion formation of leaves at five-week-old Col-0, ahk2ahk3, etr1-1, ein3 and ein2 plants the day after the PCD-inducing night (n≥13). (B) PAM measurements of leaves the day after PCD-inducing night (n = 15). (C) Pictures of representative plants that experienced a PLP. Letters indicate significant differences between groups (p ≤ 0.05). Error bars indicate SE.

Furthermore, Fv/Fm values were unchanged in all genotypes compared to wild type except for *ahk2ahk3* (Figure 35B). Importance of functional ethylene signaling was further supported by testing mutants having a constantly activated ethylene signaling. *ctr1-1* and *ctr1*/*sugar-insensitive1* (*sis1*) plants did not form any lesions in response to exposure to a PLP while *ahk2ahk3* had 2.5 times more lesions than wild type (Figure 36A).

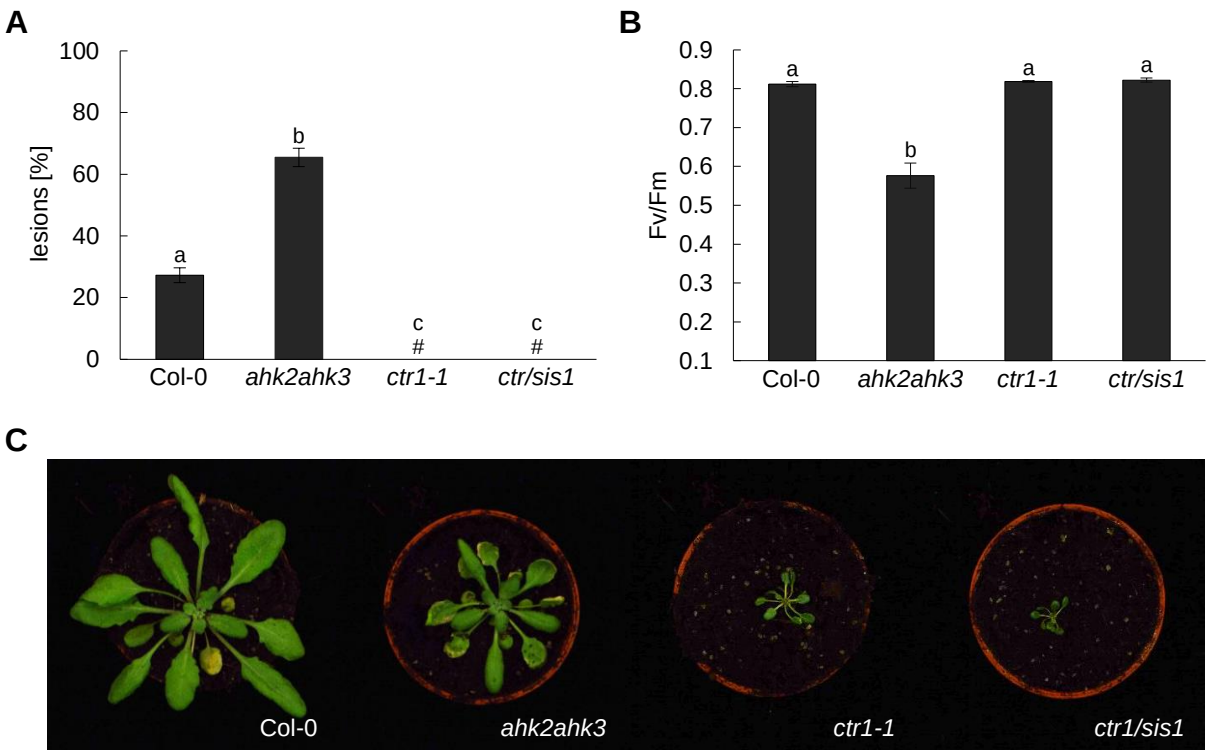

Figure 36: Loss of CTR1 causes a reduced sensitivity to photoperiod stress.
(A) Lesion formation of leaves at five-week-old Col-0, ahk2ahk3, ctr1-1 and ctr1/sis1 plants the day after the PCD-inducing night (n≥10). (B) PAM measurements of leaves the day after PCD-inducing night (n ≥ 14). (C) Pictures of representative plants that experienced a PLP. Letters indicate significant differences between groups (p ≤ 0.05). Error bars indicate SE.

Fv/Fm values of these mutants did not differ from wild type while that of *ahk2ahk3* was reduced (Figure 36B). Since *ctr1-1* and *ctr1/sis1* plants are strongly affected in growth (Figure 36C), ethylene receptor mutants, which are less growth-impaired, were exposed to photoperiod stress to exclude growth-related influences on the formation of photoperiod stress. Like *ctr* mutants, *etr1etr2ein4* and *etr2ein4ers2* did not form any lesions after exposure to photoperiod stress while *ahk2ahk3* did form 3.5 times more lesions compared to wild-type plants (Figure 37A). Furthermore, Fv/Fm was reduced in *ahk2ahk3* compared to wild type while *etr1etr2ein4* and *etr2ein4ers2* did not differ from wild type (Figure 37B).
To sum up, plants with a decreased ethylene status/impaired ethylene signaling were more sensitive to photoperiod stress whereas plants with an increased ethylene status/constantly active ethylene signaling were more sensitive to photoperiod stress.

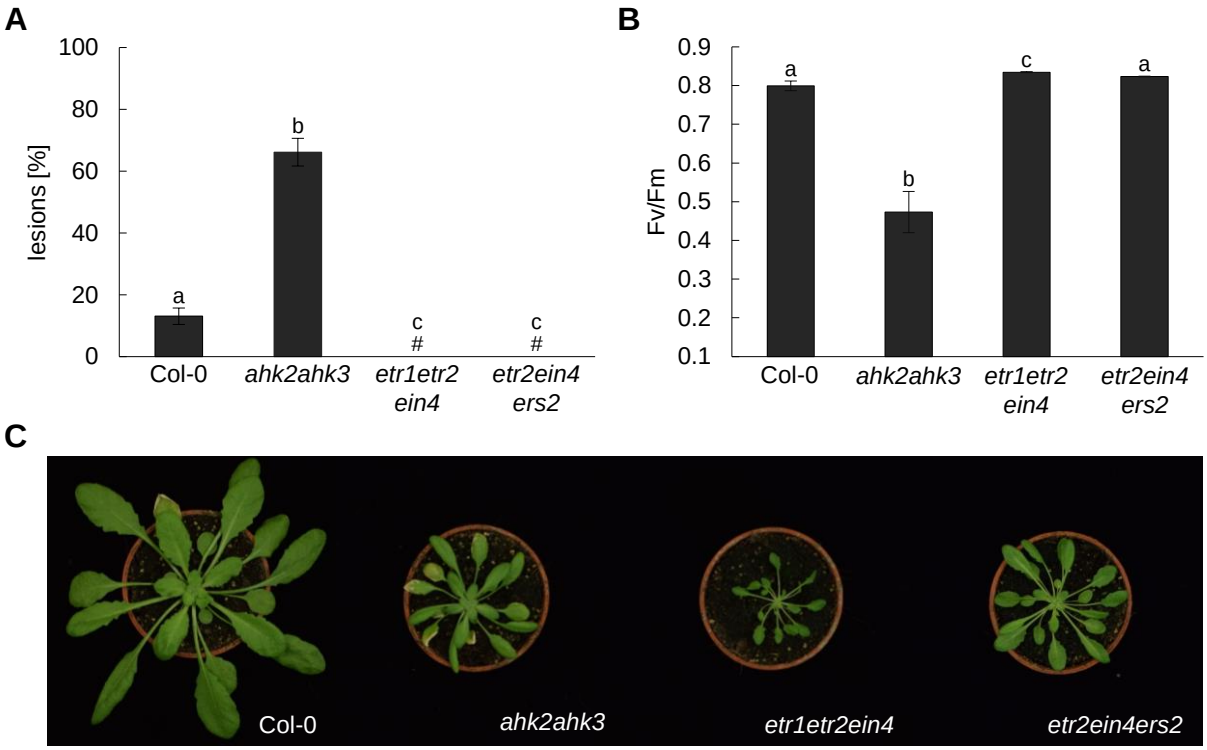

Figure 37: Loss of type-II ethylene receptors causes a reduced sensitivity to photoperiod stress.
(A) Lesion formation of leaves at five-week-old Col-0, ahk2ahk3, etr1etr2ein4 and etr2ein4ers2 plants the day after the PCD-inducing night (n ≥ 12). (B) PAM measurements of leaves the day after PCD-inducing night (n = 15). (C) Pictures of representative plants that experienced a PLP. Letters indicate significant differences between groups (p ≤ 0.05). Error bars indicate SE.

3.3.7 The GA content does not change in wild-type plants in response to a prolonged light period

In addition to auxin, different active GAs as well as their precursors and deactivated forms were measured in the same experimental setup used for cytokinin measurements in section 3.1.1. Of all active GA forms measured, GA_1 and GA_3 levels differed between control and PL plants. GA_1 levels were increased in PL plants after 24 hours of light by 50 % compared to control plants (Figure 38B; time point 1).

Furthermore, GA_3 levels were reduced in PL plants at the end of the night following PLP (Figure 38C; time point 4). Photoperiod stress did not induce changes in GA_5, GA_6 and GA_7 content (Figure 38D - F). Similarly, content of most bioactive GA-precursors was not altered upon photoperiod stress (Supplemental Figure 4). The only exception was content of GA_{13}, which was reduced by 40 % in PL samples compared to control in the middle of the night following PLP (Supplemental Figure 4B; time point 3).

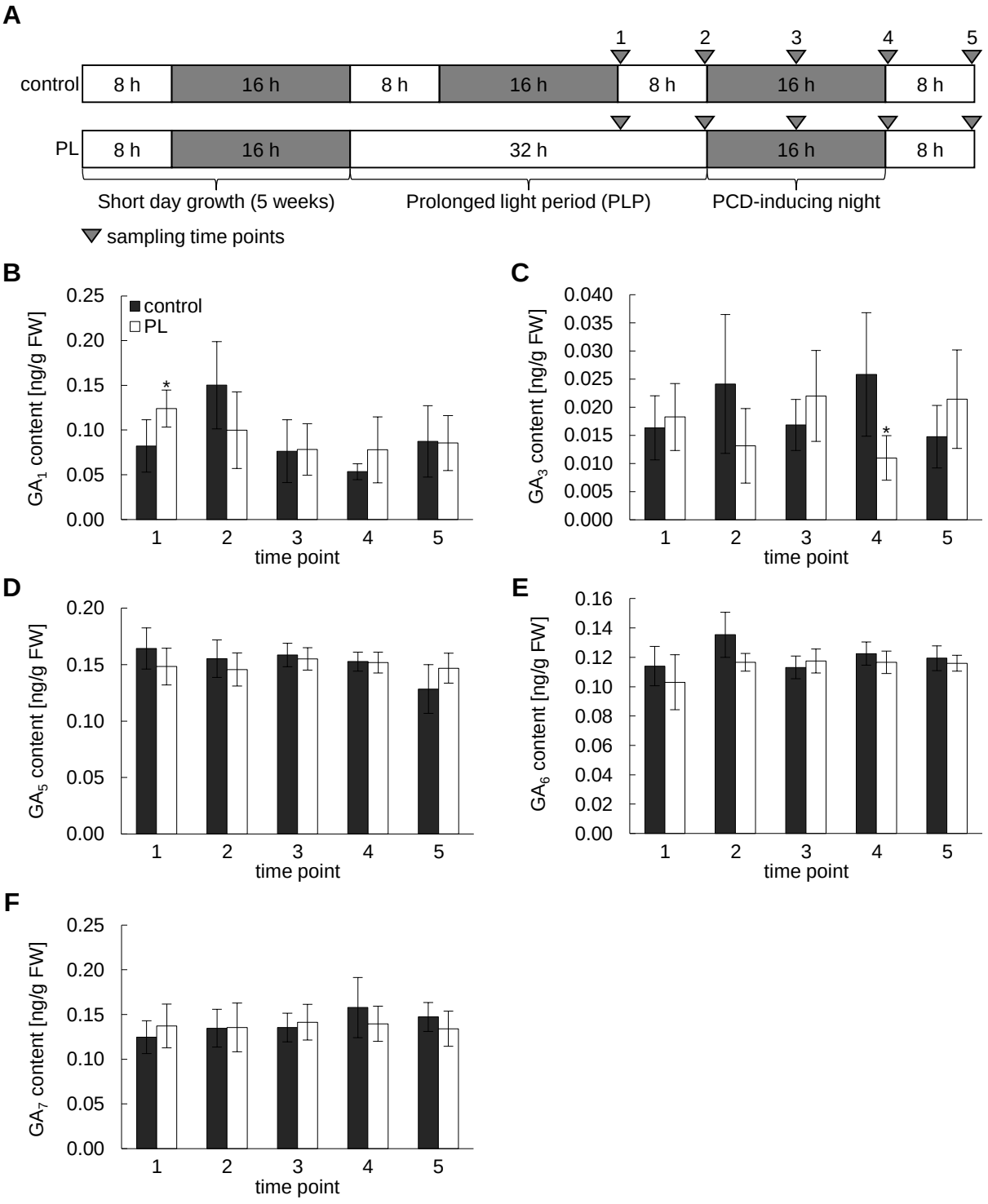

Figure 38: Photoperiod stress does not change levels of bioactive GAs in wild-type plants.
(A) Schematic overview of sampling time points for GA measurements. five-week-old wild type plants were either cultivated under SD conditions (control) or were treated with a prolonged light period (PLP) of 32 h (PL). (B - F) Content of GA_1 (B), GA_3 (C), GA_5 (D), GA_6 (E) and GA_7 (F) in control and PL samples at the time points depicted in A. Stars indicate statistically significant a difference between PL and the respective control at the given time point (1 - 5) in a paired Student's t-test ($p \leq 0.05$; $n = 5$). Error bars indicate SD.

Additionally, except for GA_{34} content no differences of GAs formed by inactivation of bioactive GAs was observed (Supplemental Figure 5). Content of GA_{34} was reduced by 10 % in PL plants compared to

control at time point 1 (Supplemental Figure 5C). Summing up, neither content of bioactive GAs nor their precursors nor their inactivation products was altered by photoperiod stress in a clear manner.

3.3.8 Expression of genes encoding GA receptors is altered in response to photoperiod stress

Next, it was examined whether genes encoding enzymes involved in GA metabolism are differently regulated in wild type and *ahk2ahk3* during the night after exposure to photoperiod stress. Under control conditions, *KS* and *GA3OX1* were less abundant in *ahk2ahk3* compared to wild type 4, 6 and 12 hours after the PLP while no other genes differed in their abundance (Figure 39B). The decreased abundance of *KS* was strongest after 12 hours, at which it was decreased nearly fivefold compared to the respective wild-type samples in *ahk2ahk3*. *GA3OX1* abundance was also decreased 5-fold in *ahk2ahk3* 12 hours after the beginning of night. In comparison, the exposure to a PLP resulted in a decrease of *KAO1* and *KAO2* abundance and an increase of *GA2OX2* and *GA2OX6* abundance in wild-type and *ahk2ahk3* plants compared to their respective control plants. Mostly, the expression of these genes occurred either earlier or stronger in *ahk2ahk3*. For example, *KAO1* was less abundant already 4 hours after the PLP-treatment, while *KAO2* abundance decreased 1.2-fold in wild-type PL plants compared to its respective control while it was decreased 1.4-fold in *ahk2ahk3* PL plants compared its control. Direct comparison of wild type PL and *ahk2ahk3* PL plants uncovered a decreased abundance of *KS* at all time points in *ahk2ahk3*, of *KAO1* and *KAO2* 12 hours after the PLP-treatment, of *GA20OX1* 4 hours after the exposure to a PLP and of *GA3OX1* 4, 6 and 12 hours after the PLP-treatment.
Furthermore, the expression of genes involved in GA signaling was elucidated. No differences were detected under control conditions except for *RGL1*, which was less abundant in *ahk2ahk3* compared to wild type at all time points (Figure 40B).

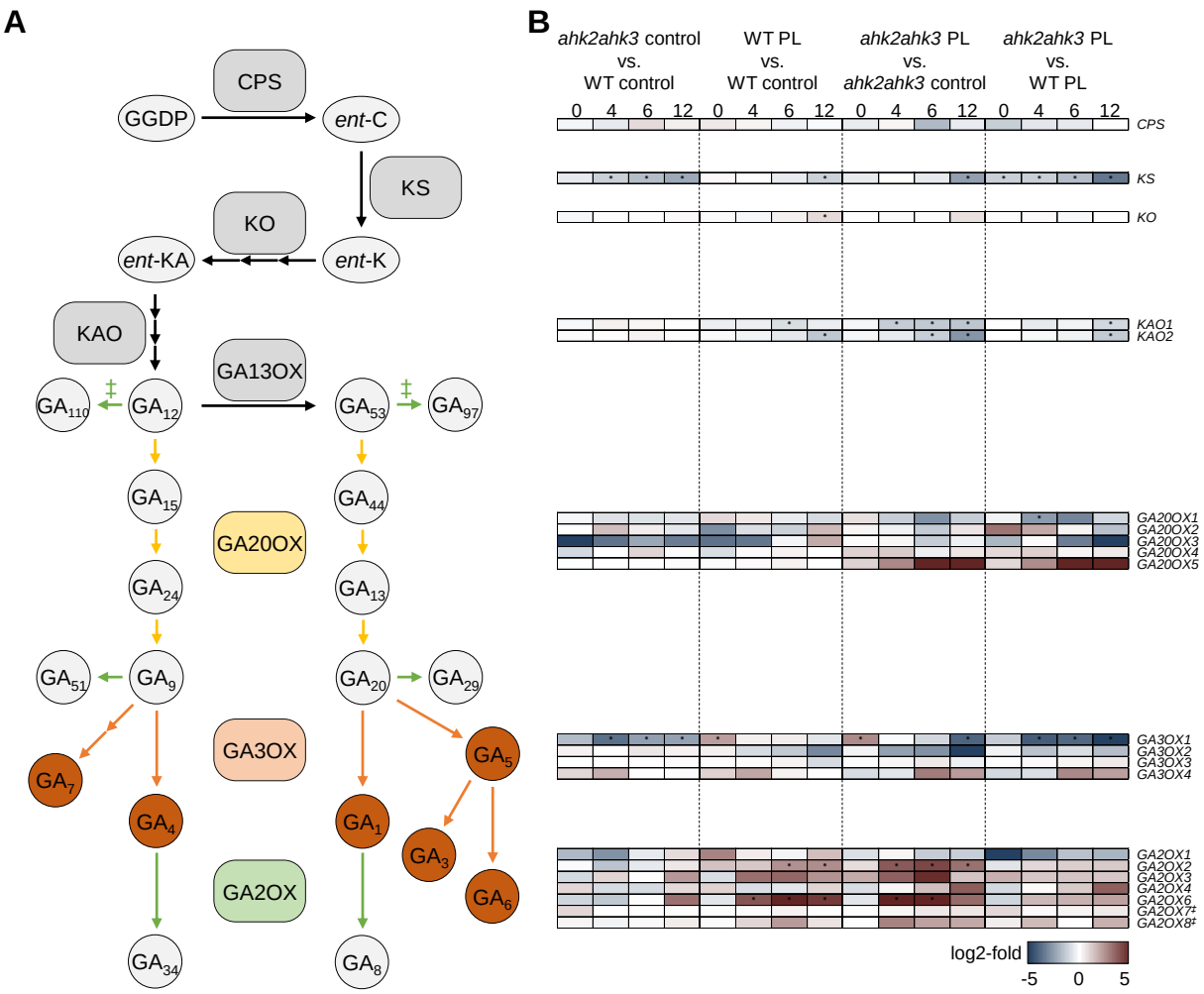

***Figure 39: Expression of GA biosynthesis and metabolism genes during photoperiod stress in wild type and* ahk2ahk3.**
(A) Simplified schematic presentation of GA metabolism. Starting from geranylgeranyl diphosphate (GGDP), the main GA-precursor GA_{12} is formed through multiple consecutive reactions involving ent-COPALYL DIPHOSPHATE SYNTHASE (CPS) that forms ent-copalyl diphosphate (ent-C), ent-KAURENE SYNTHASE (KS) that forms ent-kaurene (ent-K), ent-KAURENE OXIDASE (KO) that forms ent-kaurenoic acid (ent-KA) and ultimately ent-KAURENOIC ACID OXIDASE (KAO) enzymes. GA_{12} can be converted to either GA_{53} via GIBBERELLIN 13-OXIDASE (GA13OX) enzymes (genes have not been identified yet) or to GA_9 via GIBBERELLIN 20-OXIDASE (GA20OX) enzymes (yellow arrows). The latter also catalyze the conversion of GA_{53} to GA_{20}. GIBBERELLIN 3-OXIDASE (GA3OX) enzymes convert GA_9 to bioactive GA_4 and GA_7 (dark orange) and GA_{20} to bioactive GA_1, GA_3, GA_5 and GA_6. Inactivation of GA_1 and GA_4 is facilitated by GIBBERELLIN 2-OXIDASE (GA2OX) enzymes, which also convert GA_9 and GA_{20} precursors to inactive forms. GA2OX7 and GA2OX8 inactivate GA_{12} and GA_{53} precursors (indicated by ‡). Double arrows indicate multiple reaction steps catalyzed by the same enzyme. (B) Transcript levels 0, 4, 6 and 12 hours after the PLP in either PL plants or control plants of wild type and ahk2ahk3. Stars indicate a significant difference between groups at the given time point after Bonferroni correction ($p \leq 0.05$; $n = 3$).

12 hours after the PLP, the abundance of *GID1B*, *SCL3*, *PIF3*, *PIF4*, *PIF5* and *PIF7* was increased in wild-type PL plants compared to its control plants. In addition, the abundance of *GID1A* was reduced two-fold 6 and 12 hours after the PLP and a similar tendency was confirmed via qRT PCR (Supplemental Figure 3E). The exposure of *ahk2ahk3* to a PLP caused a decrease of *GID1A*, *GID1C*, *GAI* and *PIF1* transcript levels already 4 hours after the PLP-treatment. Furthermore, the abundance of *RGA*, *RGL1* and *PIF5* was decreased while the abundance of *GID1B*, *SCL3* and *PIF7* was increased. In comparison to wild-type PL plants, transcript levels of *GID1A*, *GID1B*, *GAI*, *RGA*, *RGL1*, *PIF1*, *PIF3*, *PIF4* and *PIF5* were decreased 12 hours after the exposure to a PLP. For some genes like *GAI*, a decreased

abundance was detected as early as 4 hours after the PLP-treatment. In contrast, *PIF7* abundance was increased 2.7-fold already 4 hours after the PLP-treatment.

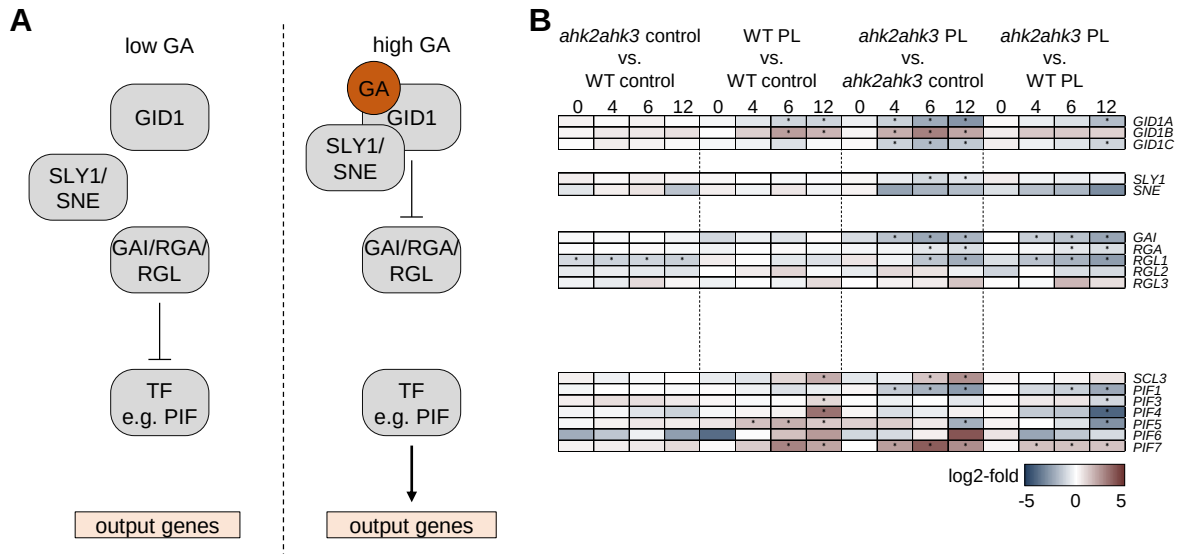

***Figure 40: Expression of GA signaling genes during photoperiod stress in wild type and* ahk2ahk3.**
(A) Schematic presentation of GA signaling. In the absence of GA (dark orange), GIBBERELLIN INSENSITIVE DWARF1 (GID1) receptors are inactive. Consequently, DELLA proteins GIBBERELLIC ACID INSENSITIVE (GAI)/ REPRESSOR OF GA1-3 (RGA)/RGA-LIKE (RGL) inhibit the function of transcription factors (TF) like e.g. PHYTOCHROME-INTERACTING FACTOR (PIF) proteins. With perception of GA by GID1 receptors, the latter associate with F-box proteins SLEEPY1 (SLY1) or SNEEZY (SNE) and inhibit DELLA function by mediating their degradation. In consequence, TFs are active and mediate the transcription of output genes. (B) Transcript levels 0, 4, 6 and 12 hours after the PLP in either PL plants or control plants of wild type and ahk2ahk3. Stars indicate a significant difference between groups at the given time point after Bonferroni correction ($p \leq 0.05$; $n = 3$).

All in all, exposure to photoperiod stress induced changes in transcript abundance mostly of genes involved in early steps of GA synthesis as well as of genes encoding GA receptors and transcription factors. Additionally, genes encoding GA signaling repressors (DELLAs) were downregulated in *ahk2ahk3* in response to photoperiod stress.

3.3.9 Plants with an impaired GA synthesis are less sensitive to photoperiod stress

To further elucidate the effect of GA on the formation of the photoperiod stress syndrome, plants with either an increased GA status (*gai* and *rga1*) or a decreased GA status (*gid1* and *ga20ox* mutants) were exposed to PLP. While *ahk2ahk3* formed more lesions in response to PLP-treatment compared to wild type, plants with a decreased GA status did not differ from wild type in their response (Figure 41A). Surprisingly, while *gid1agid1c* formed more lesions than wild type, all *ga20ox* double mutants were less responsive. The latter also had increased Fv/Fm values compared to wild type (Figure 41B). *ahk2ahk3* had the lowest Fv/Fm of all mutants tested. All in all, while an increased GA status did not alter the responsiveness to photoperiod stress, a decreased GA status caused either an increased sensitivity or an insensitivity.

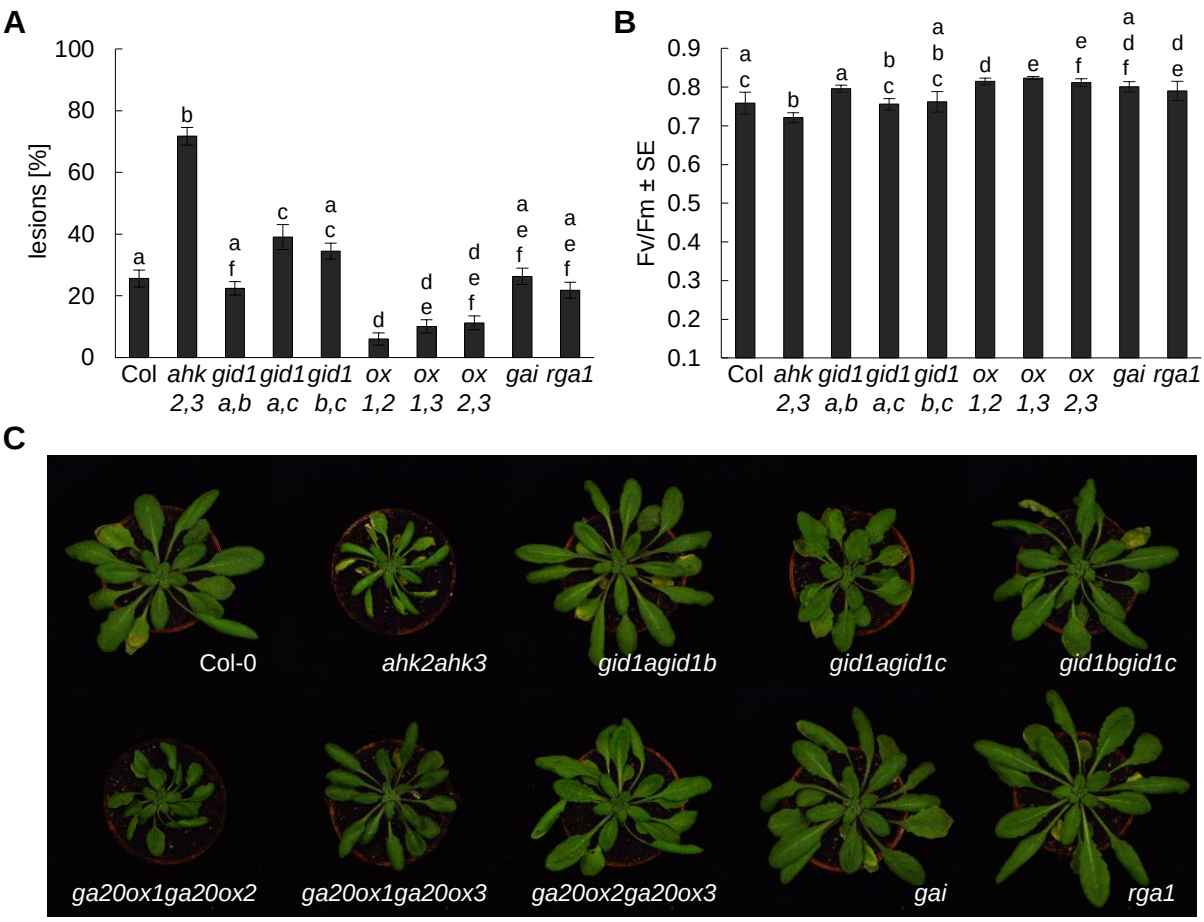

Figure 41:* ga20ox *mutants are less sensitive to photoperiod stress.
(A) Lesion formation of leaves at five-week-old Col-0, ahk2ahk3, gid1agid1b, gid1agid1c, gid1bgid1c, ga20ox1ga20ox2 *(*ox1,2*),* ga20ox1ga20ox3 *(*ox1,3*),* ga20ox2ga20ox3 *(*ox2,3*),* gai *and* rga1 *plants the day after the PCD-inducing night (n ≥ 13). (B) PAM measurements of leaves the day after PCD-inducing night (n = 12). (C) Pictures of representative plants that experienced a PLP. Letters indicate significant differences between groups (p ≤ 0.05). Error bars indicate SE.*

4 Discussion

4.1 t*Z*-type cytokinins protect plants against photoperiod stress

4.1.1 The cytokinin concentration is increased in response to photoperiod stress

As an addition to the work of Nitschke, 2014 and Nitschke *et al*., 2016 reporting a general importance of cytokinin to cope with alterations of the light-dark cycle, this work demonstrated that short-day grown wild-type plants increase the cytokinin concentration in leaves due to a 24h-prolongation of the light period. With exception of *c*Z-type cytokinins, the level of all other cytokinin types were increased in plants that experienced a prolonged light period compared to control plants (Figure 12, Table 25, Table 26, Supplemental Table 1 and Supplemental Table 2). These results are consistent with findings of Corbesier *et al*., 2003, who reported that the exposure of short-day grown plants to a prolonged light period of 16, 20 or 24 hours induced an increase in the content of *t*Z-type cytokinins but more strikingly of iP-type cytokinins. Since plants with a reduced cytokinin status develop the photoperiod stress syndrome during the night after the exposure to a prolonged light period (Nitschke *et al*., 2016), it might be assumed that the increase in endogenous cytokinin levels is crucial to reduce the symptoms induced by photoperiod stress.

One function of increased endogenous cytokinin levels could be to modulate chloroplast responses and prevent stress-induced changes in chloroplast architecture. An elevation of endogenous cytokinin levels through expression of an *IPT* gene under the control of a senescence- and maturation-induced *SARK* promoter (*SARK::IPT*) dampened the consequences of drought stress in several species like tobacco (Rivero *et al*., 2007), rice (Peleg *et al*., 2011; Reguera *et al*., 2013), peanut (Qin *et al*., 2011) or maize (Décima Oneto *et al*., 2016) by increasing or maintaining the photosynthesis rate and stomatal conductance. Other studies reported a direct influence of cytokinin on the shape and development of chloroplasts (Cortleven *et al*., 2014). Chemical inhibition of cytokinin degradation by INHIBITOR OF CYTOKININ DEGRADATION (INCYDE) protected the photosystem of tomato plants from its impediment by salt stress (Aremu *et al*., 2014). Furthermore, cytokinin protects plants by repressing the retardation of grana stacking that is caused by exposure to heat stress (Caers *et al*., 1985) and excessive starch grain and plastoglobuli formation under high light stress (Cortleven *et al*., 2014). Notably, in contrast to photoperiod stress, endogenous cytokinin levels decrease in plants after exposure to other abiotic stimuli like heat, salt or drought and moreover, mutants with a lower cytokinin status are more resistant to these stresses (Itai *et al*., 1973; Caers *et al*., 1985; Nishiyama *et al*., 2011). Another function of cytokinin might be to reduce/regulate the formation of potentially toxic compounds like H_2O_2 and other ROS by modulating the antioxidant system. Elevated cytokinin contents in tobacco by introgression of the *SARK::IPT* construct resulted in an improved antioxidant system (increased contents of ascorbic acid, glutathione, GLUTATHIONE REDUCTASE (GR), ASCORBATE PEROXIDASE (APX) and SUPEROXIDE DISMUTASE (SOD)) especially in old leaves (Dertinger *et al*., 2003; Procházková *et al*., 2008). Moreover, *ahk2ahk3* and *ipt1ipt3ipt5ipt7* roots had an elevated ROS content compared to wild type and it increased further when plants were grown under K^+-deficiency (Nam *et al*., 2012). Upon pathogen infection, *t*Z signals through AHK3 and ARR2 to regulate the

expression of the apoplastic peroxidases PRX33 and PRX34 that cause an accumulation of H_2O_2 and consequently the closure of stomata (Arnaud *et al*., 2017).

Further indications for the importance of cytokinin during photoperiod stress can be found in the expression of respective genes during the night after the PLP-treatment in wild type and the cytokinin signaling mutant *ahk2ahk3*. While most genes in cytokinin biosynthesis and metabolism were not significantly regulated, an increased abundance of cytokinin metabolism genes *UGT73C1*, *UGT73C5* and *UGT85A1* was detected (Figure 13). The increase correlates with the increase in *t*Z O-glucosides in wild type during the night following PLP treatment (Table 26). Furthermore, a similar transcriptional response of these genes could be detected in *ahk2ahk3* and thus might hint to an importance of *t*Z inactivation via O-glucosylation in order to properly balance *t*Z levels during the exposure to photoperiod stress. An importance of cytokinin O-glucosylation has been described for ovule development and for the onset of senescence in *Arabidopsis* plants that constitutively overexpressed either *UGT73C1* or *UGT85A1* (Jin *et al*., 2013; Cucinotta *et al*., 2018).

Moreover, the abundance of *ENT6* involved in cytokinin riboside transport and of several *PUP* genes that are involved in cytokinin free base transport was altered due to PLP-treatment in wild type and *ahk2ahk3* (Figure 14). This might indicate that an exposure to photoperiod stress leads to an alteration in the transport and flux of cytokinin ribosides and free bases. This work focused only on the expression profile of *ENT* and *PUP* genes known to be involved in cytokinin transport. However, the *ENT* gene family harbors eight members and the *PUP* family harbors 21 members in *Arabidopsis* (Hirose *et al*., 2005; Durán-Medina *et al*., 2017). Thus, it might be that many more genes are involved in the transport of cytokinin ribosides and free bases and that photoperiod stress also influences the transcript abundance of these genes.

Lastly, the transcript abundance of several cytokinin signaling components was altered in wild type and *ahk2ahk3* under control conditions and upon PLP treatment (Figure 15). Under control conditions, decreased abundances of *AHK2* and *AHK3* in *ahk2ahk3* compared to wild type were detected and verify the purity of the samples sent for sequencing. Moreover, decreased abundances of type-A *ARR*s especially at later time points (6 and 12 h after the PLP) in samples of stressed plants of both genotypes compared to their respective controls have been detected. This indicates that the cytokinin signaling output might be decreased in the night after the PLP treatment, as type-A *ARR* expression is part of the cytokinin signaling pathway feedback loop (see section 1.2.3, Figure 3; reviewed in e.g. Werner and Schmülling, 2009). Furthermore, these results demonstrate the validity of the RNAseq experiment for the regulation of cytokinin related genes, as the decreased abundance of type-A *ARR*s in response to photoperiod stress was described previously (Nitschke, 2014; Nitschke *et al*., 2016). All in all, the decrease in type-A *ARR* abundance, the alterations in *AHP* and type-B *ARR* abundance and the measured increase in cytokinin content taken together might be interpreted as another indication for the importance of properly balancing cytokinin function in order to cope with photoperiod stress.

4.1.2 tZ-type cytokinins act as protectants against photoperiod stress

Both *cypDM* and *abcg14* plants were very sensitive to photoperiod stress as demonstrated phenotypically by an increased lesion formation, physiologically by a decreased photosynthetic capacity and molecularly by an increased H_2O_2 formation and altered abundance of marker genes (Figure 16).

*t*Z-type cytokinins are mainly involved in development processes in the shoot and are formed by two redundant CYP735A enzymes (Kiba *et al*., 2013). Moreover, *t*Z-type cytokinins are transported from the root to the shoot via the xylem flow with the help of ABCG14 (Ko *et al*., 2014; Zhang *et al*., 2014). Thus, the results indicate that root-derived *t*Z-type cytokinins are crucial for the resistance of plants to photoperiod stress in the shoot. *ahk3* plants as well as in *ahk2ahk3* and *ahk3cre1* are more sensitive to photoperiod stress (Nitschke *et al*., 2016). The protective function of *t*Z-type cytokinins to photoperiod stress might explain why AHK3 is the receptor with the major role in this context. A first indication is that AHK3 has a higher affinity to bind *t*Z as to bind iP whereas, for example, AHK2 has a similar affinity to both iP and *t*Z (Stolz *et al*., 2011; Romanov *et al*., 2006; Lomin *et al*., 2015). Secondly, *ahk3* plants and respective *ahk* higher order mutants have a strongly increased content of *t*Z-type cytokinins whereas the content of iP-type cytokinins is not changed (Riefler *et al*., 2006). Moreover, crosses of *ahk* double mutants with *cypDM* plants showed that the additive effect in growth retardation caused by the simultaneous loss of *t*Z-type cytokinin biosynthesis and cytokinin perception was less pronounced in *ahk3cypDM* mutant combinations (Kiba *et al*., 2013). Summing up, the cause of the increased photoperiod stress sensitivity of *ahk3* single and higher order mutants is most probably an impairment in *t*Z perception.

Watering of *t*Z-type cytokinin deficient *cypDM* plants with either the major transport form *t*ZR or bioactive *t*Z demonstrated that both forms can protect plants against photoperiod stress although *t*Z was more effective (Figure 17). Furthermore, both *t*Z and *t*ZR supplementation rescued the decrease in type-A *ARR* abundance in these plants. These results suggest that *t*ZR supplementation is able to positively influence some but not all *t*Z-regulated processes. The reduced potency of *t*ZR in the context of photoperiod stress might be a consequence of the fact that *t*ZR must be converted to *t*Z to unfold its protective function (Lomin *et al*., 2015) and that *t*Z concentrations might than be lower in *t*ZR-watered plants as in those ones that were watered with *t*Z. One could further speculate that during photoperiod stress, *t*Z and *t*ZR enter different tissues. In support of that, it was recently shown that under long-day conditions, root-derived *t*Z has distinct functions in the shoot (e.g. in regulating the size of leaves or the SAM) compared to root-derived *t*ZR that is converted to *t*Z later (Osugi *et al*., 2017). Moreover, as already discussed in section 4.1.1, cytokinin ribosides and free bases are transported by different transporter families (ENTs and PUPs; Durán-Medina *et al*., 2017).

4.1.3 logS plants are insensitive to photoperiod stress

In the experiments conducted for this thesis, *logS* plants did not show an increased sensitivity to photoperiod stress neither phenotypically nor physiologically nor at the molecular level (Figure 18). LOG enzymes catalyze the activation of riboside monophosphate cytokinins to free bases (Kurakawa *et al*., 2007; Kuroha *et al*., 2009). Only the free bases can bind to the cyclase histidine kinase associated sensory extracellular (CHASE) domain of HISTIDINE KINASE receptors and activate cytokinin signaling (Lomin *et al*., 2015). Hence, the results obtained are surprising as the deficiency in cytokinin free bases should, in theory, have caused and increased photoperiod stress sensitivity. One could speculate that the consequences of photoperiod stress caused by a deficiency of active cytokinins in *logS* plants are compensated by the different developmental status. The sensitivity to photoperiod stress is to some extent dependent on the developmental stage (see section 3.2, Nitschke, 2014; Nitschke *et al*., 2016)

and *logS* plants are severely impaired in root and shoot development and accumulate cytokinin nucleotides (Tokunaga *et al*., 2012). The latter have been shown to cause growth retardation at high concentrations (Zhang *et al*., 2013). Hence, the increased amounts of cytokinin ribotides in *logS* plants could be causative for the growth retardation or could stress plants in general so that the exposure to a PLP might no longer have a reduced impact or any impact at all.

4.1.4 ARR2, ARR10 and ARR12 regulate the response to photoperiod stress in a complex manner

Upon perception of cytokinin through AHKs, five of the six-member family of AHPs become phosphorylated by AHKs and act as positive regulators of cytokinin signaling (Suzuki *et al*., 2000). This study demonstrated that AHP2, AHP3 and AHP5 act redundantly during photoperiod stress and that AHP2 and AHP3 might have a prominent role compared to AHP5 (section 3.1.7; Figure 19). A functional redundancy of AHPs has been shown before (Hutchison *et al*., 2006). The results obtained thus complement the cytokinin-dependent photoperiod stress signaling pathway with the addition of AHPs, which so far involved AHK3 as the main receptor and ARR2 as the main transcription factor (Nitschke *et al*., 2016).

AHP1 to AHP5 phosphorylate and thus activate type-B ARR transcription factors (Suzuki *et al*., 2001b). Testing of *arr2arr10arr12* triple mutant as well as its respective double and single mutants revealed that loss of ARR10 and ARR12 can rescue the phenotype of *arr2* plants and that loss of all three transcription factors results in an increased photoperiod stress sensitivity compared to respective double mutants (section 3.1.7; Figure 20). This hints at a complex regulatory mechanism during photoperiod stress signaling between ARR2 on the one hand and ARR10 and ARR12 on the other. A similar relationship between the aforementioned type-B ARRs and also other members of this family has been described in the context of root development. For example, *arr12* and *arr10arr12* root elongation was more affected by cytokinin treatment than that of *arr2arr12* and *arr2arr10arr12*, respectively (Mason *et al*., 2005). In the context of type-B ARR dependent gene regulation a model has been proposed in which simultaneous binding of multiple/different type-B ARRs and unknown factors to certain promoter regions is crucial (Ramireddy *et al*., 2013). Experimental evidence for a direct interaction between members of the type-B ARR family is rare. An interaction of ARR2 and ARR14 has been described in yeast (Dortay *et al*., 2006). Recently, it was found that the C-termini of ARR1 and ARR12 interact to regulate auxin synthesis (Yan *et al*., 2017). It could also be the case that interactions between type-B ARRs are context/status-dependent as it is known that the homodimerization of bacterial RRs depends on their phosphorylation status (Mack *et al*., 2009). Similarly, ARR18 can homodimerize when both ARR18 proteins are either both phosphorylated or not phosphorylated (Veerabagu *et al*., 2012).

The findings of this study could be explained by a model, in which ARR2, ARR10 and ARR12 interact with a yet unknown interaction partner (X) that is essential for photoperiod stress resistance. It is predicted that the affinity of ARR2 to X would be higher than affinities of ARR10 and ARR12 to X. In addition, a direct or indirect interaction of ARR10 and ARR12 is proposed. In photoperiod stress-treated wild-type plants, ARR2 would interact with X resulting in photoperiod stress resistance while ARR10 and ARR12 would directly/indirectly interact with each other to fulfill different functions. In *arr2* plants, X would not have an interaction partner and thus would be unable to function in stress protection because

ARR10 and ARR12 would not be available as interaction partners. Consequently, stress resistance would be lowered. Resistance of *arr2arr10* and *arr2arr12* plants would be caused by the loss of the ARR10-ARR12 association and the resulting interaction of X with ARR10 or ARR12. Ultimately, the enhanced stress phenotype of *arr2arr10arr12* plants would be caused by the complete loss of interaction partners for X.

Beside the interaction amongst ARRs, interactions between several type-B ARRs and other proteins exist and might give indications which protein X could be. For example, ARR1, ARR2 and ARR14 interact with DELLA proteins RGA1 and GAI to regulate root development and photomorphogenesis (Marín-de la Rosa *et al*., 2015; Yan *et al*., 2017). During the regulation of auxin synthesis, EIN3 interacts with the C-terminus of ARR1 and thereby increases ARR1 activity (Yan *et al*., 2017). As part of the crosstalk between cytokinin and abscisic acid, ARR1, ARR11 and ARR12 directly interact with SUCROSE NON-FERMENTING-1 (SNF1)-RELATED PROTEIN KINASE2 (SnRK2) kinases and thereby inhibit their function prior to drought stress (Huang *et al*., 2018).

4.2 The response to photoperiod stress is age- and tissue-specific

4.2.1 The age of plants and specific leaves influences the photoperiod stress sensitivity

In the first detailed description of the photoperiod stress syndrome, indications have been presented that the photoperiod stress syndrome develops mainly in mature, fully expanded leaves (Nitschke, 2014). In agreement with these findings, the detailed phenotypical, physiological and molecular analyses of specific wild-type and *ahk2ahk3* leaves demonstrated that the oldest, non-senescent leaves (leaves 5 to 8) of both genotypes were strongly affected by a PLP while only in more sensitive *ahk2ahk3* plants leaves 9 to 13 were also affected (Figure 21). These results indicate that there might be an effect of the developmental stage of the leaves on the sensitivity to photoperiod stress. As has been described previously, mature leaves are also more sensitive than young leaves in the context of other abiotic stresses like drought stress (Koffler *et al*., 2014), salt stress (Munns *et al*., 1995; Munns, 2002) or high light stress (Bielczynski *et al*., 2017). This indicates that the competence of mature leaves to enter senescence seems to be a general phenomenon.

As a next step, developmental programs of leaves that are influenced by cytokinin and might regulate the sensitivity to photoperiod stress were further investigated. *ahk2ahk3* had an increased number of juvenile leaves compared to wild type and an increased *MIRNA156* transcript abundance in relation to *MIRNA172* (Figure 22A-D) confirming previous findings stating that the cytokinin status influences the timing of plants to form leaves with a juvenile or adult identity by regulating the ratio of MIRNA156 to MIRNA172 (Kiba *et al*., 2013; Werner, 2016). However, neither *35S::MIR156B* nor *35S::MIM172* plants, which have also an increased number of juvenile leaves, were strongly affected by the exposure to a PLP (Figure 22E-G). Thus, it is very unlikely that the leaf identity is causative for the different sensitivities of wild type and *ahk2ahk3* to photoperiod stress.

Other experiments rather indicate that the plant- and leaf age is of importance as the phenotypic and molecular sensitivity of plants to alterations of the light-dark rhythm increased with age in *ahk2ahk3*

plants (Figure 23) and with the age of leaf 8 in both genotypes (Figure 24). In addition, the area of leaf 8 of four-week-old and five-week-old *ahk2ahk3* plants was reduced compared to wild type and leaf growth was slower in *ahk2ahk3* plants (Figure 24A). An indicator for the developmental age of a leaf is its expansion and leaf maturity is characterized by its arrest (Gonzalez *et al*., 2012; Jibran *et al*., 2013; Bar and Ori, 2014). Moreover, cytokinin is known not only to regulate leaf expansion by influencing the cell size but also to influence the very early stages of leaf development by being crucial for cell division and proliferation (Miller *et al*., 1955, 1956; Werner *et al*., 2001, 2003; Riefler *et al*., 2006). Taken together, one could argue that *ahk2ahk3* leaves end cell proliferation and enter maturity earlier as wild-type leaves.

During its life cycle, leaves undergo ARCs and in mature leaves these ARCs result in an competence to induce leaf senescence by external stimuli like abiotic and biotic stress (Jing *et al*., 2005; Jibran *et al*., 2013; Kanojia and Dijkwel, 2018). Some changes that occur with age are an increasing ROS sensitivity and ROS production in the pre-senescent state, decreasing ascorbic acid levels and chlorophyll contents, increasing JA levels and an increased sensitivity to ethylene (Dertinger *et al*., 2003; Jing *et al*., 2005; Kotchoni *et al*., 2009; Breeze *et al*., 2011). Another ARC is the decrease in cytokinin content (Hewett and Wareing, 1973; Singh *et al*., 1992a, 1992b; Skalák *et al*., 2019). Several studies have demonstrated the importance of cytokinin to inhibit leaf senescence (Richmond and Lang, 1957; Dyer and Osborne, 1971; Gan and Amasino, 1995) and to counteract the occurrence of ARCs by regulating ascorbic acid levels and chlorophyll content (Dertinger *et al*., 2003). Thus, it might be the case that the competence to induce leaf senescence by external stimuli develops earlier in plants with a reduced cytokinin status as these accumulate ARCs faster.

4.2.2 The responsiveness to photoperiod stress differs between leaves and roots

As already indicated by the results of section 3.1 and discussed in section 4.1, different tissues contribute to the responsiveness of plants to photoperiod stress. In the course of this work it was further elaborated whether different tissues show a similar response to photoperiod stress. Exposure of lines overexpressing cytokinin degradation enzyme (Myc-tagged) CKX1 tissue-specifically to photoperiod stress indicates that the vasculature and the epidermis are of crucial importance to cope with alterations of the light-dark cycle (Figure 25). The vasculature serves as the main route to distribute iP-type cytokinins (via phloem) and more importantly *t*Z-type cytokinins (via xylem) to root and shoot tissue (Ko *et al*., 2014; Zhang *et al*., 2014; Durán-Medina *et al*., 2017). Furthermore, *t*Z-type cytokinins are formed CYP735A enzymes from iP-type cytokinins (Takei *et al*., 2004; Kiba *et al*., 2013). Thus, the increased sensitivity of *SUC2::CKX1-4xMyc* and *CLV1::CKX1* might be explained by a decrease in iP-type cytokinins in the phloem, which are then missing as precursors that could be formed into *t*Z-type cytokinins ultimately resulting in a reduced *t*Z-type cytokinin content. Moreover, the epidermis-specific overexpression of *CKX1* in *ATML::CKX1-4xMyc* resulted in a fourfold reduction of the *t*Z content in shoot tissue compared to that of wild type (Werner, 2016), which provides an explanation for the increased photoperiod stress sensitivity of these plants.

In addition to the results discussed above, one could deduce the importance of certain tissues from the role of type-B ARRs in regulating the sensitivity to photoperiod stress (section 3.1.7). *ARR2*, *ARR10* and *ARR12* are expressed together in stomata, hydathodes and in the root elongation zone while *ARR2* is

expressed right next to the vasculature and *ARR10* and *ARR12* are expressed within it (Mason *et al*., 2004). Furthermore, the importance of the vasculature and of roots is indicated not only by type-B *ARR* expression patterns but also by that of *CYP735A* genes, which are mainly expressed in these tissues (Takei *et al*., 2004; Kiba *et al*., 2013).

Exposure of wild type and *ahk2ahk3* to a PLP did not alter the abundance of stress marker genes *BAP1* and *ZAT12* in roots during the night after treatment compared to respective controls (Figure 26). These results indicate that the transcriptional response to photoperiod stress differs between leaves and roots independent of the plants' photoperiod stress sensitivity as such. As the transcript abundance of *BAP1* and *ZAT12* also displays the cell death and oxidative stress response of root tissue (Yang *et al*., 2007; Le *et al*., 2016), the results indicate that roots might not have oxidative stress upon exposure to photoperiod stress and that cell death might not be induced. This is consistent with the systemic response from shoot to root tissue in the context of high light stress. While the exposure of specific leaves to high light stress induced the expression of *ZAT10* in distal leaves, no induction could be found in root tissue (Rossel *et al*., 2007). However, a systemic response from roots to shoots mediated by Ca^{2+} waves was postulated in the context of salt stress. Within one minute, an induction of respective marker genes could be measured in shoot tissue of plants of which the root had been exposed to high concentrations of NaCl (Choi *et al*., 2014).

In addition to the expression of stress marker genes, no changes in the abundance of genes involved in cytokinin biosynthesis, metabolism and transport were detected after exposure to a PLP (Figure 26). This is surprising as roots are the main source for *t*Z-type cytokinins (Kiba *et al*., 2013; Ko *et al*., 2014; Zhang *et al*., 2014; Osugi *et al*., 2017) and thus are of great importance in the context of photoperiod stress. As the cytokinin content was already increased in PL plants during PLP treatment (Figure 12), the time points chosen for transcript analyses of roots during the night after the exposure to a PLP might have been too late to detect differences in the transcript abundance of these genes between PL and control plants.

4.3 The sensitivity to photoperiod stress is influenced by the auxin and ethylene status

4.3.1 The regulation of auxin homeostasis is crucial to cope with photoperiod stress

As one of the best studied antagonists of cytokinin, auxin is involved in many developmental and stress-related processes. Within this study, several indications have been collected that the auxin status of plants might be crucial to cope with photoperiod stress. Most strikingly, an elevation in the content of endogenous IAA in *yuc1D* (Zhao *et al*., 2001) increased the sensitivity to photoperiod stress while an increasing impairment in auxin perception by the loss of *TIR/AFB* genes resulted in a decreasing sensitivity in terms of lesion formation, H_2O_2 formation and partially in marker gene expression (Figure 30 and Figure 31). Similarly, an increased auxin status in *Arabidopsis* was associated with a decreased stress resistance to cold, drought and salt (Park *et al*., 2007) while a decreased auxin status by either loss of *TIR/AFB* or by a constitutive overexpression of *GH3.5* (*wes1-D* mutant) enhanced the resistance to the previously mentioned stresses (Park *et al*., 2007; Iglesias *et al*., 2010). In rice, decreased IAA

level by a gain of *GH3.13* function improved the resistance to drought (Zhang *et al*., 2009). Vice versa, auxin supplementation and an increase in endogenous IAA content by *YUC* overexpression improved the resistance to drought stress, while *yuc* mutants were less resistant than wild type (Lee *et al*., 2012; Shi *et al*., 2014).

The importance of auxin in coping with photoperiod stress is further indicated by auxin measurements in less sensitive wild-type plants. Here, concentrations of bioactive IAA and - more pronounced - its irreversibly inactivated conjugate IAA-Asp increased during the night after exposure to a PLP while IAA-Glu levels were only slightly changed (Figure 27D, E). These results might indicate that plants which are able to cope with photoperiod stress avoid the accumulation of free IAA by inducing certain inactivation pathways. In support of this, only minor changes in the expression of genes involved in auxin biosynthesis have been detected in wild-type leaves (Figure 28). Instead, enhanced expression levels of several *GH3* genes - involved in IAA-Asp formation - were observed at earlier but also similar time points as the IAA-Asp accumulation (Figure 28). These results indicate that PLP treatment might induce the formation of GH3 enzymes, which ultimately conjugate and thus inactivate free IAA. As mentioned before, previous studies suggest that the constitutive overexpression of *GH3.5* (*wes1-D* mutant) not only causes an IAA deficiency phenotype but also increases the resistance to abiotic stress (Park *et al*., 2007). In agreement with this, *gh3.5* plants had increased IAA levels and were more affected by abiotic stress. Endogenous IAA concentrations are even more elevated in *gh3* sextuple mutants (Porco *et al*., 2016).

In addition to the conjugation of IAA to Asp and Glu, GH3 enzymes also catalyze the conjugation of IAA to other amino acids like leucine (Leu), tryptophan (Trp), phenylalanine (Phe) or alanine (Ala) (Staswick *et al*., 2002, 2005). In contrast to the conjugation with Glu and Asp, these conjugations are reversible and are catalyzed IAR3/ILR1/ILL enzymes (Davies *et al*., 1999; LeClere *et al*., 2002; Rampey, 2004). The RNAseq results presented in this study showed that the abundance of *IAR3* and *ILL1* was altered upon photoperiod stress treatment in wild type (Figure 28). These results might indicate that due to exposure to photoperiod stress, not only the irreversible but also the reversible inactivation of IAA and more importantly the reactivation of IAA amino acid conjugates must be balanced. IAR3 catalyzes the formation of bioactive IAA from IAA alanine (Davies *et al*., 1999). In *Arabidopsis*, *iar3* mutants had reduced IAA levels and were less tolerant to drought stress than wild type, demonstrating the importance of this reaction (Kinoshita *et al*., 2012). However, *in vitro* and *in vivo* experiments suggest that IAR3 not only hydrolyzes IAA conjugates but also catalyzes the inactivation of bioactive JA isoleucine as demonstrated by wounding of *IAR3* overexpressors that led to a diminished increase in JA isoleucine content compared to wild type (Zhang *et al*., 2016c). Lastly, neither the IAAox content nor the abundances of IAAox forming *DAO* genes were changed in wild type upon exposure to photoperiod stress (Figure 27C and Figure 28). These results indicate that IAAox formation is of minor importance with regard to coping with a prolongation of the light period.

What might be the mechanism behind the toxicity of bioactive IAA in the context of photoperiod stress? As the peak in free IAA correlates with the peak in H_2O_2 levels (Figure 27B, Abduelsoud *et al*., unpublished) one could assume that excessive amounts of IAA might induce H_2O_2 formation and by that induce oxidative stress ultimately resulting in the photoperiod stress syndrome. Several studies suggest that auxin induces the formation of ROS during the gravitropic response of *Arabidopsis* roots (Joo *et al*.,

2001), *Arabidopsis* lateral root and root hair development (Duan *et al*., 2010; Ma *et al*., 2014), cell wall loosening in maize coleoptiles (Schopfer, 2001) and quiescent center formation in maize roots (Jiang *et al*., 2003). Moreover, auxin induces the formation of H_2O_2 during salt stress (Iglesias *et al*., 2010). Mechanistically, auxin acts through NADPH oxidases RESPIRATORY BURST OXIDASE HOMOLOGs (RBOHs), the content of ascorbic acid and amount of SOD, GR and CATALASEs (CATs) (Duan *et al*., 2010; Peer *et al*., 2013; Shi *et al*., 2014).

One could also assume that increased IAA levels are the product of H_2O_2 accumulation. The only influence of H_2O_2 on auxin signaling has been described recently (Biswas *et al*., 2019). In a feed-forward-loop in lateral root founder cells, auxin stimulates the RBOH-dependent formation of ROS, which in turn leads to the formation of reactive carbonyl species (RCS). The latter promote the degradation of Aux/IAA proteins via the TIR1/AFB-SCF complex ultimately activating the auxin signaling pathway (Biswas *et al*., 2019).

4.3.2 An interaction of cytokinin and auxin during the regulation of photoperiod stress

As an addition to the role of auxin in forming the photoperiod stress syndrome, the decreased sensitivity of *ahk2hk3tir1afb2* to an alteration of the light-dark cycle compared to *ahk2ahk3* provided genetic evidence that the increased sensitivity of plants with a reduced cytokinin status might be due to an increased activation of the auxin signaling pathway downstream of the cytokinin signaling pathway (Figure 32). In agreement with this, previous experiments found that *ahk2ahk3* mutants accumulated more IAA than wild type in response to an applied PLP (Dr. Anne Cortleven; personal communication). Furthermore, RNAseq results in this study revealed an increased gene abundance of *IAR3* and *ILR1* and a decreased abundance of *ILL1* and *ILL2* in stressed *ahk2ahk3* compared to wild type as well as a lowered expression of auxin biosynthesis enzymes (Figure 28). One could therefore speculate that caused by a malfunctioning IAA conjugation, free IAA levels increase in plants with a lowered cytokinin status, which cause oxidative stress ultimately leading to the phenotypic shaping of the photoperiod stress syndrome. Numerous studies suggest that cytokinin and auxin regulate each other's synthesis pathways and thus their hormone levels (Eklöf *et al*., 2000; Nordström *et al*., 2004; Jones *et al*., 2010; Di *et al*., 2016; Yan *et al*., 2017). Furthermore, cytokinin perception has a substantial influence on auxin transport in the root and during de novo organogenesis (Dello Ioio *et al*., 2008; Ruzicka *et al*., 2009; Pernisova *et al*., 2009, 2016). Even though *GH3* expression in stressed *ahk2ahk3* was not altered compared to stressed wild-type plants (Figure 28), recent studies found that cytokinin directly induces the expression of several *GH3* genes and further demonstrated that cytokinin function on root meristem size is in part dependent on GH3 function (Pierdonati *et al*., 2019).

Apart from the regulation of hormone levels, RNAseq results showed that the abundances of genes involved in auxin signaling were affected in wild type, but more strongly - mostly decreased - in *ahk2ahk3* (Figure 29). For example, the abundance of *TIR1/AFB* genes was decreased markedly in response to a PLP in wild type and in *ahk2ahk3,* but the decrease was more marked in *ahk2ahk3*. The same tendencies could be observed for the abundance of *IAA/AUX* and class B and C *ARF* genes. The reduction in *TIR/AFB* abundance might indicate that the auxin signaling output is reduced in *ahk2ahk3*. Simultaneously, the decreased abundance of *IAA/AUX* and class B and C *ARF* genes might indicate a hyperactivation of the auxin signaling pathway as these all act as negative regulators of auxin signaling

(Ulmasov *et al*., 1997b, 1999b; Guilfoyle and Hagen, 2007). In contrast, several *IAA/AUX* genes were induced by auxin treatment in *Arabidopsis* seedlings (Stowe-Evans *et al*., 1998). As both genetic and physiological evidence indicate a positive relationship between auxin and the sensitivity to photoperiod stress it might be more plausible to interpret the described transcriptional deregulation as a hyperactivation. In support of this, previous studies found that *t*Z could induce the expression of *IAA3/SHORT HYPOCOTYL 2* (*SHY2*) and *IAA17/AXILLARY ROOT3* (*AXR3*) (Jones *et al*., 2010). As *t*Z-type cytokinins act as protectants against photoperiod stress and the perception of *t*Z is greatly impaired in *ahk2ahk3*, it might be that *t*Z is crucial to induce gene expression of auxin signaling components and thus, to keep them in balance.

Another explanation for the opposing functions of cytokinin and auxin in the context of photoperiod stress might be that they share components downstream of the signaling pathways of both hormones and that these are deregulated. One potential candidate gene family could be *SMALL AUXIN-UP RNAs* (*SAURs*), whose expression was decreased after photoperiod stress treatment, especially in *ahk2ahk3* (Dr. Anne Cortleven, personal communication). *SAURs* were originally found to be induced by auxin treatment (McClure and Guilfoyle, 1987, 1989) and are crucial for the regulation of the light response (Sun *et al*., 2016) but also for the development of leaves, flowers and siliques (van Mourik *et al*., 2017). Recent studies further indicate that the expression of several *SAURs* is also induced by *t*Z and other hormones (van Mourik *et al*., 2017). Hence, it might be that the differential expression of *SAURs* in *ahk2ahk3* is a cause of an imbalance between cytokinin and auxin output.

4.3.3 Loss of type-II ethylene receptors causes a reduced photoperiod stress sensitivity

In addition to the role of auxin, this thesis characterized the role of ethylene and its signaling pathway in photoperiod stress. As a first indication of a potential role for ethylene in photoperiod stress, the transcript abundance of a majority of *ACS* and *ACO* genes which are involved in ethylene biosynthesis was increased in both wild-type and *ahk2ahk3* plants, during the night after the exposure to a PLP (Figure 33). Ethylene is known to be induced by abiotic and biotic stresses and thought to activate numerous processes that result in the senescence of plants (Reviewed in Yang and Hoffman, 1984; Abeles *et al*., 1992; Schaller and Kieber, 2002). Moreover, ethylene is able to induce the expression of proteins involved in its synthesis (Van Zhong and Burns, 2003). One might therefore suggest that a decreased ethylene status might result in an improved photoperiod stress resistance of plants. However, a constitutive activation by either loss of CTR1 or loss of three of the five ethylene receptors (*etr1etr2ein4* and *etr2ein4ers2* plants) resulted in a considerably decreased photoperiod stress sensitivity (Figure 36 and Figure 37). These results indicate that ethylene might act as a positive regulator of photoperiod stress resistance.

In the context explained before, the improved resistance of plants with an increased ethylene status is contradictory at first sight. However, a protective function of a constitutive active ethylene signaling has been suggested against high concentrations of salt by a permanent increase in the amount of ROS (Cao *et al*., 2007; Jiang *et al*., 2013) and the response to ethylene does not necessarily cause the induction of senescence as a plant's responsiveness to ethylene is age-dependent (Jing *et al*., 2005). Thus, it might be that the perception of ethylene is a necessary process to induce the molecular and

phenotypical changes caused by photoperiod stress. A constitutively activated ethylene pathway might reflect a type of ethylene 'blindness' in this context as minor changes in ethylene concentration as well as a more marked increase could not be sensed properly. In fact, *ctr1* did not show a phenotypic response due to ethylene treatment (Kieber *et al*., 1993) and it has been suggested that a negative feedback regulation exists (Van Zhong and Burns, 2003). The improved photoperiod stress resistance of *ctr1*, *etr1etr2ein4* and *etr2ein4ers2* might thus be the result of the discussed ethylene insensitivity.

Based on their N-terminal structure, the five ethylene receptors in *Arabidopsis* can be divided into two subfamilies, type I receptors (ETR1 and ERS1) and type II receptors (ETR2, ERS2 and EIN4) (Hua *et al*., 1998). The phenotypic and physiological response of *etr2ein4ers2* to photoperiod stress thus indicates that the loss of type II ethylene receptors is sufficient to protect plants from the phenotypic consequences of photoperiod stress. Furthermore, *etr1etr2ein4*, *etr2ein4ers2* and *ctr1* were similarly sensitive to photoperiod stress but *ctr1* mutants were much smaller due to the maximal activation of ethylene signaling compared to *etr1etr2ein4* and *etr2ein4ers2* (Figure 36C and Figure 37C). This might indicate that the ethylene-dependent response to photoperiod stress is independent of the plant size but it might rather suggest that a constitutively active ethylene signaling induces developmental changes, which prevent plants forming the photoperiod stress syndrome.

An important role for ethylene perception by ETR/ERS/EIN4 receptors during photoperiod stress is further supported by the transcriptional response to a PLP treatment in wild type and *ahk2ahk3*. In stressed plants of both genotypes, the transcript abundance of most ethylene receptors increased in the course of the night following PLP treatment compared to respective controls (Figure 34). This might signify that in order to properly cope with a prolongation of the light period, ethylene receptor transcript - and probably protein - levels must be adjusted very precisely. In agreement with that, a differential regulation of ethylene receptor genes has been described previously in the context of drought, osmotic and salt stress (Peng *et al*., 2014b; Ren *et al*., 2017). As the expression of ethylene receptors can be induced by ethylene treatment (Hua *et al*., 1998; Van Zhong and Burns, 2003), the results could further suggest a synthesis of ethylene in response to a prolongation of the light period, which then might have induced the transcription of its receptors.

In which tissue could ethylene signaling unfold its protective function against photoperiod stress? The importance of a tissue-specific ethylene signaling is suggested by analysis of lines overexpressing F-box protein EBF2 in different tissues. An overexpression of *EBF2* caused a reduction in ethylene signaling and in the *ctr1* background, an epidermis-specific *EBF2* expression was able to rescue the *ctr1* dwarf phenotype (Vaseva *et al*., 2018). Thus, one could speculate that during photoperiod stress, ethylene signaling in the epidermis might be crucial. This would also implicate that ethylene might act in the same tissue as cytokinin (see section 4.2.2 for discussion of tissue-specific cytokinin response).

In addition to the protective function of a constitutive ethylene signaling, an impairment in ethylene perception in *etr1-1* and *ein2* but not in *ein3* increased the sensitivity of plants to photoperiod stress (Figure 35). As EIN2 stabilizes EIN3 and EIL transcription factors by direct interaction and by inducing degradation of EBF proteins (An *et al*., 2010; Wen *et al*., 2012), the results indicate that EIN3 acts redundantly with EILs as positive regulators of photoperiod stress resistance. The importance of EIN3 and EIL transcription factors in positively regulating the resistance to other abiotic stresses like salt stress was suggested before (Peng *et al*., 2014a). Downstream targets of EIN3/EIL transcription factors

during photoperiod stress could be ETHYLENE RESPONSE FACTORs that are crucial in the response to pathogen infection, salt, drought and heat (Reviewed in Müller and Munné-Bosch, 2015).
Several studies indicate that ROS and ethylene regulate each other on multiple levels during the formation of senescence/PCD after exposure to a variety of abiotic stresses (Reviewed in Zhang *et al*., 2016b; Kanojia and Dijkwel, 2018). For example, ethylene regulates the formation of ROS via RBOHF and PEROXIDASEs during salt stress (Jiang *et al*., 2013; Peng *et al*., 2014a). In cotton, ethylene-dependent induction of H_2O_2 occurred as early as 6 h after treatment while H_2O_2-dependent induction of ethylene synthesis was detected 3 days after treatment (Qin *et al*., 2008). Hence, during/after exposure to a PLP, ethylene could trigger ROS formation or vice versa, which might ultimately result in lesion formation and a PCD response.

4.3.4 Potential interactions of ethylene with cytokinin in the context of photoperiod stress

With the exception of the transcriptional regulation of genes involved in ethylene biosynthesis, metabolism and signaling in *ahk2ahk3*, which suggested that cytokinin might impact the ethylene output (Figure 33 and Figure 34), no direct interactions between these hormones have been investigated in this thesis. However, the alterations in photoperiod stress sensitivity of plants caused by changes in the ethylene and cytokinin status cannot be fully interpreted by looking at each hormone separately as their synthesis and signaling are closely interconnected (Schaller and Kieber, 2002; Iqbal *et al*., 2017; Liu *et al*., 2017).
As discussed before, an exposure to photoperiod stress led to increased contents of various types of cytokinin (Figure 12 and section 4.1.1) and it was suggested that especially *t*Z-type cytokinins have a protective function (Figure 16, Figure 17 and section 4.1.2) which required the functioning of AHPs and ARRs. Moreover, an impaired ethylene perception and signaling in *etr1-1* and *ein2* caused a lowered photoperiod stress sensitivity while an increased ethylene status caused by an absence of ethylene receptors or the protein kinase CTR1 protected plants from photoperiod stress (Figure 35, Figure 36, Figure 37 and section 4.3.3). These results could be linked as previous studies have found that ethylene production and thus the triple response is induced in seedlings by treating them with cytokinin (Cary *et al*., 1995; Vogel *et al*., 1998; Woeste *et al*., 1999a; Cortleven *et al*., 2019a).
Mechanistically, the increase in ethylene content is caused by a ARR1-dependent posttranslational stabilization of ethylene biosynthesis enzyme ACS5 and loss of function mutants were named after their inability to induce the cytokinin-dependent triple response (*cytokinin insensitive5*; *cin5*) (Vogel *et al*., 1998; Chae *et al*., 2003; Hansen *et al*., 2009). Other studies suggested a similar mechanism for ACS4 (Woeste *et al*., 1999a) and it was reported that the transcript abundance of *ACO4* and *ACS6* was reduced eight-fold in *arr2* compared to wild type, which suggests that ARR2 acts as a positive regulator of ethylene biosynthesis (Hass *et al*., 2004). Furthermore, cytokinin applied to *Arabidopsis* seedlings increased the protein abundance of ACO2 in the root (Zdárská *et al*., 2013). If the increase in cytokinin content during the exposure to a PLP is protective against photoperiod stress by signaling through the cytokinin signaling pathway and an increased ethylene status is protective as well, one could speculate that *t*Z-type cytokinins act upstream of ethylene biosynthesis to enable their protective function. Consequently, plants that are either deficient in *t*Z-type cytokinins or have an impaired *t*Z perception

would not be able to induce ethylene biosynthesis upon exposure to photoperiod stress. It is also possible that ethylene acts upstream of cytokinin synthesis. However, so far, no other study reported such a relationship.

Beside the effect of cytokinin on ethylene biosynthesis, the signal transduction of the hormones is interconnected at various levels. Numerous studies suggest that ETR1 directly interacts with AHPs which consequently regulate type-B ARRs (e.g. ARR2) and thus directly influences the output of the cytokinin signaling pathway (Hass *et al*., 2004; Binder *et al*., 2018; Zdarska *et al*., 2019). Hence, one cannot exclude that cytokinin signaling is already affected in the *etr1-1* or *etr1-6* background before and especially during photoperiod stress treatment and consequently, that the increased phenotypic sensitivity of *etr1-1* plants might not only be a result of an impaired ethylene perception. Another indicator for a shared signaling of ethylene and cytokinin could be the cytokinin-dependent induction of the constitutive triple response that is transduced through EIN2 (Cary *et al*., 1995). Similarly, cytokinin acts through EIN2 during root elongation (Ruzicka *et al*., 2009). This might indicate that the increased photoperiod stress sensitivity of *ein2* plants could also be caused by a reduced cytokinin function.

Downstream of EIN2, EIN3/EIL transcription factors regulate the ethylene signaling output (Chao *et al*., 1997; Guo and Ecker, 2003; Potuschak *et al*., 2003). Some studies demonstrated that EIN3 acts as a negative regulator of type-A *ARR* expression, thus inhibiting the cytokinin-induced feedback inhibition of its own signaling pathway (Shi *et al*., 2012). Moreover, it was suggested that EIN3 interacts with type-B ARR1 to increase ARR1 dependent *TAA1* expression (Yan *et al*., 2017). Hence, type-B ARR function and thus cytokinin signaling might be reduced in *ein3* and more considerably in *ein2* as these plants have reduced EIN3 and EIL protein levels (An *et al*., 2010). The increased photoperiod stress sensitivity of *ein2* plants could thus be a cause of a reduced cytokinin signaling output.

4.3.5 Potential interactions of ethylene with auxin in the context of photoperiod stress

As described in this thesis, plants with either an increased auxin content (*yuc1D*) or an impaired ethylene signaling (*ein2* and *ein3*) were less resistant to photoperiod stress while either an impaired auxin perception (*tir1afb2afb3* plants) or a constitutively active ethylene signaling (*ctr1*, *etr1etr2ein4* and *etr2ein4ers2* plants) improved the resistance to photoperiod stress (Figure 31, Figure 36 and Figure 37). Furthermore, auxin content was increased upon exposure to photoperiod stress (Figure 27). All these observations could be linked to each other as auxin and ethylene signaling and synthesis are interconnected (Reviewed in Benková and Hejátko, 2009; Muday *et al*., 2012; Hu *et al*., 2017) and thus will be outlined in this section.

The ethylene response in roots and hypocotyls depends on the induction of auxin synthesis via WEAK ETHYLENE INSENSITIVE2 (WEI2)/ANTHRANILATE SYNTHASE α1 (ASA1) and WEI7/ANTHRANILATE SYNTHASE β1 (ASB1) enzymes that act in the formation of Trp precursors as well as on TAA1/TAR (Stepanova *et al*., 2005, 2008). Further studies suggest that ethylene signaling in the root epidermis triggers auxin synthesis (Vaseva *et al*., 2018). Vice versa, auxin can induce ethylene synthesis in tomato by inducing expression of several *ACS* (Yip *et al*., 1992). In rice, auxin induced ethylene synthesis by positively regulating *ACO* expression (Chae *et al*., 2000). Taking this into account, one could speculate that the increase in IAA content upon exposure to photoperiod stress in wild-type

plants (Figure 27) is caused ethylene-dependently or that the increased IAA levels might render ethylene synthesis, which ultimately induces senescence and PCD (see also sections 4.3.1and 4.3.3).
The interaction of ethylene and auxin signaling was indicated by genetic studies suggesting that CTR1 acts upstream of TIR1 in the regulation of hypocotyl elongation (Alonso *et al*., 2003) and that ARF2 is necessary for ethylene function on apical hook development (Li *et al*., 2004). In the root tip, cell proliferation is inhibited by ethylene through induction of *IAA3/SHY2* gene expression (Street *et al*., 2015). Based on this, one could speculate that ethylene function is suppressed in *tir1afb2afb3* as auxin signaling might be required. If a temporarily increased ethylene signaling output were necessary to form the photoperiod stress syndrome and auxin signaling might be required for proper ethylene signaling, one could argue that *tir1afb2afb3* mutants are at least partially insensitive to ethylene and that this might be the reason for its increased photoperiod stress resistance.

4.3.6 The GA status has a minor influence on the sensitivity to photoperiod stress

In wild-type plants, concentrations of active GAs, their precursors and deactivated forms did not drastically change upon photoperiod stress exposure (Figure 38, Supplemental Figure 4 and Supplemental Figure 5). Similarly, the abundance of most genes involved in GA synthesis and metabolism did not differ in wild type and *ahk2ahk3* upon PLP-treatment (Figure 39). Furthermore, *ga20ox* double mutants were less sensitive to photoperiod stress at the phenotypical level compared to wild type (Figure 41). During cold stress, bioactive GAs are negative regulators of resistance and the amount of bioactive GAs is reduced by the cold-induced expression of *GA2OX* genes (Achard *et al*., 2008). Application of bioactive GAs reduced the resistance to salt stress and plants deficient in their synthesis had increased survival rates upon exposure to high concentrations of NaCl (Magome *et al*., 2004). A similar effect of GA application was communicated for the heat stress resistance of barley seedlings (Vettakkorumakankav *et al*., 1999). However, the data presented in this thesis indicate that GA biosynthesis and metabolism are of minor importance during the exposure to photoperiod stress itself but might be crucial during the short-day cultivation period prior to PLP treatment by influencing plant development.
As well as GA biosynthesis and metabolism, the importance of GA signaling on photoperiod stress resistance has been analyzed. RNAseq revealed that the exposure of wild type and *ahk2ahk3* to a PLP induced similar changes in the transcript abundance of GA receptors as well as downstream transcription factors like PIFs (Figure 40), which has been confirmed via qRT PCR for *GID1A* (Supplemental Figure 3E). At the same time, abundance of several *GAI*/*RGA*/*RGL* genes was reduced only in stressed *ahk2ahk3* plants. These results suggest that a PLP leads to a modulation of the GA signaling pathway at the transcriptional level in plants with differing sensitivities to photoperiod stress. Moreover, the reduced abundance of *GAI*/*RGA*/*RGL* in stressed *ahk2ahk3* compared to control plants might indicate that an increased GA signaling output could be a cause for the formation of the photoperiod stress syndrome. The importance of these genes is indicated by previously described decreased salt stress and cold stress resistance of *Arabidopsis gairga* double mutants (Achard *et al*., 2006, 2008). Genetic evidence provided in this work suggests that a loss of GA receptors leads to an increased phenotypic sensitivity to photoperiod stress whereas an increased GA signaling by a loss of GA signaling repressors (*gai* and *rga* plants) did not alter the phenotypic responsiveness to photoperiod

stress (Figure 41). Confirmative for the phenotypic sensitivity of *gid1* double mutants to photoperiod stress, *gid1agid1c* plants are impaired the most in GA signaling compared to other *gid1* double mutant combinations and thus show the strongest GA-related developmental phenotypes (Griffiths *et al*., 2006). However, especially the phenotypic response of *gid1agid1c* plants and *ga20ox* mutants contradicts each other. One reason for this observation might be that a reduction in GA content in *ga20ox* plants causes an equal reduction in the activity of all three GID1 receptors while in *gid1* double mutants, GA responses are channeled through one receptor in specific tissues. Furthermore, as all receptors have different binding affinities to bioactive GAs (Nakajima *et al*., 2006), the loss of receptors might alter the responsiveness of plants to specific but not all bioactive GAs and thus might induce changes that differ from a reduction of all bioactive GAs in *ga20ox*. All in all, the importance of GA biosynthesis and signaling to cope with photoperiod stress was not fully conclusive from the experiments conducted so far and remains to be solved by future investigations.

4.4 Differences between RNAseq and qRT data

In order to confirm the results of the RNAseq experiment, transcript abundances of some genes involved in auxin, ethylene and GA biosynthesis and signaling were tested via qRT-PCR with a different sample set (Supplemental Figure 3). While some tendencies like the decreased abundance of *TIR1* upon PLP treatment were consistent with the RNAseq data, other effects like the differences in *TIR1* and *CTR1* abundance between PL plants of wild type and *ahk2ahk3* could not be confirmed. What might be the reason for this? One explanation could be that the leaves taken for RNAseq analysis did not show any lesion formation in wild type whereas *ahk2ahk3* leaves were all affected. In addition, leaves eight to eleven of both genotypes were taken for the qRT confirmation experiment. Based on the differences in lesion formation of wild-type and *ahk2ahk3* (Figure 21), leaves eight to eleven best reflect the percentage in lesion formation of whole plants. This implicates that the data obtained by RNAseq might show the difference between an ‘all or nothing’ photoperiod stress response independent of the genotype, whereas the samples taken to confirm the RNAseq data via qRT-PCR reflect a mixture of strong and weak responding leaves. Thus, some differences found by RNAseq that have been interpreted as genotype specific could also be interpreted as being specific for a marked photoperiod stress response.

4.5 Future perspectives

4.5.1 Role of cytokinin synthesis, metabolism and signaling in photoperiod stress

This study provided experimental evidence that root-derived *t*Z-type cytokinins have a protective function against photoperiod stress (sections 3.1.3 and 3.1.4). However, even though the cytokinin content increased in leaves during and after exposure to photoperiod stress in wild type (section 3.1.1), it is still not known whether cytokinins are needed during the stress treatment or whether they affect developmental processes prior to it that influence the sensitivity to photoperiod stress later. To decipher this in future experiments, one could spray *t*Z-type cytokinins onto plants which are unable to synthesize different types of cytokinin (e.g. *ipt3ipt5ipt7* or *cypDM*) only during PLP treatment as well as in the night afterwards.

Apart from investigating the role of *t*Z-type cytokinins prior and during photoperiod stress, results of this study suggest that their transport from the root to the shoot via ABCG14 is of importance (section 3.1.3). Reciprocal grafting of wild type and *abcg14* or *cypDM* should confirm the results indicating the importance for the root-to-shoot transport of *t*Z-type cytokinins and by exchange of the wild type with other mutants, one could use grafting experiments as a fast approach to investigate the connection of other factors with cytokinin in the context of photoperiod stress (some other grafting experiments are proposed in section 4.5.3).

As a part of cytokinin signaling, AHP2, AHP3 and AHP5 act redundantly to regulate the photoperiod stress response (section 3.1.6). As all AHPs except AHP6 are mostly positively regulating cytokinin signaling (Hutchison *et al*., 2006; Mähönen *et al*., 2006) it could be the case that AHP1 and AHP4 are also involved in photoperiod stress signaling. Future experiments that test the photoperiod stress sensitivity of *ahp1*, *ahp4* as well as higher order *ahp* mutants (e.g. *ahp1ahp2ahp3*) should give further insights into the regulation of photoperiod stress through AHPs.

Downstream of AHPs, a complex regulation of the photoperiod stress sensitivity by type-B ARR2, ARR10 and ARR12 is indicated by the sensitivity of respective *arr* single, double and triple mutants to photoperiod stress (section 3.1.7) and a model explaining this regulation has been proposed (section 4.1.4). In order to test the proposed model, one could investigate the interaction of type-B ARRs by testing e.g. N-terminally truncated ARR versions in a yeast-two-hybrid assay as these were able to interact compared with each other and compared to full-length versions (Dortay *et al*., 2006; Yan *et al*., 2017). In another approach that might lead to the identification of the unknown interaction partner X, one could generate lines that express tagged ARR2, ARR10 or ARR12 under their native promoters and introgress them in the *arr2arr10arr12* background (e.g. *ARR2::ARR2-Myc*, *ARR10::ARR10-HA*, *ARR12::ARR12-Myc*). One would expect that X could be found via co-immunoprecipitation by cross-linking it to either of the tagged ARRs in *ARR2-Myc/arr2arr10arr12*, *ARR10-HA/arr2arr10arr12*, and *ARR12-Myc/arr2arr10arr12* and analyzing the interaction partners via MS. In plants expressing ARR10-HA simultaneously with ARR12-Myc in *arr2arr10arr12*, an ARR10-HA-ARR12-Myc interaction could be found and the interaction to X would be lost and thus not detected. If ARRs bind directly to promoters to regulate the sensitivity to photoperiod stress (not X), one could further perform ChiPseq experiments and find target genes and compare the overlap of these between ARR2, ARR10 and ARR12 in the same lines discussed before. A potential ARR-X interaction might be reflected by a similar set of target genes

which are bound by ARR2, ARR10 and ARR12 in *ARR2-Myc/arr2arr10arr12*, *ARR10-HA/arr2arr10arr12*, and *ARR12-Myc/arr2arr10arr12* plants, while in those expressing *ARR10-HA* simultaneously with *ARR12-Myc*, ARR10 and ARR12 might target different genes than ARR2. Depending on whether the interaction is of importance during development or during photoperiod stress treatment, one would detect the ARR-X/ARR10-ARR12 interaction either in control or in stressed plants. To explain the complex regulation of photoperiod stress by ARRs, one could also assume that B-type ARRs interact indirectly through other proteins. However, experimental evidence would be much more difficult to generate as there is no possibility of optimizing experimental conditions to stabilize the interaction of two interaction partners compared to a direct ARR-interaction.

In a forward genetic approach that might lead to the identification of factors that either interact with or are downstream targets of type B ARRs, one could mutagenize *arr2* or *arr2arr10arr12* seeds and screen for plants which show a dampened/suppressed sensitivity to photoperiod stress compared to the control mutant population.

4.5.2 The importance of leaf/plant age and different tissues in photoperiod stress and a potential influence of cytokinin

As shown and discussed in this thesis, *ahk2ahk3* leaves might end cell proliferation and enter maturity or senescence earlier than wild-type leaves (sections 3.2.3 and 4.2.1). At the molecular level, cell proliferation is positively regulated by many factors like ANT (Mizukami and Fischer, 2000), GRFs (Kim and Kende, 2004; Horiguchi *et al*., 2005), AN3/ GIF1 (Kim and Kende, 2004; Lee *et al*., 2009), ARGOS (Hu *et al*., 2003) or SWP (Autran *et al*., 2002). Moreover, senescence is regulated by NACs (Ooka *et al*., 2003; Kim *et al*., 2016, 2018a), WRKYs (Miao *et al*., 2004; Besseau *et al*., 2012), SAGs and SDGs (Hensel *et al*., 1993; Lohman *et al*., 1994; Li *et al*., 2012). To get further insights into the importance of the above mentioned factors regulating cell proliferation and senescence, one could measure the transcript and protein abundance of these factors in leaves of both genotypes in three-, four- and five-week-old plants prior to the exposure to a PLP as well as during the night after the exposure. As a next step, one could expose loss- and gain-of-function mutants of potential candidate genes to photoperiod stress and determine their phenotypic and molecular responses.

Beside the discussed molecular foundation of senescence, the increased responsiveness to ethylene and the decrease in the ability to prevent ROS accumulation, by e.g. ascorbic acid, are two major ARCs in mature leaves that could be causative for the ability to senesce in response to environmental cues like a PLP. In future experiments, one could treat wild-type plants and *ahk2ahk3* of different age (three-, four-, and five-week-old) or leaf eight of respective plants with ethylene/ethephon (Zhang and Wen, 2010) to induce ARC-dependent senescence. Moreover, five-week-old wild type and *ahk2ahk3* could be supplied with the ascorbic acid precursor L-Gal (Kotchoni *et al*., 2009) prior to exposure to a PLP to get additional insights in the importance of the antioxidant system for the responsive to photoperiod stress.

Not only the age of plants and leaves might be crucial for the formation of the photoperiod stress syndrome but also the response of different tissues within a plant might impact on its photoperiod stress sensitivity as indicated by the photoperiod stress response of *CKX(-4xMyc)* overexpressing lines (section 3.2.4). To investigate the impact of the exposure to photoperiod stress on different leaf tissues,

future experiments could compare the transcriptional changes caused by photoperiod stress in the vasculature, the mesophyll and the epidermis with those of total leaves. Moreover, to elucidate the role of the different leaf tissues in more detail, one could express *ARR2* under the control of tissue-specific promoters in the *arr2* background to rescue the mutant's phenotype. Conversely, one could express a dominant negative ARR2 (ARR2DN) variant under the same promoters in wild-type and would expect an increased sensitivity to photoperiod stress for those plants that express *ARR2DN* in an important tissue.

Roots are of importance to protect plants from the photoperiod stress syndrome (section 3.1.3) but exposure of wild type and *ahk2ahk3* to a PLP did not alter the abundance of photoperiod stress marker genes (section 3.2.5). To characterize the transcriptional responsiveness of roots in more detail, one should perform RNAseq experiments with roots of wild type and *ahk2ahk3* that would be either exposed to photoperiod stress or not. By comparing the results of these experiments with the expression data collected for leaves, one could further identify shared stress markers and might get insights into which genes are regulated specifically in the different tissues.

4.5.3 Deciphering the crosstalk between cytokinin, auxin and ethylene in photoperiod stress

During the exposure to photoperiod stress, increased IAA and IAA-Asp levels were detected in wild-type plants (section 3.3.1) and might be causative for the formation of the stress syndrome as *yuc1D* plants had an increased photoperiod stress sensitivity (section 3.3.3). Future experiments could further investigate the importance of IAA during PLP treatment by spraying wild-type plants with IAA or with the auxin transport inhibitor *N*-1-naphthylphthalamic acid (NPA). Another approach would be to create lines which induce the expression of auxin biosynthesis or degradation/conjugation genes during/after the photoperiod stress treatment. For that purpose, promoters of genes that are photoperiod stress induced like *ZAT12* or *BAP1* could be used. The developmental alterations caused by a constantly changed auxin homeostasis could thus be minimized.

In order to find out whether a constant reduction in free IAA results in a reduced sensitivity to photoperiod stress, plants impaired in auxin biosynthesis like *yuc* mutants could be exposed to a PLP. Similarly, in order to decipher whether IAA-Asp accumulation is of importance to cope with photoperiod stress by decreasing endogenous IAA concentrations, it might be of interest to expose *gh3* single and higher order mutants to photoperiod stress. Apart from IAA-Asp, altered transcript abundances of *IAR3* and *ILR3* indicate that other IAA conjugates could be of importance to cope with prolongations of the light period (section 3.3.2). To further elucidate whether these alterations in transcript abundance are relevant for auxin homeostasis during photoperiod stress, measurements of respective IAA-conjugates should be conducted in wild-type. As discussed before, *ahk2ahk3* might have increased IAA levels after exposure to photoperiod stress (section 4.3.2). Future experiments should thus measure the content IAA and all amino acid conjugates in *ahk2ahk3* as well as other cytokinin mutants.

In addition to auxin biosynthesis and metabolism, auxin signaling has a crucial function in photoperiod stress as *tir1afb2afb3* were much less sensitive to PLP treatment than wild type (section 3.3.3). Further receptor mutant analysis might give indications which auxin receptors are of major importance. In addition, future experiments testing the photoperiod stress sensitivity of *ahk2ahk3tir1afb*

quadruple/quintuple mutants and of *tir1afb2afb3/abcg14* grafts (similar setup as described in 4.5.1) might give additional proof for the crucial role of auxin perception in plants with a reduced cytokinin status.

After exposure of wild-type and *ahk2ahk3* plants, an increase in the abundance of genes involved in ethylene biosynthesis (e.g. *SAM* and *ACS* genes) and signaling (e.g. *ETR*, *ERS*, and *EBF* genes) was found (section 3.3.5). To study whether ethylene is induced in response to photoperiod stress, measurements of ethylene and its precursors during the formation of the photoperiod stress syndrome in wild type and *ahk2ahk3* should be performed. Moreover, exposure of plants with an increased or impaired ethylene biosynthesis to photoperiod stress might give further insights into its involvement.

Analysis of ethylene signaling mutants indicates that an impaired ethylene perception increases the photoperiod stress sensitivity while a constitutively active signaling has the opposite effect (section 3.3.6). To decipher which ethylene receptor has the prominent role in the regulation of photoperiod stress, lower order mutants of *etr1etr2ein4* and *etr2ein4ers2* should be exposed to a PLP. To figure out which tissues require proper ethylene signaling in the context of photoperiod stress, *ctr1* lines overexpressing *EBF2* that were used before (Vaseva *et al*., 2018), could be tested.

As discussed before (section 4.3.4), ETR1 directly interacts with components of the cytokinin signaling pathway. To analyze whether ETR1 acts independently of cytokinin signaling during photoperiod stress, generation and exposure of e.g. *etr1-1ahk2ahk3* and *etr1-6ahk2ahk3* mutants to a PLP should be considered. An increased sensitivity to photoperiod stress in *etr1-1ahk2ahk3* compared to their respective *ahk2ahk3* and *etr1-1* controls would be indicative of a separate regulation of photoperiod stress while a sensitivity of *etr1-6ahk2ahk3* that is not intermediate to *etr1-6* and *ahk2ahk3* would suggest a shared regulation. In addition, a cytokinin-ethylene interaction could be tested by exposing e.g. *etr1etr2ein4/abcg14* or *ctr1/abcg14* reciprocal grafts to photoperiod stress (similar setup as described in 4.5.1).

Not only ETR1 directly interacts with cytokinin signaling components but also EIN3 as it directly interacts with type-B ARRs and as a consequence positively regulates their function (Yan *et al*., 2017). Hence, it might be of interest in future studies to characterize an EIN3/EIL-ARR interaction in the context of photoperiod stress by e.g. exposing *ein3arr2*, *eil1arr2* and *ein3eil1arr2* mutants to a PLP. Furthermore, one could perform ChiPseq experiments with e.g. *ARR2* and *EIN3* overexpressing lines and expose these to photoperiod stress. A comparison between the targets found for each transcription factor might provide further indications for a synergistic effect of ethylene and cytokinin and could give insights into potential downstream targets of both pathways.

To investigate a potential interaction between ethylene and auxin during photoperiod stress in more detail, one could measure the content of ethylene precursor ACC or ethylene itself in wild type in a similar experimental setup as done for auxin measurements. Moreover, ACC/ethylene content could be measured in *yuc1D* or *tir1afb2afb3* and IAA/IAA-Asp contents could be determined in *ctr1* or in *ein2* plants. If one of the hormones is causative for the formation of the photoperiod stress syndrome, hormone levels should correlate with the phenotypic sensitivity of the respective genotypes. Genetic evidence for an interaction could be provided by generation and testing of *etr1etr2ein4yuc1D* plants. If auxin is acting downstream of ethylene signaling, the quadruple mutant should phenocopy the *yuc1D* photoperiod stress phenotype.

4.5.4 Photoperiod stress as a system to study the ability of plants to adapt to seasonal changes in daylength

As mentioned briefly in the introduction to photoperiod stress (section 1.1), differences in the expression of marker genes as well as an increase in H_2O_2 is detectable after a light period that has been prolonged by two hours compared to SD cultivation. Moreover, this PLP can prevent a response to a second PLP of twelve hours if the second PLP is applied within five days (Dr. Sylvia Illgen, personal communication). These results indicate that plants can perceive much shorter extensions in daylength and implicate that the given PLP of 32 hours is an extreme version of photoperiod stress. As the quantification of marker gene expression and H_2O_2 has technical limitations in detection, future experiments could indirectly prove the perception of very short extensions in daylength by testing e.g. the protective effect of a first PLP of eight hours and ten minutes to a second PLP of twelve hours. Independent of that one could speculate that an accumulation of H_2O_2 also occurs by prolonging the daylength by 5 minutes (with a much smaller amplitude). In that case, H_2O_2 might act as a signaling molecule inducing changes in e.g. the antioxidant system of chloroplasts, peroxisomes or mitochondria (Reviewed in Niu and Liao, 2016). Summing up, photoperiod stress in its current form displays a type of artificial light stress but might develop into a setup which, in future, enables us to study the ability of plants to adapt to extensions in daylength as they occur in nature during seasonal changes from winter to spring or spring to summer.

5 Summary

Photoperiod stress is a novel type of abiotic stress in plants caused by a prolongation of the light period. It has been reported that plants require a functional circadian clock as well as a functional cytokinin synthesis, metabolism and signaling to cope with photoperiod stress. Within this thesis, additional factors influencing the sensitivity to photoperiod stress have been investigated.

In the first chapter of this work, plants that are either unable to synthesize *tZ*-type cytokinins (*cypDM*) or transport them from the root to the shoot (*abcg14*) were exposed to photoperiod stress. As indicated by an increased lesion formation, a reduced photosynthetic capacity, an altered expression of marker genes and an accumulation of H_2O_2, these plants were more sensitive to a prolongation of the light period. Further experimental evidence for the importance of these type of cytokinins was provided by watering of *cypDM* plants with *tZ*-type cytokinins which rescued the photoperiod stress phenotype. Moreover, cytokinin levels were monitored throughout photoperiod stress treatment and development of stress symptoms in wild-type plants and indicated that the treatment leads to a general cytokinin accumulation. Apart from cytokinin synthesis and transport, mutant analysis led to the identification of AHP2, AHP3 and AHP5 as key components of cytokinin signaling during photoperiod stress. In addition, indications for a complex regulatory mechanism of ARR2, ARR10 and ARR12 transcription factors during photoperiod stress have been collected and based on these, a model in which ARRs either interact with each other or with unknown factors has been proposed.

In the second chapter, the photoperiod stress sensitivity of young and mature plants and leaves and the contribution of different tissues to the photoperiod stress response has been investigated. The photoperiod stress sensitivity of wild-type and *ahk2ahk3* plants and leaves of different age and the photoperiod stress response of leaves on a single rosette was determined. Results indicated that with an increasing leaf and plant age the ability to cope with prolongations of the light period decreased. Furthermore, analysis of *MIR156B* and *MIM172* overexpressors demonstrated that there is no influence of the leaf identity (juvenile vs. adult leaves) on the photoperiod stress response. Moreover, the exposure of plants tissue-specifically expressing *CKX1* to photoperiod stress indicated that the vasculature and epidermis are crucial to regulate the sensitivity to photoperiod stress. Lastly, the molecular response to photoperiod stress in leaves and roots of wild type and *ahk2ahk3* was compared and indicates that roots differ substantially in their response from leaves.

In the third chapter, the importance of the phytohormones auxin, ethylene and GA in coping with photoperiod stress was investigated. Auxin and GA measurements in wild-type leaves, transcriptome analysis of wild-type and *ahk2ahk3* leaves as well as mutant analysis hints at a protective function of ethylene and a photoperiod stress inducing the role of auxin. Strikingly, a partial loss of auxin perception in *ahk2ahk3* caused a partial rescue of the photoperiod stress phenotype and thus indicates that an imbalance in auxin homeostasis might be causative for the increased photoperiod stress sensitivity of plants with a lowered cytokinin status.

6 Zusammenfassung

Photoperiodischer Stress ist ein kürzlich entdeckter abiotischer Stress, der durch die Verlängerung der Lichtperiode hervorgerufen wird. In der Erstveröffentlichung zu photoperiodischem Stress wurde eine funktionelle Relevanz der circadianen Uhr und der Synthese, des Metabolismus und der Signaltransduktion des Pflanzenhormons Cytokinin beschrieben. In der vorliegenden Arbeit wurden weitere Faktoren, die potenziell die Sensitivität gegenüber photoperiodischem Stress beeinflussen, untersucht.

Im ersten Kapitel dieser Arbeit wurden Pflanzen, die entweder *t*Z-Typ-Cytokinine nicht mehr synthetisieren (*cypDM*) oder von der Wurzel Richtung Spross transportieren können (*abcg14*) photoperiodischem Stress ausgesetzt. Diese Pflanzen reagierten sehr sensitiv auf die Verlängerung der Lichtperiode, was eine erhöhte Läsionsbildung, eine Verringerung der photosynthetischen Kapazität, eine veränderte Expression von stressregulierten Genen und eine Akkumulation von H_2O_2 zur Folge hatte. Als weiterer experimenteller Beleg für die Wichtigkeit von *t*Z-Typ Cytokininen reduzierte das Wässern von *cypDM* Pflanzen mit *t*Z-Typ Cytokininen die Sensitivität der Pflanzen gegenüber photoperiodischem Stress. Weiterhin wurde im Wildtyp der Cytokinin-Gehalt über die Ganze Stressbehandlung hinweg verfolgt und zeigte, dass die Behandlung der Pflanzen mit photoperiodischem Stress zu einer allgemeinen Erhöhung des Cytokinin-Gehalts führt. Die Analyse von Mutanten zeigte zudem, dass die Signalkomponenten AHP2, AHP3 und AHP5 sowie die Transkriptionsfaktoren ARR2, ARR10 und ARR12 von zentraler Bedeutung für die Cytokinin-Signaltransduktion während photoperiodischem Stress ist. Des Weiteren wurde ein Modell vorgeschlagen, in dem ARR2, ARR10 und ARR12 entweder untereinander oder mit unbekannten Faktoren interagieren.

Im zweiten Kapitel wurde die Antwort von jungen und alten Pflanzen und Blättern sowie verschiedener Gewebe gegenüber photoperiodischem Stress untersucht. Hierfür wurde die Sensitivität von Pflanzen und Blättern des Wildtyps und von *ahk2ahk3* verschiedenen Alters bestimmt sowie die Antwort verschiedener Blätter einer Rosette untersucht. Die Untersuchungen deuten unter anderem auf eine reduzierte Toleranz von Pflanzen und Blättern gegenüber einer Verlängerung der Lichtperiode mit zunehmendem Alter hin. Die Analyse von *MIR156B*- und *MIM172*-überexprimierenden Pflanzen zeigte weiterhin, dass die Blattidentität (juvenile vs. adulte Blätter) keinen Einfluss auf die Stressantwort hat. Durch die Untersuchung von Pflanzen, die das Cytokinin-abbauende Enzym CKX1 gewebespezifisch exprimieren, wurde zudem eine zentrale Aufgabe der Vaskulatur und der Epidermis in der Modulation der Stressantwort demonstriert. Der Vergleich der molekularen Antwort von Wurzeln und Blättern deutet zudem auf eine unterschiedliche Antwort der Gewebe gegenüber photoperiodischem Stress hin.

Im dritten Kapitel wurde die Rolle der Pflanzenhormone Auxin, Ethylen und GA für die Sensitivität gegenüber photoperiodischem Stress bestimmt. Messungen des Auxin- und GA-Gehalts in Pflanzen des Wildtyps, eine Transkriptomanalyse des Wildtyps und von *ahk2ahk3*-Pflanzen sowie die Analyse von Auxin-, Ethylen- und GA-Mutanten demonstrierten eine schützende Wirkung von Ethylen und einen Stress-induzierenden Einfluss von Auxin. Eine Beeinträchtigung der Auxin-Signaltransduktion in *ahk2ahk3*-Pflanzen resultierte in einer Verringerung der Stressantwort. Dies könnte darauf hindeuten, dass Pflanzen mit einem verringerten Cytokinin-Status ein Ungleichgewicht der Auxin-Homöostase

aufweisen, welche für die erhöhte Sensitivität gegenüber photoperiodischem Stress verantwortlich sein könnte.

7 References

Abeles, F.B., Morgan, P.W., and Saltveit, M.E. (1992). The role of ethylene in agriculture. In Ethylene in Plant Biology (Academic Press), pp. 264–296.

Abramoff, M.D., Magalhaes, P.J., and Ram, S.J. (2004). Image processing with ImageJ. Biophotonics Int. **11**: 36–42.

Achard, P., Cheng, H., De Grauwe, L., Decat, J., Schoutteten, H., Moritz, T., Van Der Straeten, D., Peng, J., and Harberd, N.P. (2006). Integration of plant responses to environmentally activated phytohormonal signals. Science **311**: 91–94.

Achard, P., Gong, F., Cheminant, S., Alioua, M., Hedden, P., and Genschika, P. (2008). The cold-inducible CBF1 factor-dependent signaling pathway modulates the accumulation of the growth-repressing DELLA proteins via its effect on gibberellin metabolism. Plant Cell **20**: 2117–2129.

Alonso, J.M., Stepanova, A.N., Solano, R., Wisman, E., Ferrari, S., Ausubel, F.M., and Ecker, J.R. (2003). Five components of the ethylene-response pathway identified in a screen for weak ethylene-insensitive mutants in *Arabidopsis*. Proc. Natl. Acad. Sci. U. S. A. **100**: 2992–2997.

An, F., Zhao, Q., Ji, Y., Li, W., Jiang, Z., Yu, X., Zhang, C., Han, Y., He, W., Liu, Y., Zhang, S., Ecker J. R., and Guo, H. (2010). Ethylene-induced stabilization of ETHYLENE INSENSITIVE3 and EIN3-LIKE1 is mediated by proteasomal degradation of EIN3 BINDING F-BOX 1 and 2 that requires EIN2 in *Arabidopsis*. Plant Cell **22**: 2384–2401.

An, H., Roussot, C., Suárez-López, P., Corbesier, L., Vincent, C., Piñeiro, M., Hepworth, S., Mouradov, A., Justin, S., Turnbull, C., and Coupland, G. (2004). CONSTANS acts in the phloem to regulate a systemic signal that induces photoperiodic flowering of *Arabidopsis*. Development **131**: 3615–3626.

Andriankaja, M., Dhondt, S., De Bodt, S., Vanhaeren, H., Coppens, F., De Milde, L., Mühlenbock, P., Skirycz, A., Gonzalez, N., Beemster, G.T.S., and Inzé, D. (2012). Exit from proliferation during leaf development in *Arabidopsis thaliana*: A not-so-gradual process. Dev. Cell **22**: 64–78.

Aremu, A.O., Masondo, N.A., Sunmonu, T.O., Kulkarni, M.G., Zatloukal, M., Spichal, L., Doležal, K., and Van Staden, J. (2014). A novel inhibitor of cytokinin degradation (INCYDE) influences the biochemical parameters and photosynthetic apparatus in NaCl-stressed tomato plants. Planta **240**: 877–889.

Ariizumi, T., Lawrence, P.K., and Steber, C.M. (2011). The role of two F-box proteins, SLEEPY1 and SNEEZY, in *Arabidopsis* gibberellin signaling. Plant Physiol. **155**: 765–775.

Arnaud, D., Lee, S., Takebayashi, Y., Choi, D., Choi, J., Sakakibara, H., and Hwang, I. (2017). Cytokinin-mediated regulation of reactive oxygen species homeostasis modulates stomatal immunity in *Arabidopsis*. Plant Cell **29**: 543–559.

Arvidsson, S., Kwasniewski, M., Riaño-Pachón, D.M., and Mueller-Roeber, B. (2008). QuantPrime - A flexible tool for reliable high-throughput primer design for quantitative PCR. BMC Bioinformatics **9**: 465.

Aukerman, M.J. and Sakai, H. (2003). Regulation of flowering time and floral organ identity by a MicroRNA and its APETALA2-like target genes. Plant Cell **15**: 2730–2741.

Autran, D., Jonak, C., Belcram, K., Beemster, G.T.S., Kronenberger, J., Grandjean, O., Inzé, D.,

and Traas, J. (2002). Cell numbers and leaf development in *Arabidopsis*: A functional analysis of the *STRUWWELPETER* gene. EMBO J. **21**: 6036–6049.

Axtell, M.J. and Bartel, D.P. (2005). Antiquity of microRNAs and their targets in land plants. Plant Cell **17**: 1658–1673.

Bar, M. and Ori, N. (2014). Leaf development and morphogenesis. Development **141**: 4219–4230.

Bartrina, I., Jensen, H., Novak, O., Strnad, M., Werner, T., and Schmülling, T. (2017). Gain-of-function mutants of the cytokinin receptors AHK2 and AHK3 regulate plant organ size, flowering time and plant longevity. Plant Physiol. **173**: 1783–1797.

Bartrina, I., Otto, E., Strnad, M., Werner, T., and Schmülling, T. (2011). Cytokinin regulates the activity of reproductive meristems, flower organ size, ovule formation, and thus seed yield in *Arabidopsis thaliana*. Plant Cell **23**: 69–80.

Benková, E. and Hejátko, J. (2009). Hormone interactions at the root apical meristem. Plant Mol. Biol. **69**: 383–396.

Bernard, P. and Couturier, M. (1992). Cell killing by the F plasmid CCDB protein involves poisoning of DNA-topoisomerase II complexes. J. Mol. Biol. **226**: 735–745.

Bertani, G. (1951). Studies on lysogenesis. I. The mode of phage liberation by lysogenic *Escherichia coli*. J. Bacteriol. **62**: 293–300.

Besseau, S., Li, J., and Palva, E.T. (2012). WRKY54 and WRKY70 co-operate as negative regulators of leaf senescence in *Arabidopsis thaliana*. J. Exp. Bot. **63**: 2667–2679.

Bielczynski, L.W., Łącki, M.K., Hoefnagels, I., Gambin, A., and Croce, R. (2017). Leaf and plant age affects photosynthetic performance and photoprotective capacity. Plant Physiol. **175**: 1634-1648.

Binder, B.M., Kim, H.J., Mathews, D.E., Hutchison, C.E., Kieber, J.J., and Schaller, G.E. (2018). A role for two-component signaling elements in the *Arabidopsis* growth recovery response to ethylene. Plant Direct **2**: e00058.

Bishopp, A., Lehesranta, S., Vatén, A., Help, H., El-Showk, S., Scheres, B., Helariutta, K., Mähönen, A.P., Sakakibara, H., and Helariutta, Y. (2011). Phloem-transported cytokinin regulates polar auxin transport and maintains vascular pattern in the root meristem. Curr. Biol. **21**: 927–932.

Bisson, M.M.A. and Groth, G. (2010). New insight in ethylene signaling: Autokinase activity of ETR1 modulates the interaction of receptors and EIN2. Mol. Plant **3**: 882–889.

Biswas, M.S., Fukaki, H., Mori, I.C., Nakahara, K., and Mano, J. (2019). Reactive oxygen species and reactive carbonyl species constitute a feed-forward loop in the auxin signaling for lateral root formation. Plant J.: tpj.14456.

Bleecker, A.B. and Kende, H. (2000). Ethylene: a gaseous signal molecule in plants. Annu. Rev. Cell Dev. Biol. **16**: 1–18.

Brandstatter, I. and Kieber, J.J. (1998). Two genes with similarity to bacterial response regulators are rapidly and specifically induced by cytokinin in *Arabidopsis*. Plant Cell **10**: 1009–1019.

Breeze, E., Harrison, E., McHattie, S., Hughes, L., Hickman, R., Hill, C., Kiddle, S., Kim, Y., Penfold, C. A., Jenkins, D., Zhang, C., Morris, K., Jenner, C., Jackson, S., Thomas, B., Tabrett, A., Legaie, R., Moore, J. D., Wild, D. L., Ott, S., Rand, D., Beynon, J., Denby, K., Mead, A., and Buchanan-Wollaston, V. (2011). High-resolution temporal profiling of transcripts during

Arabidopsis leaf senescence reveals a distinct chronology of processes and regulation. Plant Cell **23**: 873–894.

Bürkle, L., Cedzich, A., Döpke, C., Stransky, H., Okumoto, S., Gillissen, B., Kühn, C., and Frommer, W.B. (2003). Transport of cytokinins mediated by purine transporters of the PUP family expressed in phloem, hydathodes, and pollen of *Arabidopsis*. Plant J. **34**: 13–26.

Caers, M., Rudelsheim, P., Onckelen, H. Van, and Horemans, S. (1985). Effect of heat stress on photosynthetic activity and chloroplast ultrastructure in correlation with endogenous cytokinin concentration in maize seedlings. Plant Cell Physiol. **26**: 47–52.

Cao, W.-H., Liu, J., He, X.-J., Mu, R.-L., Zhou, H.-L., Chen, S.-Y., and Zhang, J.-S. (2007). Modulation of ethylene responses affects plant salt-stress responses. Plant Physiol. **143**: 707–719.

Cardon, G., Höhmann, S., Klein, J., Nettesheim, K., Saedler, H., and Huijser, P. (1999). Molecular characterisation of the *Arabidopsis* SBP-box genes. Gene **237**: 91–104.

Cary, A.J., Liu, W., and Howell, S.H. (1995). Cytokinin action is coupled to ethylene in its effects on the inhibition of root and hypocotyl elongation in *Arabidopsis thaliana* seedlings. Plant Physiol. **107**: 1075–1082.

Cedzich, A., Stransky, H., Schulz, B., and Frommer, W.B. (2008). Characterization of cytokinin and adenine transport in *Arabidopsis* cell cultures. Plant Physiol. **148**: 1857–67.

Chae, H.S., Cho, Y.G., Park, M.Y., Lee, M.C., Eun, M.Y., Kang, B.G., and Kim, W.T. (2000). Hormonal cross-talk between auxin and ethylene differentially regulates the expression of two members of the *1-AMINOCYCLOPROPANE-1-CARBOXYLATE OXIDASE* gene family in rice (*Oryza sativa* L.). Plant Cell Physiol. **41**: 354–362.

Chae, H.S., Faure, F., and Kieber, J.J. (2003). The *eto1*, *eto2*, and *eto3* mutations and cytokinin treatment increase ethylene biosynthesis in *Arabidopsis* by increasing the stability of ACS protein. Plant Cell **15**: 545–559.

Chao, Q., Rothenberg, M., Solano, R., Roman, G., Terzaghi, W., and Ecker, J.R. (1997). Activation of the ethylene gas response pathway in *Arabidopsis* by the nuclear protein ETHYLENE-INSENSITIVE3 and related proteins. Cell **89**: 1133-1144.

Chen, C., Ridzon, D. A., Broomer,A. J., Zhou, Z., Lee, D. H., Nguyen, J. T., Barbisin, M., Xu, N. L., Mahuvakar, V. R., Andersen, M. R., Lao, K. Q., Livak, K. J., and Guegler, K. J. (2005). Real-time quantification of microRNAs by stem-loop RT-PCR. Nucleic Acids Res. **33**: e179–e179.

Chen, X. (2004). A microRNA as a Translational Repressor of APETALA2 in *Arabidopsis* flower development. Science **303**: 2022–2025.

Cheng, H. (2004). Gibberellin regulates *Arabidopsis* floral development via suppression of DELLA protein function. Development **131**: 1055–1064.

Cheng, Y., Dai, X., and Zhao, Y. (2006). Auxin biosynthesis by the YUCCA flavin monooxygenases controls the formation of floral organs and vascular tissues in *Arabidopsis*. Genes Dev. **20**: 1790–1799.

Chien, J.C. and Sussex, I.M. (1996). Differential regulation of trichome formation on the adaxial and abaxial leaf surfaces by gibberellins and photoperiod in *Arabidopsis thaliana* (L.) Heynh. Plant Physiol. **111**: 1321–1328.

Choi, W.G., Toyota, M., Kim, S.H., Hilleary, R., and Gilroy, S. (2014). Salt stress-induced Ca^{2+} waves

are associated with rapid, long-distance root-to-shoot signaling in plants. Proc. Natl. Acad. Sci. U. S. A. **111**: 6497–6502.

Clough, S.J. and Bent, A.F. (1998). Floral dip: A simplified method for *Agrobacterium*-mediated transformation of *Arabidopsis thaliana*. Plant J. **16**: 735–743.

Coenen, C. and Lomax, T.L. (1997). Auxin-cytokinin interactions in higher plants: Old problems and new tools. Trends Plant Sci. **2**: 351–356.

Corbesier, L., Prinsen, E., Jacqmard, A., Lejeune, P., Van Onckelen, H., Périlleux, C., and Bernier, G. (2003). Cytokinin levels in leaves, leaf exudate and shoot apical meristem of *Arabidopsis thaliana* during floral transition. J. Exp. Bot. **54**: 2511–2517.

Cortleven, A., Ehret, S., Schmülling, T., and Johansson, H. (2019a). Ethylene-independent promotion of photomorphogenesis in the dark by cytokinin requires COP1 and the CDD complex. J. Exp. Bot. **70**: 165–178.

Cortleven, A., Leuendorf, J.E., Frank, M., Pezzetta, D., Bolt, S., and Schmülling, T. (2019b). Cytokinin action in response to abiotic and biotic stress in plants. Plant. Cell Environ. **42**: 998–1018.

Cortleven, A., Nitschke, S., Klaumünzer, M., Abdelgawad, H., Asard, H., Grimm, B., Riefler, M., and Schmülling, T. (2014). A novel protective function for cytokinin in the light stress response is mediated by the ARABIDOPSIS HISTIDINE KINASE2 and ARABIDOPSIS HISTIDINE KINASE3 receptors. Plant Physiol. **164**: 1470–1483.

Cucinotta, M., Manrique, S., Cuesta, C., Benkova, E., Novak, O., and Colombo, L. (2018). CUP-SHAPED COTYLEDON1 (CUC1) and CUC2 regulate cytokinin homeostasis to determine ovule number in *Arabidopsis*. J. Exp. Bot. **69**: 5169–5176.

Darwin, C. and Darwin, F. (1880). The power of movement in plants (John Murray: London).

Davière, J.-M. and Achard, P. (2013). Gibberellin signaling in plants. Development **140**: 1147–1151.

Davies, R.T., Goetz, D.H., Lasswell, J., Anderson, M.N., and Bartel, B. (1999). IAR3 encodes an auxin conjugate hydrolase from *Arabidopsis*. Plant Cell **11**: 365–376.

Davis, A.M., Hall, A., Millar, A.J., Darrah, C., and Davis, S.J. (2009). Protocol: Streamlined sub-protocols for floral-dip transformation and selection of transformants in *Arabidopsis thaliana*. Plant Methods **5**: 3.

Décima Oneto, C., Otegui, M.E., Baroli, I., Beznec, A., Faccio, P., Bossio, E., Blumwald, E., and Lewi, D. (2016). Water deficit stress tolerance in maize conferred by expression of an *ISOPENTENYLTRANSFERASE* (*IPT*) gene driven by a stress- and maturation-induced promoter. J. Biotechnol. **220**: 66–77.

Dertinger, U., Schaz, U., and Schulze, E.D. (2003). Age-dependence of the antioxidative system in tobacco with enhanced glutathione reductase activity or senescence-induced production of cytokinins. Physiol. Plant. **119**: 19–29.

Dharmasiri, N., Dharmasiri, S., and Estelle, M. (2005a). The F-box protein TIR1 is an auxin receptor. Nature **435**: 441–445.

Dharmasiri, N., Dharmasiri, S., Weijers, D., Lechner, E., Yamada, M., Hobbie, L., Ehrismann, J.S., Jürgens, G., and Estelle, M. (2005b). Plant development is regulated by a family of auxin receptor F box proteins. Dev. Cell **9**: 109–119.

Di, D.-W., Wu, L., Zhang, L., An, C.-W., Zhang, T.-Z., Luo, P., Gao, H.-H., Kriechbaumer, V., and Guo, G.-Q. (2016). Functional roles of *Arabidopsis CKRC2/YUCCA8* gene and the involvement of PIF4 in the regulation of auxin biosynthesis by cytokinin. Sci. Rep. **6**: 36866.

Dill, A., Thomas, S.G., Hu, J., Steber, C.M., and Sun, T. (2004). The *Arabidopsis* F-box protein SLEEPY1 targets gibberellin signaling repressors for gibberellin-induced degradation. Plant Cell **16**: 1392–1405.

Donnelly, P.M., Bonetta, D., Tsukaya, H., Dengler, R.E., and Dengler, N.G. (1999). Cell cycling and cell enlargement in developing leaves of *Arabidopsis*. Dev. Biol. **215**: 407–419.

Dortay, H., Mehnert, N., Bürkle, L., Schmülling, T., and Heyl, A. (2006). Analysis of protein interactions within the cytokinin-signaling pathway of *Arabidopsis thaliana*. FEBS J. **273**: 4631–4644.

Duan, Q., Kita, D., Li, C., Cheung, A.Y., and Wu, H.-M. (2010). FERONIA receptor-like kinase regulates RHO GTPase signaling of root hair development. Proc. Natl. Acad. Sci. U. S. A. **107**: 17821–17826.

Durán-Medina, Y., Díaz-Ramírez, D., and Marsch-Martínez, N. (2017). Cytokinins on the move. Front. Plant Sci. **8**: 146.

Dyer, T.A. and Osborne, D.J. (1971). Leaf nucleic acids:: II. Metabolism during senescence and the effect of kinetin. J. Exp. Bot. **22**: 552–560.

Ecker, J.R. (1995). The ethylene signal transduction pathway in plants. Science **268**: 667–675.

Eklöf, S., Åstot, C., Sitbon, F., Moritz, T., Olsson, O., and Sandberg, G. (2000). Transgenic tobacco plants co-expressing *Agrobacterium IAA* and *IPT* genes have wild-type hormone levels but display both auxin- and cytokinin-overproducing phenotypes. Plant J. **23**: 279–284.

El-Showk, S., Ruonala, R., and Helariutta, Y. (2013). Crossing paths: cytokinin signalling and crosstalk. Development **140**: 1373–83.

Endo, M., Shimizu, H., Nohales, M.A., Araki, T., and Kay, S.A. (2014). Tissue-specific clocks in *Arabidopsis* show asymmetric coupling. Nature **515**: 419–422.

Feng, S., Martinez, C., Gusmaroli, G., Wang, Y., Zhou, J., Wang, F., Chen, L., Yu, L., Iglesias-Pedraz, J. M., Kircher, S., Schäfer, E., Fu, X., Fan, L. M., and Deng, X. W. (2008). Coordinated regulation of *Arabidopsis thaliana* development by light and gibberellins. Nature **451**: 475–479.

Franco-Zorrilla, J.M., Valli, A., Todesco, M., Mateos, I., Puga, M.I., Rubio-Somoza, I., Leyva, A., Weigel, D., García, J.A., and Paz-Ares, J. (2007). Target mimicry provides a new mechanism for regulation of microRNA activity. Nat. Genet. **39**: 1033–1037.

Gan, S. and Amasino, R.M. (1995). Inhibition of leaf senescence by autoregulated production of cytokinin. Science **270**: 1986–1988.

Gao, Y., Zhang, Y., Zhang, D., Dai, X., Estelle, M., and Zhao, Y. (2015). AUXIN BINDING PROTEIN 1 (ABP1) is not required for either auxin signaling or *Arabidopsis* development. Proc. Natl. Acad. Sci. U. S. A. **112**: 2275–2280.

Gibson, S.I., Laby, R.J., and Kim, D. (2001). The *sugar-insensitive 1* (*sis1*) mutant of *Arabidopsis* is allelic to *ctr1*. Biochem. Biophys. Res. Commun. **280**: 196–203.

Gillissen, B., Bürkle, L., André, B., Kühn, C., Rentsch, D., Brandl, B., and Frommer, W.B. (2000). A new family of high-affinity transporters for adenine, cytosine, and purine derivatives in

Arabidopsis. Plant Cell **12**: 291–300.

Gonzalez, N., Vanhaeren, H., and Inzé, D. (2012). Leaf size control: Complex coordination of cell division and expansion. Trends Plant Sci. **17**: 332–340.

Granier, C., Massonnet, C., Turc, O., Muller, B., Chenu, K., and Tardieu, F. (2002). Individual leaf development in *Arabidopsis thaliana*: A stable thermal-time-based programme. Ann. Bot. **89**: 595–604.

Grant, S.G., Jessee, J., Bloom, F.R., and Hanahan, D. (1990). Differential plasmid rescue from transgenic mouse DNAs into *Escherichia coli* methylation-restriction mutants. Proc. Natl. Acad. Sci. U. S. A. **87**: 4645–4649.

Griffiths, J., Murase, K., Rieu, I., Zentella, R., Zhang, Z.-L., Powers, S.J., Gong, F., Phillips, A.L., Hedden, P., Sun, T., and Thomas, S.G. (2006). Genetic characterization and functional analysis of the GID1 gibberellin receptors in *Arabidopsis*. Plant Cell **18**: 3399–3414.

Guilfoyle, T.J. and Hagen, G. (2007). Auxin response factors. Curr. Opin. Plant Biol. **10**: 453–460.

Guo, H. and Ecker, J.R. (2003). Plant responses to ethylene gas are mediated by SCFEBF1/EBF2-dependent proteolysis of EIN3 transcription factor. Cell **115**: 667–677.

Guzman, P. and Ecker, J.R. (1990). Exploiting the triple response of *Arabidopsis* to identify ethylene-related mutants. Plant Cell **2**: 513–523.

Hanahan, D. (1983). Studies on transformation of *Escherichia coli* with plasmids. J. Mol. Biol. **166**: 557–580.

Hansen, M., Chae, H.S., and Kieber, J.J. (2009). Regulation of ACS protein stability by cytokinin and brassinosteroid. Plant J. **57**: 606–614.

Hass, C., Lohrmann, J., Albrecht, V., Sweere, U., Hummel, F., Yoo, S. D. Hwang, I., Zhu, T., Schäfer, E., Kudla, J., and Harter, K. (2004). The RESPONSE REGULATOR 2 mediates ethylene signalling and hormone signal integration in *Arabidopsis*. EMBO J. **23**: 3290–3302.

Hedden, P. and Phillips, A.L. (2000). Gibberellin metabolism: New insights revealed by the genes. Trends Plant Sci. **5**: 523–530.

Hedden, P. and Sponsel, V. (2015). A century of gibberellin research. J. Plant Growth Regul. **34**: 740–760.

Helliwell, C.A., Chandler, P.M., Poole, A., Dennis, E.S., and Peacock, W.J. (2001). The CYP88A cytochrome P450, ent-kaurenoic acid oxidase, catalyzes three steps of the gibberellin biosynthesis pathway. Proc. Natl. Acad. Sci. U. S. A. **98**: 2065–2070.

Helliwell, C.A., Sheldon, C.C., Olive, M.R., Walker, A.R., Zeevaart, J.A.D., Peacock, W.J., and Dennis, E.S. (1998). Cloning of the *Arabidopsis* ent-kaurene oxidase gene *GA3*. Proc. Natl. Acad. Sci. U. S. A. **95**: 9019–9024.

Hensel, L.L., Grbić, V., Baumgarten, D.A., and Bleecker, A.B. (1993). Developmental and age-related processes that influence the longevity and senescence of photosynthetic tissues in *Arabidopsis*. Plant Cell **5**: 553–564.

Hewett, E.W. and Wareing, P.F. (1973). Cytokinins in *PopulusXrobusta*: Qualitative changes during development. Physiol. Plant. **29**: 386–389.

Hirose, N., Makita, N., Yamaya, T., and Sakakibara, H. (2005). Functional characterization and expression analysis of a gene, *OsENT2*, encoding an equilibrative nucleoside transporter in rice

suggest a function in cytokinin transport. Plant Physiol. **138**: 196–206.

Hirose, N., Takei, K., Kuroha, T., Kamada-Nobusada, T., Hayashi, H., and Sakakibara, H. (2008). Regulation of cytokinin biosynthesis, compartmentalization and translocation. J. Exp. Bot. **59**: 75–83.

Hori, S. (1898). Some observations on 'bakanae' disease of the rice plant. Mem Agric Res Sta **12**: 110–119.

Horiguchi, G., Kim, G.T., and Tsukaya, H. (2005). The transcription factor AtGRF5 and the transcription coactivator AN3 regulate cell proliferation in leaf primordia of *Arabidopsis thaliana*. Plant J. **43**: 68–78.

Hou, B., Lim, E.-K., Higgins, G.S., and Bowles, D.J. (2004). N-glucosylation of cytokinins by glycosyltransferases of *Arabidopsis thaliana*. J. Biol. Chem. **279**: 47822–47832.

Hu, J., Mitchum, M. G., Barnaby, N., Ayele, B. T., Ogawa, M., Nam, E., Lai, W., Hanada, A., Alonso, J. M., Ecker, J. R., Swain, S. M., Yamaguchi, S., Kamiya, Y., and Sun, T. (2008). Potential sites of bioactive gibberellin production during reproductive growth in *Arabidopsis*. Plant Cell **20**: 320–336.

Hu, Y., Vandenbussche, F., and Van Der Straeten, D. (2017). Regulation of seedling growth by ethylene and the ethylene–auxin crosstalk. Planta **245**: 467–489.

Hu, Y., Xie, Q., and Chua, N.-H. (2003). The *Arabidopsis* auxin-inducible gene ARGOS controls lateral organ size. Plant Cell **15**: 1951–1961.

Hua, J., Chang, C., Sun, Q., and Meyerowitz, E.M. (1995). Ethylene insensitivity conferred by *Arabidopsis ERS* gene. Science **269**: 1712–4.

Hua, J. and Meyerowitz, E.M. (1998). Ethylene responses are negatively regulated by a receptor gene family in *Arabidopsis thaliana*. Cell **94**: 261–271.

Hua, J., Sakai, H., Nourizadeh, S., Chen, Q.G., Bleecker, A.B., Ecker, J.R., and Meyerowitz, E.M. (1998). *EIN4* and *ERS2* are members of the putative ethylene receptor gene family in *Arabidopsis*. Plant Cell **10**: 1321–1332.

Huang, X., Hou, L., Meng, J., You, H., Li, Z., Gong, Z., Yang, S., and Shi, Y. (2018). The antagonistic action of abscisic acid and cytokinin signaling mediates drought stress response in *Arabidopsis*. Mol. Plant **11**: 970-982.

Huijser, P. and Schmid, M. (2011). The control of developmental phase transitions in plants. Development **138**: 4117–4129.

Hutchison, C.E., Li, J., Argueso, C., Gonzalez, M., Lee, E., Lewis, M.W., Maxwell, B.B., Perdue, T.D., Schaller, G.E., Alonso, J.M., Ecker, J.R., and Kieber, J.J. (2006). The ARABIDOPSIS HISTIDINE PHOSPHOTRANSFER PROTEINs are redundant positive regulators of cytokinin signaling. Plant Cell **18**: 3073–3087.

Ichihashi, Y., Horiguchi, G., Gleissberg, S., and Tsukaya, H. (2010). The bHLH transcription factor SPATULA controls final leaf size in *Arabidopsis thaliana*. Plant Cell Physiol. **51**: 252–261.

Iglesias, M.J., Terrile, M.C., Bartoli, C.G., D'Ippólito, S., and Casalongué, C.A. (2010). Auxin signaling participates in the adaptative response against oxidative stress and salinity by interacting with redox metabolism in *Arabidopsis*. Plant Mol. Biol. **74**: 215–222.

Imamura, A., Hanaki, N., Nakamura, A., Suzuki, T., Taniguchi, M., Kiba, T., Ueguchi, C., Sugiyama,

T., and Mizuno, T. (1999). Compilation and characterization of ARABIOPSIS THALIANA RESPONSE REGULATORs implicated in His-Asp phosphorelay signal transduction. Plant Cell Physiol. **40**: 733–742.

Inoue, T., Higuchi, M., Hashimoto, Y., Seki, M., Kobayashi, M., Kato, T., Tabata, S., Shinozaki, K., and Kakimoto, T. (2001). Identification of CRE1 as a cytokinin receptor from *Arabidopsis*. Nature **409**: 1060–1063.

Dello Ioio, R., Nakamura, K., Moubayidin, L., Perilli, S., Taniguchi, M., Morita, M.T., Aoyama, T., Costantino, P., and Sabatini, S. (2008). A genetic framework for the control of cell division and differentiation in the root meristem. Science **322**: 1380–1384.

Iqbal, N., Khan, N.A., Ferrante, A., Trivellini, A., Francini, A., and Khan, M.I.R. (2017). Ethylene role in plant growth, development and senescence: Interaction with other phytohormones. Front. Plant Sci. **08**: 475.

Ishida, K., Yamashino, T., Yokoyama, A., and Mizuno, T. (2008). Three type-B response regulators, ARR1, ARR10 and ARR12, play essential but redundant roles in cytokinin signal transduction throughout the life cycle of *Arabidopsis thaliana*. Plant Cell Physiol. **49**: 47–57.

Itai, C., Ben-Zioni, A., and Ordin, L. (1973). Correlative changes in endogenous hormone levels and shoot growth induced by short heat treatments to the root. Physiol. Plant. **29**: 355–360.

Jiang, C., Belfield, E.J., Cao, Y., Smith, J.A.C., and Harberd, N.P. (2013). An *Arabidopsis* soil-salinity-tolerance mutation confers ethylene-mediated enhancement of sodium/potassium homeostasis. Plant Cell **25**: 3535–3552.

Jiang, K., Meng, Y.L., and Feldman, L.J. (2003). Quiescent center formation in maize roots is associated with an auxin-regulated oxidizing environment. Development **130**: 1429–1438.

Jibran, R., A. Hunter, D., and P. Dijkwel, P. (2013). Hormonal regulation of leaf senescence through integration of developmental and stress signals. Plant Mol. Biol. **82**: 547–561.

Jin, S.H., Ma, X.M., Kojima, M., Sakakibara, H., Wang, Y.W., and Hou, B.K. (2013). Overexpression of glucosyltransferase UGT85A1 influences *trans*-zeatin homeostasis and *trans*-zeatin responses likely through O-glucosylation. Planta **237**: 991–999.

Jing, H.C., Schippers, J.H.M., Hille, J., and Dijkwel, P.P. (2005). Ethylene-induced leaf senescence depends on age-related changes and *OLD* genes in *Arabidopsis*. J. Exp. Bot. **56**: 2915–2923.

Jones, B., Gunneråas, S.A., Petersson, S. V, Tarkowski, P., Graham, N., May, S., Dolezal, K., Sandberg, G., and Ljung, K. (2010). Cytokinin regulation of auxin synthesis in *Arabidopsis* involves a homeostatic feedback loop regulated via auxin and cytokinin signal transduction. Plant Cell **22**: 2956–2969.

Ju, C. Yoon, G. M., Shemansky, J. M., Lin, D. Y. Ying, Z. I., Chang, J., Garrett, W. M., Kessenbrock, M., Groth, G., Tucker, M. L., Cooper, B., Kieber, J. J., and Chang, C. (2012). CTR1 phosphorylates the central regulator EIN2 to control ethylene hormone signaling from the ER membrane to the nucleus in *Arabidopsis*. Proc. Natl. Acad. Sci. U. S. A. **109**: 19486–19491.

Joo, H. J., Bae, Y. S., and Lee, J. S. (2001). Role of auxin-induced reactive oxygen species in root gravitropism. Plant Physiol. **126**: 1055–1060.

Kakimoto, T. (2001). Identification of plant cytokinin biosynthetic enzymes as dimethylallyl diphosphate:ATP/ADP isopentenyltransferases. Plant Cell Physiol. **42**: 677–685.

Kang, J., Lee, Y., Sakakibara, H., and Martinoia, E. (2017). Cytokinin transporters: GO and STOP in signaling. Trends Plant Sci. **22**: 455–461.

Kanojia, A. and Dijkwel, P.P. (2018). Abiotic stress responses are governed by reactive oxygen species and age. Ann. Plant Rev. **1**: 1-32.

Karimi, M., De Meyer, B., and Hilson, P. (2005). Modular cloning in plant cells. Trends Plant Sci. **10**: 103–105.

Kasahara, H., Takei, K., Ueda, N., Hishiyama, S., Yamaya, T., Kamiya, Y., Yamaguchi, S., and Sakakibara, H. (2004). Distinct isoprenoid origins of cis- and *trans*-zeatin biosyntheses in *Arabidopsis*. J. Biol. Chem. **279**: 14049–14054.

Kazama, T., Ichihashi, Y., Murata, S., and Tsukaya, H. (2010). The mechanism of cell cycle arrest front progression explained by a KLUH/CYP78A5-dependent mobile growth factor in developing leaves of *Arabidopsis thaliana*. Plant Cell Physiol. **51**: 1046–1054.

Kazan, K. (2015). Diverse roles of jasmonates and ethylene in abiotic stress tolerance. Trends Plant Sci. **20**: 219–229.

Kiba, T., Takei, K., Kojima, M., and Sakakibara, H. (2013). Side-chain modification of cytokinins controls shoot growth in *Arabidopsis*. Dev. Cell **27**: 452–461.

Kieber, J.J., Rothenberg, M., Roman, G., Feldmann, K. A., and Ecker, J. R. (1993). CTRI , a negative regulator of the ethylene pathway in *Arabidopsis*, encodes a member of the raf family of protein kinases. Cell **72**: 427–441.

Kieber, J.J. and Schaller, G.E. (2014). Cytokinins. Arab. B. **12**: e0168.

Kim, H.J., Nam, H.G., and Lim, P.O. (2016). Regulatory network of NAC transcription factors in leaf senescence. Curr. Opin. Plant Biol. **33**: 48–56.

Kim, H.J., Park, J.-H., Kim, J., Kim, J.J., Hong, S., Kim, J., Kim, J.H., Woo, H.R., Hyeon, C., Lim, P.O., Nam, H.G., and Hwang, D. (2018a). Time-evolving genetic networks reveal a NAC troika that negatively regulates leaf senescence in *Arabidopsis*. Proc. Natl. Acad. Sci. U. S. A. **115**: E4930–E4939.

Kim, H.J., Ryu, H., Hong, S.H., Woo, H.R., Lim, P.O., Lee, I.C., Sheen, J., Nam, H.G., and Hwang, I. (2006). Cytokinin-mediated control of leaf longevity by AHK3 through phosphorylation of ARR2 in *Arabidopsis*. Proc. Natl. Acad. Sci. U. S. A. **103**: 814–819.

Kim, J., Park, S.J., Lee, I.H., Chu, H., Penfold, C.A., Kim, J.H., Buchanan-Wollaston, V., Nam, H.G., Woo, H.R., and Lim, P.O. (2018b). Comparative transcriptome analysis in *Arabidopsis ein2*/*ore3* and *ahk3*/*ore12* mutants during dark-induced leaf senescence. J. Exp. Bot. **69**: 3023–3036.

Kim, J.H. and Kende, H. (2004). A transcriptional coactivator, AtGIF1, is involved in regulating leaf growth and morphology in *Arabidopsis*. Proc. Natl. Acad. Sci. U. S. A. **101**: 13374–13379.

Kinoshita, N., Wang, H., Kasahara, H., Liu, J., MacPherson, C., Machida, Y., Kamiya, Y., Hannah, M.A., and Chuaa, N.H. (2012). IAA-Ala Resistant3, an evolutionarily conserved target of miR167, mediates *Arabidopsis* root architecture changes during high osmotic stress. Plant Cell **24**: 3590–3602.

Ko, D., Kang, J., Kiba, T., Park, J., Kojima, M., Do, J., Kim, K. Y., Kwon, M., Endler, A., Song, W.-Y., Martinoia, E., Sakakibara, H., and Lee, Y.. (2014). *Arabidopsis* ABCG14 is essential for the root-to-shoot translocation of cytokinin. Proc. Natl. Acad. Sci. U. S. A. **111**: 7150–7155.

Koffler, B.E., Luschin-Ebengreuth, N., Stabentheiner, E., Müller, M., and Zechmann, B. (2014). Compartment specific response of antioxidants to drought stress in *Arabidopsis*. Plant Sci. **227**: 133–144.

Köllmer, I., Novák, O., Strnad, M., Schmülling, T., and Werner, T. (2014). Overexpression of the cytosolic *CYTOKININ OXIDASE/DEHYDROGENASE* (*CKX7*) from *Arabidopsis* causes specific changes in root growth and xylem differentiation. Plant J. **78**: 359–371.

Koncz, C. and Schell, J. (1986). The promoter of TL-DNA gene 5 controls the tissue-specific expression of chimaeric genes carried by a novel type of *Agrobacterium* binary vector. MGG Mol. Gen. Genet. **204**: 383–396.

Korasick, D.A., Enders, T.A., and Strader, L.C. (2013). Auxin biosynthesis and storage forms. J. Exp. Bot. **64**: 2541–2555.

Kotchoni, S.O., Larrimore, K.E., Mukherjee, M., Kempinski, C.F., and Barth, C. (2009). Alterations in the endogenous ascorbic acid content affect flowering time in *Arabidopsis*. Plant Physiol. **149**: 803–815.

Krishnakumar, V., Contrino, S., Cheng, C.Y., Belyaeva, I., Ferlanti, E.S., Miller, J.R., Vaughn, M.W., Micklem, G., Town, C.D., and Chan, A.P. (2017). Thalemine: A warehouse for *Arabidopsis* data integration and discovery. Plant Cell Physiol. **58**: e4.

Kurakawa, T., Ueda, N., Maekawa, M., Kobayashi, K., Kojima, M., Nagato, Y., Sakakibara, H., and Kyozuka, J. (2007). Direct control of shoot meristem activity by a cytokinin-activating enzyme. Nature **445**: 652–655.

Kuroha, T., Tokunaga, H., Kojima, M., Ueda, N., Ishida, T., Nagawa, S., Fukuda, H., Sugimoto, K., and Sakakibara, H. (2009). Functional Analyses of LONELY GUY Cytokinin-Activating Enzymes Reveal the Importance of the Direct Activation Pathway in *Arabidopsis*. Plant Cell **21**: 3152–3169.

Le, C.T.T., Brumbarova, T., Ivanov, R., Stoof, C., Weber, E., Mohrbacher, J., Fink-Straube, C., and Bauer, P. (2016). ZINC FINGER OF ARABIDOPSIS THALIANA12 (ZAT12) interacts with FER-LIKE IRON DEFICIENCY-INDUCED TRANSCRIPTION FACTOR (FIT) linking iron deficiency and oxidative stress responses. Plant Physiol. **170**: 540–557.

LeClere, S., Tellez, R., Rampey, R.A., Matsuda, S.P.T., and Bartel, B. (2002). Characterization of a family of IAA-amino acid conjugate hydrolases from *Arabidopsis*. J. Biol. Chem. **277**: 20446–20452.

Lee, B.H., Ko, J.-H., Lee, S., Lee, Y., Pak, J.-H., and Kim, J.H. (2009). The *Arabidopsis* GRF-INTERACTING FACTOR gene family performs an overlapping function in determining organ size as well as multiple developmental properties. Plant Physiol. **151**: 655–668.

Lee, M., Jung, J.-H., Han, D.-Y., Seo, P.J., Park, W.J., and Park, C.-M. (2012). Activation of a flavin monooxygenase gene *YUCCA7* enhances drought resistance in *Arabidopsis*. Planta **235**: 923–938.

Lee, S., Cheng, H., King, K.E., Wang, W., He, Y., Hussain, A., Lo, J., Harberd, N.P., and Peng, J. (2002). Gibberellin regulates *Arabidopsis* seed germination via RGL2, a GAI/RGA-like gene whose expression is up-regulated following imbibition. Genes Dev. **16**: 646–658.

Li, G., Liu, K., Baldwin, S.A., and Wang, D. (2003). Equilibrative nucleoside transporters of *Arabidopsis thaliana*: cDNA cloning, expression pattern, and analysis of transport activities. J. Biol.

Chem. **278**: 35732–35742.

Li, H., Johnson, P., Stepanova, A., Alonso, J.M., and Ecker, J.R. (2004). Convergence of signaling pathways in the control of differential cell growth in *Arabidopsis*. Dev. Cell **7**: 193–204.

Li, Z., Peng, J., Wen, X., and Guo, H. (2012). Gene network analysis and functional studies of senescence-associated genes reveal novel regulators of *Arabidopsis* leaf senescence. J. Integr. Plant Biol. **54**: 526–539.

Liang, X., Oono, Y., Shen, N.F., Köhler, C., Li, K., Scolnik, P.A., and Theologis, A. (1995). Characterization of two members (*ACS1* and *ACS3*) of the *1-AMINOCYCLOPROPANE-1-CARBOXYLATE SYNTHASE* gene family of *Arabidopsis thaliana*. Gene **167**: 17–24.

Linkies, A., Muller, K., Morris, K., Tureckova, V., Wenk, M., Cadman, C.S.C., Corbineau, F., Strnad, M., Lynn, J.R., Finch-Savage, W.E., and Leubner-Metzger, G. (2009). Ethylene interacts with abscisic acid to regulate endosperm rupture during germination: A comparative approach using *Lepidium sativum* and *Arabidopsis thaliana*. Plant Cell **21**: 3803–3822.

Liu, J., Moore, S., Chen, C., and Lindsey, K. (2017). Crosstalk complexities between auxin, cytokinin, and ethylene in *Arabidopsis* root development: From experiments to systems modeling, and back again. Mol. Plant **10**: 1480–1496.

Lohman, K.N., Gan, S., John, M.C., and Amasino, R.M. (1994). Molecular analysis of natural leaf senescence in *Arabidopsis thaliana*. Physiol. Plant. **92**: 322–328.

Lomin, S.N., Krivosheev, D.M., Steklov, M.Y., Arkhipov, D. V, Osolodkin, D.I., Schmülling, T., and Romanov, G.A. (2015). Plant membrane assays with cytokinin receptors underpin the unique role of free cytokinin bases as biologically active ligands. J. Exp. Bot. **66**: 1851–1863.

De Lucas, M., Davière, J.M., Rodríguez-Falcón, M., Pontin, M., Iglesias-Pedraz, J.M., Lorrain, S., Fankhauser, C., Blázquez, M.A., Titarenko, E., and Prat, S. (2008). A molecular framework for light and gibberellin control of cell elongation. Nature **451**: 480–484.

Lumba, S., Tsuchiya, Y., Delmas, F., Hezky, J., Provart, N.J., Shi Lu, Q., McCourt, P., and Gazzarrini, S. (2012). The embryonic leaf identity gene FUSCA3 regulates vegetative phase transitions by negatively modulating ethylene-regulated gene expression in *Arabidopsis*. BMC Biol. **10**: 8.

Ma, F., Wang, L., Li, J., Samma, M.K., Xie, Y., Wang, R., Wang, J., Zhang, J., and Shen, W. (2014). Interaction between HY1 and H_2O_2 in auxin-induced lateral root formation in *Arabidopsis*. Plant Mol. Biol. **85**: 49–61.

Mack, T.R., Gao, R., and Stock, A.M. (2009). Probing the roles of the two different dimers mediated by the receiver domain of the response regulator PHOB. J. Mol. Biol. **389**: 349–364.

Magome, H., Yamaguchi, S., Hanada, A., Kamiya, Y., and Oda, K. (2004). *Dwarf and delayed-flowering 1*, a novel *Arabidopsis* mutant deficient in gibberellin biosynthesis because of overexpression of a putative AP2 transcription factor. Plant J. **37**: 720–729.

Mähönen, A.P., Bishopp, A., Higuchi, M., Nieminen, K.M., Kinoshita, K., Törmäkangas, K., Ikeda, Y., Oka, A., Kakimoto, T., and Helariutta, Y. (2006). Cytokinin signaling and its inhibitor AHP6 regulate cell fate during vascular development. Science **311**: 94–98.

Mao, D., Yu, F., Li, J., Van de poel, B., Tan, D., Li, J., Liu, Y., Li, X., Dong, M., Chen, L., Li, D., and Luan, S. (2015). FERONIA receptor kinase interacts with S-adenosylmethionine synthetase and

suppresses S-adenosylmethionine production and ethylene biosynthesis in *Arabidopsis*. Plant Cell Environ. **38**: 2566–2574.

Marín-de la Rosa, N., Pfeiffer, A., Hill, K., Locascio, A., Bhalerao, R. P., Miskolczi, P., Grønlund, A. L., Wanchoo-Kohli, A., Thomas, S. G., Bennett, M. J., Lohmann, J. U., Blázquez, M. A. Alabadí, D., and Yu, H. (2015). Genome wide binding site analysis reveals transcriptional coactivation of cytokinin-responsive genes by DELLA proteins. PLoS Genet. **11**: e1005337.

Martin, M.N., Saladores, P.H., Lambert, E., Hudson, A.O., and Leustek, T. (2007). Localization of members of the gamma-glutamyl transpeptidase family identifies sites of glutathione and glutathione S-conjugate hydrolysis. Plant Physiol. **144**: 1715–1732.

Martínez-Zapater, J.M., Jarillo, J.A., Cruz-Alvarez, M., Roldán, M., and Salinas, J. (1995). *Arabidopsis* late-flowering fve mutants are affected in both vegetative and reproductive development. Plant J. **7**: 543–551.

Mashiguchi, K., Tanaka, K., Sakai, T., Sugawara, S., Kawaide, H., Natsume, M., Hanada, A., Yaeno, T., Shirasu, K., Yao, H., McSteen, P., Zhao, Y., Hayashi, K., Kamiya, Y., and Kasahara, H. (2011). The main auxin biosynthesis pathway in *Arabidopsis*. Proc. Natl. Acad. Sci. U. S. A.**108**: 18512–18517.

Mason, M.G., Li, J., Mathews, D.E., Kieber, J.J., and Schaller, G.E. (2004). Type-B RESPONSE REGULATORs display overlapping expression patterns in *Arabidopsis*. Plant Physiol. **135**: 927–937.

Mason, M.G., Mathews, D.E., Argyros, D.A., Maxwell, B.B., Kieber, J.J., Alonso, J.M., Ecker, J.R., and Schaller, G.E. (2005). Multiple type-B RESPONSE REGULATORs mediate cytokinin signal transduction in *Arabidopsis*. Plant Cell **17**: 3007–3018.

Mathieu, J., Yant, L.J., Mürdter, F., Küttner, F., and Schmid, M. (2009). Repression of Flowering by the miR172 Target SMZ. PLoS Biol. **7**: e1000148.

Matschi, S., Hake, K., Herde, M., Hause, B., and Romeis, T. (2015). The calcium-dependent protein kinase CPK28 regulates development by inducing growth phase-specific, spatially restricted alterations in jasmonic acid levels independent of defense responses in *Arabidopsis*. Plant Cell **27**: 591–606.

Matsumoto-Kitano, M., Kusumoto, T., Tarkowski, P., Kinoshita-Tsujimura, K., Vaclavikova, K., Miyawaki, K., and Kakimoto, T. (2008). Cytokinins are central regulators of cambial activity. Proc. Natl. Acad. Sci. U. S. A. **105**: 20027–20031.

McClure, B.A. and Guilfoyle, T. (1987). Characterization of a class of small auxin-inducible soybean polyadenylated RNAs. Plant Mol. Biol. **9**: 611–623.

McClure, B.A. and Guilfoyle, T. (1989). Rapid redistribution of auxin-regulated RNAs during gravitropism. Science **243**: 91–93.

McDonnell, L., Plett, J.M., Andersson-Gunnerås, S., Kozela, C., Dugardeyn, J., Van Der Straeten, D., Glick, B.R., Sundberg, B., and Regan, S. (2009). Ethylene levels are regulated by a plant encoded 1-AMINOCYCLOPROPANE-1-CARBOXYLIC ACID DEAMINASE. Physiol. Plant. **136**: 94–109.

McGinnis, K.M., Thomas, S.G., Soule, J.D., Strader, L.C., Zale, J.M., Sun, T., and Steber, C.M. (2003). The *Arabidopsis* SLEEPY1 gene encodes a putative F-box subunit of an SCF E3 ubiquitin

ligase. Plant Cell **15**: 1120–1130.

Miao, Y., Laun, T., Zimmermann, P., and Zentgraf, U. (2004). Targets of the WRKY53 transcription factor and its role during leaf senescence in *Arabidopsis*. Plant Mol. Biol. **55**: 853–867.

Miller, C.O., Skoog, F., Okumura, F.S., Von Saltza, M.H., and Strong, F.M. (1956). Isolation, structure and synthesis of kinetin, a substance promoting cell division. J. Am. Chem. Soc. **78**: 1375–1380.

Miller, C.O., Skoog, F., Von Saltza, M.H., and Strong, F.M. (1955). Kinetin, a cell division factor from deoxyribonucleic acid. J. Am. Chem. Soc. **77**: 1392.

Mitchum, M.G., Yamaguchi, S., Hanada, A., Kuwahara, A., Yoshioka, Y., Kato, T., Tabata, S., Kamiya, Y., and Sun, T. (2006). Distinct and overlapping roles of two GIBBERELLIN 3-OXIDASEs in *Arabidopsis* development. Plant J. **45**: 804–818.

Miyawaki, K., Matsumoto-Kitano, M., and Kakimoto, T. (2004). Expression of cytokinin biosynthetic *ISOPENTENYLTRANSFERASE* genes in *Arabidopsis* : tissue specificity and regulation by auxin, cytokinin, and nitrate. Plant J. **37**: 128–138.

Miyawaki, K., Tarkowski, P., Matsumoto-Kitano, M., Kato, T., Sato, S., Tarkowska, D., Tabata, S., Sandberg, G., and Kakimoto, T. (2006). Roles of *Arabidopsis* ATP/ADP ISOPENTENYLTRANSFERASEs and tRNA ISOPENTENYLTRANSFERASEs in cytokinin biosynthesis. Proc. Natl. Acad. Sci. U. S. A. **103**: 16598–16603.

Mizukami, Y. and Fischer, R.L. (2000). Plant organ size control: AINTEGUMENTA regulates growth and cell numbers during organogenesis. Proc. Natl. Acad. Sci. U. S. A. **97**: 942–947.

van Mourik, H., van Dijk, A.D.J., Stortenbeker, N., Angenent, G.C., and Bemer, M. (2017). Divergent regulation of *Arabidopsis SAUR* genes: A focus on the SAUR10-clade. BMC Plant Biol. **17**: 245.

Muday, G.K., Rahman, A., and Binder, B.M. (2012). Auxin and ethylene: Collaborators or competitors? Trends Plant Sci. **17**: 181–195.

Müller-Moulé, P., Nozue, K., Pytlak, M.L., Palmer, C.M., Covington, M.F., Wallace, A.D., Harmer, S.L., and Maloof, J.N. (2016). *YUCCA* auxin biosynthetic genes are required for *Arabidopsis* shade avoidance. PeerJ **4**: e2574.

Müller, M. and Munné-Bosch, S. (2015). ETHYLENE RESPONSE FACTORs: A key regulatory hub in hormone and stress signaling. Plant Physiol. **169**: 32–41.

Munns, R. (2002). Comparative physiology of salt and water stress. Plant, Cell Environ. **25**: 239–250.

Munns, R., Schachtman, D.P., and Condon, A.G. (1995). The significance of a two-phase growth response to salinity in wheat and barley. Aust. J. Plant Physiol. **22**: 561–569.

Nakajima, M., Shimada, A., Takashi, Y., Kim, Y. C., Park, S. H., Ueguchi-Tanaka, M., Suzuki, H., Katoh, E., Iuchi, S., Kobayashi, M., Maeda, T., Matsuoka, M., and Yamaguchi, I. (2006). Identification and characterization of *Arabidopsis* gibberellin receptors. Plant J. **46**: 880–889.

Nam, Y.J., Tran, L.S.P., Kojima, M., Sakakibara, H., Nishiyama, R., and Shin, R. (2012). Regulatory roles of cytokinins and cytokinin signaling in response to potassium deficiency in *Arabidopsis*. PLoS One **7**: e47797.

Narita, N.N., Moore, S., Horiguchi, G., Kubo, M., Demura, T., Fukuda, H., Goodrich, J., and Tsukaya, H. (2004). Overexpression of a novel small peptide ROTUNDIFOLIA4 decreases cell proliferation and alters leaf shape in *Arabidopsis thaliana*. Plant J. **38**: 699–713.

Nelissen, H., Gonzalez, N., and Inzé, D. (2016). Leaf growth in dicots and monocots: so different yet

so alike. Curr. Opin. Plant Biol. **33**: 72–76.

Neljubow, D. (1901). Ueber die horizontale Nutation der Stengel von *Pisum sativum* und einiger anderen Pflanzen. Pflanz. Beih. Bot. Zentralb **70**: 128–139.

Nishiyama, R., Watanabe, Y., Fujita, Y., Le, D. T., Kojima, M., Werner, T., Vankova, R., Yamaguchi-Shinozaki, K., Shinozaki, K., Kakimoto, T., Sakakibara, H., Schmülling, T., and Tran, L. P. (2011). Analysis of cytokinin mutants and regulation of cytokinin metabolic genes reveals important regulatory roles of cytokinins in drought, salt and abscisic acid responses, and abscisic acid biosynthesis. Plant Cell **23**: 2169–2183.

Nitschke, S. (2014). Novel roles for cytokinin in the responses to high light and circadian stress.

Nitschke, S., Cortleven, A., Iven, T., Feussner, I., Havaux, M., Riefler, M., and Schmülling, T. (2016). Circadian stress regimes affect the circadian clock and cause jasmonic acid-dependent cell death in cytokinin-deficient *Arabidopsis* plants. Plant Cell **28**: 1616–1639.

Nitschke, S., Cortleven, A., and Schmülling, T. (2017). Novel stress in plants by altering the photoperiod. Trends Plant Sci. **22**: 913–916.

Niu, L. and Liao, W. (2016). Hydrogen peroxide signaling in plant development and abiotic responses: Crosstalk with nitric oxide and calcium. Front. Plant Sci. **7**: 230.

Nordström, A., Tarkowski, P., Tarkowska, D., Norbaek, R., Astot, C., Dolezal, K., and Sandberg, G. (2004). Auxin regulation of cytokinin biosynthesis in *Arabidopsis thaliana*: A factor of potential importance for auxin-cytokinin-regulated development. Proc. Natl. Acad. Sci. U. S. A. **101**: 8039–8044.

Novák, O., Hauserová, E., Amakorová, P., Doležal, K., and Strnad, M. (2008). Cytokinin profiling in plant tissues using ultra-performance liquid chromatography–electrospray tandem mass spectrometry. Phytochemistry **69**: 2214–2224.

Okushima, Y., Overvoorde, P. J., Arima, K., Alonso, J. M., Chan, A., Chang, C., Ecker, J. R., Hughes, B., Lui, A., Nguyen, D., Onodera, C., Quach, H., Smith, A., Yu, G., and Theologis, A. (2005). Functional genomic analysis of the *AUXIN RESPONSE FACTOR* gene family members in *Arabidopsis thaliana*: unique and overlapping functions of ARF7 and ARF19. Plant Cell **17**: 444–463.

Ooka, H., Satoh, K., Doi, K., Nagata, T., Otomo, Y., Murakami, K., Matsubara, K., Osato, N., Kawai, J., Carninci, P., Hayashizaki, Y., Suzuki, K., Kojima, K., Takahara, Y., Yamamoto, K., and Kikuchi, S. (2003). Comprehensive analysis of *NAC* family genes in *Oryza sativa* and *Arabidopsis thaliana*. DNA Res. **10**: 239–247.

Osugi, A., Kojima, M., Takebayashi, Y., Ueda, N., Kiba, T., and Sakakibara, H. (2017). Systemic transport of *trans*-zeatin and its precursor have differing roles in *Arabidopsis* shoots. Nat. Plants **3**: 17112.

Otto, E. (2013). Der Einfluss von Cytokinin auf die Entwicklung des Sprossmeristems und auf den Ertrag von *Arabidopsis thaliana* und *Brassica napus*.

Overvoorde, P.J., Okushima, Y., Alonso, J. M., Chan, A., Chang, C., Ecker, J. R., Hughes, B., Liu, A., Onodera, C., Quach, H., Smith, A., Yu, G., and Theologis, A. (2005). Functional genomic analysis of the *AUXIN/INDOLE-3-ACETIC ACID* gene family members in *Arabidopsis thaliana*. Plant Cell **17**: 3282–3300.

Pant, B.D., Buhtz, A., Kehr, J., and Scheible, W.R. (2008). MicroRNA399 is a long-distance signal for the regulation of plant phosphate homeostasis. Plant J. **53**: 731–738.

Park, J., Nguyen, K.T., Park, E., Jeon, J.-S., and Choi, G. (2013). DELLA proteins and their interacting RING finger proteins repress gibberellin responses by binding to the promoters of a subset of gibberellin-responsive genes in *Arabidopsis*. Plant Cell **25**: 927–943.

Park, J., Oh, D.-H., Dassanayake, M., Nguyen, K.T., Ogas, J., Choi, G., and Sun, T. (2017). Gibberellin Signaling Requires Chromatin Remodeler PICKLE to Promote Vegetative Growth and Phase Transitions. Plant Physiol. **173**: 1463–1474.

Park, J.E., Park, J.Y., Kim, Y.S., Staswick, P.E., Jeon, J., Yun, J., Kim, S.Y., Kim, J., Lee, Y.H., and Park, C.M. (2007). GH3-mediated auxin homeostasis links growth regulation with stress adaptation response in *Arabidopsis*. J. Biol. Chem. **282**: 10036–10046.

Parry, G., Calderon-Villalobos, L.I., Prigge, M., Peret, B., Dharmasiri, S., Itoh, H., Lechner, E., Gray, W.M., Bennett, M., and Estelle, M. (2009). Complex regulation of the TIR1/AFB family of auxin receptors. Proc. Natl. Acad. Sci. U. S. A. **106**: 22540–22545.

Peer, W.A., Cheng, Y., and Murphy, A.S. (2013). Evidence of oxidative attenuation of auxin signalling. J. Exp. Bot. **64**: 2629–2639.

Peleg, Z., Reguera, M., Tumimbang, E., Walia, H., and Blumwald, E. (2011). Cytokinin-mediated source/sink modifications improve drought tolerance and increase grain yield in rice under water-stress. Plant Biotechnol. J. **9**: 747–758.

Pěnčík, A., Rolčík, J., Novák, O., Magnus, V., Barták, P., Buchtík, R., Salopek-Sondi, B., and Strnad, M. (2009). Isolation of novel indole-3-acetic acid conjugates by immunoaffinity extraction. Talanta **80**: 651–655.

Peng, J. and Harberd, N.P. (1993). Derivative alleles of the *Arabidopsis gibberellin-insensitive* (*gai*) mutation confer a wild-type phenotype. Plant Cell **5**: 351–360.

Peng, J., Li, Z., Wen, X., Li, W., Shi, H., Yang, L., Zhu, H., and Guo, H. (2014a). Salt-induced stabilization of EIN3/EIL1 confers salinity tolerance by deterring ROS accumulation in *Arabidopsis*. PLoS Genet. **10**: e1004664.

Peng, Z., He, S., Gong, W., Sun, J., Pan, Z., Xu, F., Lu, Y., and Du, X. (2014b). Comprehensive analysis of differentially expressed genes and transcriptional regulation induced by salt stress in two contrasting cotton genotypes. BMC Genomics **15**: 760.

Pernisova, M., Klima, P., Horak, J., Valkova, M., Malbeck, J., Soucek, P., Reichman, P., Hoyerova, K., Dubova, J., Friml, J., Za;zimalova, E., and Hejatko, J. (2009). Cytokinins modulate auxin-induced organogenesis in plants via regulation of the auxin efflux. Proc. Natl. Acad. Sci. U. S. A. **106**: 3609–3614.

Pernisova, M., Prat, T., Grones, P., Harustiakova, D., Matonohova, M., Spichal, L., Nodzynski, T., Friml, J., and Hejatko, J. (2016). Cytokinins influence root gravitropism via differential regulation of auxin transporter expression and localization in *Arabidopsis*. New Phytol. **212**: 497–509.

Phillips, A.L., Ward, D.A., Uknes, S., Appleford, N.E., Lange, T., Huttly, A.K., Gaskin, P., Graebe, J.E., and Hedden, P. (1995). Isolation and expression of three *GIBBERELLIN 20-OXIDASE* cDNA clones from *Arabidopsis*. Plant Physiol. **108**: 1049–1057.

Plackett, A.R.G., Powers, S. J., Fernandez-Garcia, N., Urbanova, T., Takebayashi, Y., Seo, M.,

Jikumaru, Y., Benlloch, R., Nilsson, O., Ruiz-Rivero, O., Phillips, A. L., Wilson, Z. A., Thomas, S. G., and Hedden, P. (2012). Analysis of the Developmental Roles of the *Arabidopsis* Gibberellin 20-Oxidases Demonstrates That GA20OX1, -2, and -3 are the dominant paralogs. Plant Cell **24**: 941–960.

Poethig, R.S. (2003). Phase change and the regulation of developmental timing in plants. Science **301**: 334–336.

Porco, S., Pěnčík, A., Rashed, A., Voß, U., Casanova-Sáez, R., Bishopp, A., Golebiowska, A., Bhosale, R., Swarup, R., Swarup, K., Peňáková, P., Novák, O., Staswick, P., Hedden, P., Phillips, A. L., Vissenberg, K., Bennett, M. J., Ljung, K. (2016). Dioxygenase-encoding *AtDAO1* gene controls IAA oxidation and homeostasis in *Arabidopsis*. Proc. Natl. Acad. Sci. U. S. A. **113**: 11016–11021.

Potuschak, T., Lechner, E., Parmentier, Y., Yanagisawa, S., Grava, S., Koncz, C., and Genschik, P. (2003). EIN3-dependent regulation of plant ethylene hormone signaling by two *Arabidopsis* F box proteins: EBF1 and EBF2. Cell **115**: 679–689.

Procházková, D., Haisel, D., and Wilhelmová, N. (2008). Antioxidant protection during ageing and senescence in chloroplasts of tobacco with modulated life span. Cell Biochem. Funct. **26**: 582–590.

Qiao, H., Chang, K.N., Yazaki, J., and Ecker, J.R. (2009). Interplay between ethylene, ETP1/ETP2 F-box proteins, and degradation of EIN2 triggers ethylene responses in *Arabidopsis*. Genes Dev. **23**: 512–521.

Qin, H., Gu, Q., Zhang, J., Sun, L., Kuppu, S., Zhang, Y., Burow, M., Payton, P., Blumwald, E., and Zhang, H. (2011). Regulated expression of an *ISOPENTENYLTRANSFERASE* gene (*IPT*) in peanut significantly improves drought tolerance and increases yield under field conditions. Plant Cell Physiol. **52**: 1904–14.

Qin, Y.M., Hu, C.Y., and Zhu, Y.X. (2008). The ascorbate peroxidase regulated by H_2O_2 and ethylene is involved in cotton fiber cell elongation by modulating ROS homeostasis. Plant Signal. Behav. **3**: 194–196.

Ramireddy, E., Brenner, W.G., Pfeifer, A., Heyl, A., and Schmülling, T. (2013). In planta analysis of a cis-regulatory cytokinin response motif in *Arabidopsis* and identification of a novel enhancer sequence. Plant Cell Physiol. **54**: 1079–1092.

Ramos, J.A., Zenser, N., Leyser, O., and Callis, J. (2001). Rapid degradation of AUXIN/INDOLEACETIC ACID proteins requires conserved amino acids of domain II and is proteasome dependent. Plant Cell **13**: 2349–2360.

Rampey, R.A. (2004). A family of auxin-conjugate hydrolases that contributes to free indole-3-acetic acid levels during *Arabidopsis* germination. Plant Physiol. **135**: 978–988.

Regnault, T., Davière, J.-M., Wild, M., Sakvarelidze-Achard, L., Heintz, D., Carrera Bergua, E., Lopez Diaz, I., Gong, F., Hedden, P., and Achard, P. (2015). The gibberellin precursor GA12 acts as a long-distance growth signal in *Arabidopsis*. Nat. Plants **1**: 15073.

Regnault, T., Daviere, J.M., Heintz, D., Lange, T., and Achard, P. (2014). The gibberellin biosynthetic genes *AtKAO1* and *AtKAO2* have overlapping roles throughout *Arabidopsis* development. Plant J. **80**: 462–474.

Reguera, M., Peleg, Z., Abdel-Tawab, Y.M., Tumimbang, E.B., Delatorre, C.A., and Blumwald, E. (2013). Stress-induced cytokinin synthesis increases drought tolerance through the coordinated regulation of carbon and nitrogen assimilation in rice. Plant Physiol. **163**: 1609–1622.

Ren, M.Y., Feng, R. J., Shi, H. R., Lu, L. F., Yun, T. Y., Peng, M., Guan, X., Zhang, H., Wang, J. Y., Zhang, X. Y., Li, Cheng L., Chen, Y. J., He, P., Zhang, Y. D., and Xie, J. H. (2017). Expression patterns of members of the ethylene signaling-related gene families in response to dehydration stresses in cassava. PLoS One **12**: e0177621.

Richmond, A.E. and Lang, A. (1957). Effect of kinetin on protein content and survival of detached xanthium leaves. Science **125**: 650–651.

Riefler, M., Novak, O., Strnad, M., and Schmülling, T. (2006). *Arabidopsis* cytokinin receptor mutants reveal functions in shoot growth, leaf senescence, seed size, germination, root development, and cytokinin metabolism. Plant Cell **18**: 40–54.

Rivero, R.M., Kojima, M., Gepstein, A., Sakakibara, H., Mittler, R., Gepstein, S., and Blumwald, E. (2007). Delayed leaf senescence induces extreme drought tolerance in a flowering plant. Proc. Natl. Acad. Sci. U. S. A. **104**: 19631–19636.

Romanov, G.A., Lomin, S.N., and Schmülling, T. (2006). Biochemical characteristics and ligand-binding properties of *Arabidopsis* cytokinin receptor AHK3 compared to CRE1/AHK4 as revealed by a direct binding assay. J. Exp. Bot. **57**: 4051–4058.

Romanov, G.A., Lomin, S.N., and Schmülling, T. (2018). Cytokinin signaling: from the ER or from the PM? That is the question! New Phytol. **218**: 41-53.

Rossel, J.B., Wilson, P.B., Hussain, D., Woo, N.S., Gordon, M.J., Mewett, O.P., Howell, K.A., Whelan, J., Kazan, K., and Pogsona, B.J. (2007). Systemic and intracellular responses to photooxidative stress in *Arabidopsis*. Plant Cell **19**: 4091–4110.

Rothenberg, M. and Ecker, J.R. (1993). Mutant analysis as an experimental approach towards understanding plant hormone action. Semin. Dev. Biol. **4**: 3–13.

Ruzicka, K., Simaskova, M., Duclercq, J., Petrasek, J., Zazimalova, E., Simon, S., Friml, J., Van Montagu, M.C.E., and Benkova, E. (2009). Cytokinin regulates root meristem activity via modulation of the polar auxin transport. Proc. Natl. Acad. Sci. U. S. A. **106**: 4284–4289.

Sakai, H., Aoyama, T., Bono, H., and Oka, A. (1998a). Two-component RESPONSE REGULATORs from *Arabidopsis thaliana* contain a putative DNA-binding motif. Plant Cell Physiol. **39**: 1232–1239.

Sakai, H., Hua, J., Chen, Q.G., Chang, C., Medrano, L.J., Bleecker, A.B., and Meyerowitz, E.M. (1998b). *ETR2* is an *ETR1-LIKE* gene involved in ethylene signaling in *Arabidopsis*. Proc. Natl. Acad. Sci. U. S. A. **95**: 5812–5817.

Sakakibara, H. (2006). Cytokinins: Activity, biosynthesis, and translocation. Annu. Rev. Plant Biol. **57**: 431–449.

Schaller, G.E. (2012). Ethylene and the regulation of plant development. BMC Biol. **10**: 9.

Schaller, G.E. and Kieber, J.J. (2002). Ethylene. Arab. B. **1**: e0071.

Schippers, J.H.M. (2015). Transcriptional networks in leaf senescence. Curr. Opin. Plant Biol. **27**: 77–83.

Schomburg, F.M., Bizzell, C.M., Lee, D.J., Zeevaart, J.A.D., and Amasino, R.M. (2003). Overexpression of a novel class of *GIBBERELLIN 2-OXIDASEs* decreases gibberellin levels and

creates dwarf plants. Plant Cell **15**: 151–163.

Schopfer, P. (2001). Hydroxyl radical-induced cell-wall loosening in vitro and in vivo: Implications for the control of elongation growth. Plant J. **28**: 679–688.

Schwab, R., Palatnik, J.F., Riester, M., Schommer, C., Schmid, M., and Weigel, D. (2005). Specific effects of microRNAs on the plant transcriptome. Dev. Cell **8**: 517–527.

Schwechheimer, C. (2012). Gibberellin signaling in plants – the extended version. Front. Plant Sci. **2**: 107.

Shi, H., Chen, L., Ye, T., Liu, X., Ding, K., and Chan, Z. (2014). Modulation of auxin content in *Arabidopsis* confers improved drought stress resistance. Plant Physiol. Biochem. **82**: 209–217.

Shi, Y., Tian, S., Hou, L., Huang, X., Zhang, X., Guo, H., and Yang, S. (2012). Ethylene signaling negatively regulates freezing tolerance by repressing expression of *CBF* and Type-A *ARR* genes in *Arabidopsis*. Plant Cell **24**: 2578–2595.

Shyh-Chang, N., Locasale, J. W., Lyssiotis, C. A. Zheng, Y., Teo, R. Y., Ratanasirintrawoot, S., Zhang, J., Onder, T., Unternaehrer, J. J., Zhu, H., Asara, J. M. Daley, G. Q., and Cantley, L. C. (2013). Influence of threonine metabolism on S-adenosylmethionine and histone methylation. Science **339**: 222–226.

Silverstone, A.L., Ciampaglio, C.N., and Sun, T. (1998). The *Arabidopsis RGA* gene encodes a transcriptional regulator repressing the gibberellin signal transduction pathway. Plant Cell **10**: 155–169.

Singh, S., Letham, D.S., and Palni, L.M.S. (1992a). Cytokinin biochemistry in relation to leaf senescence. VII: Endogenous cytokinin levels and exogenous applications of cytokinins in relation to sequential leaf senescence of tobacco. Physiol. Plant. **86**: 388–397.

Singh, S., Palni, L.M.S., and Letham, D.S. (1992b). Cytokinin biochemistry in relation to leaf senescence V: Endogenous cytokinin levels and metabolism of zeatin riboside in leaf discs from green and senescent tobacco (*Nicotiana rustica*) leaves. J. Plant Physiol. **139**: 279–283.

Skalák, J., Vercruyssen, Li., Claeys, H., Hradilová, J., Černý, M., Novák, O., Plačková, L., Saiz-Fernández, I., Skaláková, P., Coppens, F., Dhondt, S., Koukalová, Š., Zouhar, J., Inzé, D., and Brzobohatý, B. (2019). Multifaceted activity of cytokinin in leaf development shapes its size and structure in *Arabidopsis*. Plant J. **97**: 805–824.

Staswick, P.E., Serban, B., Rowe, M., Tiryaki, I., Maldonado, M.T., Maldonado, M.C., and Suza, W. (2005). Characterization of an *Arabidopsis* enzyme family that conjugates amino acids to indole-3-acetic acid. Plant Cell **17**: 616–27.

Staswick, P.E., Tiryaki, I., and Rowe, M.L. (2002). Jasmonate response locus *JAR1* and several related *Arabidopsis* genes encode enzymes of the firefly luciferase superfamily that show activity on jasmonic, salicylic, and indole-3-acetic acids in an assay for adenylation. Plant Cell **14**: 1405–1415.

Stepanova, A.N., Hoyt, J.M., Hamilton, A.A., and Alonso, J.M. (2005). A link between ethylene and auxin uncovered by the characterization of two root-specific ethylene-insensitive mutants in *Arabidopsis*. Plant Cell **17**: 2230–2242.

Stepanova, A.N., Robertson-Hoyt, J., Yun, J., Benavente, L.M., Xie, D.Y., Doležal, K., Schlereth, A., Jürgens, G., and Alonso, J.M. (2008). TAA1-mediated auxin biosynthesis is essential for

hormone crosstalk and plant development. Cell **133**: 177–191.

Stolz, A., Riefler, M., Lomin, S.N., Achazi, K., Romanov, G.A., and Schmülling, T. (2011). The specificity of cytokinin signalling in *Arabidopsis thaliana* is mediated by differing ligand affinities and expression profiles of the receptors. Plant J. **67**: 157–168.

Stowe-Evans, E.L., Harper, R.M., Motchoulski, A. V, and Liscum, E. (1998). NPH4, a conditional modulator of auxin-dependent differential growth responses in *Arabidopsis*. Plant Physiol. **118**: 1265–1275.

Street, I.H., Aman, S., Zubo, Y., Ramzan, A., Wang, X., Shakeel, S.N., Kieber, J.J., and Schaller, G.E. (2015). Ethylene inhibits cell proliferation of the *Arabidopsis* root meristem. Plant Physiol. **169**: 338–350.

Sun, J., Hirose, N., Wang, X., Wen, P., Xue, L., Sakakibara, H., and Zuo, J. (2005). *Arabidopsis SOI33*/*AtENT8* gene encodes a putative equilibrative nucleoside transporter that is involved in cytokinin transport in planta. J. Integr. Plant Biol. **47**: 588–603.

Sun, N., Wang, J., Gao, Z., Dong, J., He, H., Terzaghi, W., Wei, N., Deng, X.W., and Chen, H. (2016). *Arabidopsis* SAURs are critical for differential light regulation of the development of various organs. Proc. Natl. Acad. Sci. U. S. A. **113**: 6071–6076.

Sun, T. (2008). Gibberellin metabolism, perception and signaling pathways in *Arabidopsis*. Arab. B. **6**: e0103.

Sun, T.P. and Kamiya, Y. (1994). The *Arabidopsis GA1* locus encodes the cyclase *ent*-kaurene SYNTHETASE A of gibberellin biosynthesis. Plant Cell **6**: 1509–1518.

Suzuki, T., Miwa, K., Ishikawa, K., Yamada, H., Aiba, H., and Mizuno, T. (2001a). The *Arabidopsis* sensor HIS-KINASE, AHK4, can respond to cytokinins. Plant Cell Physiol. **42**: 107–113.

Suzuki, T., Sakurai, K., Imamura, A., Nakamura, A., Ueguchi, C., and Mizuno, T. (2000). Compilation and characterization of histidine-containing phosphotransmitters implicated in His-to-Asp phosphorelay in plants: AHP signal transducers of *Arabidopsis thaliana*. Biosci. Biotechnol. Biochem. **64**: 2486–2489.

Suzuki, T., Sakurai, K., Ueguchi, C., and Mizuno, T. (2001b). Two types of putative nuclear factors that physically interact with histidine-containing phosphotransfer (Hpt) domains, signaling mediators in His-to-Asp phosphorelay, in *Arabidopsis thaliana*. Plant Cell Physiol. **42**: 37–45.

Takei, K., Sakakibara, H., and Sugiyama, T. (2001). Identification of genes encoding ADENYLATE ISOPENTENYLTRANSFERASE, a cytokinin biosynthesis enzyme, in *Arabidopsis thaliana*. J. Biol. Chem. **276**: 26405–26410.

Takei, K., Yamaya, T., and Sakakibara, H. (2004). *Arabidopsis CYP735A1* and *CYP735A2* encode cytokinin hydroxylases that catalyse the biosynthesis of *trans*-zeatin. J. Biol. Chem. **279**: 41866–41872.

Teale, W.D., Paponov, I.A., and Palme, K. (2006). Auxin in action: signalling, transport and the control of plant growth and development. Nat. Rev. Mol. Cell Biol. **7**: 847–859.

Telfer, A., Bollman, K.M., and Poethig, R.S. (1997). Phase change and the regulation of trichome distribution in *Arabidopsis thaliana*. Development **124**: 645–654.

Thomas, S.G., Phillips, A.L., and Hedden, P. (1999). Molecular cloning and functional expression of *GIBBERELLIN 2-OXIDASE*s, multifunctional enzymes involved in gibberellin deactivation. Proc.

Natl. Acad. Sci. U. S. A. **96**: 4698–4703.

Tiwari, S.B., Hagen, G., and Guilfoyle, T. (2003). The roles of auxin response factor domains in auxin-responsive transcription. Plant Cell **15**: 533–543.

Todesco, M., Rubio-Somoza, I., Paz-Ares, J., and Weigel, D. (2010). A collection of target mimics for comprehensive analysis of microRNA function in *Arabidopsis thaliana*. PLoS Genet. **6**: e1001031.

Tokunaga, H., Kojima, M., Kuroha, T., Ishida, T., Sugimoto, K., Kiba, T., and Sakakibara, H. (2012). *Arabidopsis lonely guy* (*log*) multiple mutants reveal a central role of the LOG-dependent pathway in cytokinin activation. Plant J. **69**: 355–365.

Tsuchisaka, A., Yu, G., Jin, H., Alonso, J.M., Ecker, J.R., Zhang, X., Gao, S., and Theologis, A. (2009). A combinatorial interplay among the 1-AMINOCYCLOPROPANE-1-CARBOXYLATE isoforms regulates ethylene biosynthesis in *Arabidopsis thaliana*. Genetics **183**: 979–1003.

Tsukaya, H. (2013). Leaf development. Arab. B. **11**: e0163.

Ueguchi-Tanaka, M., Ashikari, M., Nakajima, M., Itoh, H., Katoh, E., Kobayashi, M., Chow, T.Y., Hsing, Y.I., Kitano, H., Yamaguchi, I., and Matsuoka, M. (2005). GIBBERELLIN INSENSITIVE DWARF1 encodes a soluble receptor for gibberellin. Nature **437**: 693–698.

Ueguchi, C., Sato, S., Kato, T., and Tabata, S. (2001). The AHK4 gene involved in the cytokinin-signaling pathway as a direct receptor molecule in *Arabidopsis thaliana*. Plant Cell Physiol. **42**: 751–755.

Ulmasov, T., Hagen, G., and Guilfoyle, T.J. (1999a). Activation and repression of transcription by auxin-response factors. Proc. Natl. Acad. Sci. U. S. A. **96**: 5844–5849.

Ulmasov, T., Hagen, G., and Guilfoyle, T.J. (1997a). ARF1, a transcription factor that binds to auxin response elements. Science **276**: 1865–8.

Ulmasov, T., Hagen, G., and Guilfoyle, T.J. (1999b). Dimerization and DNA binding of auxin response factors. Plant J. **19**: 309–319.

Ulmasov, T., Murfett, J., Hagen, G., and Guilfoyle, T.J. (1997b). AUX/IAA proteins repress expression of reporter genes containing natural and highly active synthetic auxin response elements. Plant Cell **9**: 1963–71.

Urbanová, T., Tarkowská, D., Novák, O., Hedden, P., and Strnad, M. (2013). Analysis of gibberellins as free acids by ultra performance liquid chromatography–tandem mass spectrometry. Talanta **112**: 85–94.

Vandesompele, J., De Preter, K., Pattyn, F., Poppe, B., Van Roy, N., De Paepe, A., and Speleman, F. (2002). Accurate normalization of real-time quantitative RT-PCR data by geometric averaging of multiple internal control genes. Genome Biol. **3**: research0034.

Vaseva, I.I., Qudeimat, E., Potuschak, T., Du, Y., Genschik, P., Vandenbussche, F., and Van Der Straeten, D. (2018). The plant hormone ethylene restricts *Arabidopsis* growth via the epidermis. Proc. Natl. Acad. Sci. U. S. A. **115**: E4130–E4139.

Veerabagu, M., Elgass, K., Kirchler, T., Huppenberger, P., Harter, K., Chaban, C., and Mira-Rodado, V. (2012). The *Arabidopsis* B-type rESPONSE REGULATOR 18 homomerizes and positively regulates cytokinin responses. Plant J. **72**: 721–731.

Vervliet, G., Holsters, M., Teuchy, H., Van Montagu, M., and Schell, J. (1975). Characterization of different plaque forming and defective temperate phages in *Agrobacterium* strains. J. Gen. Virol.

26: 33–48.

Vettakkorumakankav, N.N., Falk, D., Saxena, P., and Fletcher, R.A. (1999). A crucial role for gibberellins in stress protection of plants. Plant Cell Physiol. **40**: 542–548.

Vogel, J.P., Woeste, K.E., Theologis, A., and Kieber, J.J. (1998). Recessive and dominant mutations in the ethylene biosynthetic gene *ACS5* of *Arabidopsis* confer cytokinin insensitivity and ethylene overproduction, respectively. Proc. Natl. Acad. Sci. U. S. A. **95**: 4766–4771.

Wang, H., Caruso, L. V, Downie, A.B., and Perry, S.E. (2004). The embryo MADS domain protein AGAMOUS-Like 15 directly regulates expression of a gene encoding an enzyme involved in gibberellin metabolism. Plant Cell **16**: 1206–1219.

Wang, J., Ma, X.M., Kojima, M., Sakakibara, H., and Hou, B.K. (2013). Glucosyltransferase UGT76C1 finely modulates cytokinin responses via cytokinin N-glucosylation in *Arabidopsis thaliana*. Plant Physiol. Biochem. **65**: 9–16.

Wang, J., Ma, X.M., Kojima, M., Sakakibara, H., and Hou, B.K. (2011). N-glucosyltransferase UGT76C2 is involved in cytokinin homeostasis and cytokinin response in *Arabidopsis thaliana*. Plant Cell Physiol. **52**: 2200–2213.

Wang, K.L.-C., Li, H., and Ecker, J.R. (2002). Ethylene biosynthesis and signaling networks. Plant Cell **14**: 131–151.

Wen, J., Lease, K.A., and Walker, J.C. (2004). DVL, a novel class of small polypeptides: Overexpression alters *Arabidopsis* development. Plant J. **37**: 668–677.

Wen, X., Zhang, C., Ji, Y., Zhao, Q., He, W., An, F., Jiang, L., and Guo, H. (2012). Activation of ethylene signaling is mediated by nuclear translocation of the cleaved EIN2 carboxyl terminus. Cell Res. **22**: 1613–1616.

Went, F. (1926). On growth-accelerating substances in the coleoptile of *Avena sativa*.

Werner, S. (2016). Einfluss von Cytokinin auf die Organgröße und auf Entwicklungsübergänge in *Arabidopsis thaliana*.

Werner, T., Motyka, V., Laucou, V., Smets, R., Van Onckelen, H., and Schmülling, T. (2003). Cytokinin-deficient transgenic *Arabidopsis* plants show multiple developmental alterations indicating opposite functions of cytokinins in the regulation of shoot and root meristem activity. Plant Cell **15**: 2532–2550.

Werner, T., Motyka, V., Strnad, M., and Schmulling, T. (2001). Regulation of plant growth by cytokinin. Proc. Natl. Acad. Sci. U. S. A. **98**: 10487–10492.

Werner, T., Nehnevajova, E., Köllmer, I., Novák, O., Strnad, M., Krämer, U., and Schmülling, T. (2010). Root-specific reduction of cytokinin causes enhanced root growth, drought tolerance, and leaf mineral enrichment in *Arabidopsis* and tobacco. Plant Cell **22**: 3905–20.

Werner, T. and Schmülling, T. (2009). Cytokinin action in plant development. Curr. Opin. Plant Biol. **12**: 527–538.

Woeste, K.E., Vogel, J.P., and Kieber, J.J. (1999a). Factors regulating ethylene biosynthesis in etiolated *Arabidopsis thaliana* seedlings. Physiol. Plant. **105**: 478–484.

Woeste, K.E., Ye, C., and Kieber, J.J. (1999b). Two *Arabidopsis* mutants that overproduce ethylene are affected in the posttranscriptional regulation of 1-AMINOCYCLOPROPANE-1-CARBOXYLIC ACID SYNTHASE. Plant Physiol. **119**: 521–530.

Woo, H.R., Kim, H.J., Nam, H.G., and Lim, P.O. (2013). Plant leaf senescence and death - regulation by multiple layers of control and implications for aging in general. J. Cell Sci. **126**: 4823–4833.

Woodward, A.W. and Bartel, B. (2005). Auxin: regulation, action, and interaction. Ann. Bot. **95**: 707–735.

Worley, C.K., Zenser, N., Ramos, J., Rouse, D., Leyser, O., Theologis, A., and Callis, J. (2000). Degradation of AUX/IAA proteins is essential for normal auxin signalling. Plant J. **21**: 553–562.

Wu, G., Park, M.Y., Conway, S.R., Wang, J.W., Weigel, D., and Poethig, R.S. (2009). The sequential action of miR156 and miR172 regulates developmental timing in *Arabidopsis*. Cell **138**: 750–759.

Wu, G. and Poethig, R.S. (2006). Temporal regulation of shoot development in *Arabidopsis thaliana* by miR156 and its target SPL3. Development **133**: 3539–3547.

Xie, Y., Huhn, K., Brandt, R., Potschin, M., Bieker, S., Straub, D., Doll, J., Drechsler, T., Zentgraf, U., and Wenkel, S. (2014). REVOLUTA and WRKY53 connect early and late leaf development in *Arabidopsis*. Development **141**: 4772–4783.

Yabuta, T. and Sumiki, Y. (1938). On the crystal of gibberellin, a substance to promote plant growth. J. Agric. Chem. Soc. Japan **14**: 1526.

Yamada, H., Suzuki, T., Terada, K., Takei, K., Ishikawa, K., Miwa, K., Yamashino, T., and Mizuno, T. (2001). The *Arabidopsis* AHK4 HISTIDINE KINASE is a cytokinin-binding receptor that transduces cytokinin signals across the membrane. Plant Cell Physiol. **42**: 1017–1023.

Yamagami, T., Tsuchisaka, A., Yamada, K., Haddon, W.F., Harden, L.A., and Theologis, A. (2003). Biochemical diversity among the 1-AMINO-CYCLOPROPANE-1-CARBOXYLATE SYNTHASE isozymes encoded by the *Arabidopsis* gene family. J. Biol. Chem. **278**: 49102–49112.

Yamaguchi, S. (2008). Gibberellin metabolism and its regulation. Annu. Rev. Plant Biol. **59**: 225–251.

Yamaguchi, S., Sun, T., Kawaide, H., and Kamiya, Y. (1998). The *GA2* locus of *Arabidopsis thaliana* encodes *ent*-KAURENE SYNTHASE of gibberellin biosynthesis. Plant Physiol. **116**: 1271–1278.

Yan, Z., Liu, X., Ljung, K., Li, S., Zhao, W., Yang, F., Wang, M., and Tao, Y. (2017). Type B RESPONSE REGULATORs Act as central integrators in transcriptional control of the auxin biosynthesis enzyme TAA1. Plant Physiol. **175**: 1438–1454.

Yang, H., Yang, S., Li, Y., and Hua, J. (2007). The *Arabidopsis BAP1* and *BAP2* genes are general inhibitors of programmed cell death. Plant Physiol. **145**: 135–146.

Yang, S.F. and Hoffman, N.E. (1984). Ethylene biosynthesis and its regulation in higher plants. Annu. Rev. Plant Physiol. **35**: 155–189.

Yip, W.K., Moore, T., and Yang, S.F. (1992). Differential accumulation of transcripts for four tomato 1-AMINOCYCLOPROPANE-1-CARBOXYLATE SYNTHASE homologs under various conditions. Proc. Natl. Acad. Sci. U. S. A. **89**: 2475–2479.

Zdarska, M., Cuyacot, A.R., Tarr, P.T., Yamoune, A., Szmitkowska, A., Hrdinová, V., Gelová, Z., Meyerowitz, E.M., and Hejátko, J. (2019). ETR1 Integrates response to ethylene and cytokinins into a single multistep phosphorelay pathway to control root growth. Mol. Plant. **?**: 1-15.

Zdárská, M., Zatloukalová, P., Benítez, M., Šedo, O., Potěšil, D., Novák, O., Svačinová, J., Pešek, B., Malbeck, J., Vašíčková, J., Zdráhal, Z., and Hejátko, J. (2013). Proteome analysis in *Arabidopsis* reveals shoot- and root-specific targets of cytokinin action and differential regulation of hormonal homeostasis. Plant Physiol. **161**: 918–930.

Zhang, J., Lin, J.E., Harris, C., Campos Mastrotti Pereira, F., Wu, F., Blakeslee, J.J., and Peer, W.A. (2016a). DAO1 catalyzes temporal and tissue-specific oxidative inactivation of auxin in *Arabidopsis thaliana*. Proc. Natl. Acad. Sci. U. S. A. **113**: 11010–11015.

Zhang, K., Novak, O., Wei, Z., Gou, M., Zhang, X., Yu, Y., Yang, H., Cai, Y., Strnad, M., and Liu, C.J. (2014). *Arabidopsis* ABCG14 protein controls the acropetal translocation of root-synthesized cytokinins. Nat. Commun. **5**: 3274.

Zhang, M., Smith, J.A.C., Harberd, N.P., and Jiang, C. (2016b). The regulatory roles of ethylene and reactive oxygen species (ROS) in plant salt stress responses. Plant Mol. Biol. **91**: 651–659.

Zhang, S.W., Li, C.H., Cao, J., Zhang, Y.C., Zhang, S.Q., Xia, Y.F., Sun, D.Y., and Sun, Y. (2009). Altered architecture and enhanced drought tolerance in rice via the down-regulation of Indole-3-acetic acid by TLD1/OsGH3.13 activation. Plant Physiol. **151**: 1889–1901.

Zhang, T., Poudel, A.N., Jewell, J.B., Kitaoka, N., Staswick, P., Matsuura, H., and Koo, A.J. (2016c). Hormone crosstalk in wound stress response: Woundinducible amidohydrolases can simultaneously regulate jasmonate and auxin homeostasis in *Arabidopsis thaliana*. J. Exp. Bot. **67**: 2107–2120.

Zhang, W. and Wen, C.-K. (2010). Preparation of ethylene gas and comparison of ethylene responses induced by ethylene, ACC, and ethephon. Plant Physiol. Biochem. **48**: 45–53.

Zhang, X., Chen, Y., Lin, X., Hong, X., Zhu, Y., Li, W., He, W., An, F., and Guo, H. (2013). ADENINE PHOSPHORIBOSYL TRANSFERASE 1 is a Key enzyme catalyzing cytokinin conversion from nucleobases to nucleotides in *Arabidopsis*. Mol. Plant **6**: 1661–1672.

Zhao, Y. (2012). Auxin biosynthesis: A simple two-step pathway converts tryptophan to indole-3-acetic acid in plants. Mol. Plant **5**: 334–338.

Zhao, Y., Christensen, S.K., Fankhauser, C., Cashman, J.R., Cohen, J.D., Weigel, D., and Chory, J. (2001). A role for flavin monooxygenase-like enzymes in auxin biosynthesis. Science **291**: 306–309.

Van Zhong, G. and Burns, J.K. (2003). Profiling ethylene-regulated gene expression in *Arabidopsis thaliana* by microarray analysis. Plant Mol. Biol. **53**: 117–131.

Zhu, F.Y., Chen, M. X., Ye, N. H., Qiao, W. M., Gao, B., Law, W. K., Tian, Y., Zhang, D., Zhang, D., Liu, T. Y., Hu, Q. J., Cao, Y. Y., Su, Z. Z., Zhang, J., and Liu, Y. (2018). Comparative performance of the BGISEQ-500 and Illumina HiSeq4000 sequencing platforms for transcriptome analysis in plants. Plant Methods **14**: 69.

Zürcher, E., Liu, J., di Donato, M., Geisler, M., and Müller, B. (2016). Plant development regulated by cytokinin sinks. Science **353**: 1027–1030.

Zwack, P.J., Robinson, B.R., Risley, M.G., and Rashotte, A.M. (2013). CYTOKININ RESPONSE FACTOR 6 negatively regulates leaf senescence and is induced in response to cytokinin and numerous abiotic stresses. Plant Cell Physiol. **54**: 971–981.

Supplementary Information

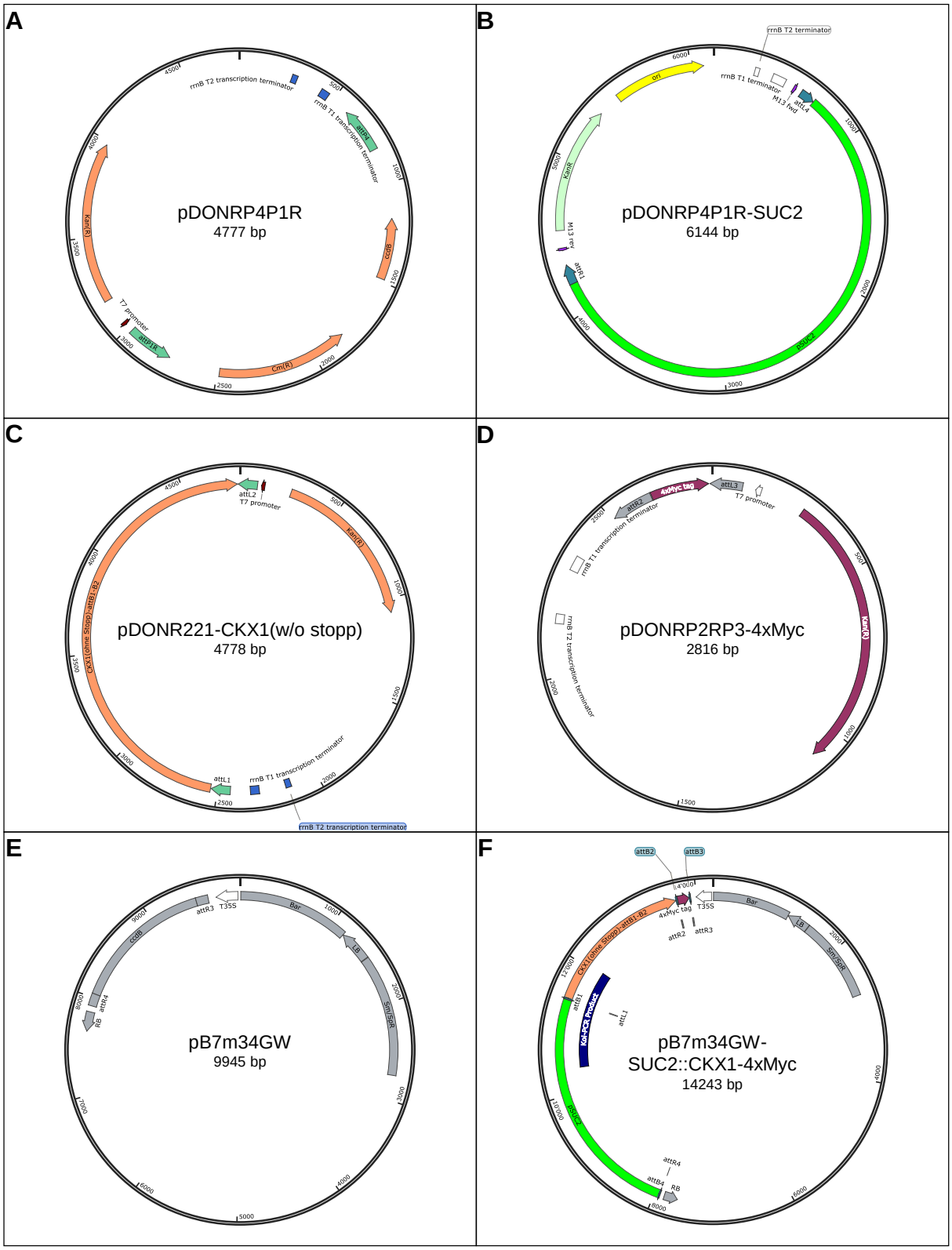

Supplemental Figure 1: Maps of vectors used and cloned in this study.
(A) pDONRP4P1R, (B) pDONRP4P1R-SUC2, (C) pDONR221-CKX1(w/o stopp), (D) pDONRP2RP3-4xMyc, (E) pB7m34GW, (F) pB7m34GW-SUC2::CKX1-4xMyc.

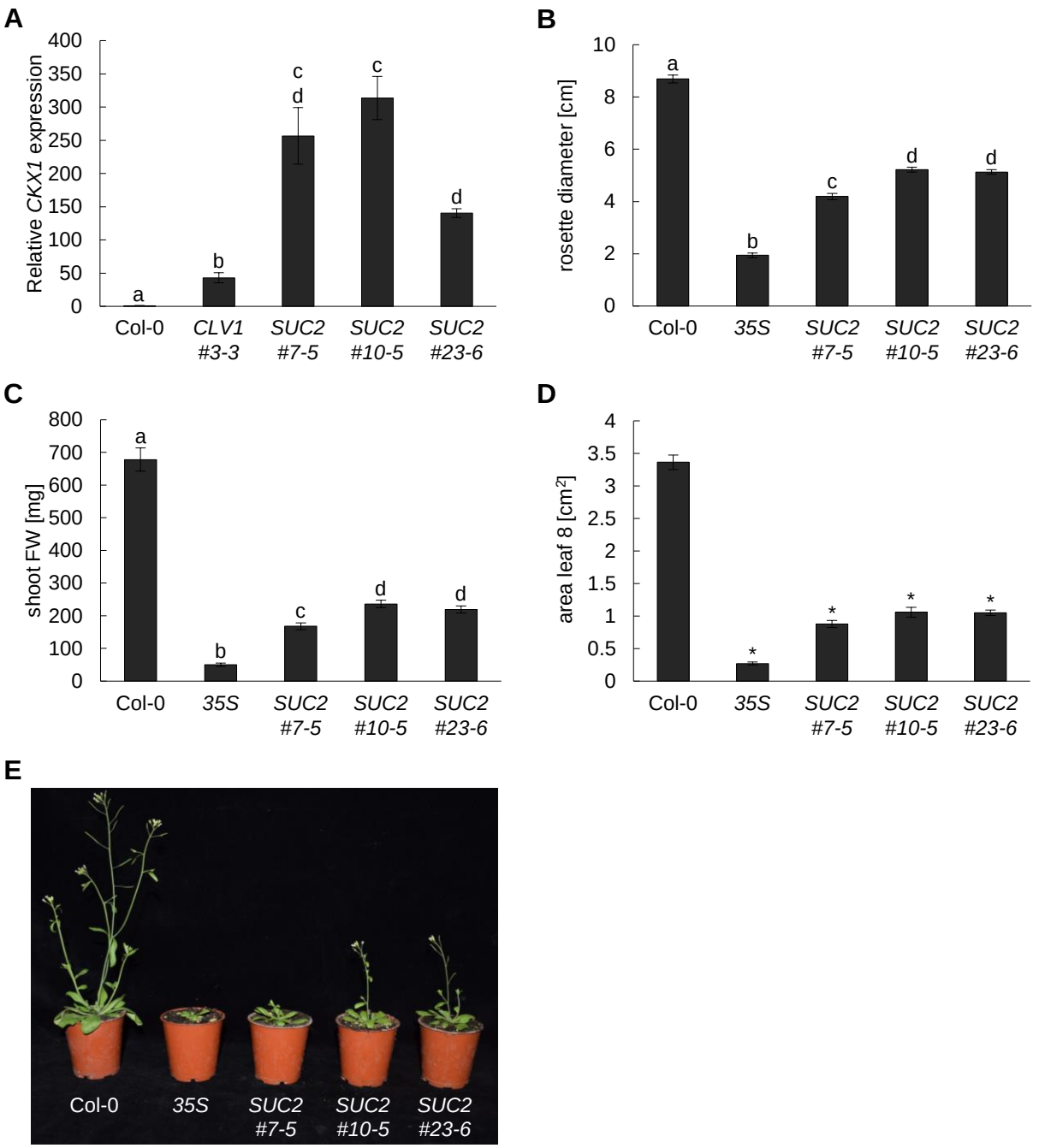

Supplemental Figure 2: Expression of* CKX1 *in* SUC2::CKX1-4xMyc *lines and shoot phenotypes.
(A) Expression of CKX1 in five-week-old long-day cultivated Col-0, CLV1::CKX1 *(*CLV1*) line #3-3 and* SUC2::CKX1-4xMyc *(*SUC2*) lines #7-5, #10-5 and #23-6 (n ≥ 3). (B) Rosette diameter, (C) shoot FW and (D) area of leaf 8 of four-week-old long-day cultivated Col-0,* 35S::CKX1 *(*35S*) and* SUC2::CKX1-4xMyc *(*SUC2*) lines #7-5, #10-5 and #23-6 (n = 10). (E) Pictures of representative plants grown for experiments shown in B to D. Letters indicate significant differences between groups and stars indicate a significant difference to Col-0 wild type (p ≤ 0.05). Error bars indicate SE.*

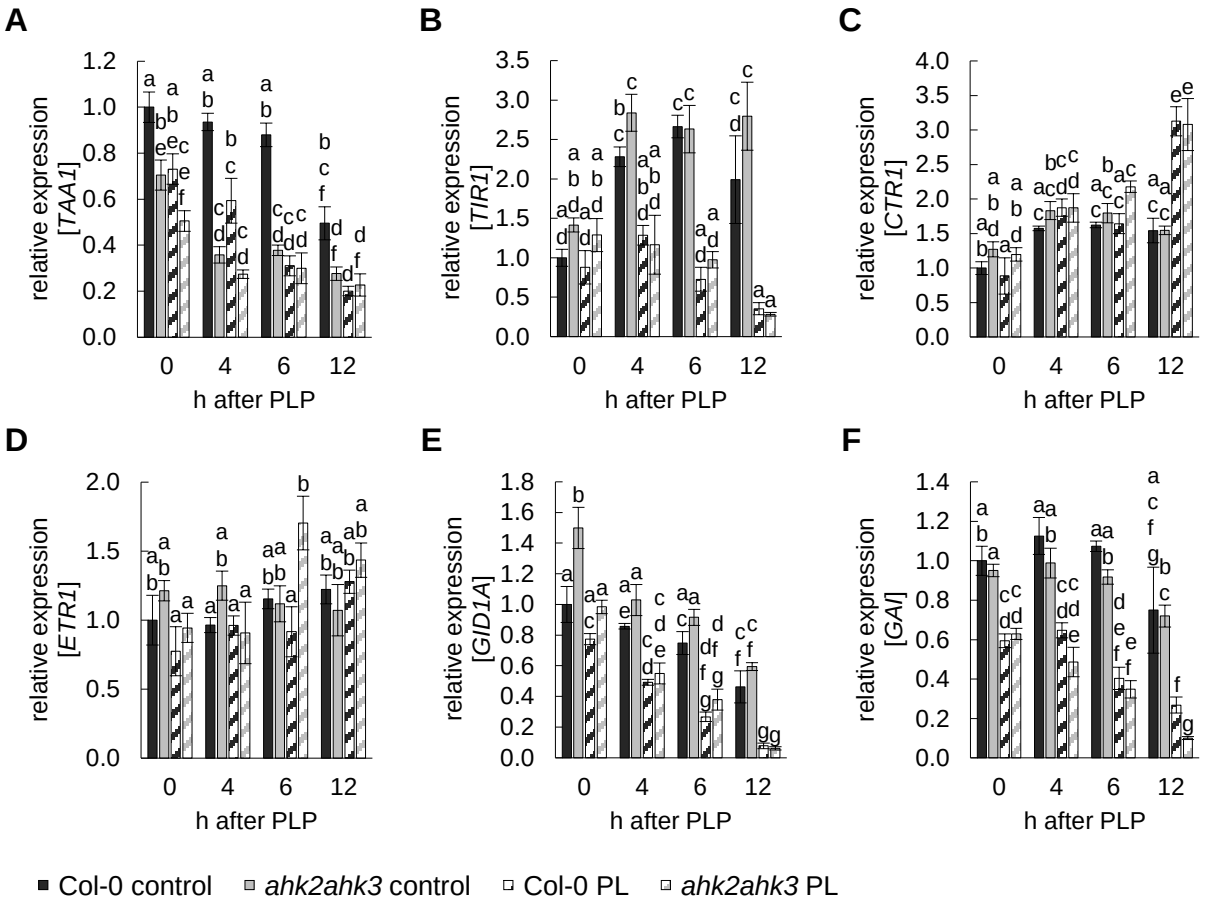

Supplemental Figure 3: Confirmation of RNAseq results via qRT-PCR.
Transcript abundances of TAA1 *(A),* TIR1 *(B),* CTR1 *(C),* ETR1 *(D),* GID1A *(E) and* GAI *(F) 0 h, 4 h, 6 h and 12 h after the PLP-treatment in control and stressed (PL) leaves of* ahk2ahk3 *and wild type. Letters indicate significant differences between groups (p ≤ 0.05; n = 4). Error bars indicate SE.*

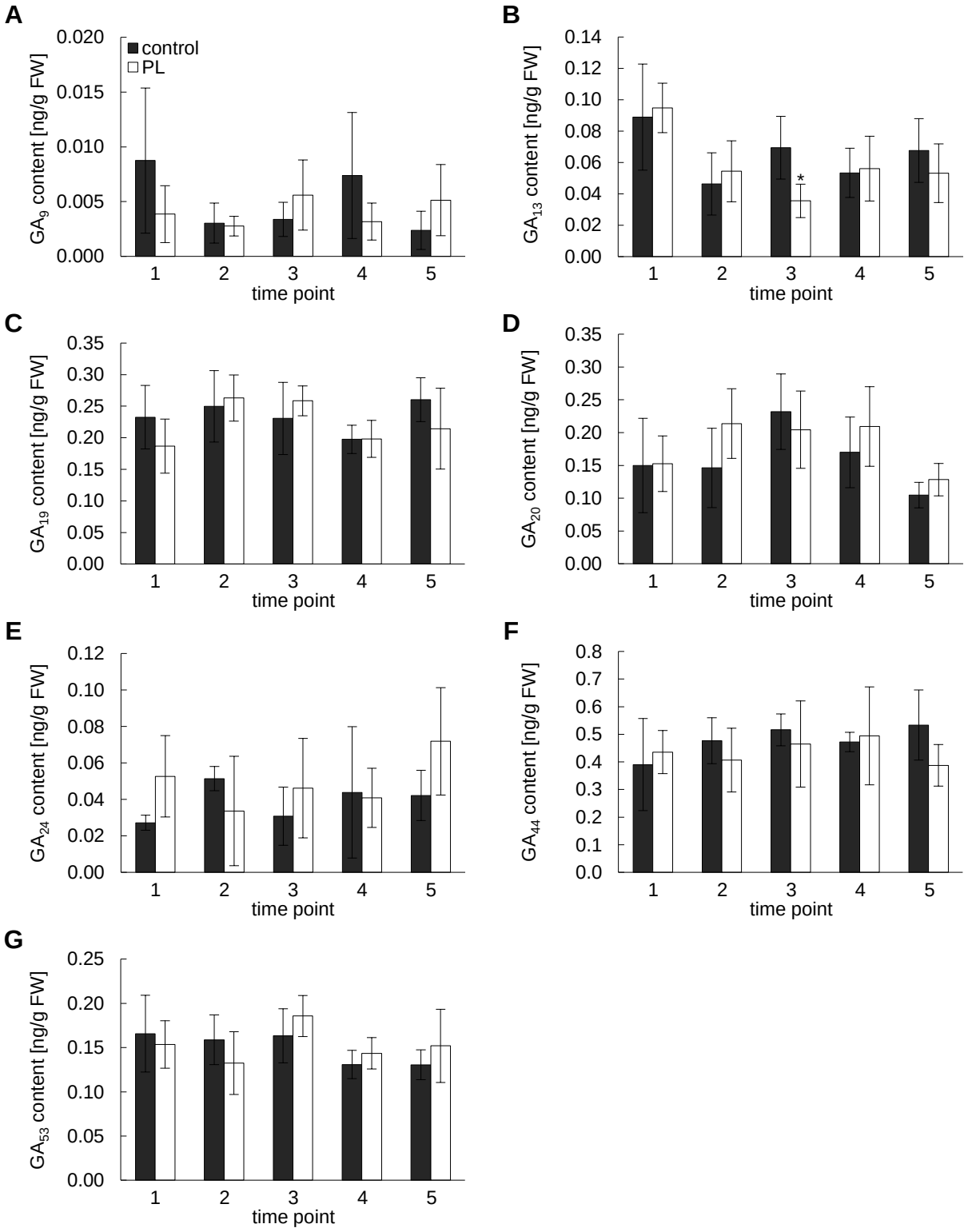

Supplemental Figure 4: Photoperiod stress does not change levels of GA-precursors in wild-type plants. *Content of GA_9 (A), GA_{13} (B), GA_{19} (C), GA_{20} (D), GA_{24} (E), GA_{44} (F) and GA_{53} (G) in control and PL samples at the time points depicted in Figure XA. Stars indicate statistically a significant difference between PL plants and the respective control at the given time point (1 - 5) in a paired Student's t-test ($p \leq 0.05$; $n = 5$). Error bars indicate SD.*

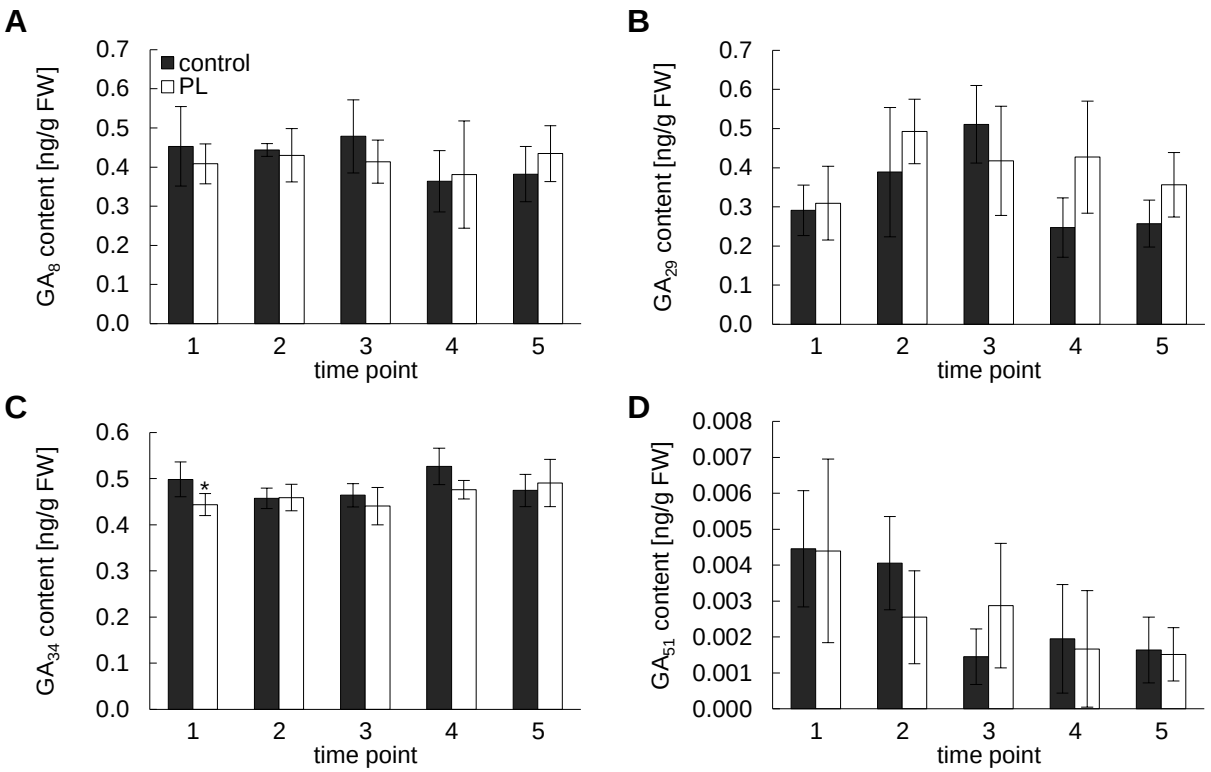

Supplemental Figure 5: Photoperiod stress does not change levels of deactivated GAs in wild-type plants. *Content of GA_8 (A), GA_{29} (B), GA_{34} (C) and GA_{51} (D) in control and PL samples at the time points depicted in Figure 38A. Stars indicate statistically a significant difference between PL and the respective control at the given time point (1 - 5) in a paired Student's t-test ($p \leq 0.05$; $n = 5$). Error bars indicate SD.*

Supplemental Table 1: DHZ-type cytokinin content in control and PL plants at the time points depicted in Figure 12A.
Bold numbers indicate statistically a significant difference in PL samples versus the controls under each sampling time point (1 - 5) in a paired Student's t-test. Values indicate pmol/g FW ± SD.

Condition	Total DHZ-types	DHZ	DHZR	DHZRMP	DHZOG	DHZROG	DHZ7G	DHZ9G
control 1	6.05±0.15	<LOD	0.026±0.007	<LOD	0.059±0.005	0.059±0.005	5.73±0.17	0.17±0.03
PL 1	5.87±0.46	<LOD	**0.053±0.015**	<LOD	0.057±0.003	0.062±0.013	5.56±0.43	0.14±0.01
control 2	5.41±0.21	<LOD	0.027±0.008	<LOD	0.054±0.002	0.067±0.006	5.13±0.20	0.14±0.01
PL 2	5.87±0.43	<LOD	**0.049±0.010**	<LOD	0.055±0.006	0.072±0.015	5.58±0.39	0.12±0.01
control 3	5.35±0.21	<LOD	0.031±0.009	<LOD	0.048±0.006	0.057±0.009	5.11±0.20	0.11±0.02
PL 3	**6.45±0.33**	<LOD	**0.075±0.021**	<LOD	**0.062±0.005**	**0.096±0.021**	**6.11±0.35**	0.10±0.01
control 4	4.93±0.29	<LOD	0.023±0.002	<LOD	0.042±0.006	0.056±0.007	4.70±0.28	0.11±0.01
PL 4	**6.51±0.92**	<LOD	**0.138±0.037**	<LOD	**0.064±0.006**	**0.122±0.036**	**6.02±0.86**	**0.16±0.04**
control 5	4.69±0.26	<LOD	0.023±0.005	<LOD	0.041±0.003	0.056±0.010	4.46±0.24	0.11±0.01
PL 5	4.66±0.59	<LOD	**0.067±0.020**	<LOD	0.051±0.008	0.068±0.017	4.38±0.54	0.10±0.02

Supplemental Table 2: cZ-type cytokinin content in control and PL plants at the time points depicted in Figure 12A.
Bold numbers indicate statistically a significant difference in PL samples versus the controls under each sampling time point (1 - 5) in a paired Student's t-test. Values indicate pmol/g FW ± SD.

Condition	Total *c*Z-types	*c*Z	*c*ZR	*c*ZRMP	*c*ZOG	*c*ZROG	*c*Z7G	*c*Z9G
control 1	21.6 ± 1.6	<LOD	0.41 ± 0.04	3.72 ± 0.58	1.14 ± 0.08	2.73 ± 0.16	13.32 ± 0.99	0.28 ± 0.01
PL 1	**18.1 ± 1.6**	<LOD	**0.10 ± 0.02**	**1.54 ± 0.15**	1.20 ± 0.12	2.48 ± 0.21	12.53 ± 1.36	**0.23 ± 0.03**
control 2	17.1 ± 0.8	<LOD	0.30 ± 0.10	2.84 ± 0.42	1.02 ± 0.07	2.30 ± 0.13	10.46 ± 0.46	0.21 ± 0.02
PL 2	16.7 ± 0.8	<LOD	0.21 ± 0.06	2.22 ± 0.46	**1.18 ± 0.09**	2.07 ± 0.17	10.82 ± 1.04	**0.17 ± 0.02**
control 3	21.6 ± 1.0	<LOD	0.33 ± 0.02	4.39 ± 0.23	1.16 ± 0.11	2.64 ± 0.12	12.88 ± 0.79	0.24 ± 0.03
PL 3	22.0 ± 1.0	<LOD	0.34 ± 0.03	4.43 ± 0.57	1.29 ± 0.06	**3.20 ± 0.30**	12.59 ± 0.93	**0.17 ± 0.01**
control 4	20.1 ± 1.5	<LOD	0.44 ± 0.01	3.56 ± 0.19	0.99 ± 0.04	2.73 ± 0.11	12.13 ± 1.30	0.22 ± 0.02
PL 4	**24.7 ± 3.1**	<LOD	**3.22 ± 0.92**	**6.18 ± 0.81**	**1.29 ± 0.04**	3.17 ± 0.38	10.67 ± 1.22	0.20 ± 0.02
control 5	17.2 ± 1.7	<LOD	0.16 ± 0.03	1.74 ± 0.34	1.04 ± 0.08	2.54 ± 0.25	11.46 ± 1.05	0.25 ± 0.02
PL 5	20.5 ± 2.4	<LOD	**1.55 ± 0.46**	**4.62 ± 0.88**	**1.72 ± 0.42**	2.56 ± 0.31	**9.83 ± 0.73**	**0.18 ± 0.02**

Acknowledgements

First of all, I want to thank Prof. Dr. Thomas Schmülling for giving me the opportunity to work in his lab, for all the discussions and guidance and for letting me switch from the cold stress field to the photoperiod stress topic. Thank you for giving me the freedom and support to explore the topic on my own and to follow the directions I found the most interesting.

Many thanks to Prof. Dr. Wolfgang Schuster for all the technical support, for the scientific discussions and exchange of experiences and for always being motivating and of course thank you for reviewing this work.

A big thank you to Dr. Anne Cortleven for taking so much time for supervising me. It was always nice to know that if there is a problem, I could come to you and we would fix it together. I really enjoyed working together with you and enjoyed learning from you how to be a well-structured scientist.

I also want to thank Dr. Jan Erik Leuendorf for supervising me during the first year of my PhD and for spending countless hours together during lunch discussing all different issues. Thank you for always being positive and supportive.

A big hug to my student helpers Milena and Sarah for taking care of the lab work in my absence (including the alphabetical sorting of all bottles), for staying curious and positive and for attempting to bake/cook ketogenic diet friendly.

Many thanks to the gardeners. Without you I would have exposed my plants not only to photoperiod stress but also to drought stress and to different biotic stresses.

Special thanks to all co-workers in Lab 101 and 109 and to the other members of the institute. You have always kept the atmosphere in the institute warm, productive and positive. I will never forget how supportive you have been.

I am grateful to the DRS and the CRC973 for financing this work and all the conferences I have attended.

Janet and Paul, I thank you for reading and correcting my thesis and for sending me all these funny mails. It always made me laugh no matter the circumstances.

Thank you, Julia, for helping me to improve my presentation skills and for the many hours we have talked about science and all other important things. You have inspired me with the way you handle life and science.

Nora, Lars, Jonathan, Kevin and Marcus, I thank you for always being there and especially for supporting me during the last couple of months that might have been the most difficult during my PhD.

Lastly, I want to thank my family and especially my godmothers. Without you I would not have been able to study and to live my dream.

Sandra, you have been the reason I wanted to become a scientist. There is not one day I do not miss you. I dedicate this work to you.

Bescheinigung bei Einreichung einer Monographie

gem. § 7 Abs. 2a und Abs. 4 der Promotionsordnung basierend auf den Mitteilungen im Amtsblatt der Freien Universität Berlin Nr. 21/2018 vom 31.05.2018

Hierdurch versichere ich, dass ich meine Dissertation mit dem Titel

The involvement of phytohormones, tissue and age in the response to photoperiod stress in *Arabidopsis thaliana*

selbstständig und ohne unerlaubte Hilfe angefertigt habe.

☒ Hierdurch versichere ich, dass meine Dissertation nicht auf meiner Diplomarbeit/Masterarbeit aufbaut bzw. nicht daraus erwachsen ist.

☐ Hierdurch versichere ich, dass meine Dissertation auf meiner Diplomarbeit / Masterarbeit mit dem Titel

.....

.....

aufbaut bzw. daraus erwachsen ist.

☒ Hierdurch versichere, dass ich meine Dissertation (ganz oder in Teilen) nicht veröffentlicht habe.

☐ Hierdurch versichere, dass ich meine Dissertation im Einvernehmen mit meinem/meiner Betreuer/in.....
ganz oder in Teilen veröffentlicht habe.

↳ Die _____ Publikation/en
(Anzahl eintragen)
werden jeder Kopie meiner Monographie als Ausdruck beigelegt.

Hierdurch versichere ich, dass ich meine Dissertation nicht schon einmal in einem anderen Promotionsverfahren eingereicht habe.

26.09.2019 .....
Datum Unterschrift